FINAL REPORT

NYSEG CONTRACT NO. 94-063

MILLIKEN STATION PROJECT

Submitted to
New York State Electric and Gas Corporation
Corporate Drive, Kirkwood Industrial Park
P.O. Box 5224
Binghamton, New York, 13902-5224
Attention: Mr. Charles Tisch

Principal Investigators
John N. Cannon
Brent W. Webb
Mardson Q. McQuay

Prepared by
Brigham Young University
Advanced Combustion Engineering Research Center
45 CTB, BYU
Provo, UT, 84602

September 1997

DISCLAIMER OF WARRANTIES AND LIMITATION OF LIABILITIES

This report was prepared by the organization(s) named below as an account of work sponsored or cosponsored by NYSEG (New York State Electric & Gas Corporation). Neither NYSEG, nor any of the organization(s) listed below, nor any person acting on behalf of any of them:

(A) Makes any warranty or representation whatsoever, express or implied, (1) with respect to the use of any information, apparatus, method, process or similar item disclosed in this report, including merchantability and fitness for a particular purpose; or (2) that such use does not infringe on or interfere with privately owned rights, including any party's intellectual property; or (3) that this report is suitable to any particular user's circumstance; or

(B) Assumes any responsibility for any damages or other liability whatsoever (including any consequential damages, even if NYSEG or any NYSEG representative has been advised of the possibility of such damages) resulting from your selection or use of this report or any information, apparatus, method, process or similar item disclosed in this report.

(C) Reference herein to any specific commercial product, process, or service by trade name, trademark, manufacturer, or otherwise, does not necessarily constitute or imply its endorsement, recommendation, or favoring by the United States government or any agency thereof. The views and opinions of authors expressed herein do not necessarily state or reflect those of the United States government or any agency thereof.

ORGANIZATION(S) THAT COFUNDED THIS REPORT:

New York State Electric & Gas Corporation
Corporate Drive, Kirkwood Industrial Park
P.O. Box 5224
Binghamton, NY 13902-5224
Attn: James J. Harvilla

US Department of Energy
FETC
P.O. Box 10940
Pittsburgh, PA 15129-9566
Attn: James Watts

Electric Power Research Institute
3412 Hillview Avenue
P.O. Box 10412
Palo Alto, CA 94303
Attn: Richard Rhudy

CONSOL, Inc.
Research & Development
4000 Brownsville Road
Library, PA 15129-9566
Attn: Robert Statnick

Empire State Electric Energy Research Corporation
1515 Broadway, 43rd Floor
New York, NY 10036-5701
Attn: Debra Dimeo

NYS Energy Research and Development Authority
Two Rockefeller Plaza
Albany, NY 12223
Attn: Joseph H. Sayer

ORDERING INFORMATION

For information about ordering this report, contact James J. Harvilla, Project Manager, New York State Electric & Gas Corporation, Corporate Drive, Kirkwood Industrial Park, P.O. Box 5224, Binghamton, NY 13902-5224, (607) 762-8630.

"LEGAL NOTICE"

"This report was prepared by Brigham Young University/ACERC as an account of work sponsored by New York State Electric and Gas Corporation (NYSEG). Neither NYSEG, nor any person acting on behalf of NYSEG:

a. Makes any warranty or representation, express or implied, with respect to the accuracy, completeness, or usefulness of the information, apparatus method or process disclosed in this report; or

b. Assumes any liabilities with respect to the use, or for damages resulting from the use, of any information, apparatus, method or process disclosed in this report."

TABLE OF CONTENTS

LIST OF TABLES iv

LIST OF ABBRIVATIONS v

ABSTRACT 1

INTRODUCTION 3

Background 3

Milliken Program 3

Test Matrix and Instrumentation 3

OBJECTIVES AND APPROACH 4

ANTICIPATED PRODUCTS 5

RESULTS 5

Test Conditions 5

Prediction Schedule and Conditions 7

Comparisons between Measurements and Predictions 8

Ignition Point Effects (Test 3) 17

NO_x and Carbon Burnout Effects (Tests 3, 4, & 5) 17

Near-field Comparisons (Test 4) 20

Far-field Comparisons (Test 5) 25

CONCLUSIONS 25

REFERENCES 27

ACKNOWLEDGMENTS 27

APPENDIXES 28

LIST OF FIGURES

FIGURE 1. SCHEMATIC OF MILLIKEN FURNACE AND ACCESS PORTS 6
FIGURE 2. MILLIKEN CASE CONVERGENCE CRITERIA (TEST 3) WITH 192K GRID AND HIGH TURBULENCE 9
FIGURE 3. BURNER INLET COMPARTMENTS SKETCH COMPARED TO 192K AND 337K GRID MODELS 10
FIGURE 4. COMPARISON OF PROBE MEASURED AND PREDICTEDTRANSVERSE VALUES FOR CASES 1, 4, AND 9 OF TABLE 3 AT LEVEL 5 FOR VARIOUS GRID SIZES. 12
FIGURE 5. COMPARISON OF AVERAGE MEASURED AND PREDICTED VERTICAL VALUES FOR CASES 1, 4, AND 9 FOR VARIOUS GRID SIZES 13
FIGURE 6. PERCENTAGE DIFFERENCE BETWEEN PREDICTED AND MEASURED AVERAGED VALUES AT VARIOUS BOILER HEIGHTS FOR CASES 1, 4, AND 9 OF TABLE 3. 14
FIGURE 7. AVERAGE MEASURED AND PREDICTED TURBULENCE INTENSITIES FOR ELEVEN PREDICTED CASES AND SEVEN TESTS FOR THREE BOILER LEVELS. 15
FIGURE 8. OVERLAY OF BURNER ORIENTATION (STRAIGHT SOLID LINE) ON O_2 PREDICTIONS (DOTTED LINE) AT LEVEL 2 16
FIGURE 9. COMPARISON OF MEASURED TEST 3 AND PREDICTED CASES 1,4,9 AT PORT 2E4 FOR VARIOUS NUMBERS OF GRID NODES 18
FIGURE 10. COMPARISON BETWEEN AVERAGED MEASURED AND PREDICTED VALUES FOR TEST 3 CONTRASTING THE EFFECTS OF THE ORIGINAL AND REVISED DEVOLATILEIZATION CONSTANTS. 19
FIGURE 11. (A ABOVE & B BELOW) AVERAGE PREDICTED AND MEASURED CARBON-IN-ASH PERCENTAGES BY BOILER LEVEL FOR CASES 6, 4, AND 10 (337 GRID) WITH MEASUREMENTS FROM TESTS 3,4,5. 21
FIGURE 12. TOP VIEW OF THE NEAR-FIELD DEMONSTRATES THE EFFECT ON O_2 STEEP GRADIENT CHANGE IN JUST 5 FEET OF LINEAR SPACE AT LEVEL 2. (I.E. BETWEEN DASHED AND UPPER SOLID LINE, SEE ALSO FIGURE 13) 22
FIGURE 13. ILLUSTRATES THE NEAR-FIELD EFFECTS OF ORIGINAL VS REVISED DEVOLATILIZATION RATE CONSTANTS COMPARED TO MEASURED PROBE TRAVERSES AT LEVEL 2 ON THE SIX NOTED VARIABLES. 23
FIGURE 14. COMPARISON BETWEEN TEST 3 AVERAGE MEASURED AND PREDICTED IN-PLANE GAS VELOCITYS (337K GRID) BY PORT ORDED BY BOILER HEIGHT. 24
FIGURE 15. COMPARISONS BETWEEN MEASURED AND PREDICTED VALUES FOR TWO DIFFERENT GRID SIZES AT THE FIFTH FLOOR LEVEL (FAR-FIELD COMPARISON) USING THE 192K AND 337K NODE GRIDS. 26

LIST OF TABLES

TABLE 1. BURNER SCALES AT WHICH PCGC-3 VALIDATION IS ADDRESSED 4
TABLE 2. MILLIKEN TEST PARAMETERS 6
TABLE 3. SIMULATIONS ON PCGC-3 TO PREDICT THE MILLIKEN FURNACE PROPERTIES 7
TABLE 4. COMPARISONS OF MEASURED (TESTS 3,4,5)AND PREDICTED (CASES 3, 4, 6, 7, 8, 10) FOR OUTLET O_2 AND NO_X CONCENTRATIONS WITH OVERFIRE AIR VARIATION 17

LIST OF ABBRIVATIONS

ABB/CE	Asea Brown Boveri/Combustion Engineering
ACERC	Advanced Combustion Engineering Research Center
BTU	British Thermal Unit
BYU	Brigham Young University
CCL	Combustion Computations Laboratory
CCOFA	Close-Coupled Overfire Air
CPR	Controlled Profile Reactor
DOE	U. S. Department of Energy
CTB	Crabtree Technology Building
EPRI	Electric Power Research Institute
ESEERCO	Empire State Electric Energy Research Co.
F	degrees Farenheit
FGD	Flue-gas Desulphurization
FPTF	Fireside Performance Test Facility
K	degree Kelvin or kilo or one-thousand
M.S.	Master of Science
MW_e	Megawatts electric
NO_x	Nitrogen Oxide Compounds
NY	New York
NYSEG	New York State Electric & Gas Corporation
PCGC-3	Pulverized Coal Gasification or Combustion Code-three dimensions
PCSV	Particle, concentration, sizer, velometer
ppm	parts per million
SOFA	Separate Overfire Air
WDPF	Westinghouse Distributed Processing Family
3-D	Three-dimensional

Abstract

The major objective of this study was to compare test data from a large-scale electric utility boiler (Milliken Station furnace) with predictions from the coal-qualified PCGC-3 combustion code. Additional objectives were to identify and evaluate code submodels and code geometrical input models that yielded appropriate validation comparisons. The contract called for sixteen predicted cases. Twenty-one prediction cases were run, of which twelve are presented in this report. The cases not presented are for the smaller size grid cases (65K nodes) where prediction results indicate that grid independence was not achieved.

Spatially resolved, point-for-point comparisons are presented herein between Milliken Station predictions and measurements for gas composition (CO_2, CO, SO_2, NO_x, O_2), gas temperatures, gas and particle velocities and particle composition. Where available, turbulence intensities are also presented. Probe traverse averages and boiler level averages at the Milliken furnace are also presented for the same variables. Comparisons are presented for the effects of grid size, over-fire air injection point and flow rate, and ignition point variation. Initial particle size distribution was obtained from data and the low- NO_x burner geometry was obtained from construction drawings. Grid density, limited by computational time requirements and ABB/CE proprietary restrictions, did not allow more detailed geometrical modeling of the burner input parameters, though near-field measurements in the burner were made to help alleviate this deficiency.

In general, combustion code computations show acceptable trends with very good point-for-point comparisons in the far-field but less reliable comparisons in the near-burner field. This inexactness in the near-field is attributed to the crude nature of the largest grid (337K nodes), even with variable grid spacing, being unable to represent the construction drawing details in the burner-input region. Lack of geometrical detail of the burner ports configuration, and lack of precise mass distribution information between primary coal/air, auxiliary air, over-fire air, and concentric firing air flow rates are also contributing factors.

The conclusions from this phase ot the study are:

1. Full-scale furnace testing with sensitive laboratory instruments can be successful and internal evaluation of such data gives assurance as to the data's accuracy.

2. A larger number of grid nodes is required for 3-D combustion model solutions to yield adequate predictions for a boiler as large as Milliken Station.

3. The coal devolatilization rate constants (ignition point location model) have a significant influence on the predicted results, especially in the near-field.

4. Far-field comparisons between measured and predicted data are better than near-field comparisons. Analysis suggests that near-field comparisions can be improved with larger numbers of grid nodes and improved code submodels.

5. Trends for important variables like NO_x and carbon-in-ash are correctly represented, but quantitative comparisons can be improved, especially in the near-field.

6. Continued efforts in evaluation of computerized computational methods should yield improved comparison results. Emphasis will need to be placed on improved near-field burner geometric models, turbulence intensity models, grid size effects, and more precise wall heat flux predictions.

These comparison results suggest that computerized predictions of large-scale utility furnaces can successfully be made. This is particularly encouraging considering the vast number of computations that a code must execute without error to accomplish these kinds of predictions.

Introduction

Background

Full-scale power plant testing provides practical process data for evaluation of combustion models and helps to assure that the submodels used in the code are adequate to model the physical processes on a large scale. This is especially true of 3-dimensional (3-D) models under development at ACERC and elsewhere which require increased computing power and more exacting convergence and stability criteria and hence more thorough evaluation using 3-D measured data. The coal-qualified version of PCGC-3 demonstrated good prediction comparisons with the 1991 Goudey Station test data as reported previously (Cannon et al, 1994). The next phase of PCGC-3 validation was to make predictions and measurements for the Milliken Station pulverized coal boiler. The Milliken Station boiler is twice the size of the Goudey Station, with a rectangular boiler cross section and newly installed low NO_x burners. The test data for the Milliken Station were obtained in July, 1995 (NYSEG Report 1995).

Milliken Program

This work was associated with the ACERC/NYSEG contract to test and simulate NYSEG's Milliken Station boiler combustion using PCGC-3. The Milliken contract with NYSEG included cost sharing with NYSEG, EPRI and ESEERCO.

The Milliken Station unit #2, where the testing was accomplished, is one of two near identical plants belonging to NYSEG located on the Finger Lakes near Lansing in New York State. The Milliken units are each designed for 160 MW_e gross load. The boilers are rectangular rather than square in cross-section, and are about twice the size of the Goudey Station tested in 1989 and 1991 by ACERC personnel (see Cannon, et al. June 1992 and Oct. 1995 and NYSEG First Semi-Annual Report, 14 Oct. 1994). The Milliken unit #2 has been fitted with thirteen new, 6" probe ports specifically provided for the ACERC tests and is part of a DOE Clean Coal Technology Program where new low-NO_x burners and a multi-million dollar Flue-Gas Desulphurization (FGD) unit has been installed.

Test Matrix and Instrumentation

Testing at the Milliken Station was patterned after the Goudey Station testing. The final testing matrix was modified to more thoroughly evaluate the newly installed ABB/CE low NO_x burners. The major test variables were coal type, over-fire air, load and burner tilt variation.

Objectives and Approach

Modeling of combustion processes by computer simulation has been a major thrust in ACERC combustion research. One obstacle to efforts at modeling 3-D combustion processes is the lack of definitive validation data from representative large-scale processes (Phillips and Smoot, 1989). A general purpose of this project was to acquire test data at a range of scales that could be used to support and evaluate the computer modeling of 3-D combustion devices over a significant range of different sizes.

In the summer of 1989, ACERC full-scale testing at the Goudey Station, 80 MW_e power plant in Johnson City, New York was initiated in cooperation with the owner utility NYSEG and ASEA Brown Boveri/Combustion Engineering (ABB/CE) and with funding help from ESEERCO. This was a first step in the process of testing at multiple-scale levels with a mobile testing trailer equipped to carry the instruments and probes necessary for remote testing from BYU. In July 1991, BYU returned to the Goudey Station for further testing on the same boiler that had been reclad and redesigned with a new super-heat/re-heat section. The Milliken Station Project was a continuance of that program with a doubling of plant scale and a more advanced burner system. This final report is the culmination of a series of reports delivered to NYSEG by contractual agreement that include the Field Measurement Report (NYSEG 1995) and the Comparison Report (NYSEG 1997).

Instrumentation was designed to gather data at strategic locations to not only support validation of combustion models, but also to refine the computerized combustion model program inputs. The long-term goal of comprehensive combustion modeling has been to develop validated programs that adequately simulate combustion in small, lab-scale burners as well as full-scale utility boilers. To fit this broad scale size range (10^6), ACERC has saught to validate submodels and the overall code at different combustor scale levels as shown in Table 1.

Table 1. Burner scales at which PCGC-3 validation is addressed.

	Scale	Furnace Heat Release Rate	Test Locations
1.	Lab Scale	~0.01 - 0.1 Million BTU/hr	-at BYU/CPR
2.	Pilot Scale	~2 - 4 Million BTU/hr	-BYU/CPR, FPTF, & Consol Reactors
3.	Small Scale Utility Boiler	~70 - 700 Million BTU/hr	-Goudey Station, NY
4.	Large Scale Utility Boiler	~1000 - 7500 Million BTU/hr	-Milliken Station tests

It is anticipated that in the absence of commonly accepted scaling laws for combustion, the computer modeling programs will become the most likely scaling mode

for combustion processes. This is particularly true for the large-scale, low-frequency, turbulent eddies that are a major factor in the time-space scales in combustion processes described by PCGC-3.

Anticipated Products

Error! No table of figures entries found.

The anticipated products of this test program were two-fold. The tests were intended to evaluate the capability of comprehensive codes for large-scale boiler simulation. Once validation is well along, the combustion codes can be used to improve the operation and upgrading of existing power plants as well as provide guidance for future power plant designs and pollutant retrofits. Thus, the key product from this phase of the effort is a documented assessment of 3-D combustion code reliability in predicting furnace behavior.

Results

Test Conditions

The Milliken experimental data set covers gas composition (CO, CO_2, SO_2, NO_x, O_2), gas temperature, particle elemental composition (C, H, N, S), particle size distribution (both gathered samples and in-situ measurements), particle velocity and concentration measurements, gas velocity for 2-D directional measurements, along with turbulence intensity and power spectral decomposition. The measurements were extracted from the Milliken Station 160 MW_e boiler during steady operation of the station. The test matrix covered five different steady-state tests that included two coal types, two different loads, and three over-fire air (SOFA) configurations as noted in Table 2.

Tests 1 and 3 were conducted to evaluate the effects of coal type on the furnace flow field. Tests 4 and 5 were conducted to evaluate the effects of SOFA injection variation with test 3 serving as a mid-point verification that represents normal plant operation.. Tests 2A, 2B and 2C were conducted to evaluate the effects of burner tilt and load at port 3e2 for gas composition. Other ports were used for gas temperature, particle size, and gas velocity. Test 2 was an abbreviated test where probes remained at a single port during the entire test time. The test data were gathered at five different boiler levels and nine-6 inch ports distributed about the furnace as noted in Figure 1. Half of the data was gathered in the near-field, the other half above the fire-ball, near the nose, and into the entrance of the convective pass. The raw data have been compiled and reported in a single report without analysis (NYSEG 1995) and in three theses with analysis (Groberg,T., 1996, Groberg, C., 1996 and Brooks, B., 1997.)

Table 2. Milliken Test Parameters

Test	1	2A	2B	2C	3	4	5
Gross Load (MWe)	156	**132**	**155**	158	157	156	157
Net Load (MWe)	147	123	145	148	147	146	146
Coal Feed (t/hr)	55.3	46.1	54.8	54.8	55.6	53.3	54.7
Excess Air (%)	3.9	3.9	4.0	4.1	3.9	3.9	3.7
Tilt (degrees)	- 5	- 5	**- 5**	**+ 5**	- 5	- 5	- 5
SOFA (% open)	40	40	40	40	**40**	**0**	**100**
Coal Type	**B**	C	**C**	C	**A**	A	A

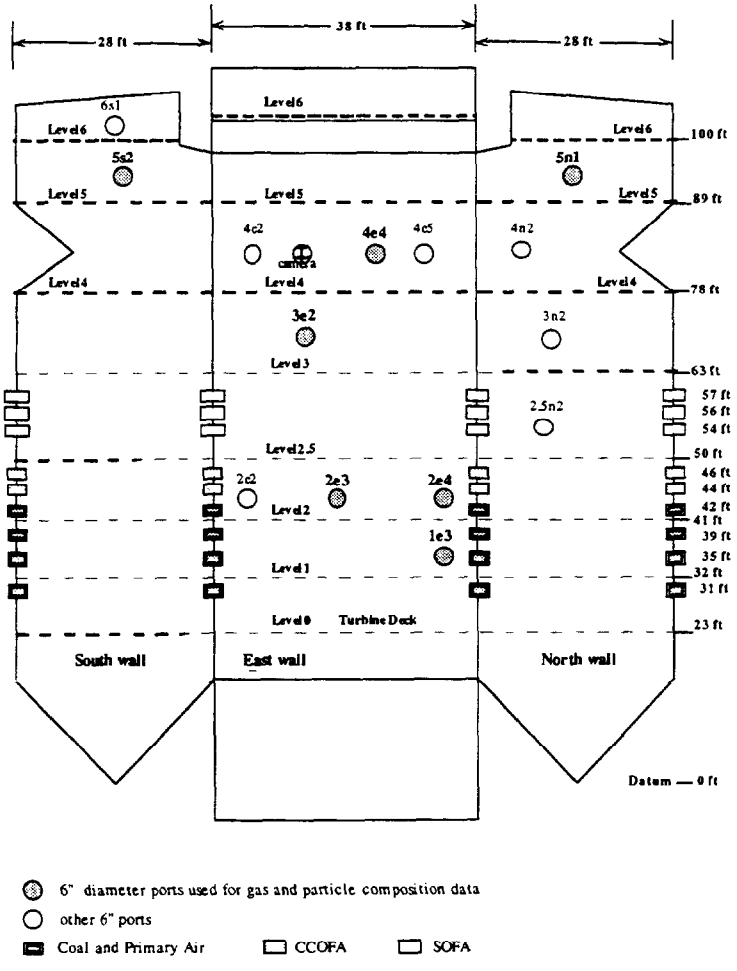

Figure 1. Schematic of Milliken furnace and access ports

Prediction Schedule and Conditions

Comparisons of the measurements to computerized predictions have been accomplished for 12 different cases as noted in Table 3. An additional nine 3-D code computations were completed as a part of this effort toward producing this set of twelve acceptable solutions. These comparisons have identified areas where improvements are required in the computational grid input conditions, physical constants in the various submodels, and grid resolution.

Table 3. Simulations on PCGC-3 to Predict the Milliken Furnace Properties

Case number	Grid Size	Milliken Test No.	Devolatilization activation energy constants	Minimum residual achieved	Enthalpy balance (%)	Mass balance (%)
1	192K	3	Ubhayakar 1976	3.5	-5.0	0.01
2	192K	4	Ubhayakar	4.4	-5.9	-0.20
3	192K	4	1.2*Ubhayakar	3.8	-8.0	-0.16
4	337K	3	Ubhayakar	4.3	-7.2	-0.79
5	337K	4	Ubhayakar	4.6	-5.0	-0.19
6	337K	4	1.2*Ubhayakar	4.1	-5.2	-0.24
7	192K	3	1.2*Ubhayakar	4.1	-6.2	-0.05
8	192K	5	1.2*Ubhayakar	3.9	-4.5	-0.03
9	65K	3	Ubhayakar	3.7	-11	-0.27
10	337K	5	1.2*Ubhayakar	3.4	-3.3	-0.01
12	337K	3	1.2*Ubhayakar	3.2	-2.7	-0.02
13	192K	5	Ubhayakar	4.5	-6.1	-0.03

All cases had a constant wall temperature boundary condition of 1160 F (900 K). Since the exact wall temperature was not known, this was used as an estimate; however, the bulk of the predicted temperatures agreed well with the measured values as can be seen from the data reported in the Appendix.

The convergence criteria for the twelve cases as noted in Table 3 are a) the maximum of the minimized residual values, b) acceptable enthalpy balance, and c) acceptable mass balance. In all 12 cases, the computations were allowed to continue until the convergence criteria bounds were met and the average of the iteration variation changed very little as noted in Figure 2. Time is noted in the upper right corner as a bench mark to aid the operator in tracking the convergence progress. In Figure 2, the case noted is not yet converged as the convergence bounds on the mass and enthalpy error had not yet been met, though the maximum residual and the wall radiation and convection seem to be changing very little. In some cases, convergence for the 65,000 node cases could be accomplished within a week. For the 337,000 node cases, over a month of computer time was typically consumed for each separate case. Convergence of a modeled computer case requires practical experience and often involves stopping a case to change a parameter, or reset a parameter once variation of other parameters have settled down, etc.

The finite nature of a numerical solution can be expressed with grid size. For example, a laboratory-scale experiment using a 20,000 node grid can be used to model a 50 cubic foot region with a very fine grid, with grid independence achieved. In this Milliken modeling effort, a 337,000 node grid was the largest practical grid size used to model a 126,000 cubic foot region and full grid independence was not necessarily always achieved. Compared to the physical burner geometry, the numerical grid pattern models noted in Figure 3 are crude and while the mass flows, velocity directions and areas were reliably modeled, the velocity magnitude and location were less precisely modeled due to lack of exact burner dimensions and correlative damper settings. This lack of precision tends to make near-field validation comparisons less precise as will be noted later.

The point-for-point comparisons between measurement and prediction, along with selected averages by boiler elevation are contained in some 700 graphs in the noted theses (Groberg,T., 1996, Groberg, C., 1996 and Brooks, B., 1997) as well as in this NYSEG comparison report. The detailed results of the 12 predictive cases are stored in the ACERC CCL computers and if printed out would exceed 20,000 pages of data. The Appendixes of this report contain a nearly complete set of comparison figures that are summarized in the following discussion.

Comparisons between Measurements and Predictions

In the overall Milliken study, there were two major objectives. First, the data were to be obtained and their accuracy assured (see Groberg, T., 1996). Secondly, these data were to be compared with model predictions from the PCGC-3 model (Groberg, C., 1996,and Brooks, 1997). A comparison of predictions with measured values on a point-

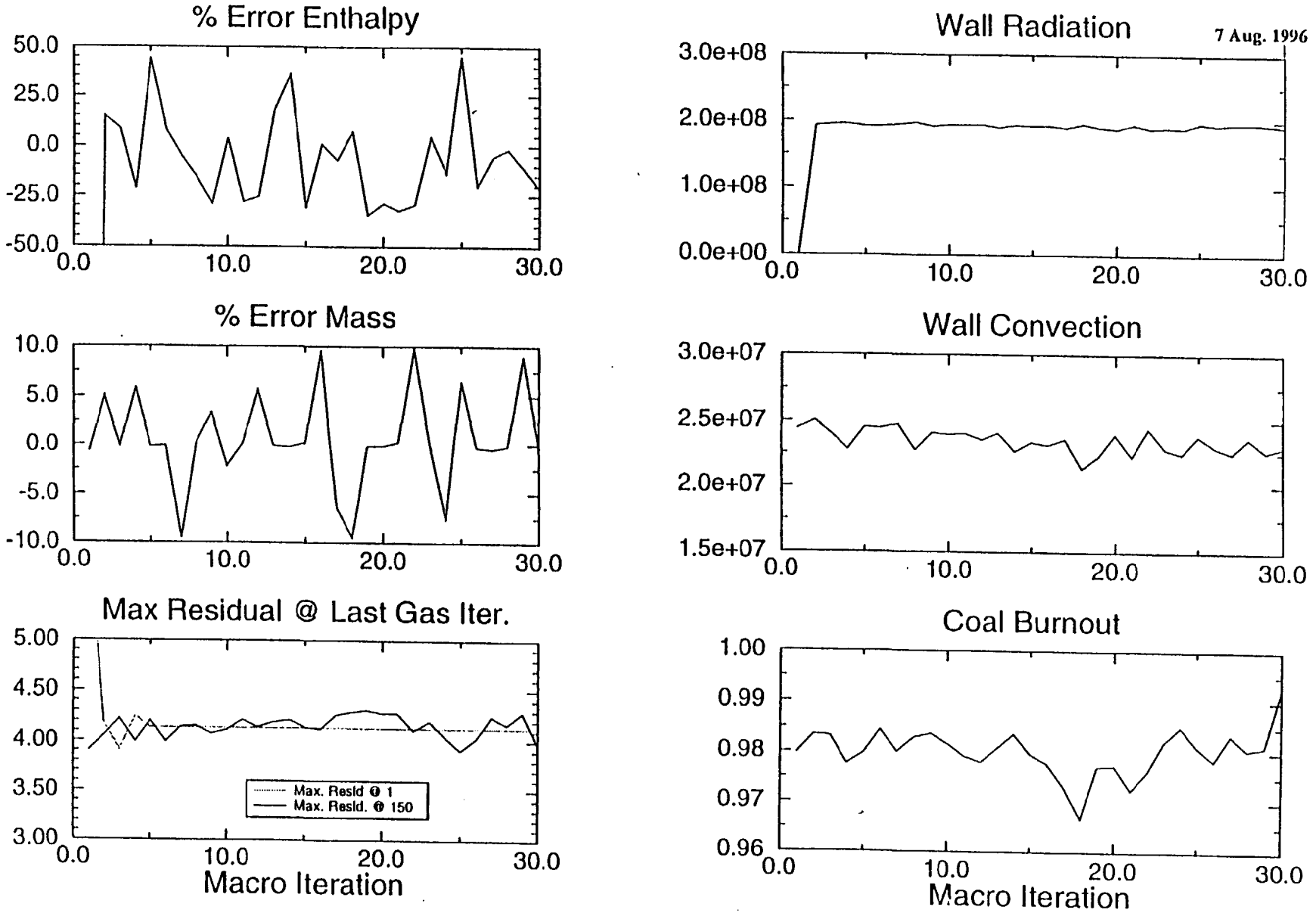

Figure 2. Milliken case convergence criteria (Test 3) with 192K grid and high turbulence.

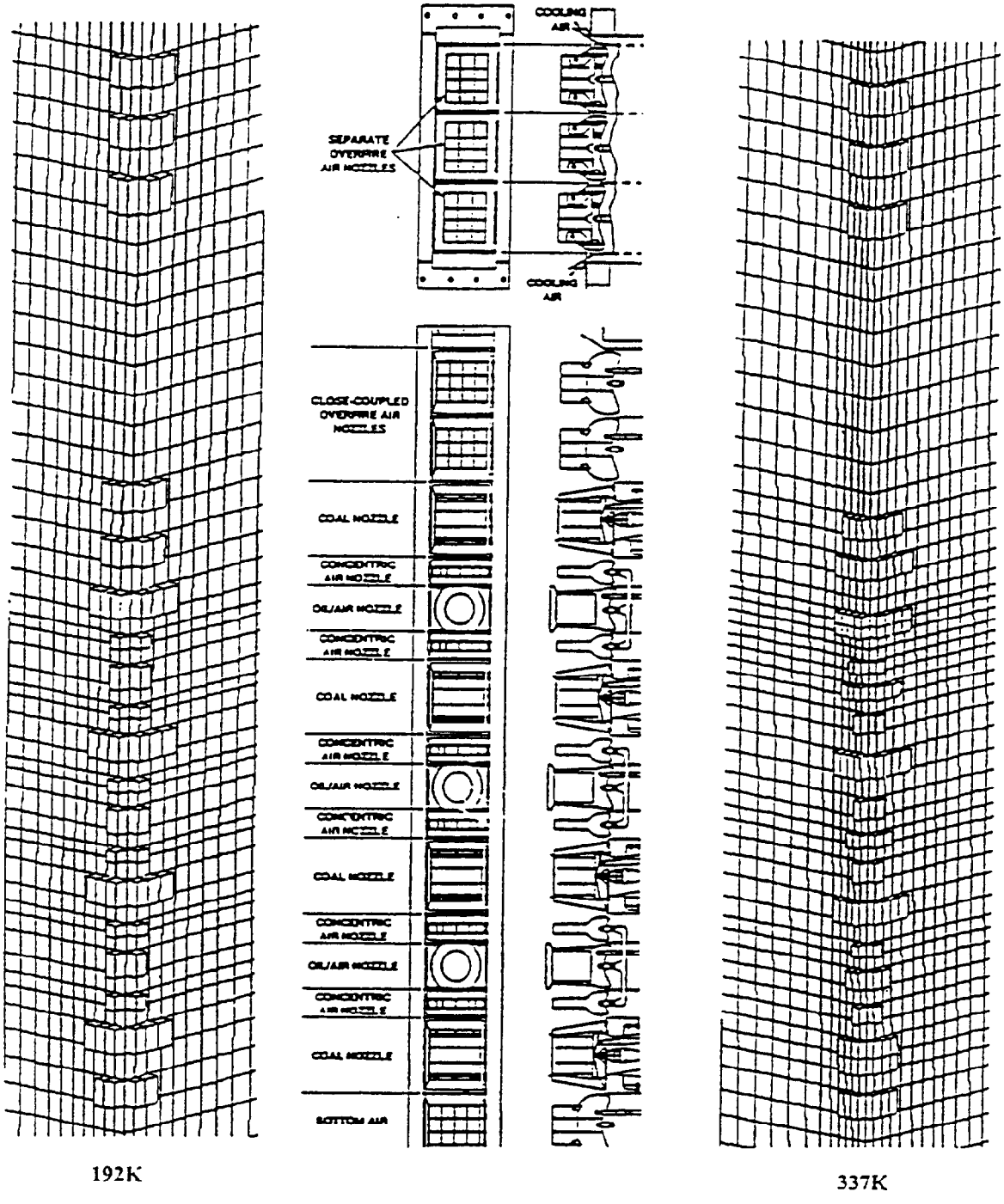

Figure 3. Burner inlet compartments sketch compared to 192K and 337K grid models.

for-point basis as well as at probe traverse level averages and furnace level averages, yield substantial insight into the PCGC-3 computer code modeling capability for a medium-scale, corner-fired coal furnace. Examples of point-for-point and averaged data are shown in Figures 4 and 5. What follows is a summary of some of the conclusions that can be drawn along with illustrations used to support these conclusions. All of the comparisons are contained in the Appendixes and are segregated by mode of comparison.

Figure 4 illustrates the point-for-point comparison between measured data and model predictions for three different grid sizes at level five in the far-field where the better comparisons typically resulted. The example shown is for Test 3 (normal plant operation). In three of the six graphs (temperature., NO_x, and CO), the 337K grid comparison is best. In the other three (O_2, SO_2, CO_2) the 192K grid comparison is the best. In general, the 337K predictions are better than the 192K predictions, both of which are usually better than the 65K predictions (See Appendix A).

An overall comparison can be shown where each port profile is averaged by port and plotted vs. the axis of the boiler. This type of comparison is depicted in Figure 5. Here again, the 337K grid prediction data best fits the measured data (though not perfectly). In order to bring quantification to this comparison process, Figure 6 has been constructed. In Figure 6, the % difference between point-for-point measurements and predictions is noted for each grid size. Figure 5 compares port profile averages, whereas Figure 6 shows the average of the point-for-point differences and is therefore a more stringent validation condition than is Figure 5 besause the profile shape is a factor. Comparisons of the type in Figure 6 are particularly valuable as they provide a means to quantify changes in boundary conditions and/or submodel improvements as the computer cases are exercised and converged.

Figure 6 shows three significant items. First, it is notable that the 337K grid is generally the best. Second, the comparison improves as the flow proceeds toward the top of the furnace. Moving from the near-field to the far-field generally improves the quality of the predictions. This is partially explained by the crude nature of even the large 337K grid in geometrically modeling the input configuration of the burner as noted in Figure 3. Thirdly, the CO difference comparison in Figure 6 shows very large numbers. Initially this would appear to be poor comparison, but Figure 5 provides the explanation. Where the large differences occur, the measured values are close to zero, resulting in an exaggerated % difference with the near-zero division. This is further complicated by the extremely large gradients in the CO field, changing by a factor of four orders of magnitude with one floor level (see Figure 10). This substantial gradient strains the ability of the CO measuring instruments, where two separate electro-chemical cells had to be used, one for a range from 0-2000 ppm and another for range from 2000 ppm to 100,000 ppm. Thus, in order to avoid misunderstanding, the numerical scale on all CO difference figures has been removed. The Figures thus show relative differences only.

Another factor that contributes to these near-field comparison interpretations is noted in Figures 7 and 8. In Figure 7, the comparison is made between the measured and predicted turbulence intensities, which tends to drive the mixing processes in the burner

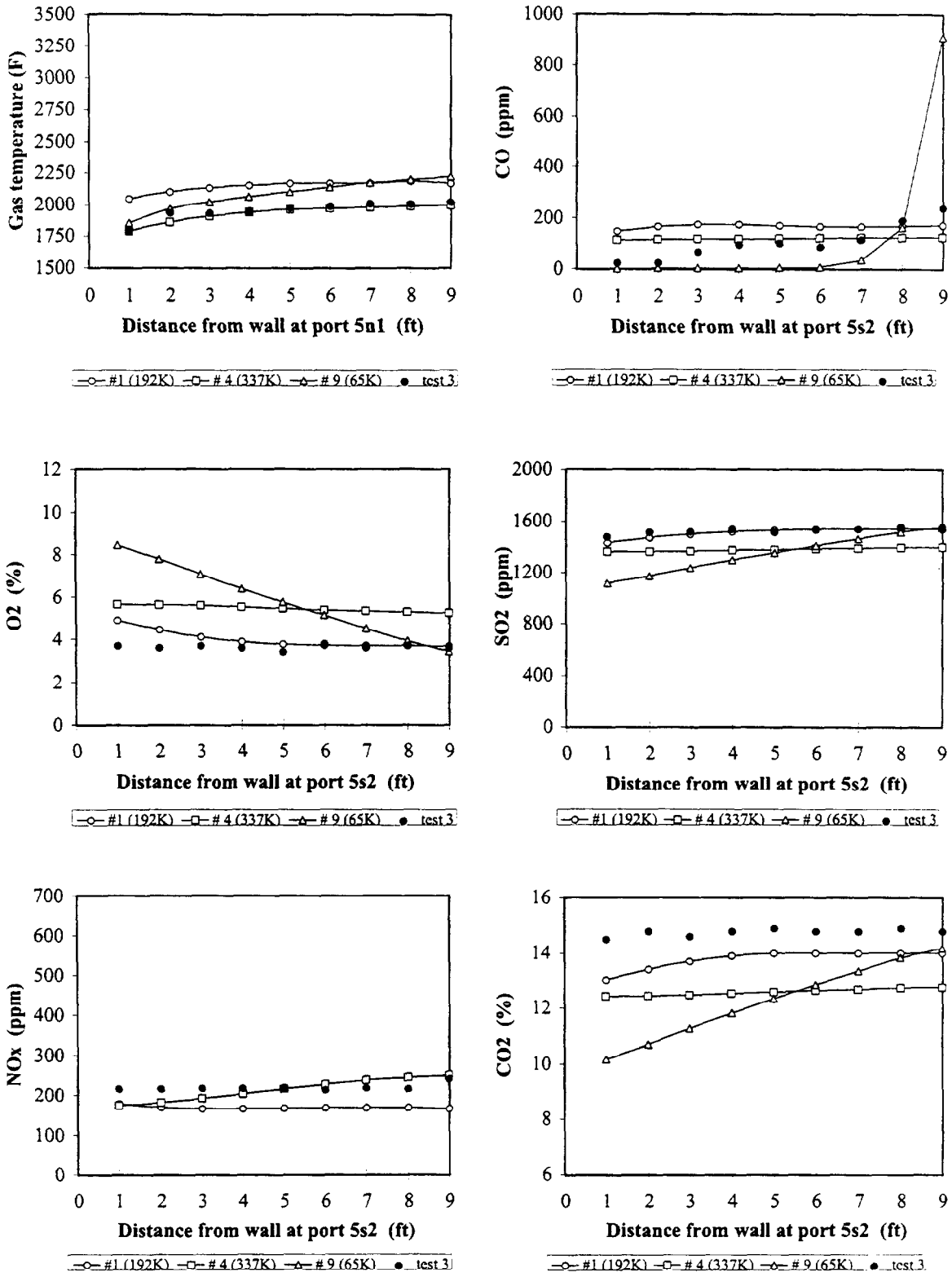

Figure 4. Comparison of probe measured and predicted traverse values for cases 1,4 and 9 of Table 3 at level 5 for various grid sizes.

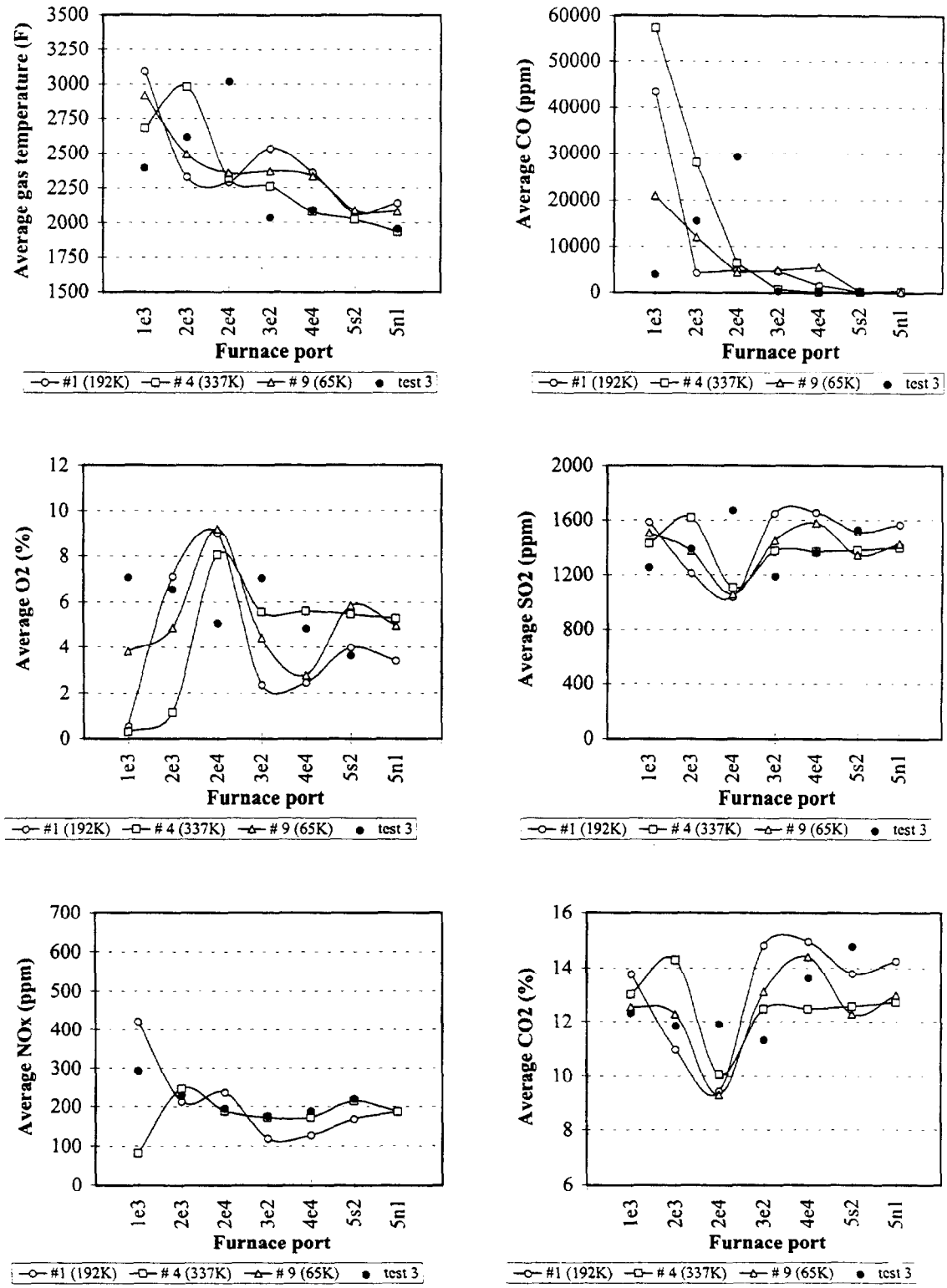

Figure 5. Comparison of average measured and predicted vertical values for cases 1, 4 and 9 for various grid sizes.

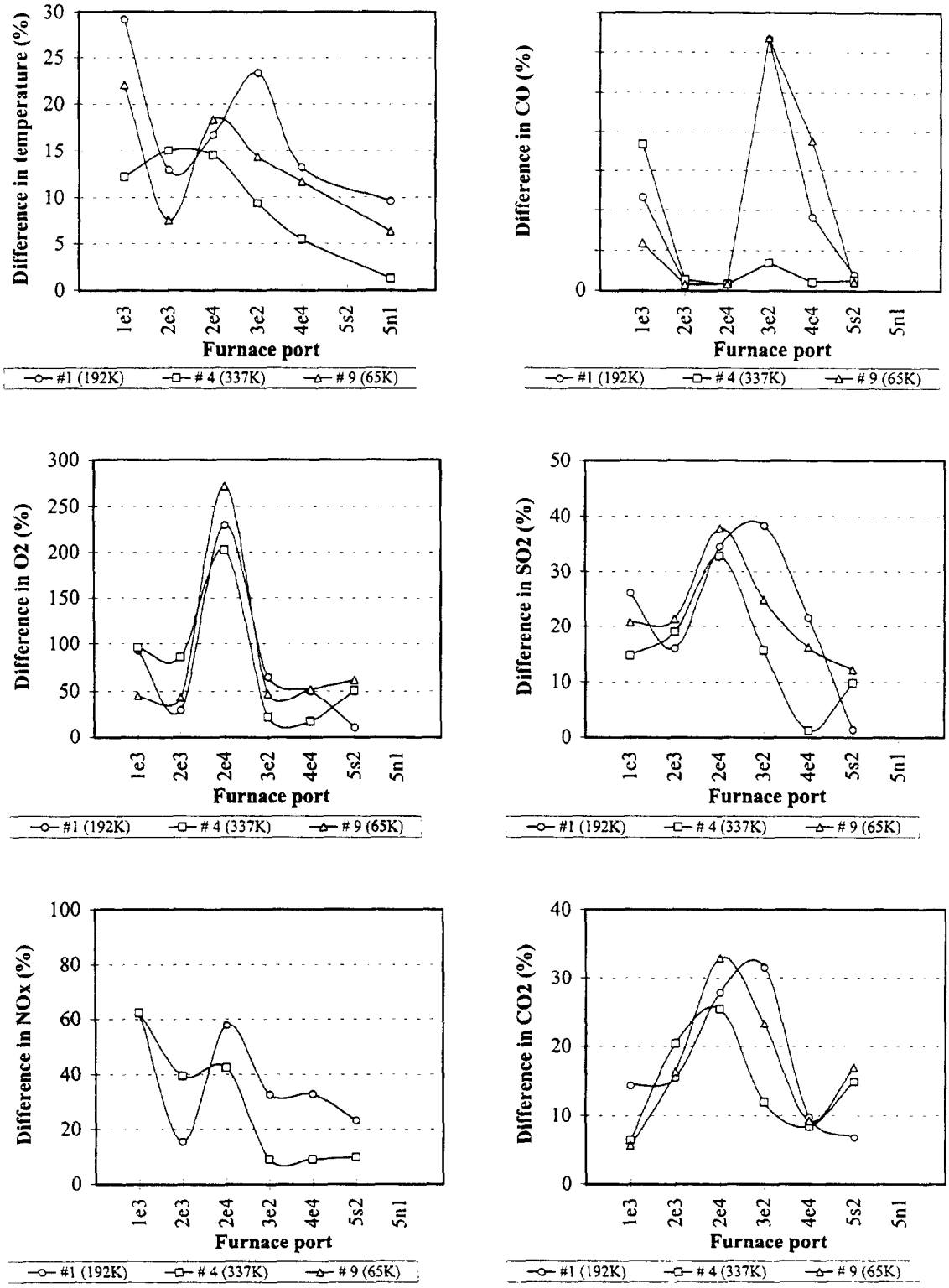

Figure 6. Percentage difference between predicted and measured average values at various boiler heights for cases 1,4 and 9 of Table 3.

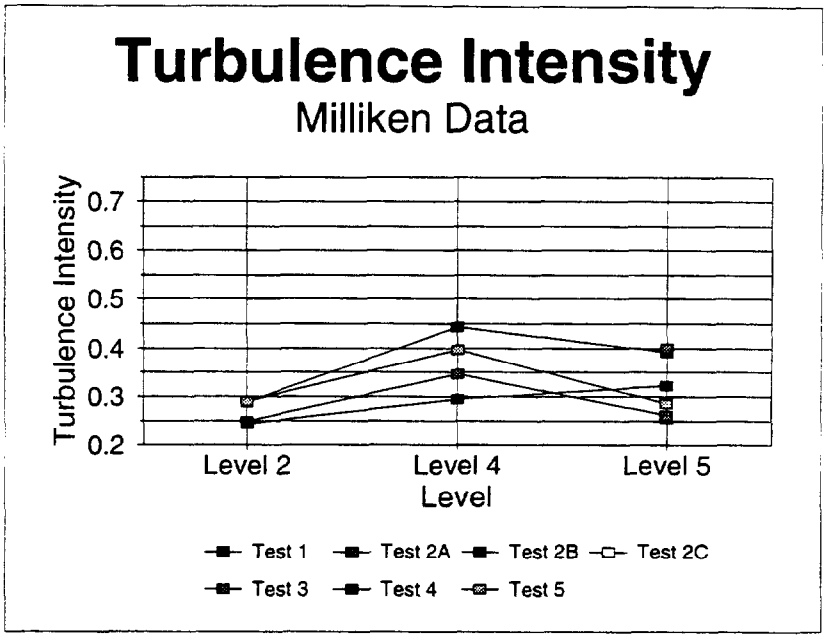

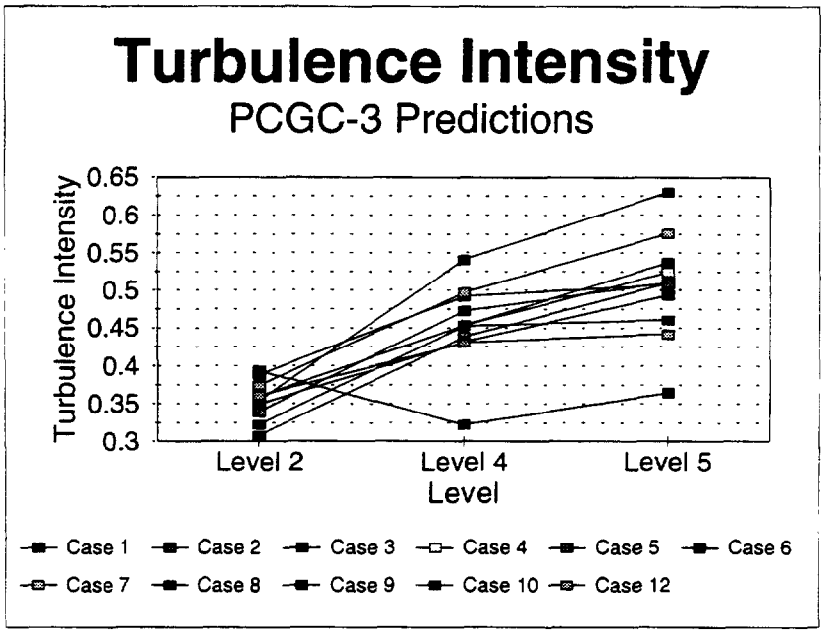

Figure 7. Average measured and predicted turbulence intensities for eleven predicted cases and seven tests for three boiler levels.

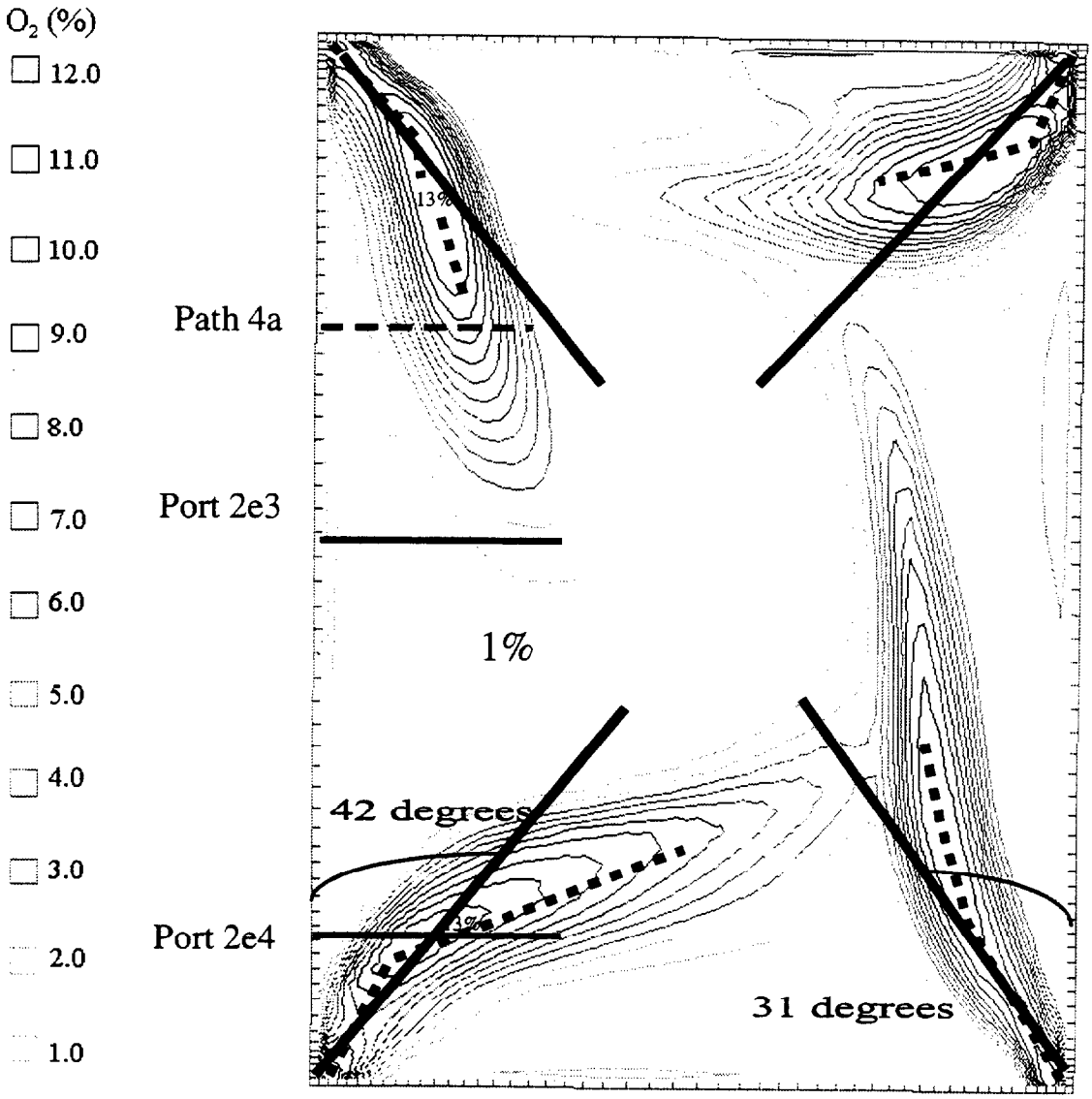

Figure 8. Overlay of burner orientation (straight solid line) on meandering predicted path of O_2 predictions (dotted line) at level 2.

region. In most cases, the predicted turbulence intensities (derived from the k value in the turbulence k-ε model) are larger than the measured values by as much as 1.8 times. Thus, the fluid mechanics of the near-field are not exactly simulated. This is further illustrated in Figure 8 where the predicted O_2 flame contours from the close-coupled over-fire air inlet (CCOFA) are viewed from above at level 2. The measured O_2 data (Figure 9) suggests an unbounded O_2 burner jet whereas the predictions show a displaced and meandering O_2 jet, indicating a strong fireball vortex with some interference from the opposite corner O_2 jet (see also Figure 8). This kind of analysis lends insight as the modeler evaluates how to achieve the best geometric burner models to simulate new or different furnace configurations.

Ignition Point Effects (Test 3)

Another factor that influences the near-field fluid mechanics is the ignition point of the coal-air stream. This is varied by adjusting the devolatilization rate constants and is illustrated in Figure 10. (Adjusting the devolatilization rate constants is not unrealistic as the original constants were derived from single particle drop-tube furnace data (Ubhayakar 1976) whereas an industrial burner is more nearly imitated by particle cloud data and seems better simulated with the revised constants.) These devolitilization rate constants are referred to herein as "old" (original) and "new" (revised) values.

Figure 10 is also a comparison of the original vs. revised devolatilization rate constants averaged over the port traverse for data from test 4. In general, the revised devolatilization rate constants seem to fit the measurements best, though the change in devolatilization rate constants is not seen as the major overall effect, having the strongest influence in the near-field.

NO_x and Carbon Burnout Effects (Tests 3, 4, & 5)

Two of the measurements that are particularly important to an electric utility are NO_x and carbon-burn-out. Table 4 has been constructed to evaluate the No_x.

Table 4. Comparisons of Measured (tests 3,4,5)and Predicted (cases 3, 4, 6, 7, 8, 10) for Outlet O_2 and NO_x Concentrations with Overfire Air Variation

Case	Measured O_2 (%)	Predicted O_2 (%)	**O_2 Diff. (%)**	Measured NOx (ppm)	Predicted NOx (ppm)	**NO_x Diff. (%)**	SOFA NO_x Test condition
337K							
4	3.8	5.0	**32**	220	203	**7**	3, Base
6	4.6	4.4	**4**	250	367	**47**	4, High
10	3.4	5.8	**41**	170	127	**25**	5, Low
192K							
7	3.8	4.0	**32**	220	880	**280**	3, Base
3	4.4	3.8	**36**	250	444	**78**	4, High
8	3.4	3.0	**12**	170	216	**27**	5, Low

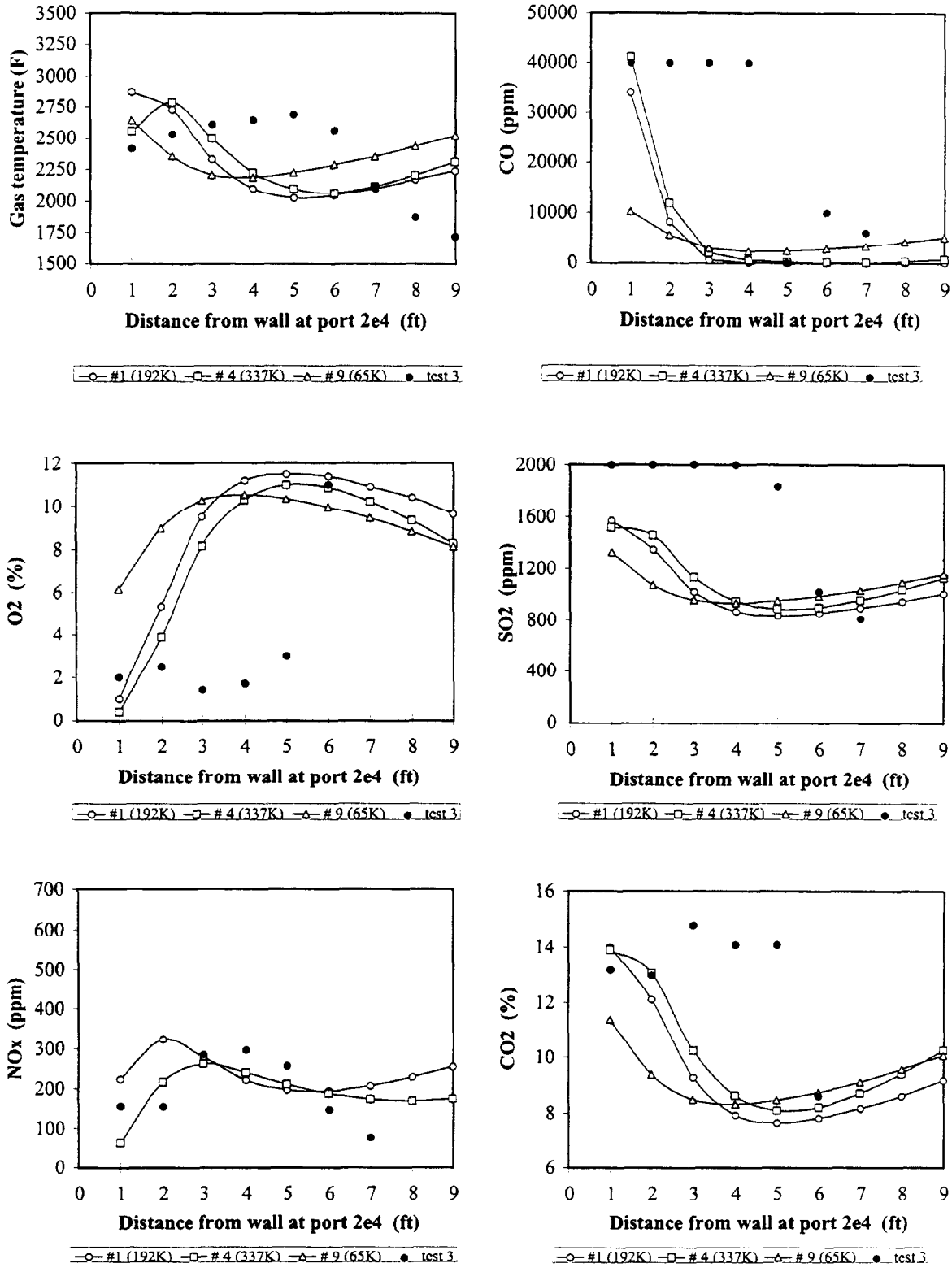

Figure 9. Comparison of measured test 3 and predicted cases 1,4,9 at port 2e4 for various numbers of grid nodes.

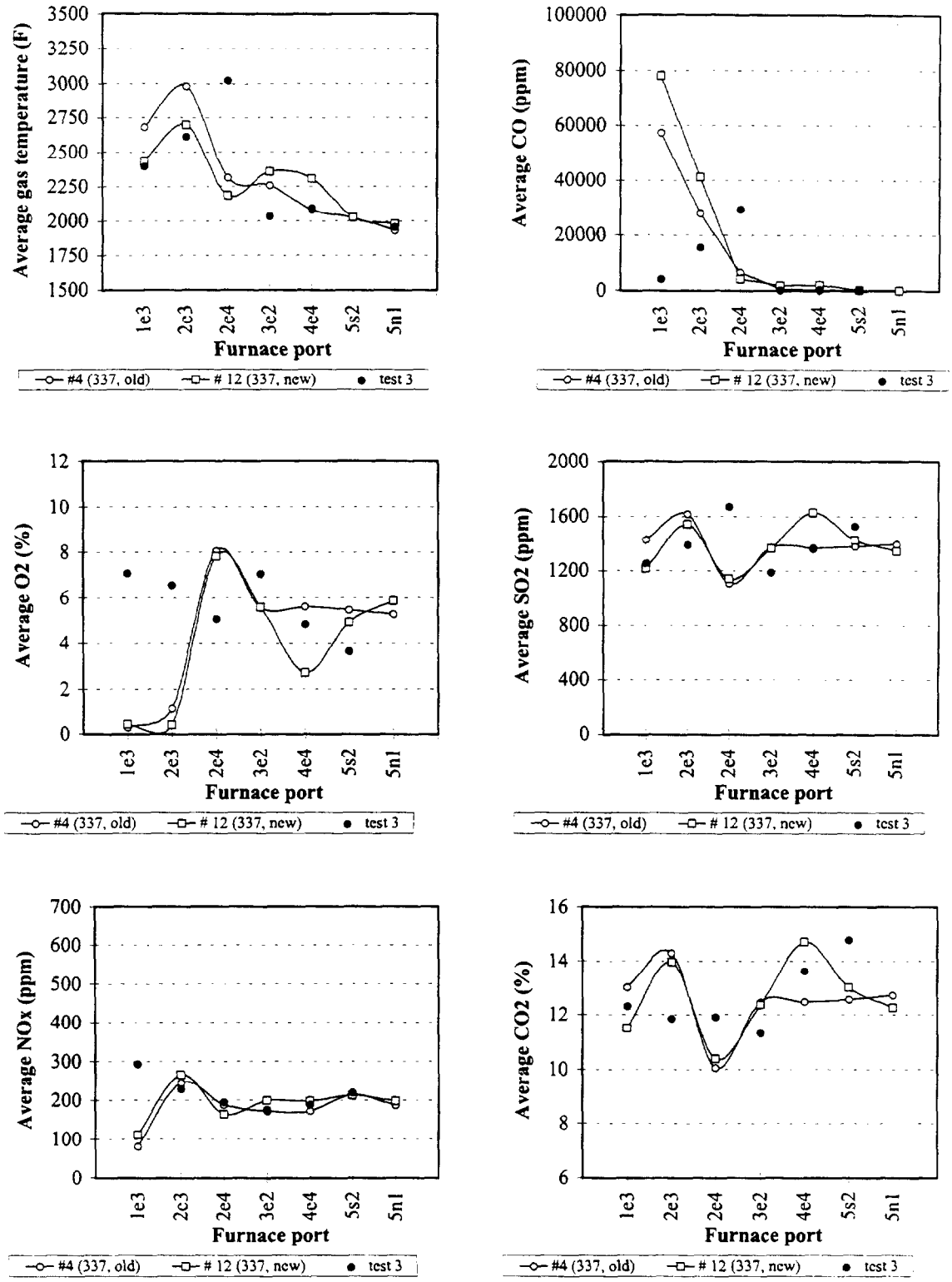

Figure 10. Comparison between averaged measured and predicted values for test 3 contrasting the effects of the original and revised devolatileization constants.

In Table 4, the effect of separate over-fire air on NO_x and O_2 has been constructed from predicted and measured probe traverse averages and vertical exit plane averages. The comparisons show that the 337K grid data are better than the 192K grid data and that the trends are predicted and the absolute numerical values are typically within an error band of 30% for the measured data.

A similar result is illustrated in Figure 11 for burnout and carbon-in-ash, where level 4 has both predicted and measured data. Figure 11b is plotted as "carbon-in-ash" which is used by plant testers vs. "carbon burn-out". While both quantities relate to the same measurement, it is clear that the carbon-in-ash is the more sensitive method of illustrating the carbon burnout data and gives a distinguishable difference in parameter effects on carbon burnout. Agreement is quite good though the computerized sub-model used for carbon burnout can be refined by more advanced sub-models. As such, future improvement is expected in the carbon burnout comparisons.

Near-field Comparisons (Test 4)

Figure 12 shows predicted O_2 contours in the near-field for test 4. Near-field comparisons are shown with Figure 13 where prediction/measurement comparisons are made for test 4 adjusted to match the measured and predicted locations of the high gradients that exist in the near-field (i.e., traverse of port 2e3 (case #6) vs. traverse path 6a (case #6a) in Figures 12 and 13, corresponding to about a 5 foot location adjustment). The new location (case #6a) fits the measured data better than the case #6 prediction at the physical port location as noted in Figure 13. This illustrates the near-field problem where point-for-point numerical comparisons, while not exact, do have similar gradients and appropriate bounds when adjusted for gradients being shifted due to burner input modeling and alignment inaccuracies. This further illustrates the need for better geometrical modeling of the burner where the models used are crude due to the course grid and withholding of proprietary information. Also, using the inlet areas taken from the construction drawings yields too high near-field velocities. Figure 14 illustrates that, while burner areas and mass flows have been used to model the burner input data, some of the predicted velocities (case 12) in the near-field are too high compared to the measured data (test 3). Improved geometric modeling of the burners with finer grids and more accurate burner dimensions may improve near-field prediction differences with measured values. Reducing the inlet velocities will tend to decrease the predicted relative turbulence intensities thus improving the comparison. This geometrical input problem arose when ABB/CE indicated they could not supply exact burner geometrical data for proprietary reasons. Also, the non-linear correspondence between the damper settings and the mass flow rates were not made available.

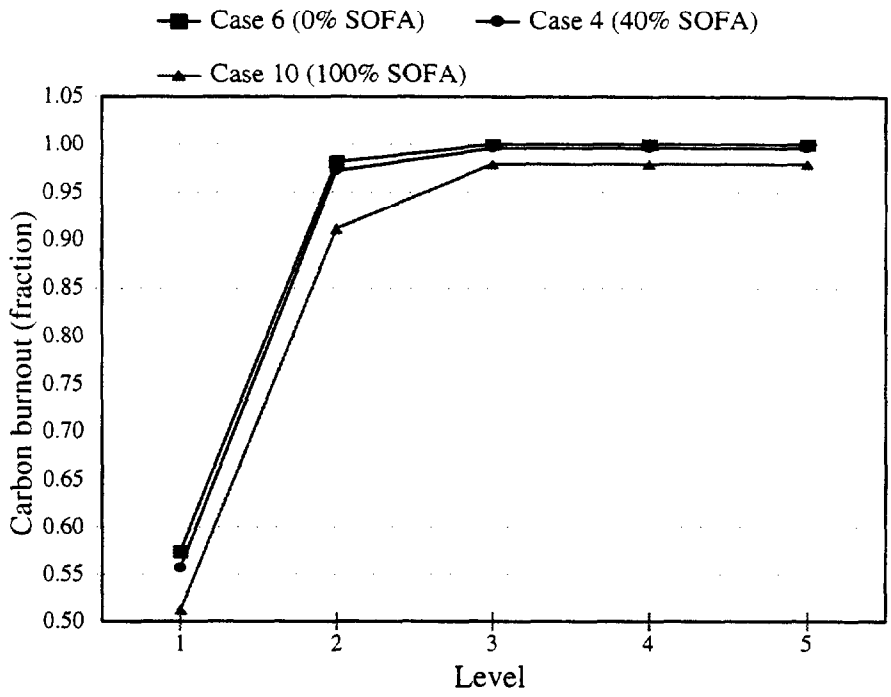

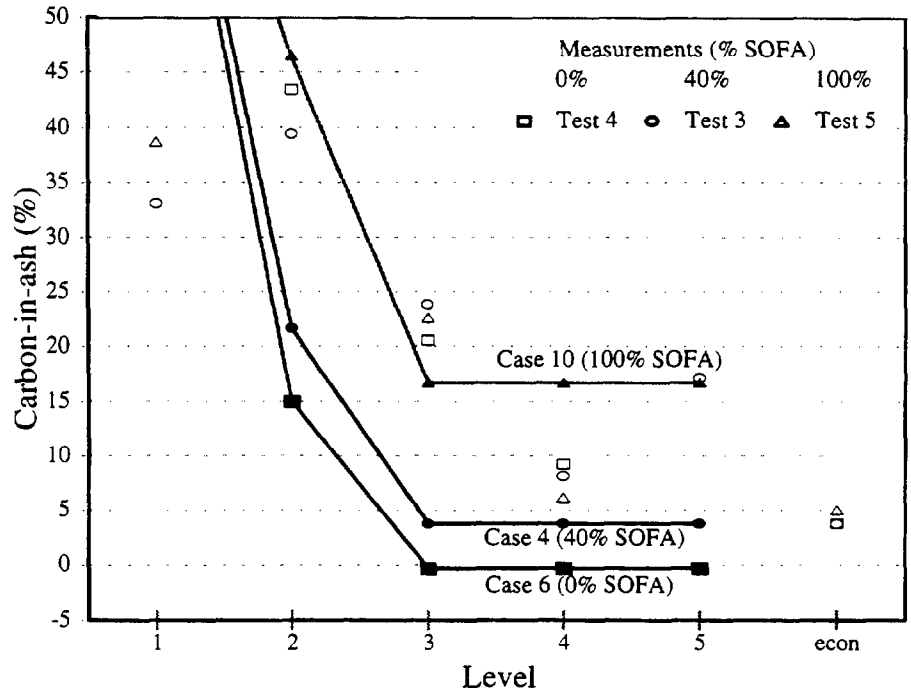

Figure 11(a above & b below). Average predicted and measured carbon-in-ash percentages by boiler level for cases 6, 4 and 10 (337K grid) with measurements from tests 3,4,5.

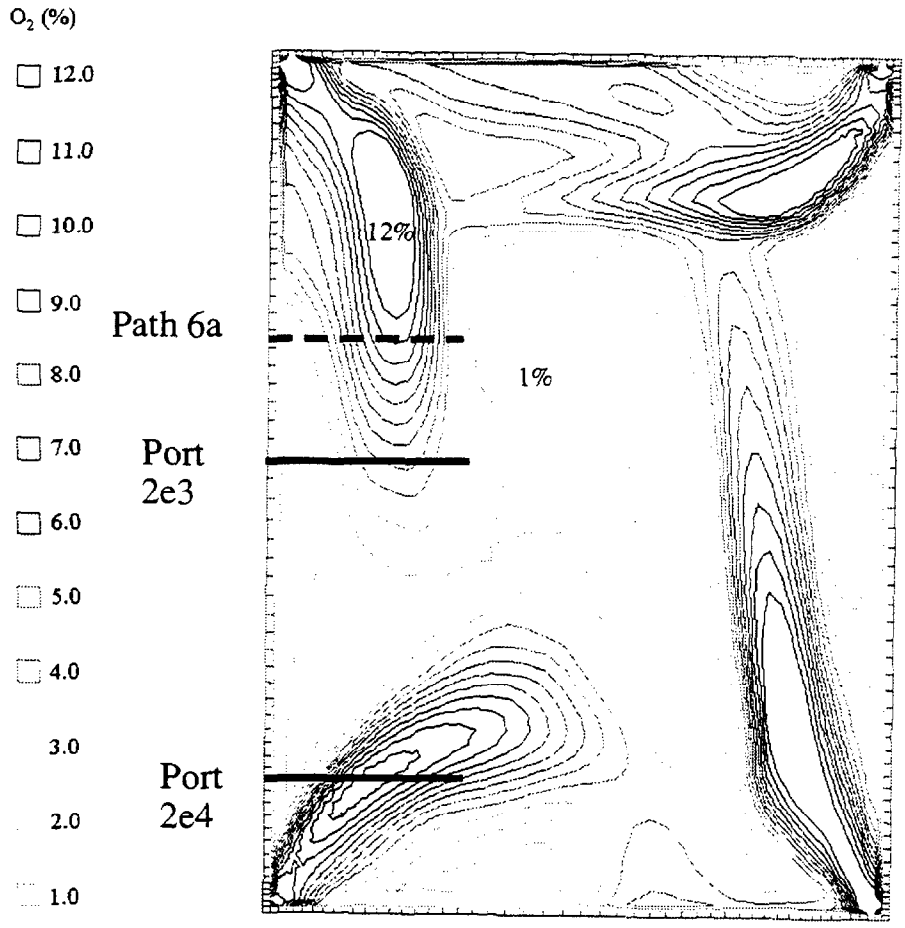

Figure 12. Top view of the O_2 near-field demonstrates the large gradient effect of 5 feet of position change on O_2 (i.e., between dashed and upper solid line) at level 2.

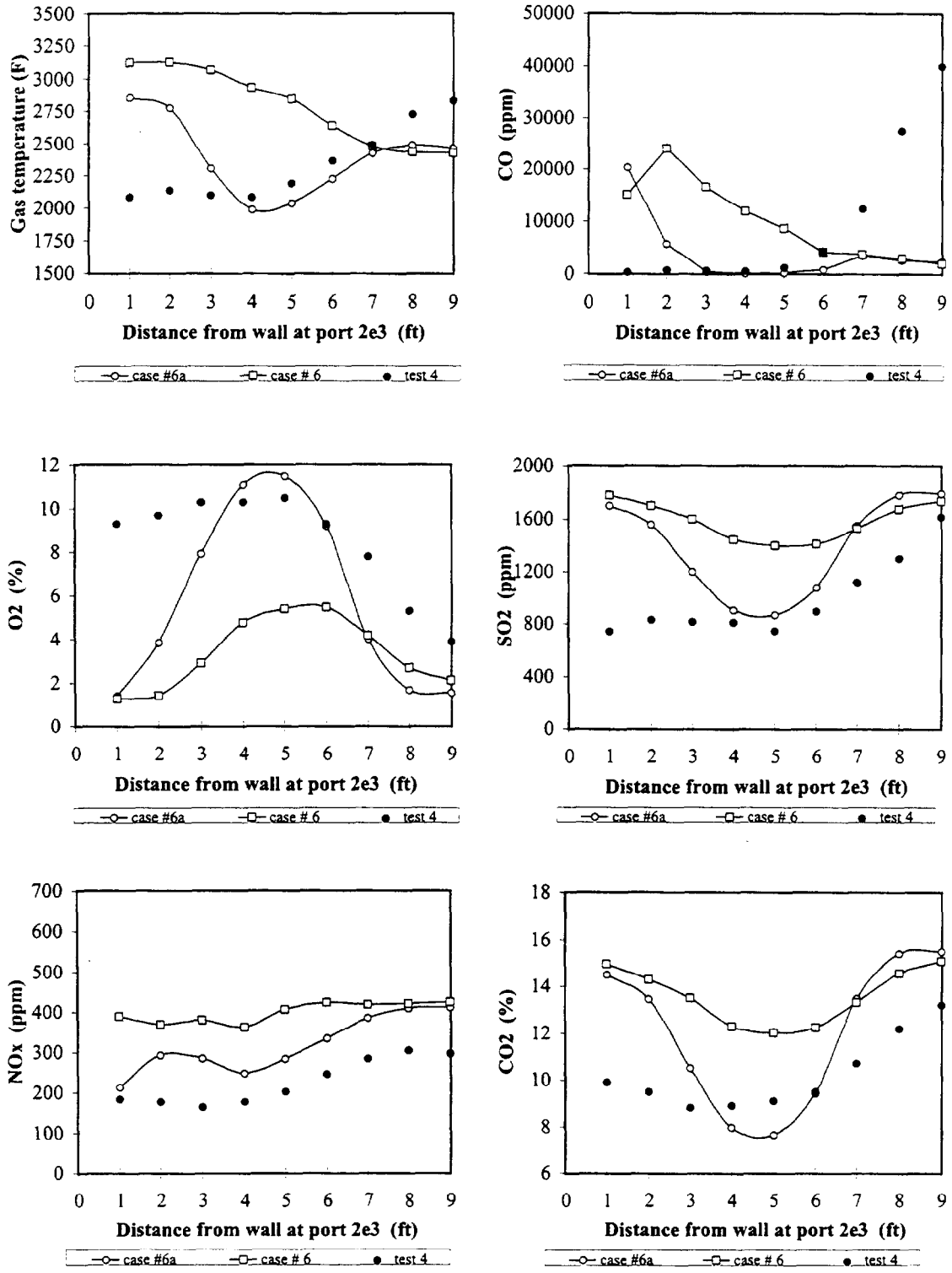

Figure 13. Illustrates the near-field effects of original vs revised devolatilization rate constants compared to measured probe traverses at level 2 on the six noted variables.

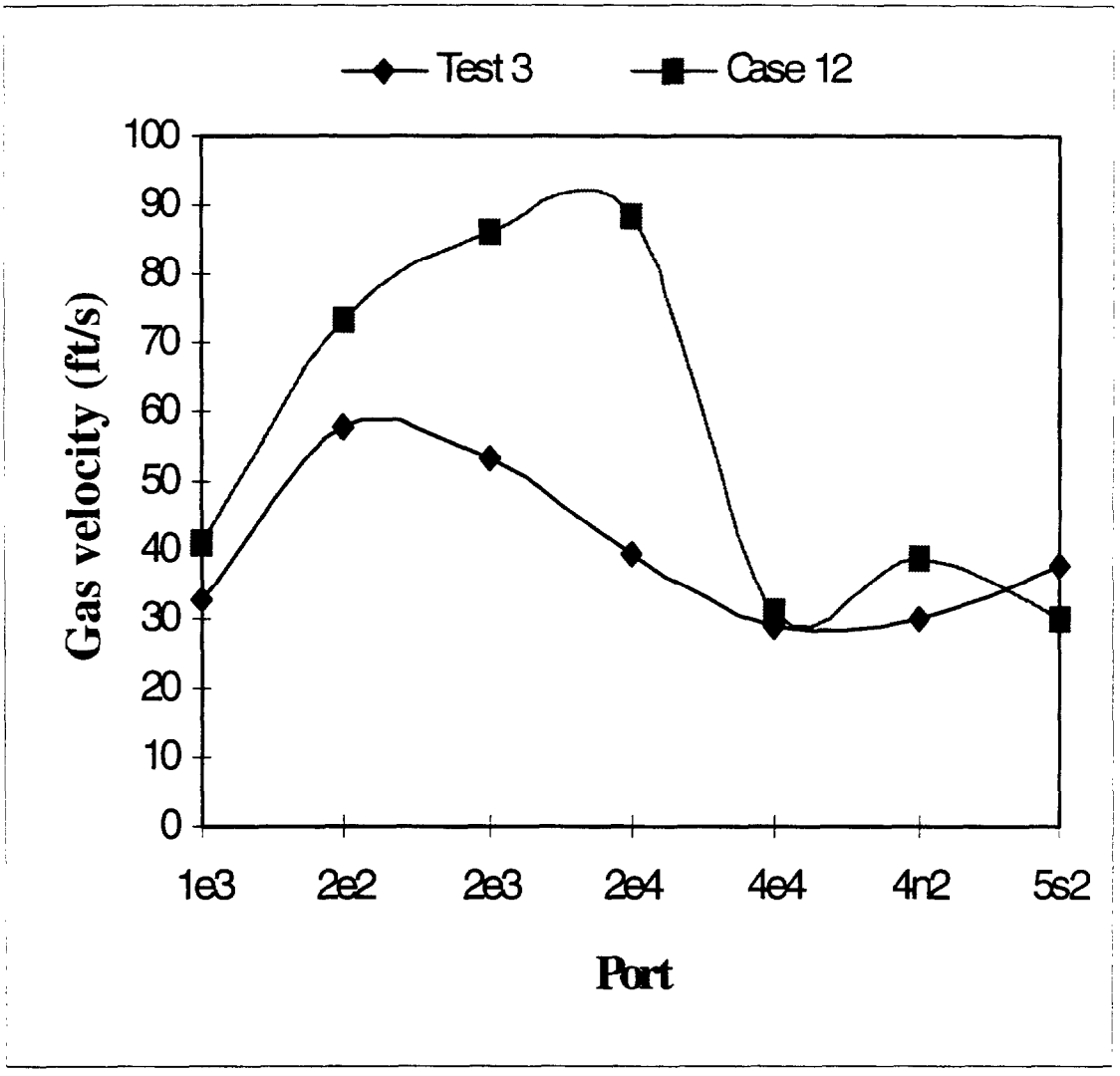

Figure 14. Comparison between test 3 average measured and predicted in-plane gas velocities (337K grid) by port and ordered by height.

Far-field Comparisons (Test 5)

In Figure 15, the far-field effects are shown for test 5, along with the effects of grid size. The larger grid number gives the better results and predicted NO_x values straddle the measured values and trends are correctly predicted. It should be noted that in the far-field (Figure 15), the differences between measured and predicted values are smaller than in the near-field (compare Figure 5 and Figure 6).

Conclusions

1. Full-scale furnace testing with sensitive laboratory instruments can provide useful data and internal evaluation of such data gives assurance as to the data's accuracy.

2. A larger number of grid nodes is required for 3-D combustion model solutions to yield adequate predictions for a boiler as large as Milliken Station.

3. The coal devolatilization rate constants (which affect the point of gaseous ignition) have a significant influence on the predicted results, especially in the near-field.

4. Far-field comparisons between measured and predicted data are better than near-field comparisons. Analysis suggests that near-field comparisions can be improved with larger numbers of grid nodes and improved code submodels.

5. Trends for important variables like NO_x and carbon-in-ash are correctly represented, but quantitative comparisons can be improved, especially in the near-field.

6. Continued efforts in evaluation of computerized computational methods should yield improved comparison results. Emphasis will need to be placed on improved near-field burner geometric models, turbulence intensity models, grid size effects, and more precise wall heat flux predictions.

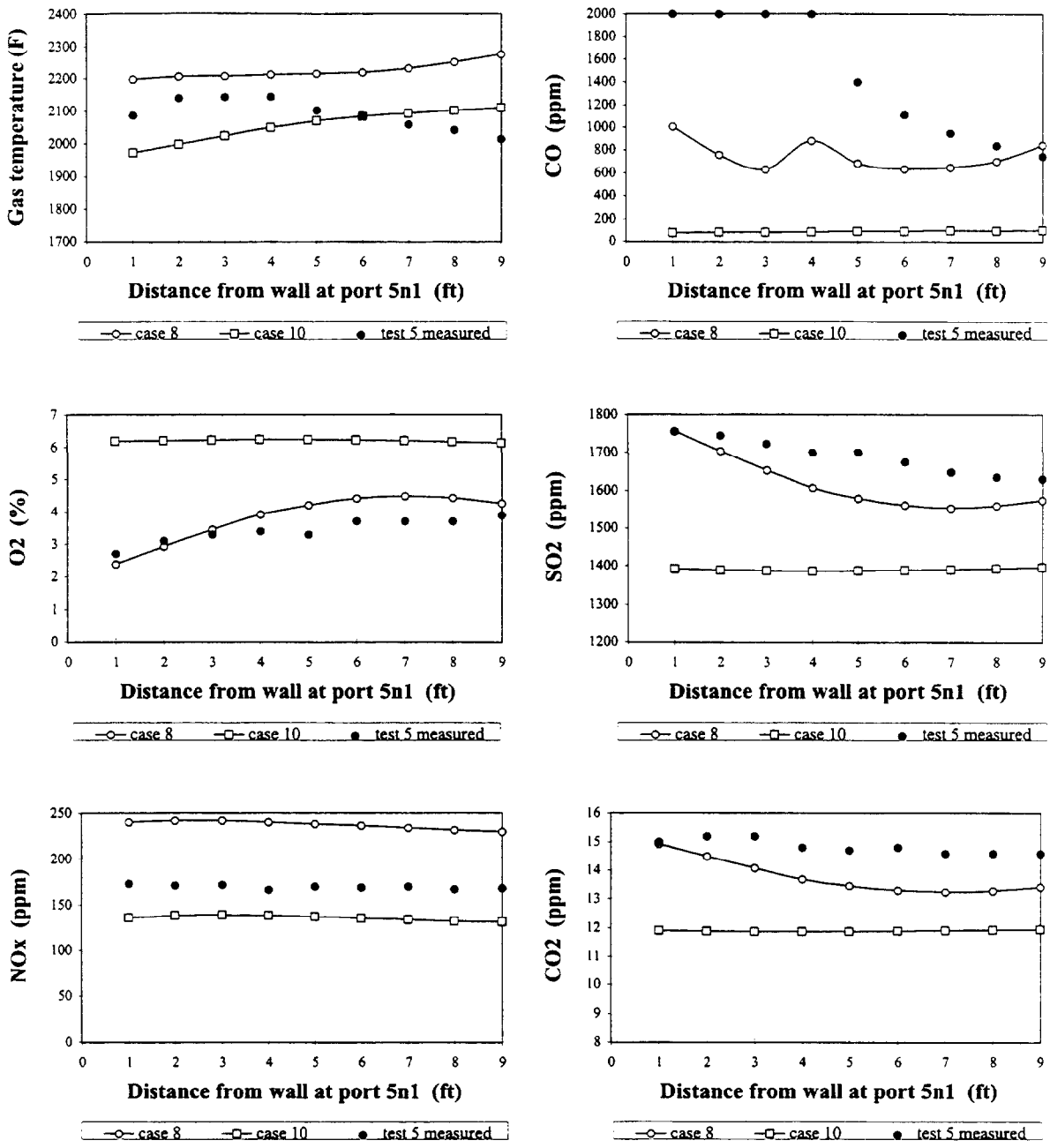

Figure 15. Comparison between measured and predicted values for two different grid sizes at the fifth floor level (far-field comparison) using the 192K and 337k node grids.

References

Brooks, B., "Gas Velocity Measurements in a Coal Fired Furnace with Comparisons to PCGC-3 Predictions" M.S. Thesis, Mechanical Engineering Dept., BYU, 1997.

Cannon, J.N., Webb, B.W.,and Queiroz, M., "Validation of 3-D Combustion Model" ESEERCO Interim Report EP 89-09, June 1992

Cannon, J.N., Webb, B. W., and McQuay, M.Q. "Validation of 3-D Combustion Model" ESEERCO Final Report EP 89-09, Oct. 1995

Groberg, C. "Comparisons of Measured Gas Temperatures and Specie Concentrations at the Milliken Furnace to PCGC-3 Predictions", M.S. Thesis, Mechanical Engineering Dept., BYU, 1996.

Groberg, T., "Validation of the Gas Species and Particle Composition Data taken at the Milliken Power Plant Furnace", M.S. Thesis, Mechanical Engineering Dept., BYU, 1996.

NYSEG Report, "First Semi-Annual Report", NYSEG Contract No. 94-063, Milliken Testing Project, 14 Oct. 1994

NYSEG Report, "Field Measurement Report", NYSEG Contract No. 94-063, Milliken Testing Project, 1995.

NYSEG Report, "Comparison Report", NYSEG Contract No. 94-063, Milliken Testing Project, April 1997

Phillips.S.D. and Smoot, L.D., Volume III. Data Book for Evaluation of Three-Dimensional Combustion Models, Final Report, Combustion Laboratory, BYU, Provo, Ut, (1989).

Ubhayakar, S.K.,Stickler, D.B., Von Rosenberg, C.W., and Gammon, R.E., "Raped Devolatilization of Pulverized Coal in Hot Combustion Gases" 16th Symposium (International) on Combustion, The Combustion Institute, Pittsburgh, PA, 427, 1976

Acknowledgments

The principal investigators on this project acknowledge the financial support of EPRI, NYSEG, ACERC/NSF, and ESSERCO with gratitude. The excellent efforts of graduate students Bradley Brooks, Christopher Groberg, Taylor Groberg, David Black, David Wang, and Waseem Nazeer; undergraduate students Adam Clark, Richard Groom, Douglas Kennedy, and Jacob Peart; and Mechanical Engineering faculty member Dr. Dale Tree, are particularly acknowledged as well as the strong support received from thrust area 5 via Dr. Scott Hill along with Dr. L. Douglas Smoot, the ACERC Director. The very cooperative atmosphere at the Milliken Station, a part of the NYSEG system is also gratefully acknowledged with special thanks to Charles Tisch, Kevin Mooney and Joseph Nogaret.

APPENDIXES

Appendix A This appendix compares the effect of grid size.

Appendix B This appendix compares the effect of separate over-fire air (SOFA) injection point and amount.

Appendix C This appendix compares the effect of changing the devolitilization constants (simulating ignition point variation).

Appendix D-1 This appendix compares the effect of grid size and devolitilization rate constants combined.

Appendix D-2 This appendix presents each of the twelve prediction cases separatly along with comparitive measured data for gas and particle velocities.

Appendix A

Compares the effect of numerical grid size

Appendix A illustrates the effect of grid size (65K, 192K, 337K) on the PCGC-3 predictions for the Milliken Station and compares the results with the measured data for test #3 using the "old" devolatilization constants

Test #3 is the "base case" for the test series having the CCOFA ducts fully open and the SOFA ducts open ~40%. The nominal NO_x value measured at the stack by the Westinghouse Distributed Processing Family (WDPF) system was 386 #/MBTU. The plant operation was at full load (158 Mw_e gross) and the tilts were at -5 degrees from horizontal and fired Blacksville coal at 4% excess O_2 in the exhaust gases.

The general conclusions drawn from these comparisons are that the 65K data has the poorest comparison and that the 337K data has the best, but not perfect comparison. There is no indication that the grid independence has consistently been reached but the 337K grid was the largest attempted and took over two months to converge to the condition noted in Table 2.

These Appendix A figures are separated for ease of comparison as follows:

A.1 compare grid size effects using the 65K, 192K, and 337K grids for test 3 (40% SOFA).

A.1.1-6 - Point-for-point comparisons by port for the noted six variables

A.1.7 - Average of the point-for-point differences by port arranged in ascending order up the furnace axis with levels 2 and 5 having two ports each.

A.1.8 - Comparisons of the port traverse averages arranged in ascending order up the furnace axis with levels 2 and 5 having two ports each.

A.2 compares the grid size effects of the 192K and 337K grids using the "new" devolatilization constants for Test 5 (100% SOFA).

A.2.1-6 same as A.1.1-6

A.2.7 same as A.1.7

A.2.8 same as A.1.8

A.3 compares the grid size effects of the 192K and 337 grids using the "new" devolatilization constants for test 4 (0% SOFA).

A.4.1 compares point-for-point data on the effect of grid size (65K, 192K, and 337K) for measured gas velocities by port in ascending order up the axis of the furnace with levels 2 and 5 having two ports each.

A.4.2 shows the effect of point-for-point average differences by port in ascending order up the furnace axis. The sensitivity to grid size is particularly noted in the lower furnace, where grid size modeling effects are most evident.

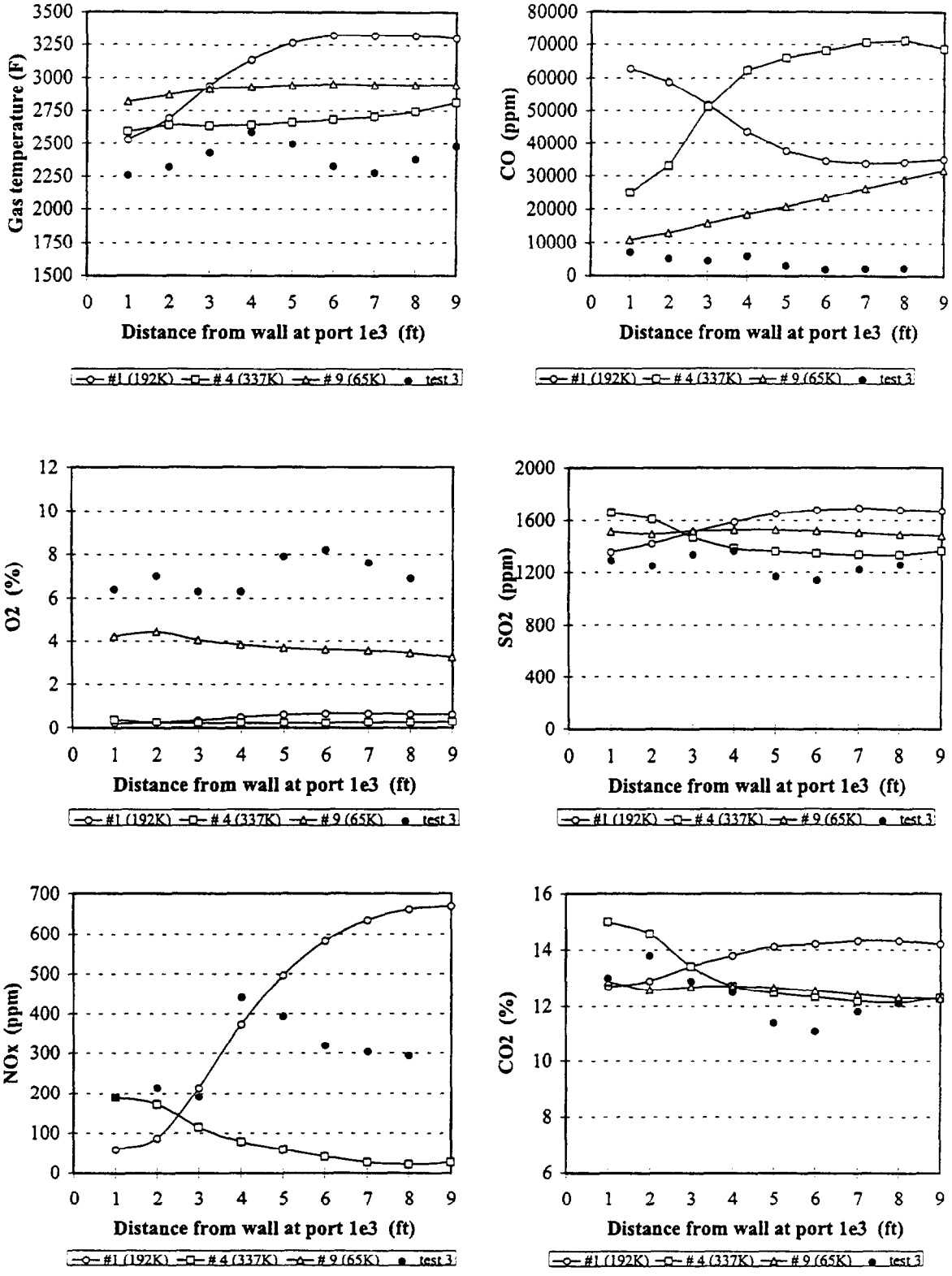

Figure A.1.1 Measured and predicted values for cases 1, 4, and 9 at port 1e3

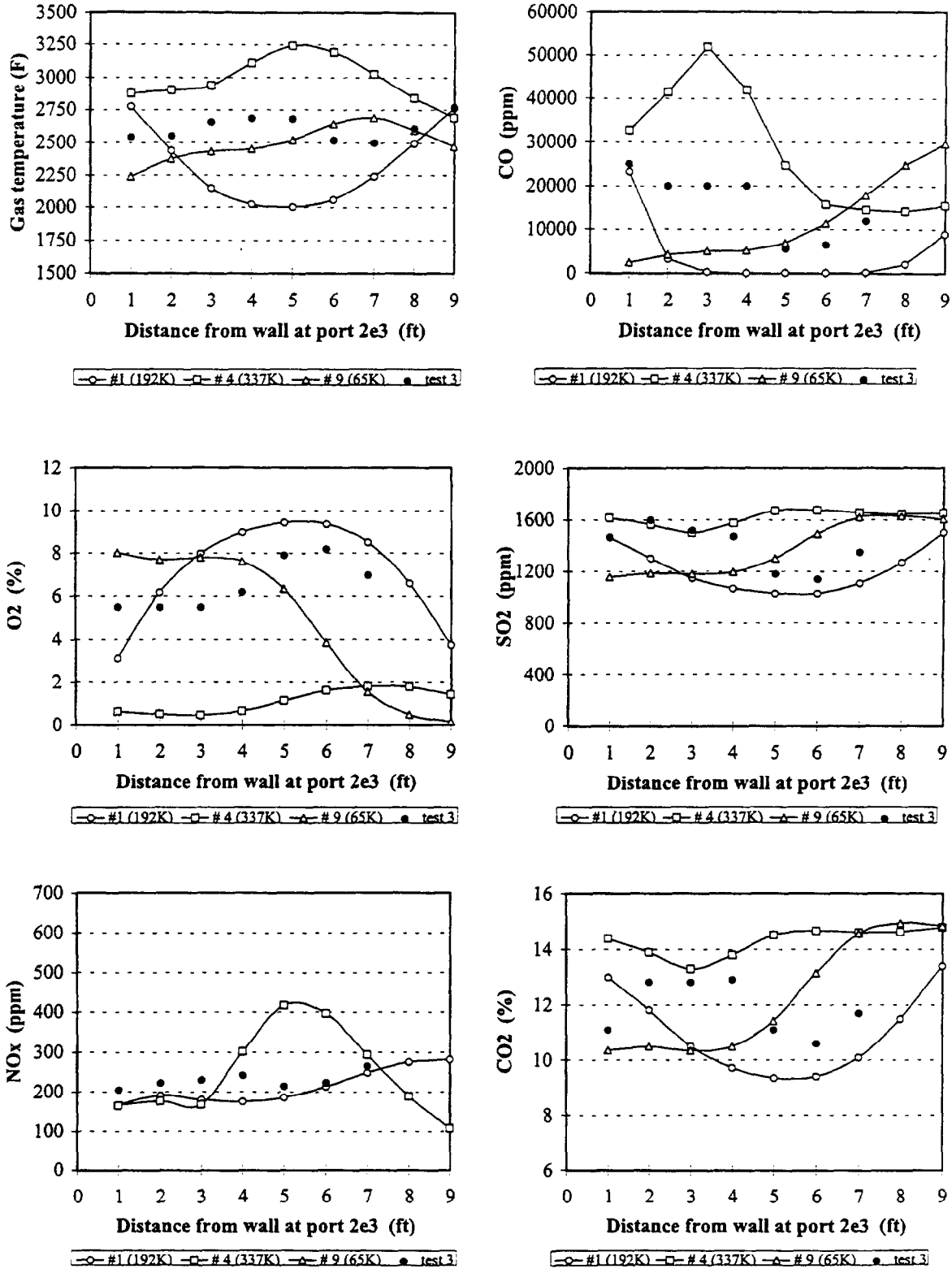

Figure A.1.2 Measured and predicted values for cases 1, 4, and 9 at port 2e3

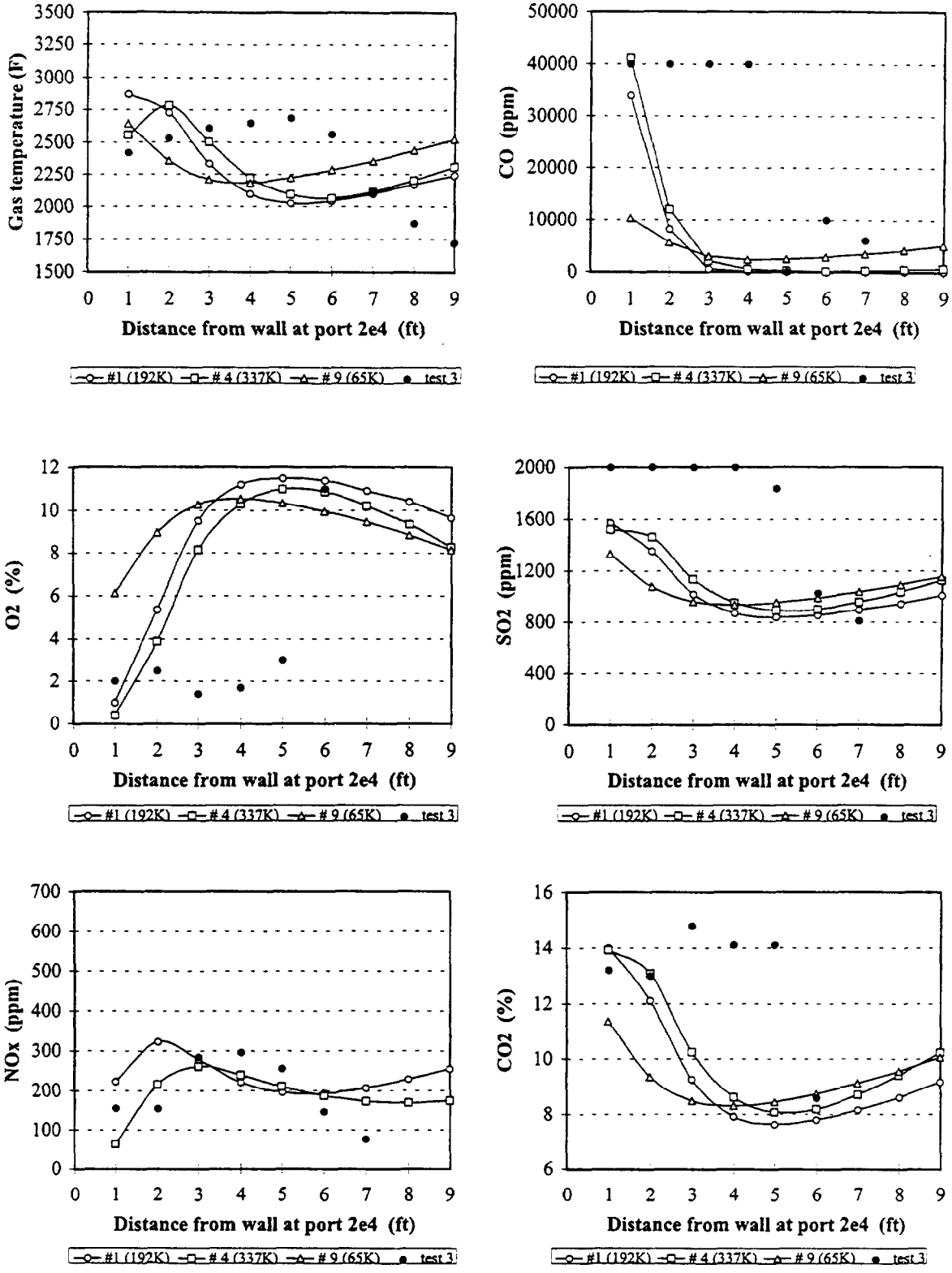

Figure A.1.3 Measured and predicted values for cases 1, 4, and 9 at port 2e4

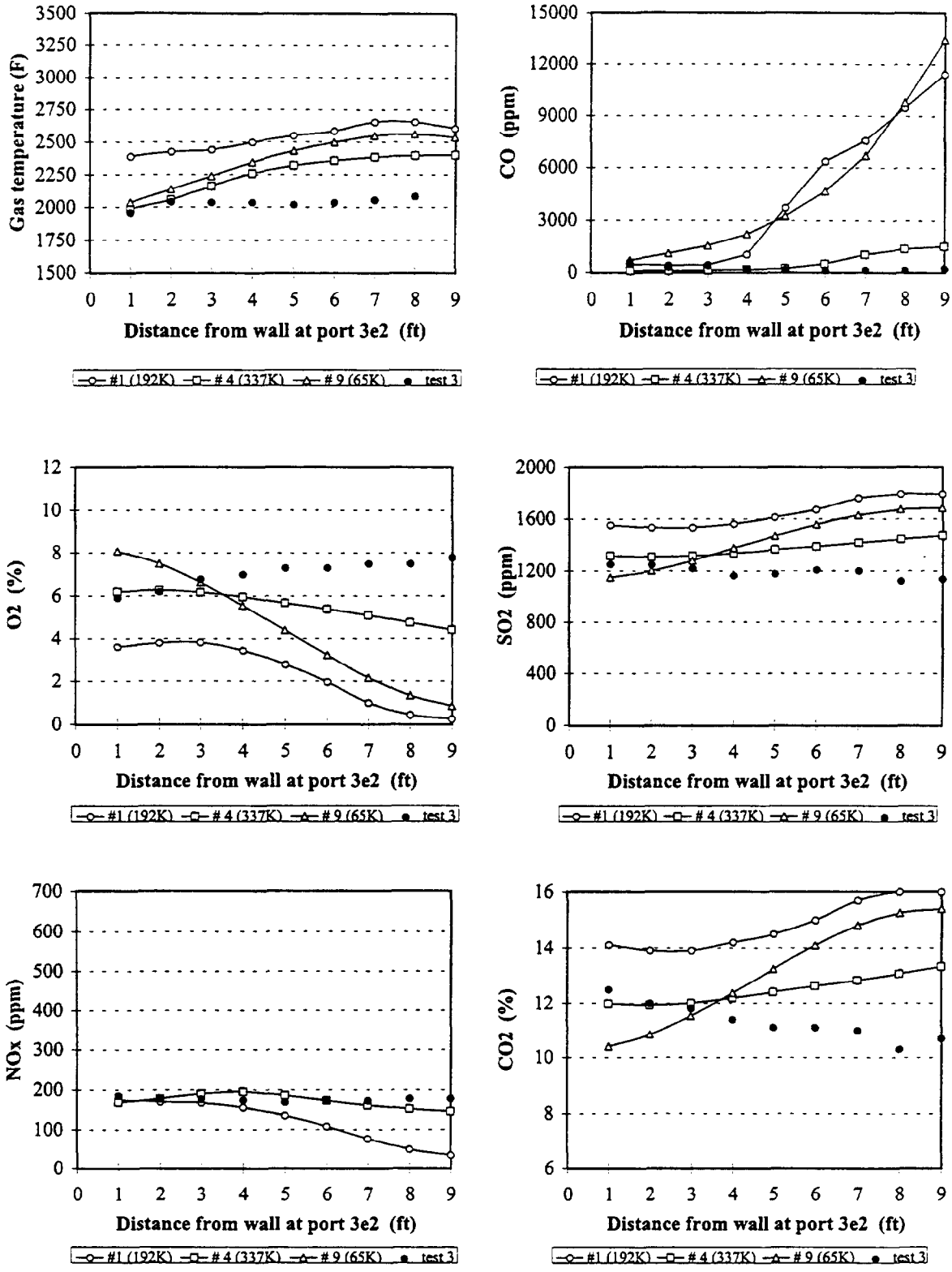

Figure A.1.4 Measured and predicted values for cases 1, 4, and 9 at port 3e2

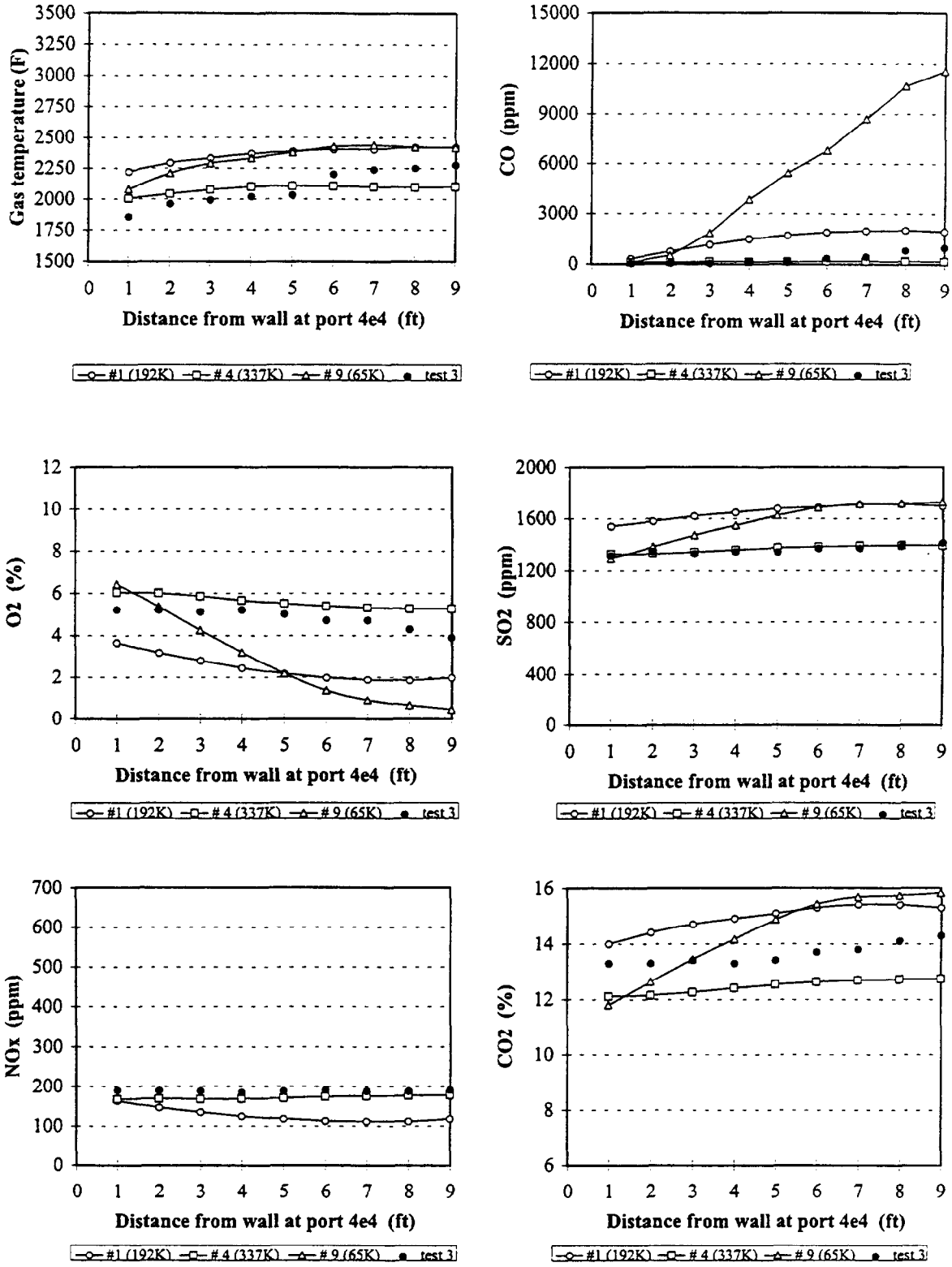

Figure A.1.5 Measured and predicted values for cases 1, 4, and 9 at port 4e4

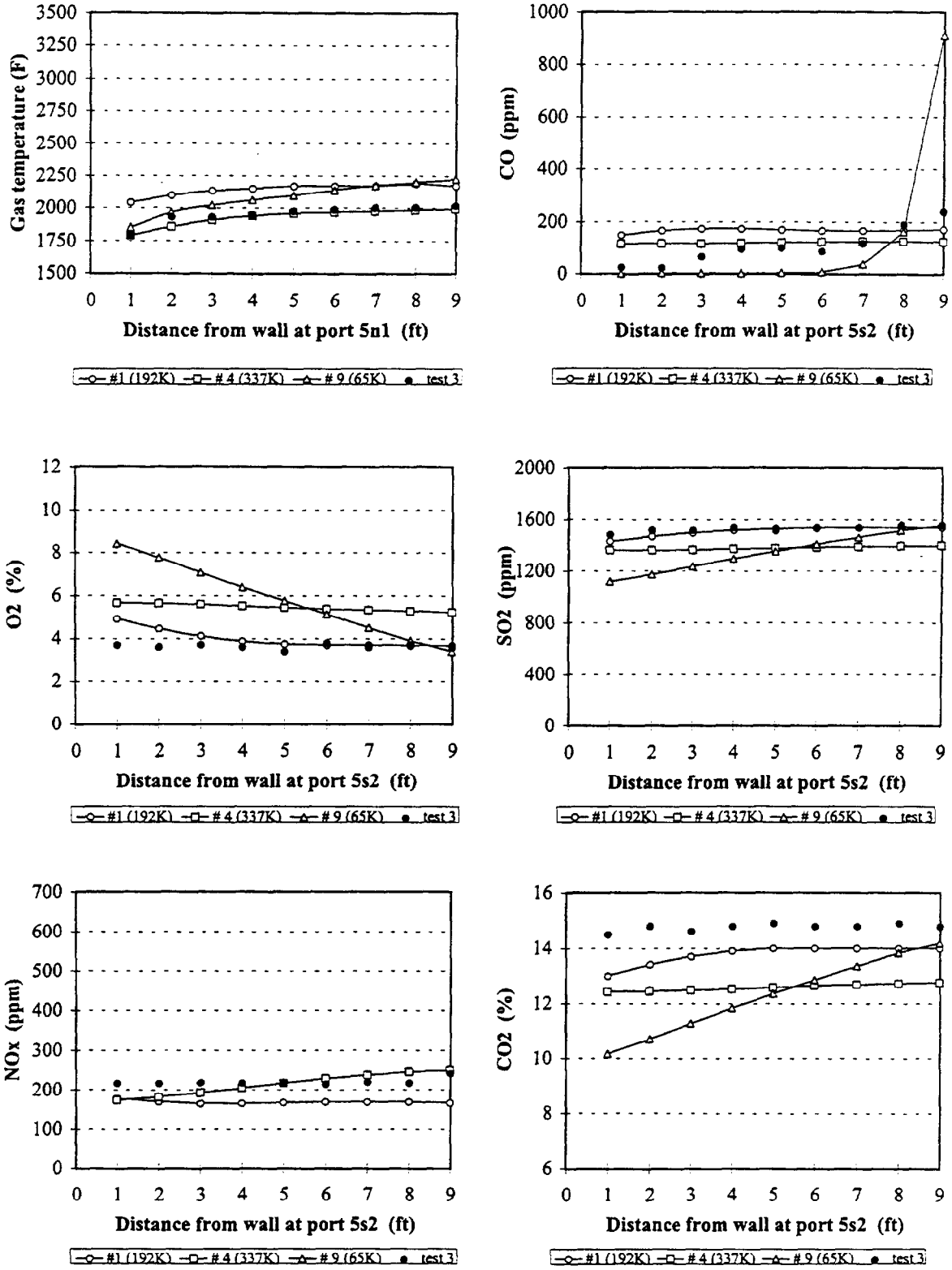

Figure A.1.6 Measured and predicted values for cases 1, 4, and 9 at level 5

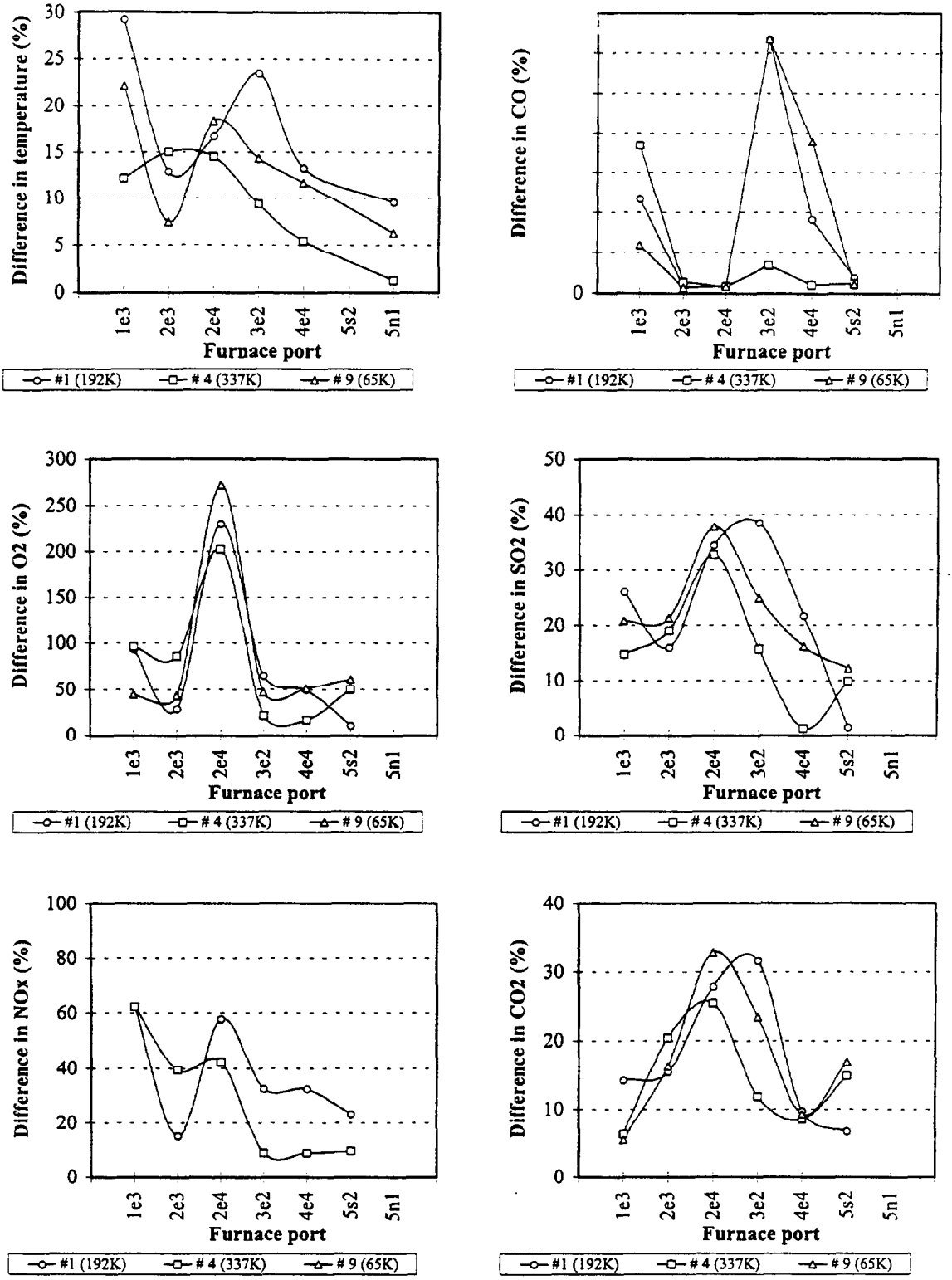

Figure A.1.7 Difference between predictions and measurements for cases 1, 4, and 9

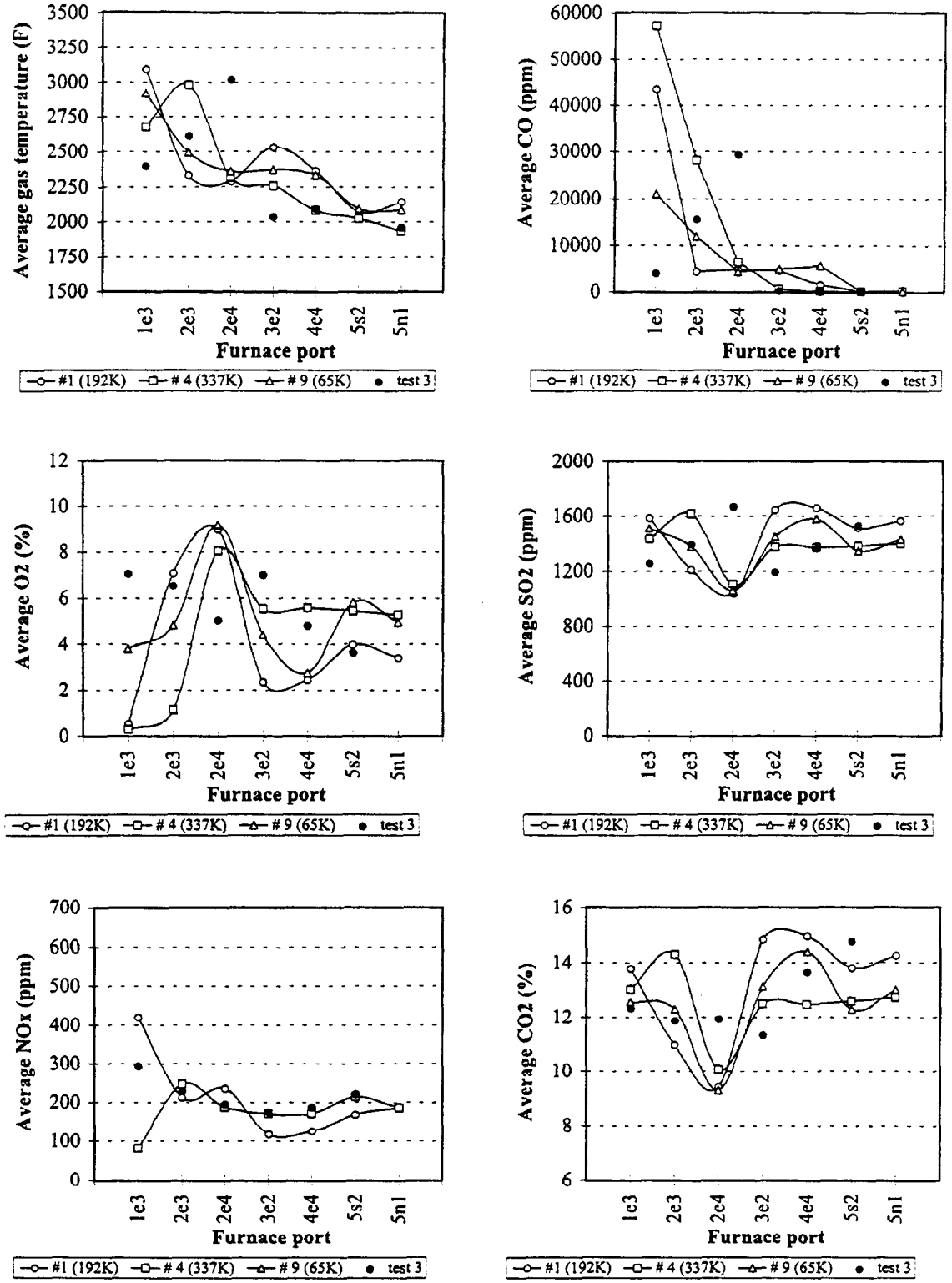

Figure A.1.8 Averaged measured and predicted values for cases 1, 4, and 9

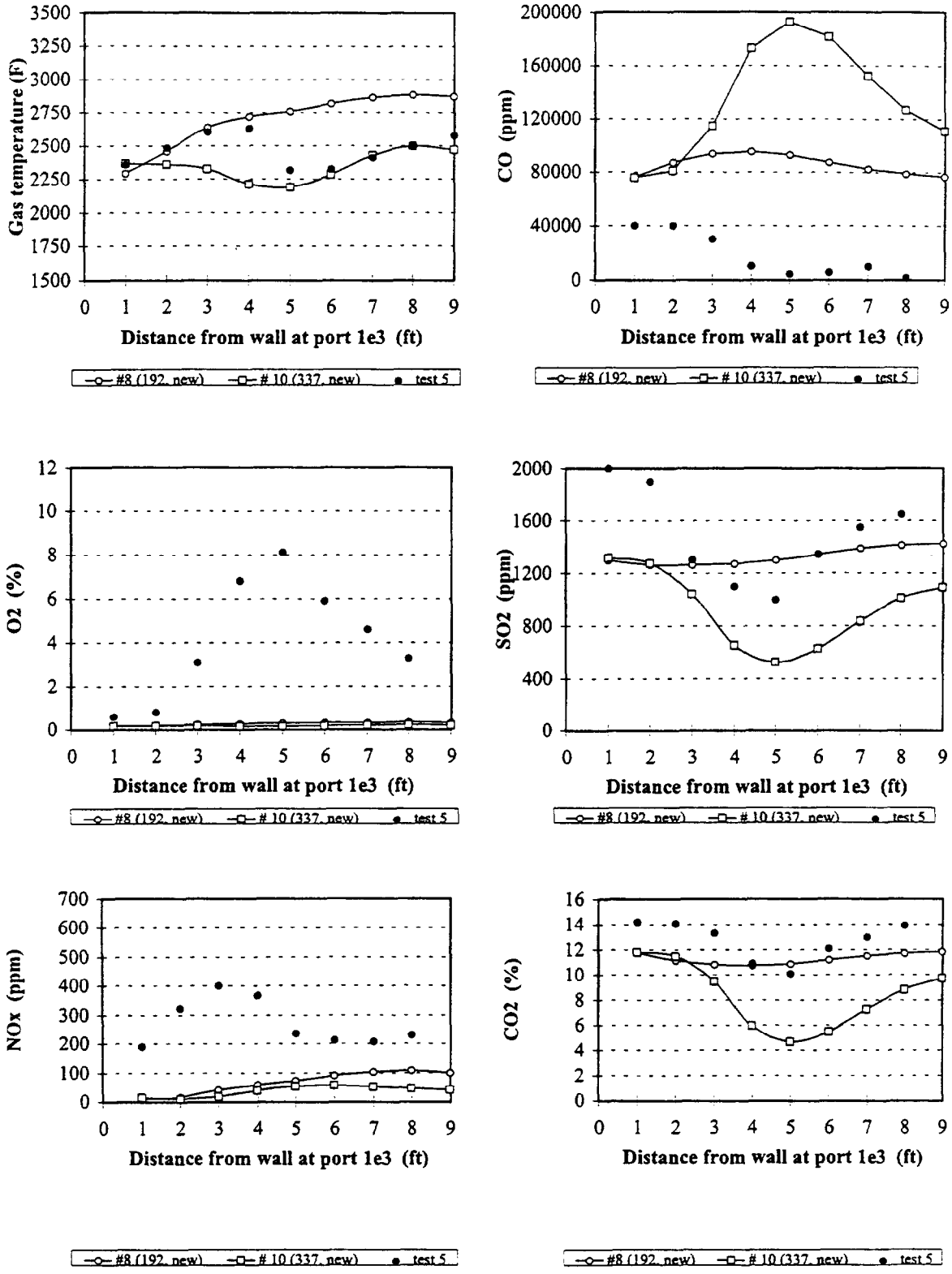

Figure A.2.1 Measured and predicted value for cases 8 and 10 at port 1e3

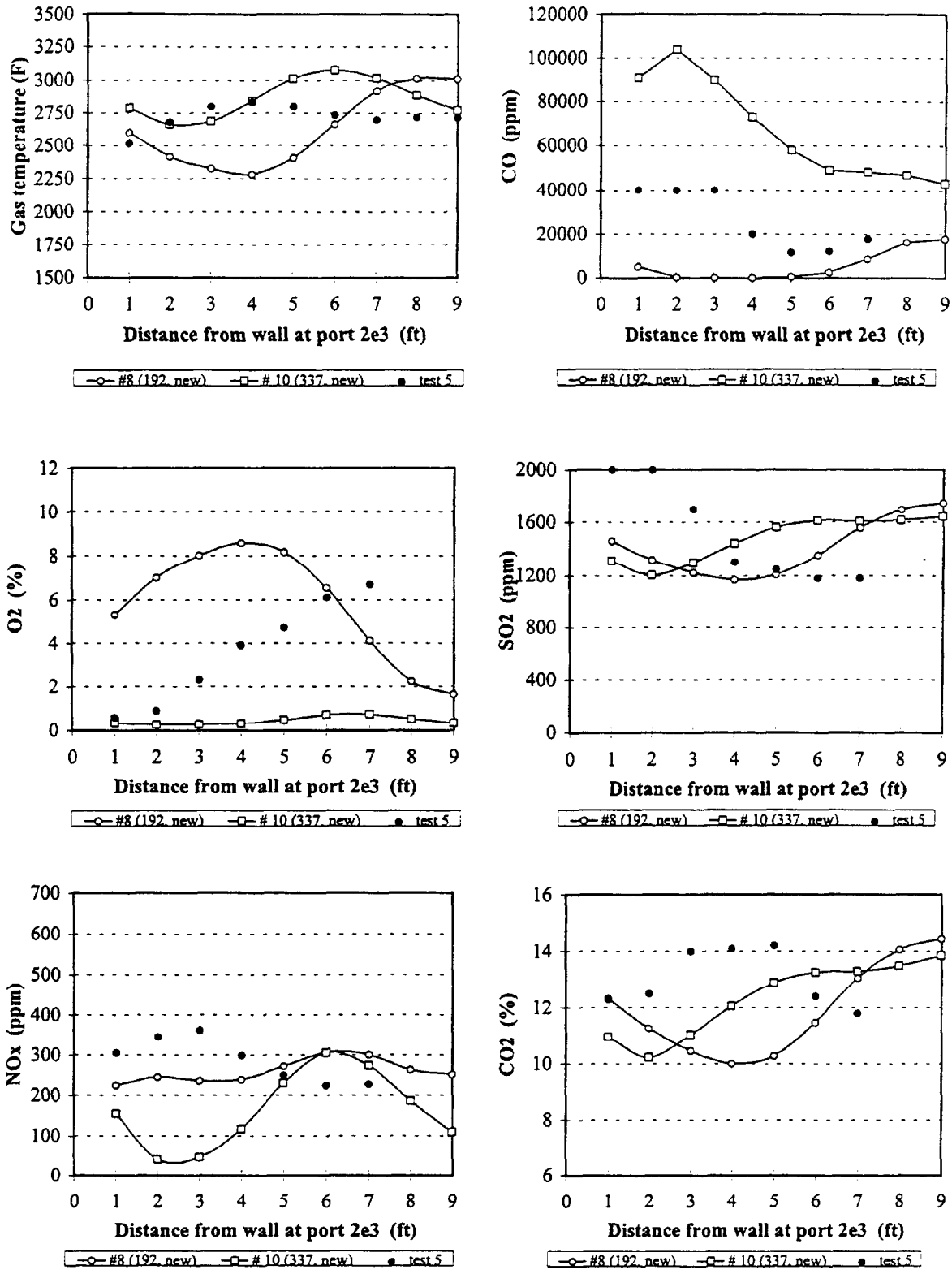

Figure A.2.2 Measured ans predicted values for cases 8 and 10 at port 2e3

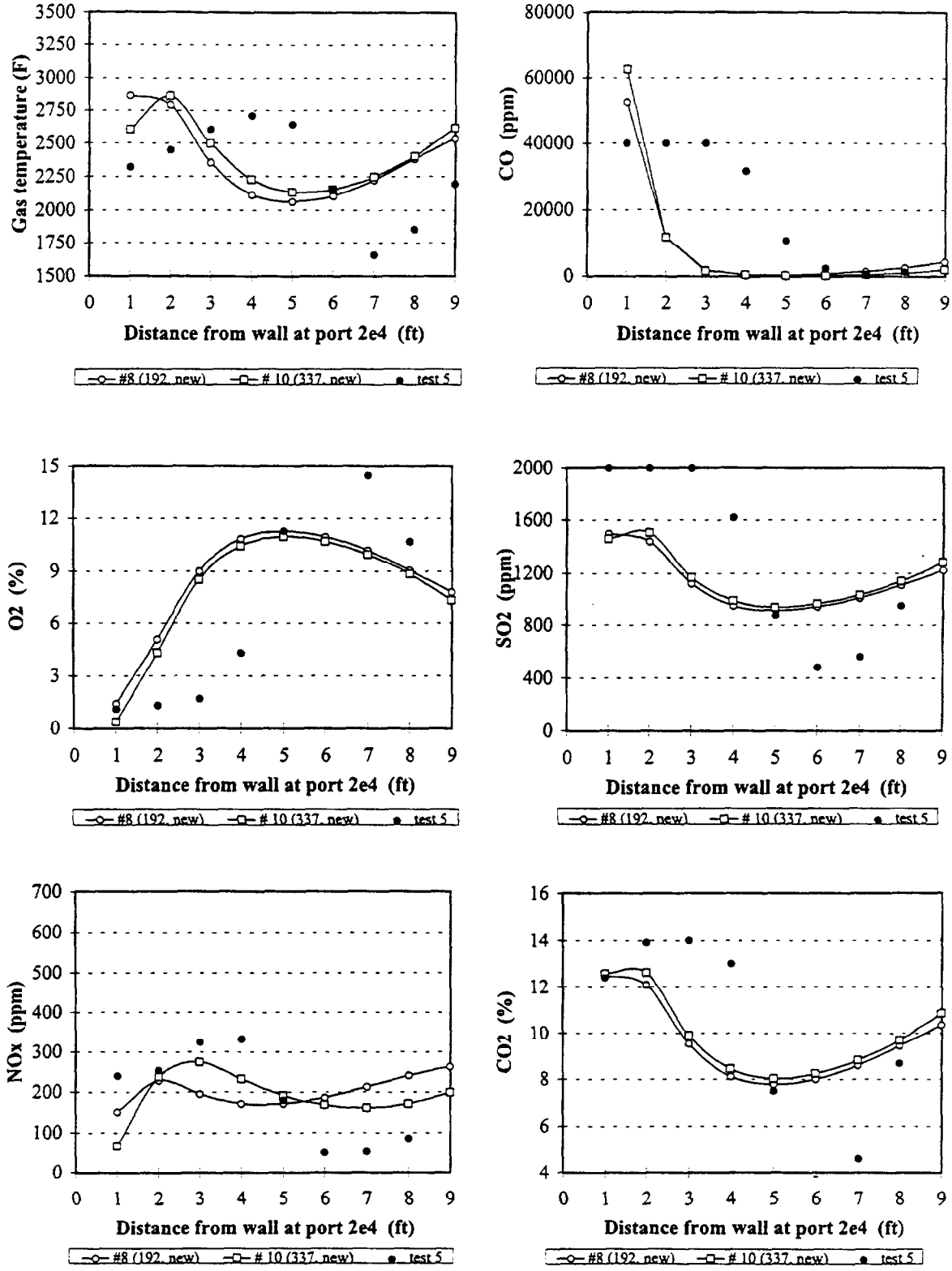

Figure A.2.3 Measured and predicted values for cases 8 and 10 at port 2e4

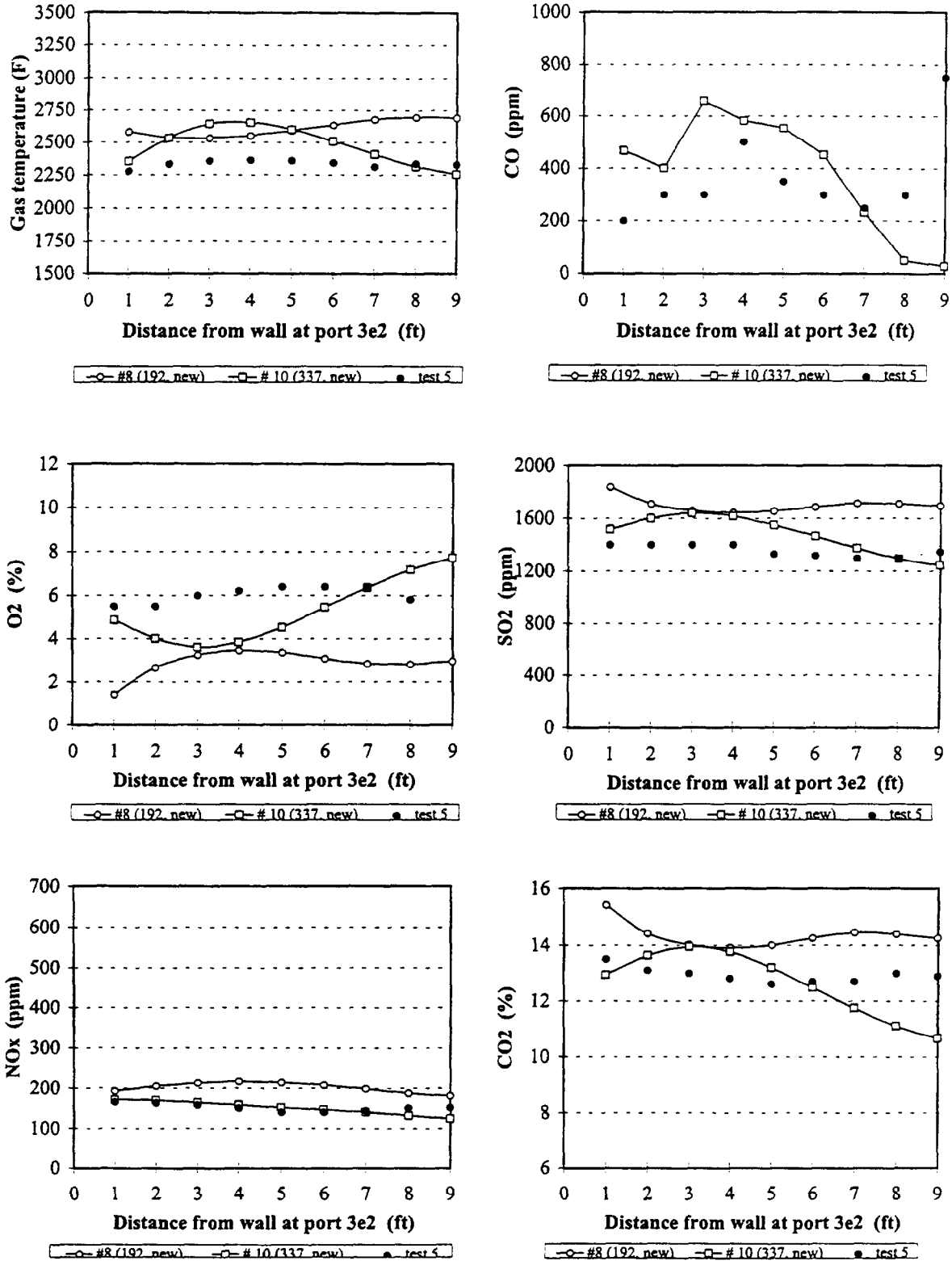

Figure A.2.4 Measured and predicted values for cases 8 and 10 at port 3e2

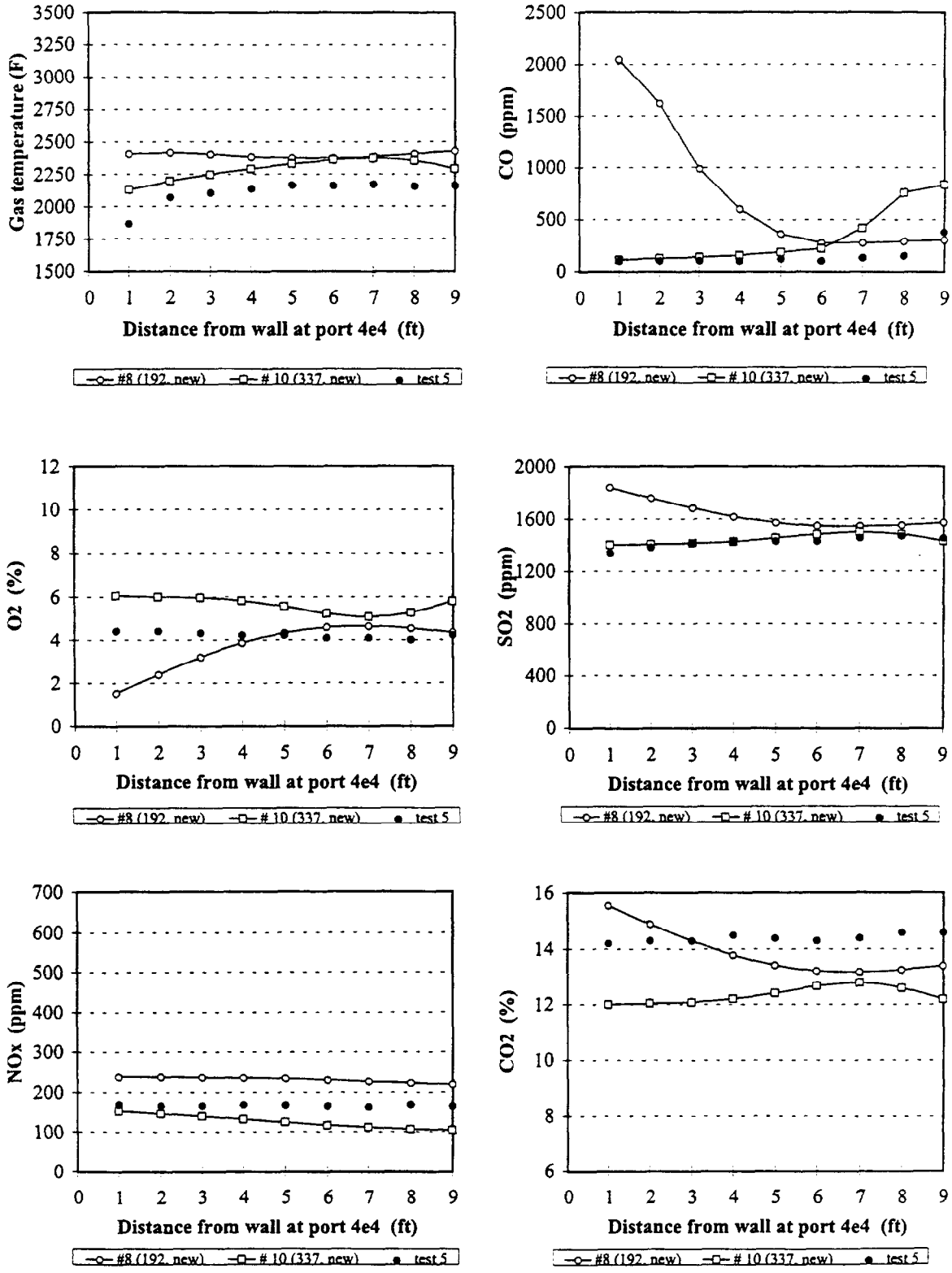

Figure A.2.5 Measured and predicted values for cases 8 and 10 at port 4e4

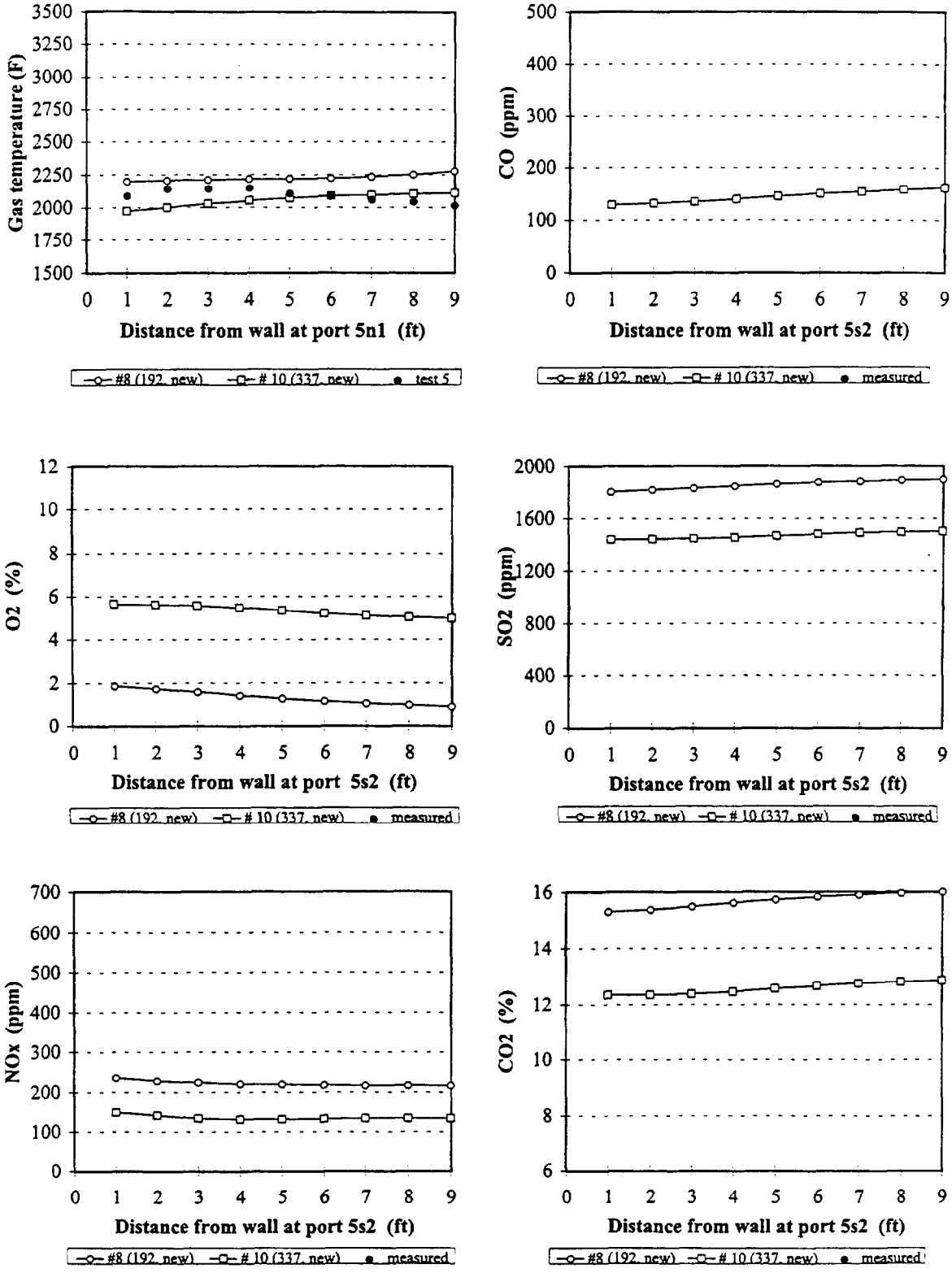

Figure A.2.6 Measured and predicted values for cases 8 and 10 at level 5

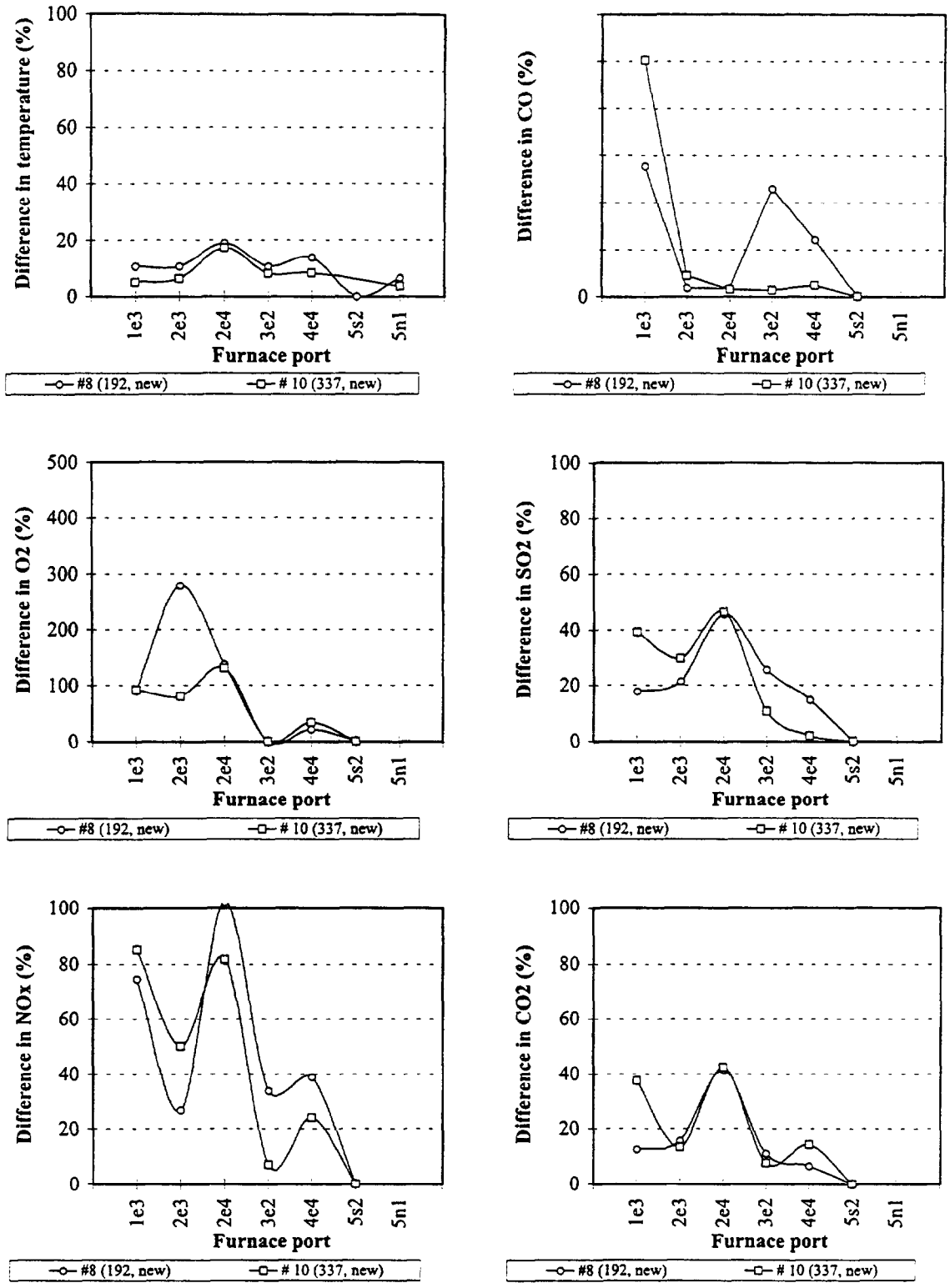

Figure A.2.7 Average difference between prediction and measurement for cases 8 and 10

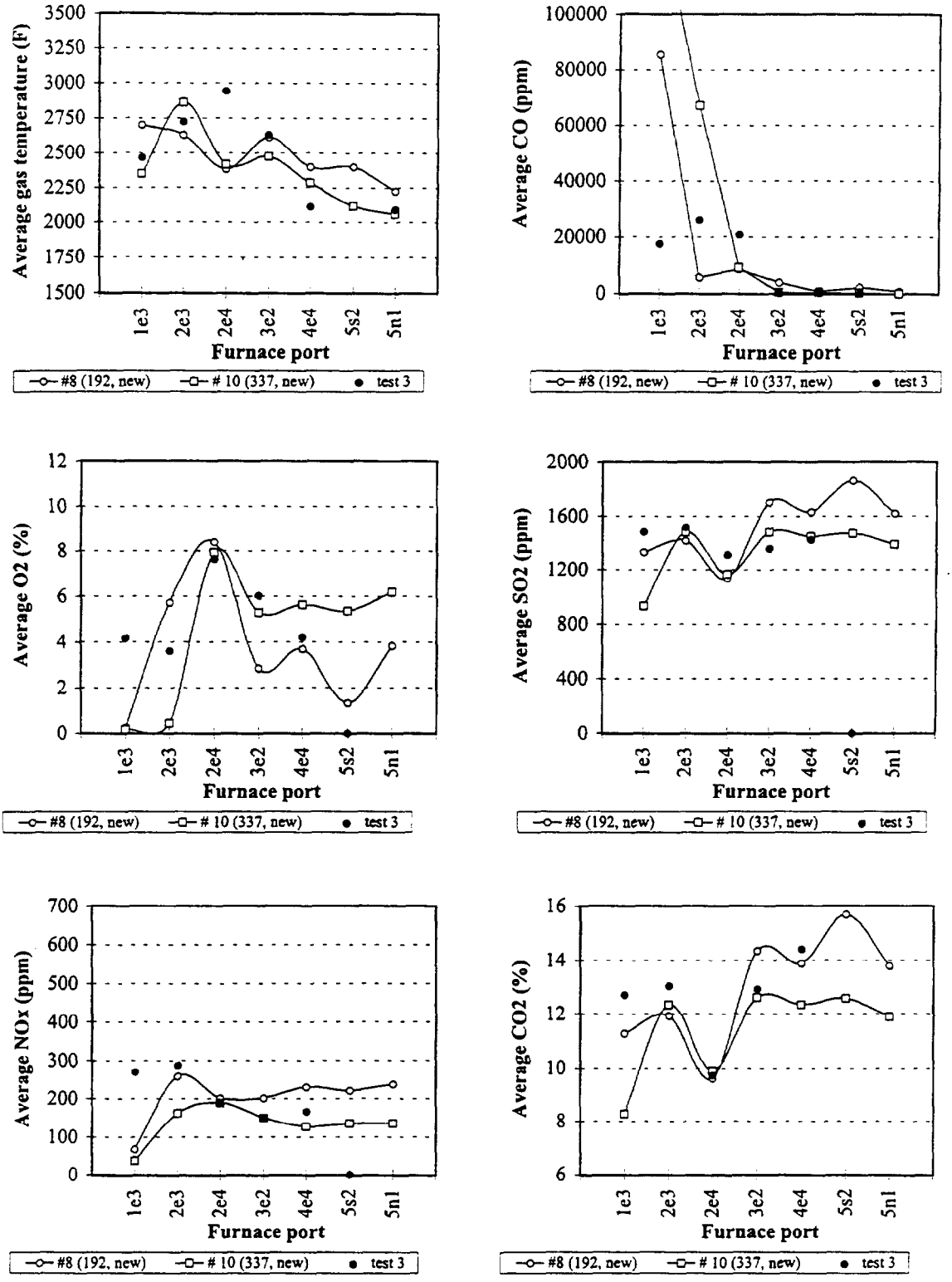

Figure A.2.8 Average predicted and measured values for cases 8 and 10

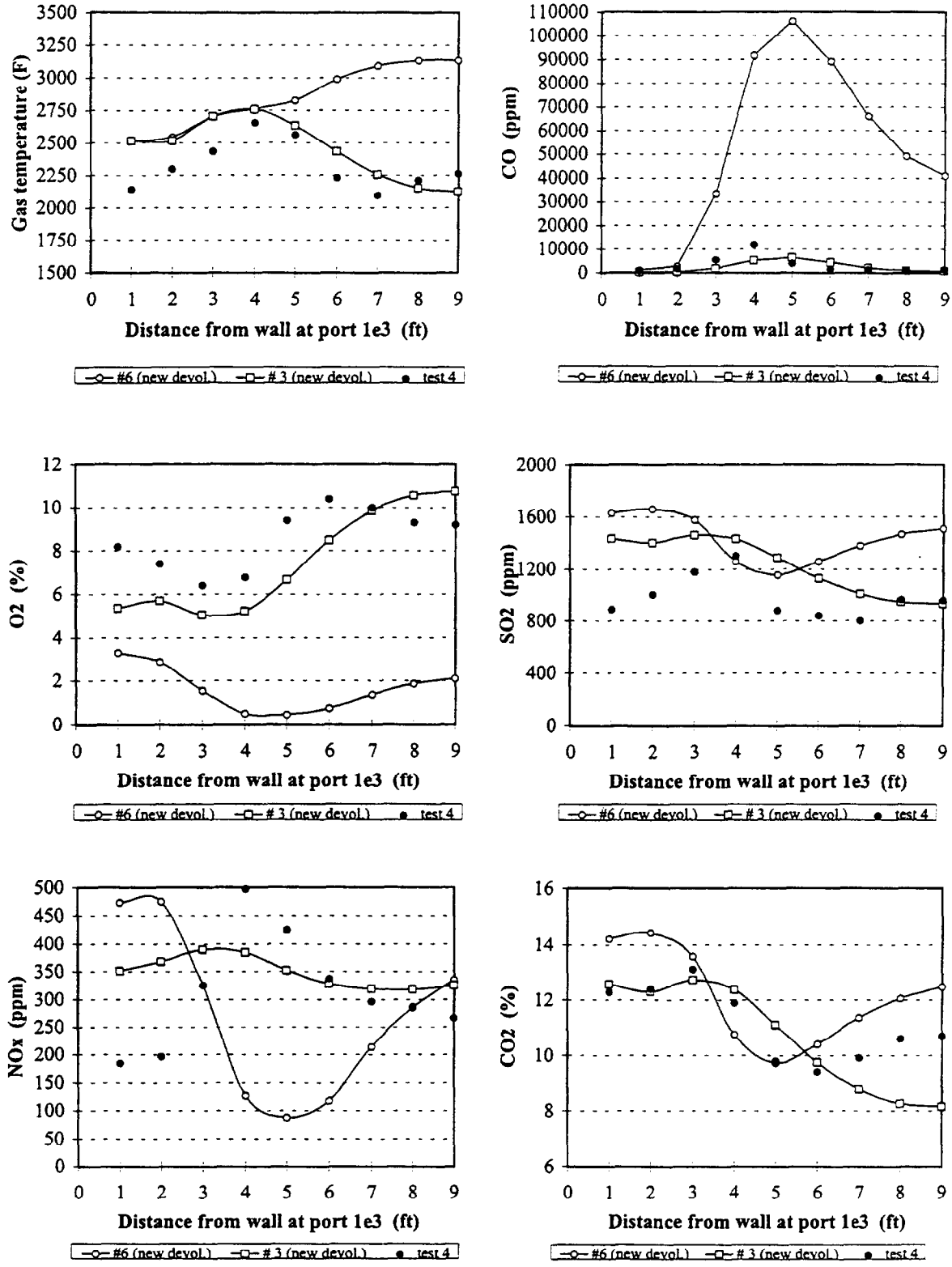

Figure A.3.1 Measured and predicted values for cases 6 and 3 at port 1e3

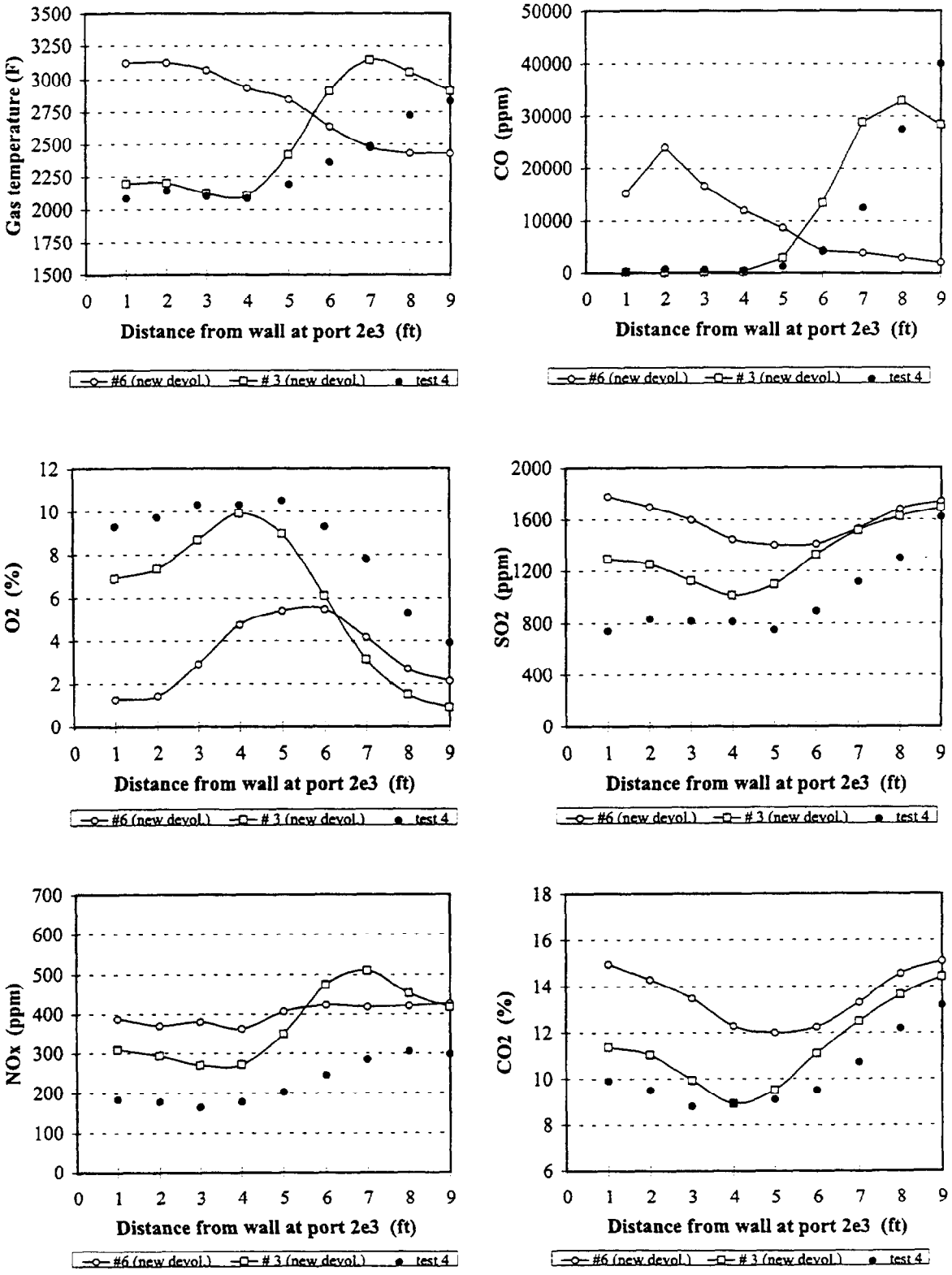

Figure A.3.2 Measured and predicted values for cases 6 and 3 at port 2e3

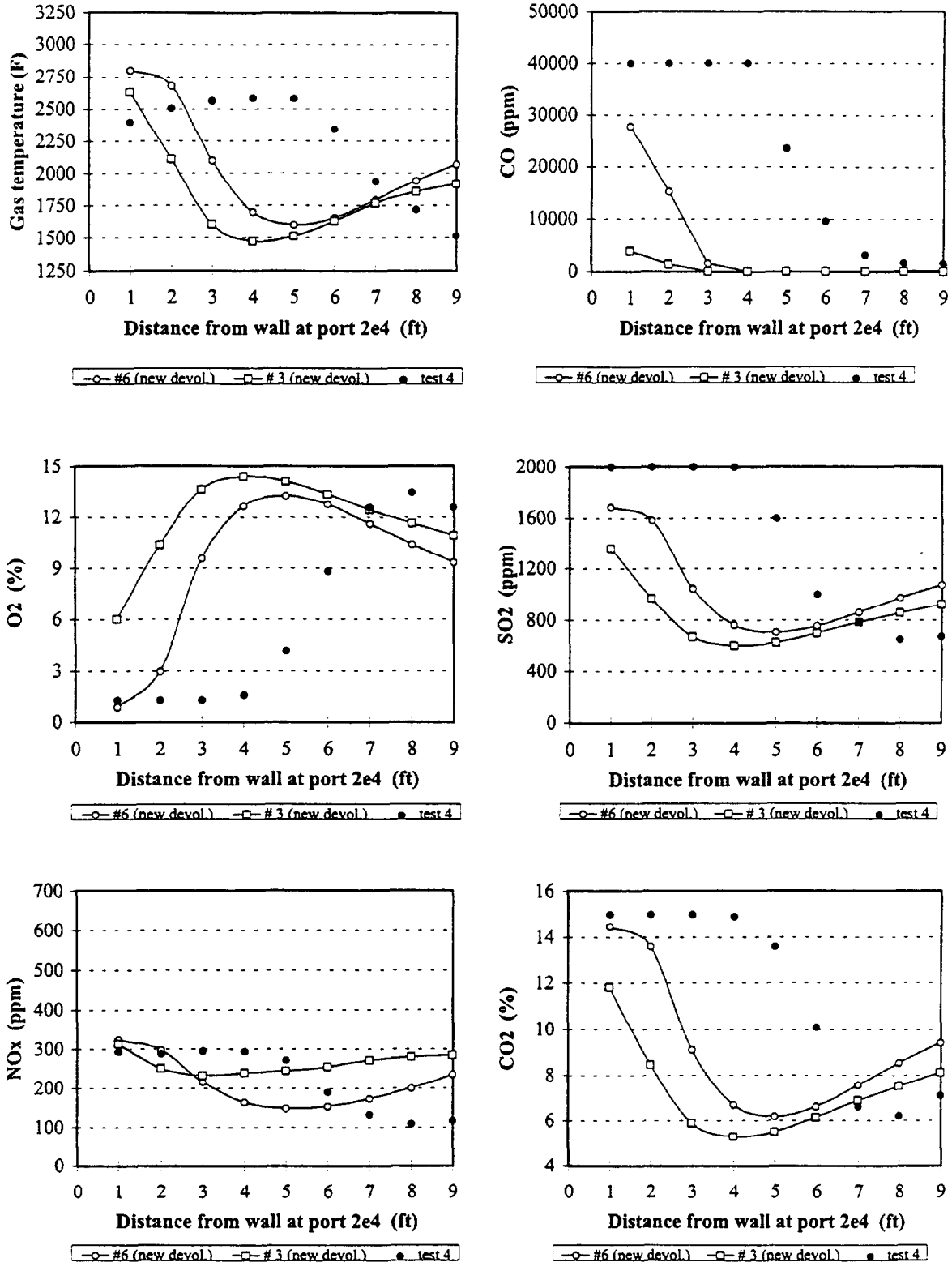

Figure A.3.3 Measured and predicted values for cases 6 and 3 at port 2e4

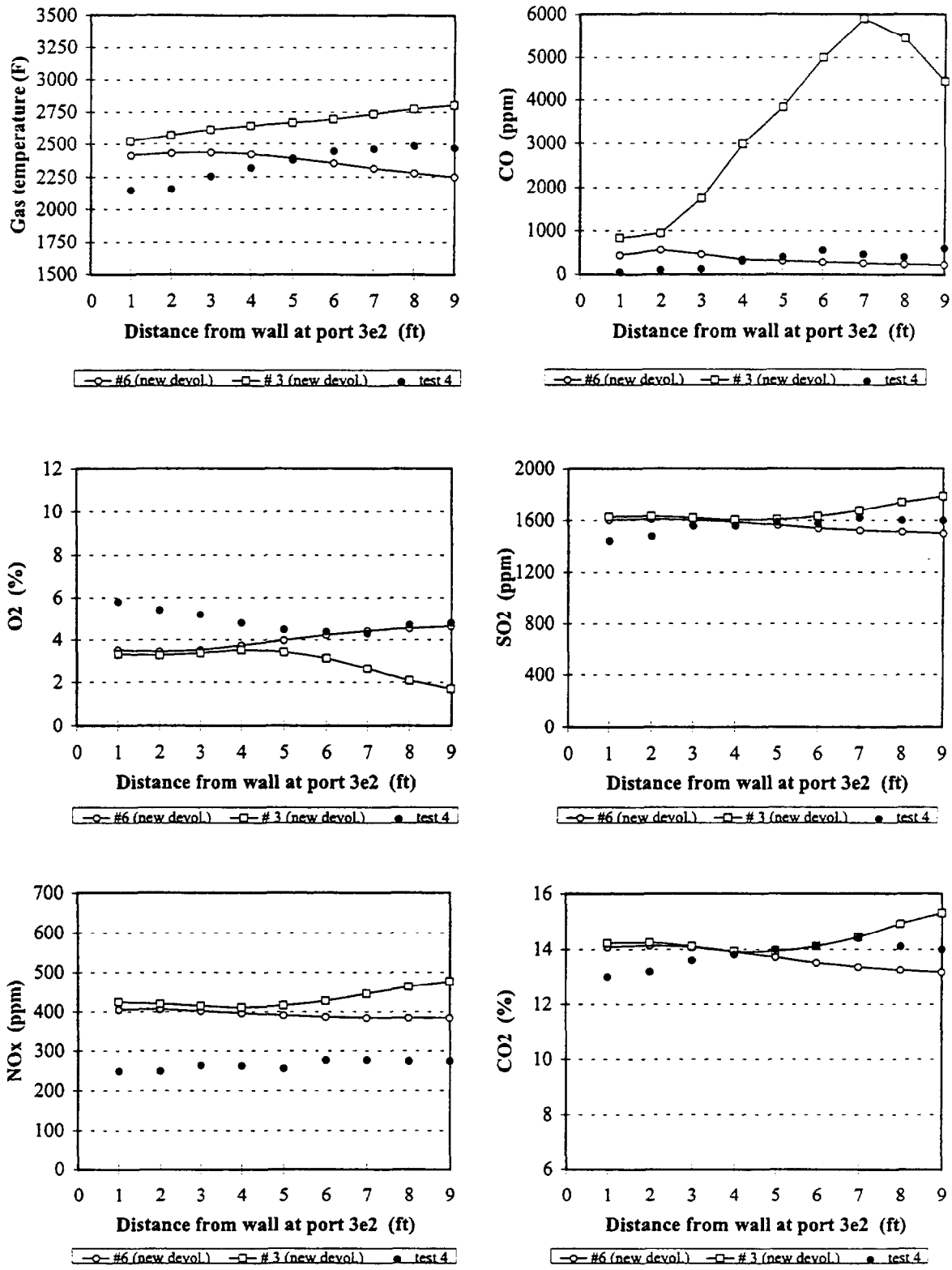

Figure A.3.4 Measured and predicted values for cases 6 and 3 at port 3e2

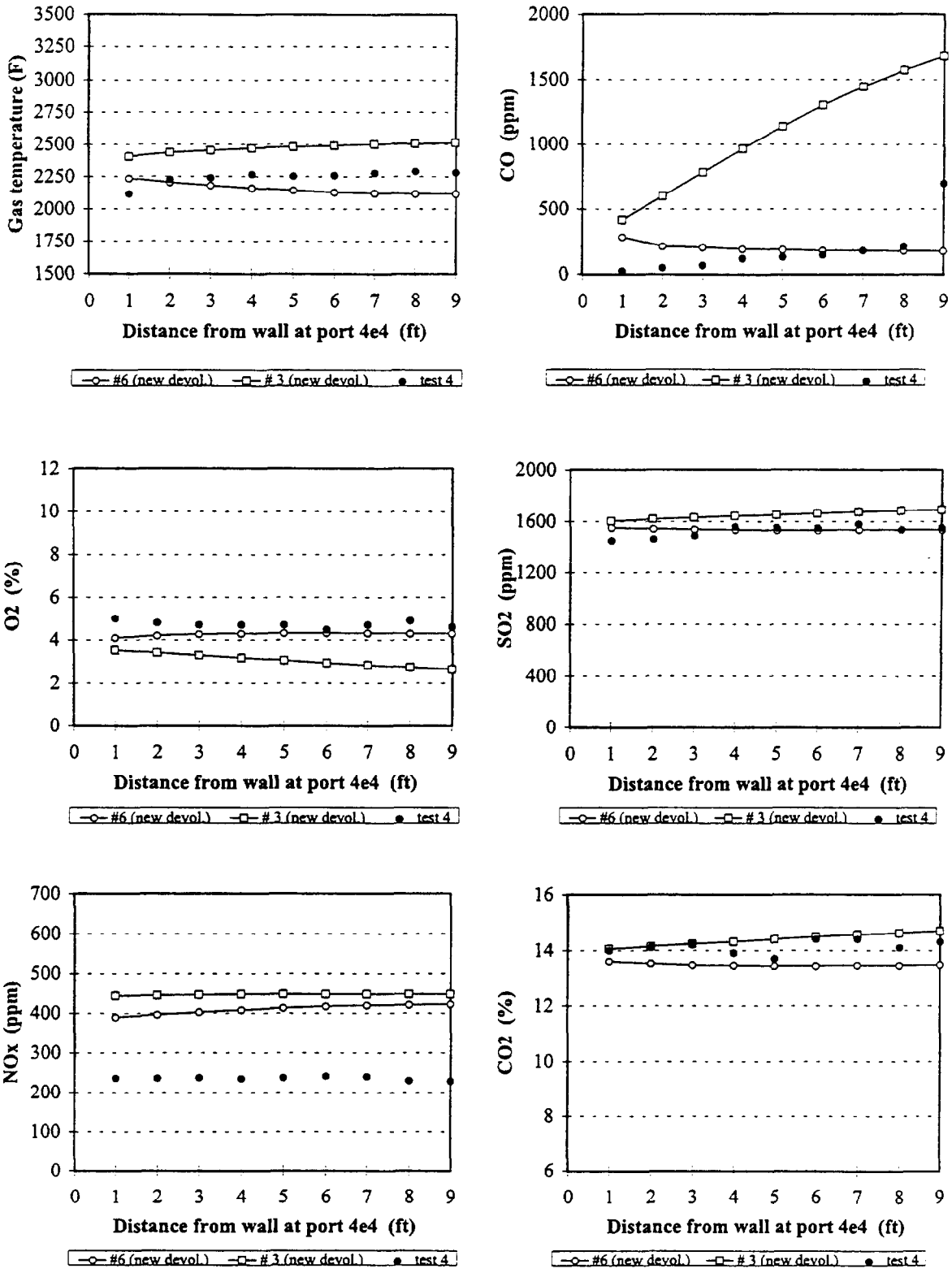

Figure A.3.5 Measured and predicted values for cases 6 and 3 at port 4e4

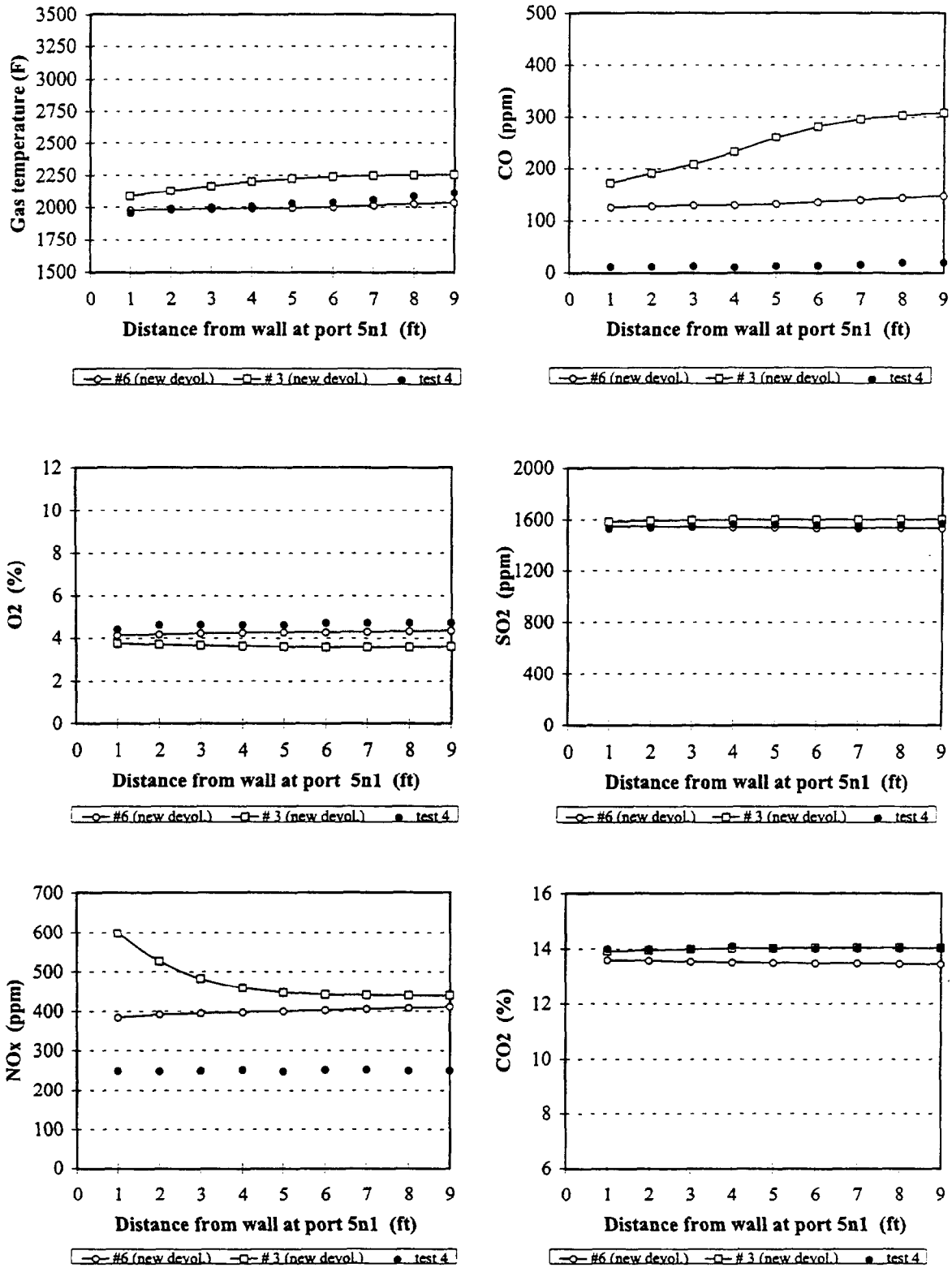

Figure A.3.6 Measured and predicted values for cases 6 and 3 at port 5n1

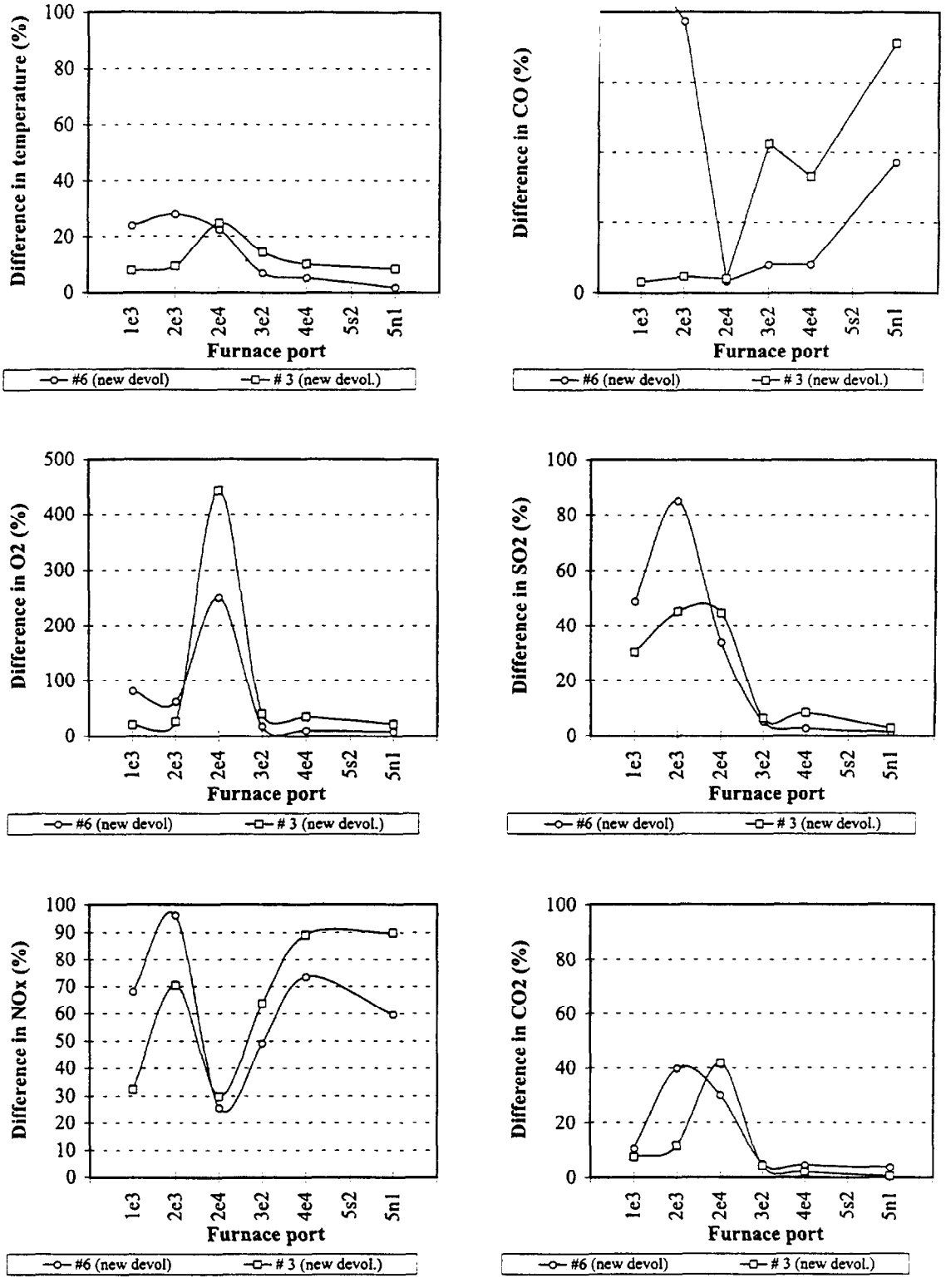

Figure A.3.7 Difference between predictions and measurements for cases 6 and 3

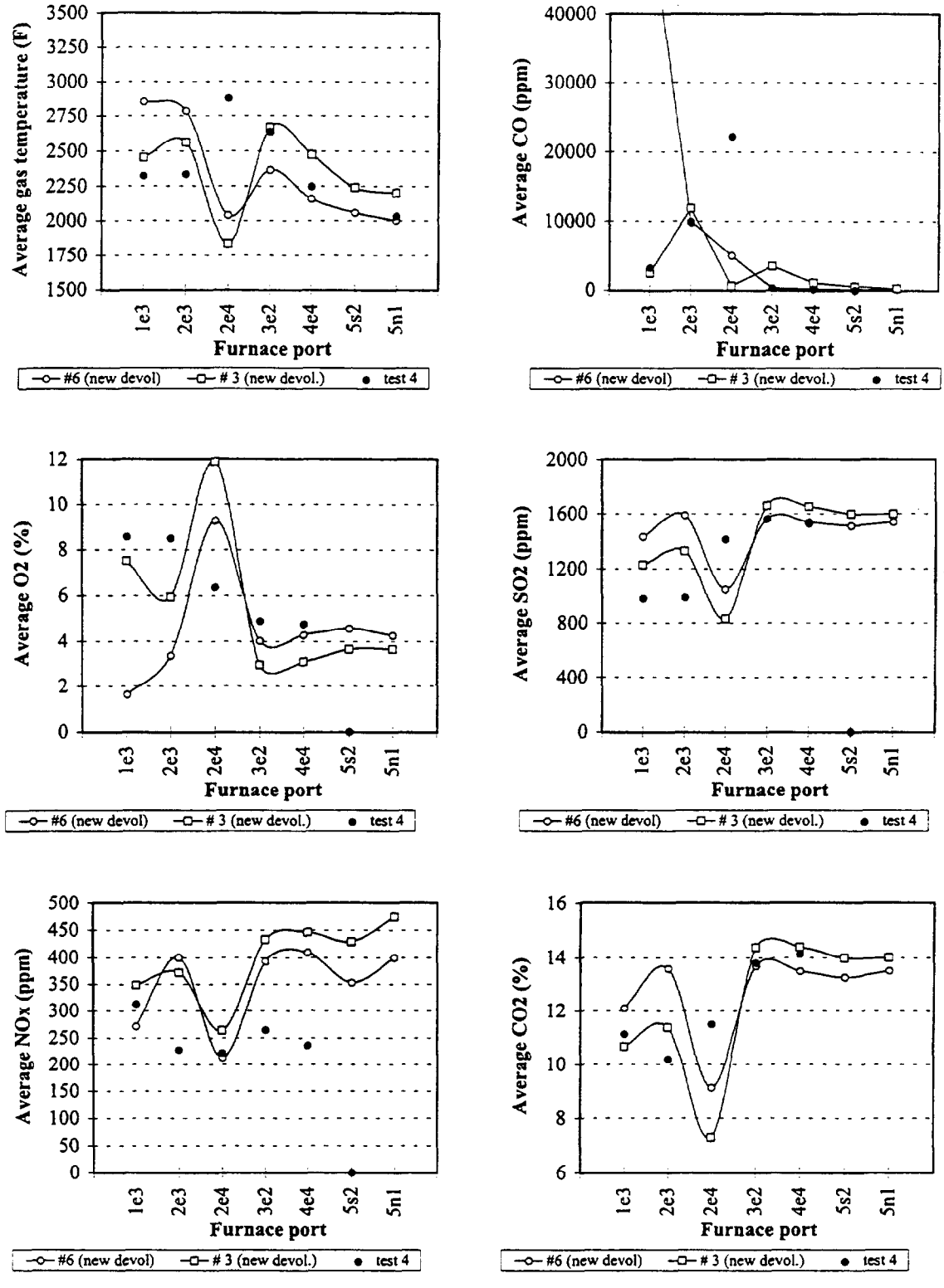

Figure A.3.8 Averaged measured and predicted values for cases 6 and 3

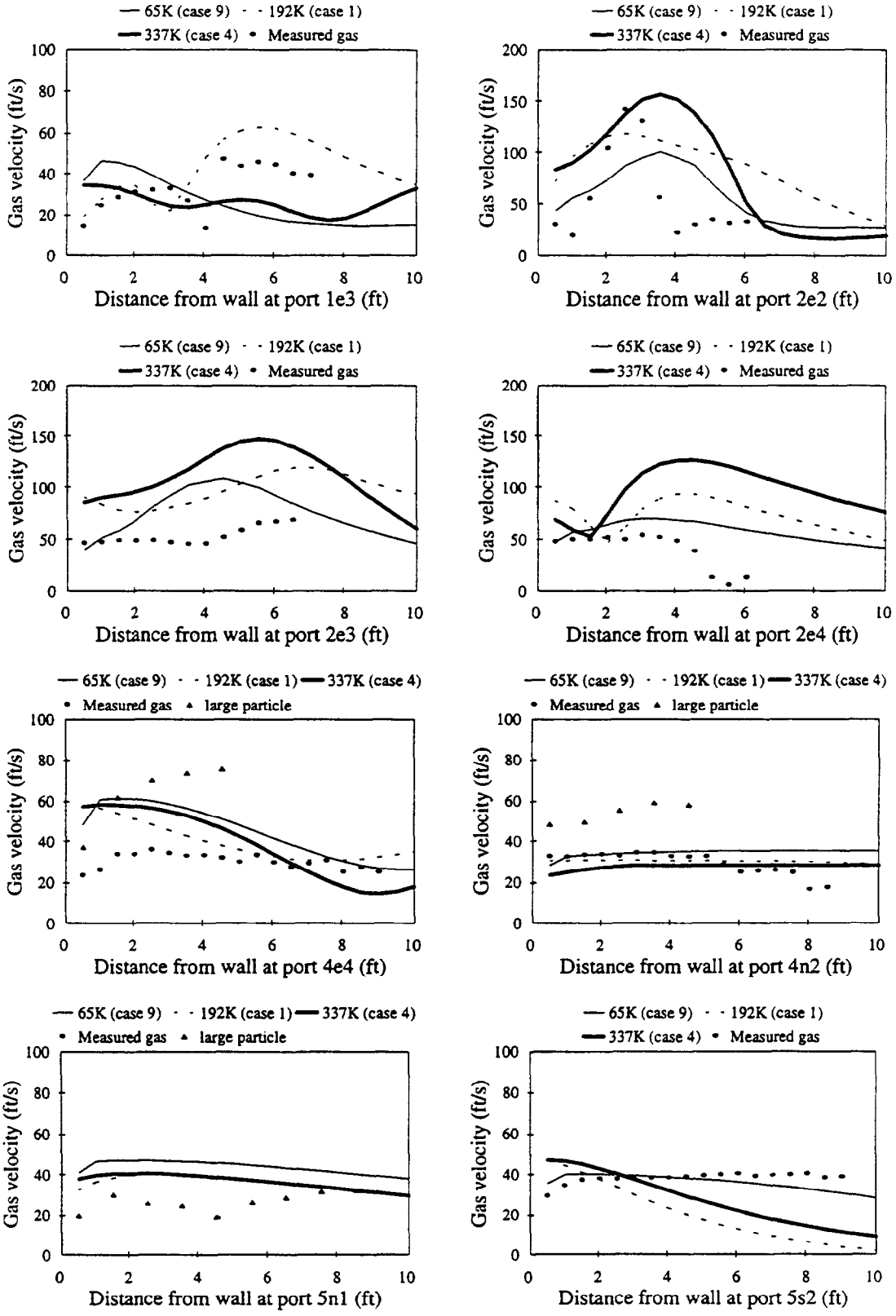

Figure A.4.1 Effect of grid size on gas velocity predictions (test 3, old devol.).

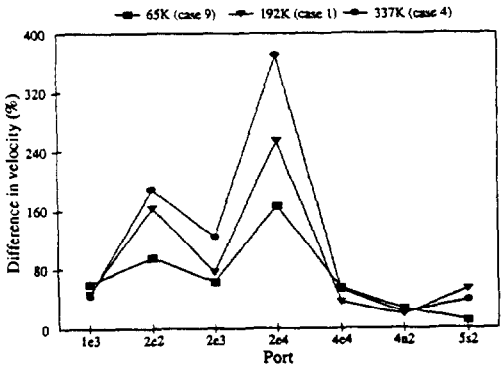

Figure A.4.2 Average port percent differences for 65K, 192K, and 337K grids (test 3, old Devil)

Appendix B

Compares the effect of over-fire air (SOFA) injection point and amount

Appendix B illustrates the effect of SOFA variation and compares the 337K predictions with the "new" devolatilization constants with the comparable measurements from Test 3 (B.1), test 4 (B.2), & test 5 (B.3). The better comparisons are in the upper part of the furnace. It is believed that the near-burner region can be improved with better burner flow modeling. This is most evident not only in the O_2 comparisons (Figures B.1.1-8), but in the velocity comparisons (Figure B.4) where the difference between the predicted and measured quantities is the largest in the near-burner region (see figures B.4.4 and B.4.5). This difficulty arose when ABB/CE indicated that the details of their burner were proprietary along with damper correlation uncertainties. The first inputs for burner velocity were estimated from the secondary air flow areas from the construction drawings. Also, there is not a linear relationship between damper setting and air flow. Thus, the best estimate for division of air flow in the burner region probably comes from the measured dusty pitot tube values even when considering the problems associated with pitot tube measurements in a high turbulence field.

The Appendix B figures are separated for ease of comparison as follows:

B.1 Comparisons for Test 3 (40% SOFA).

B.2 Comparisons for Test 4 (0% SOFA).

B.3 Comparisons for Test 5 (100% SOFA).

B.4.1-2 Comparisons for the 337K grid.

B.4.3-4 Comparisons for point-for-point average differences for each test and the noted predictions (It is significant to note that the near-field velocity differences are larger for the test 3 and 5 models than for the test 4 model. This illuminates the difficulty of modeling the SOFA flows in near-burner field.

B.4.5-7 Average percent difference between predicted and measured values for tests 3, 4, and 5.

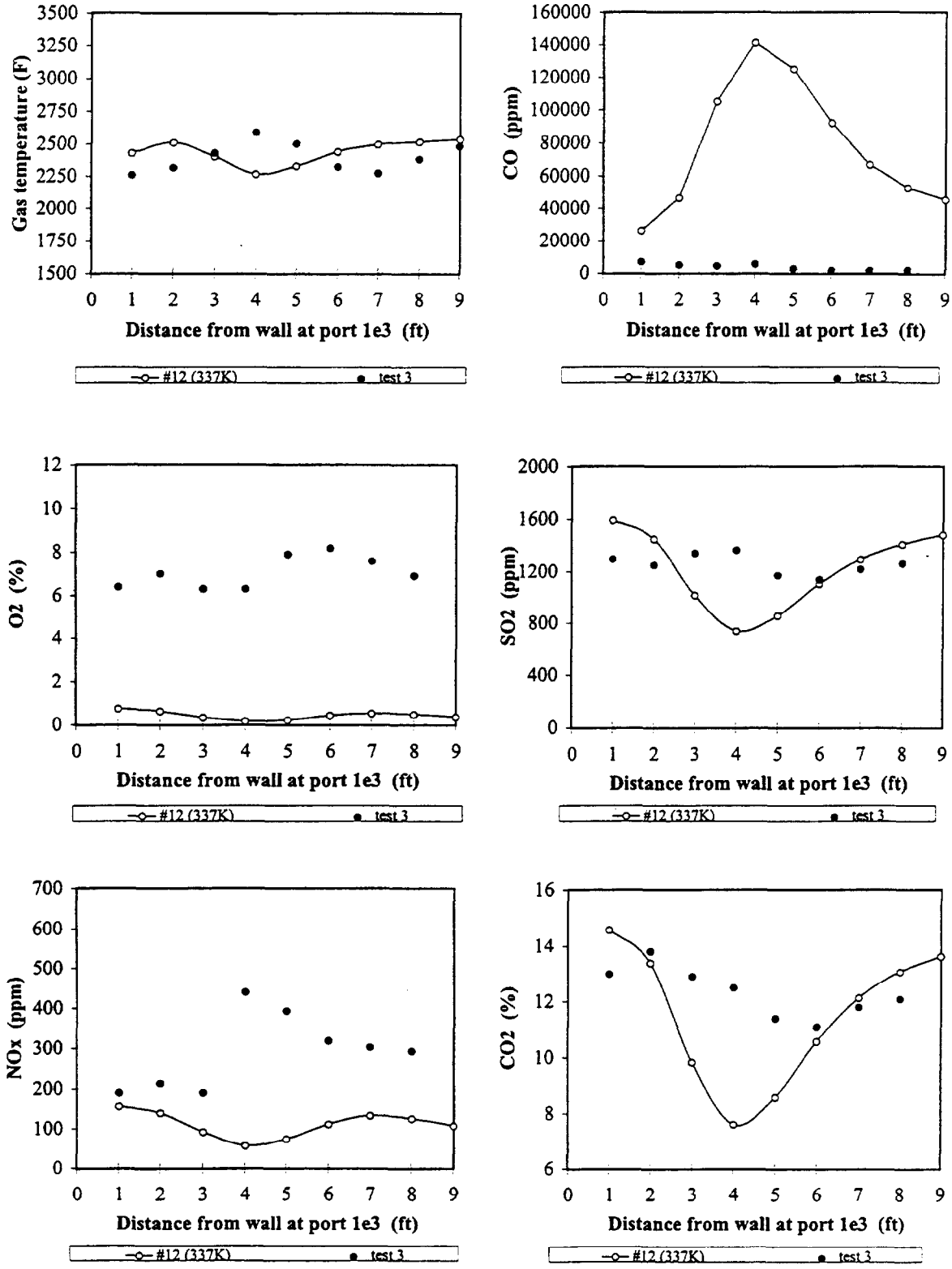

Figure B.1.1 Measured and predicted values for case 12 at port 1e3

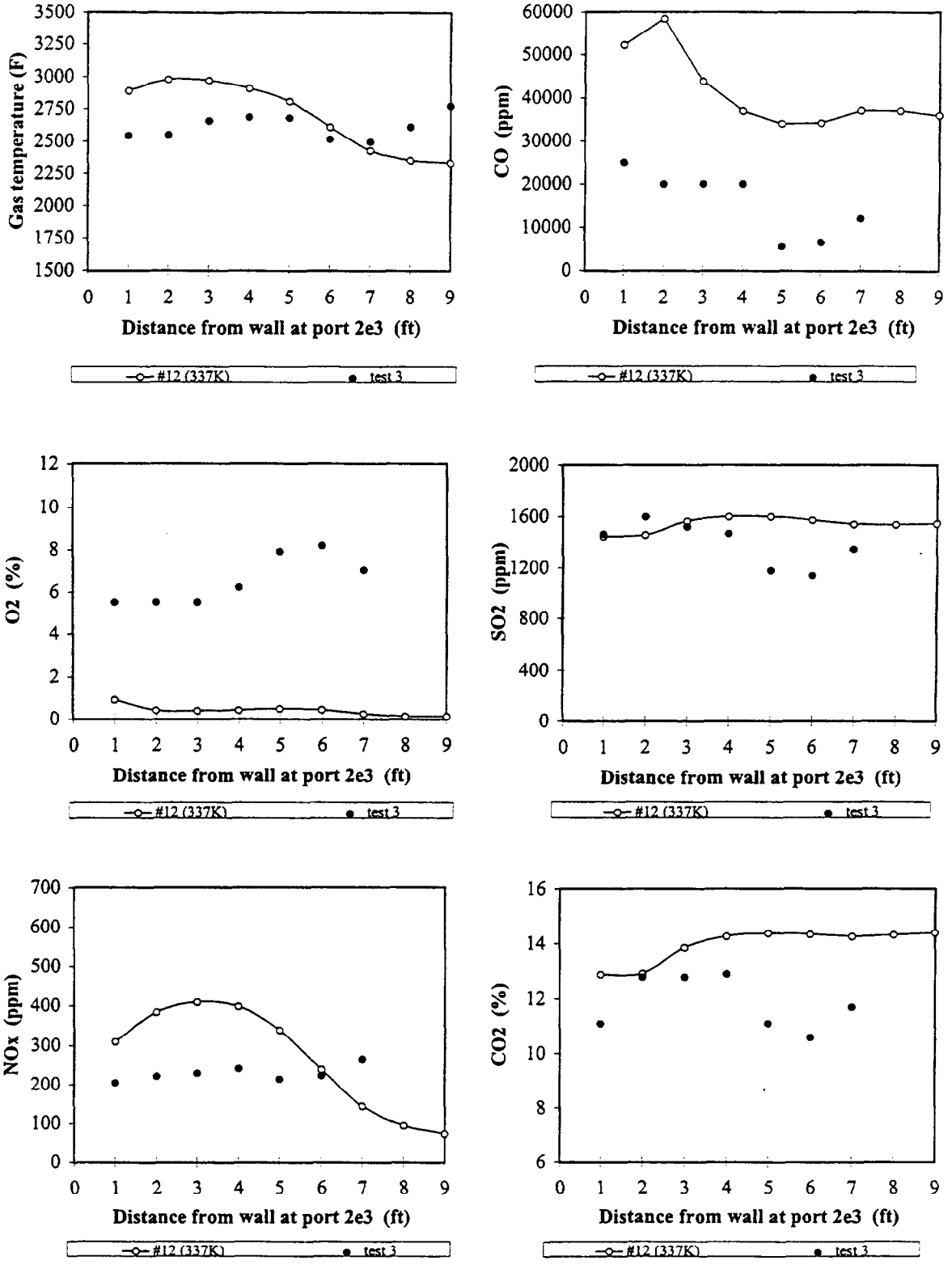

Figure B.1.2 Measured and predicted values for case 12 at port 2e3

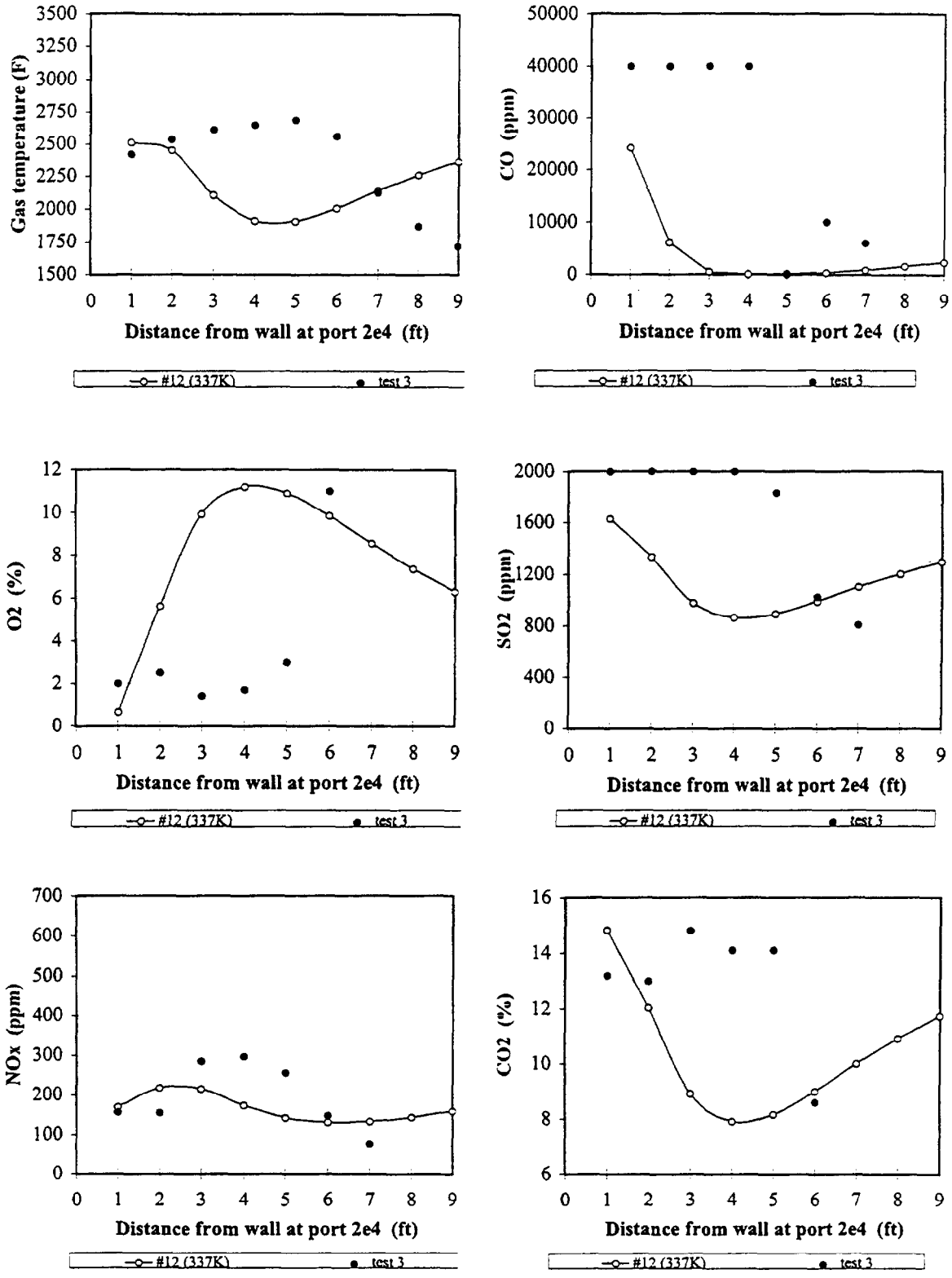

Figure B.1.3 Measured and predicted values for case 12 at port 2e4

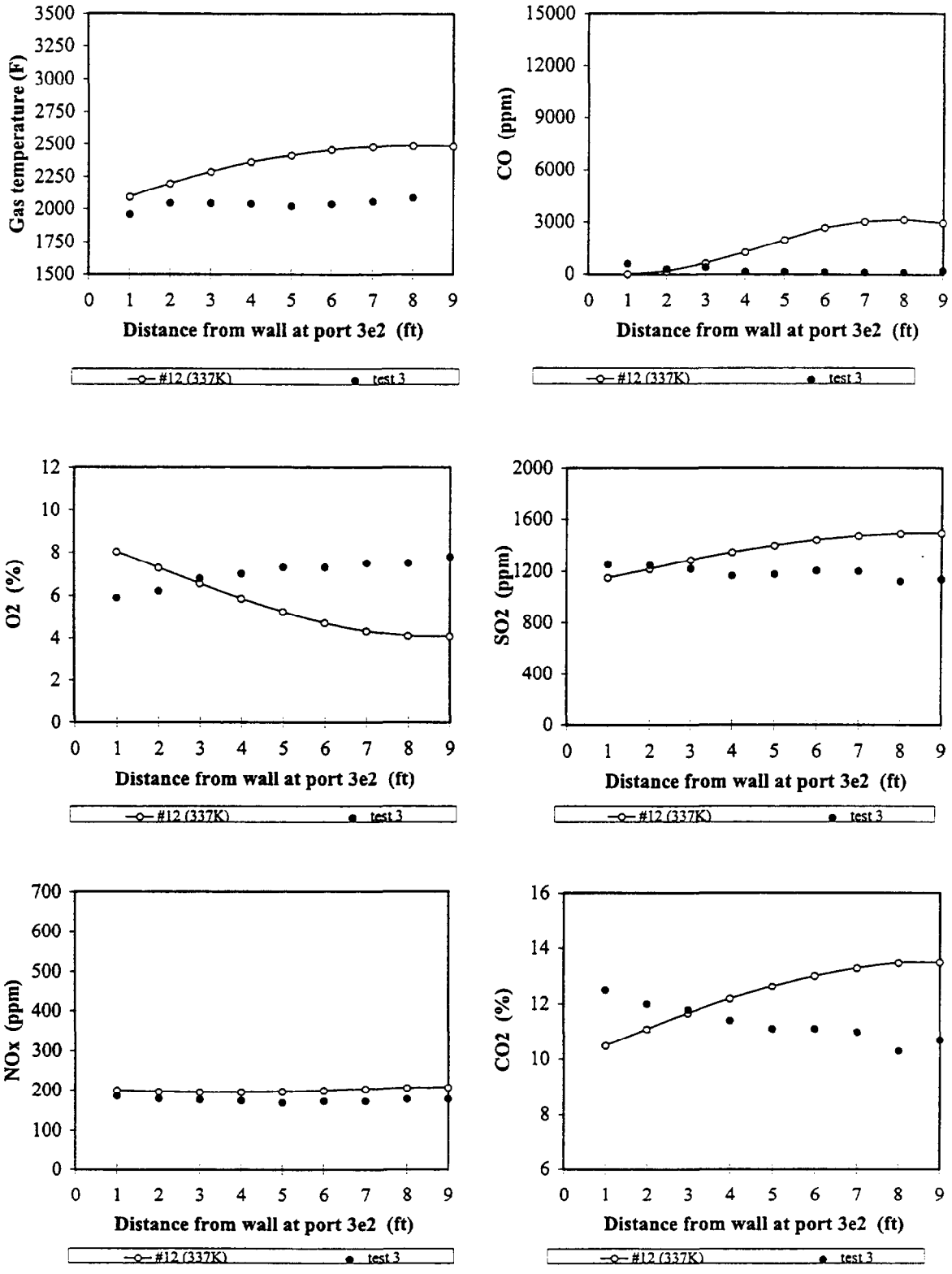

Figure B.1.4 Measured and predicted values for case 12 at port 3e2

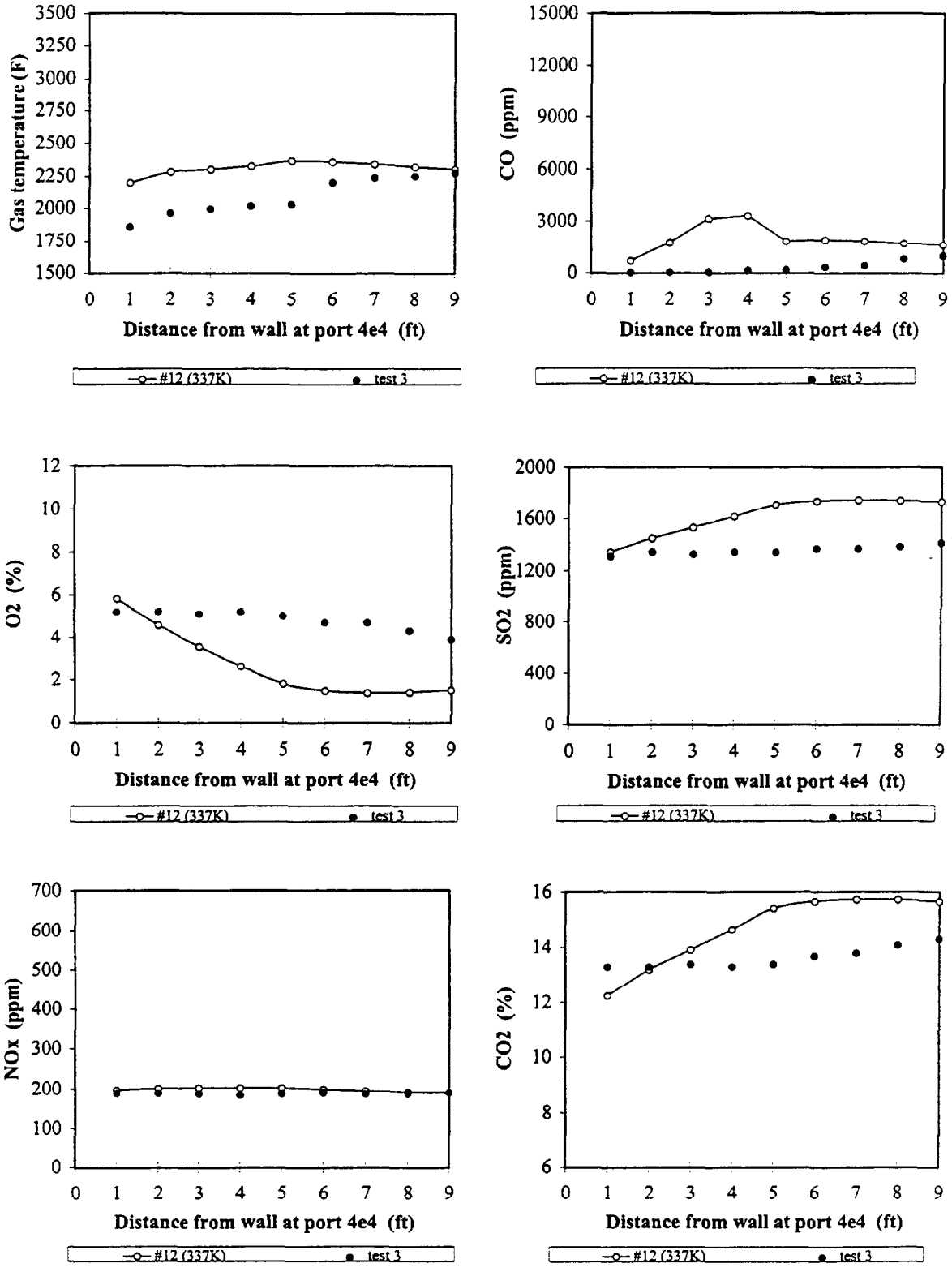

Figure B.1.5 Measured and predicted values for case 12 at port 4e4

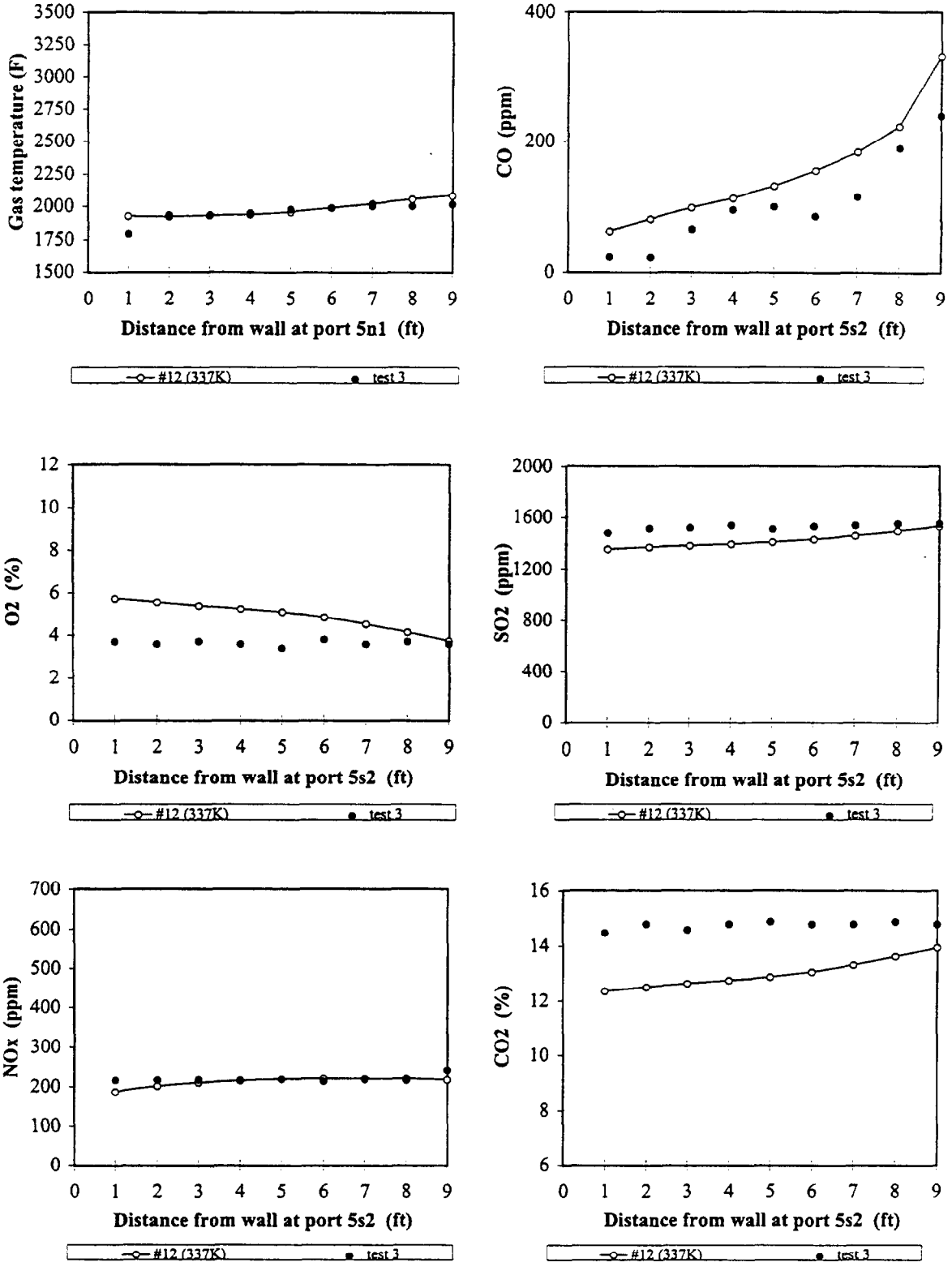

Figure B.1.6 Measured and predicted values for case 12 at level 5

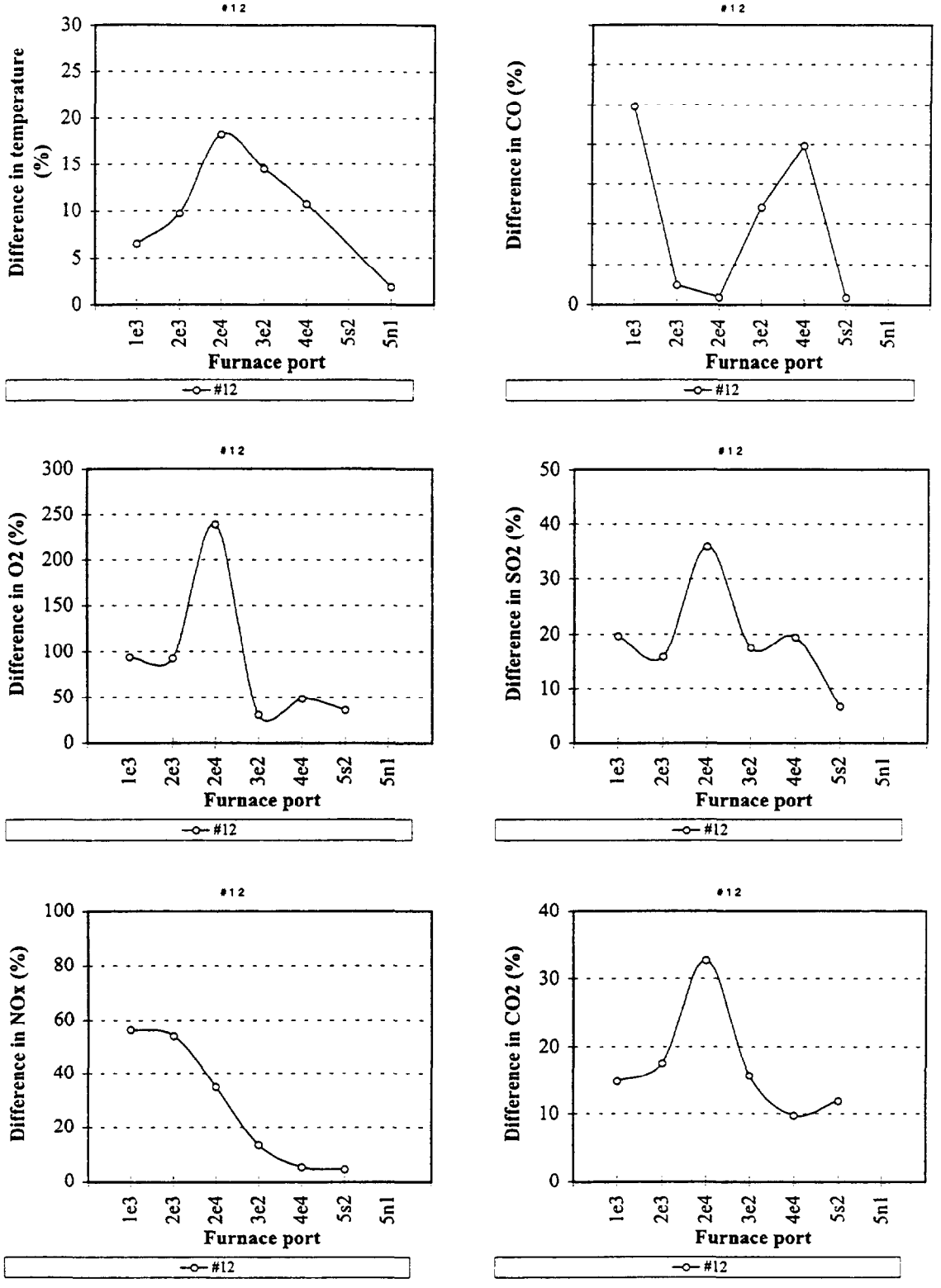

Figure B.1.7 Difference between predictions and measurements for case 12.

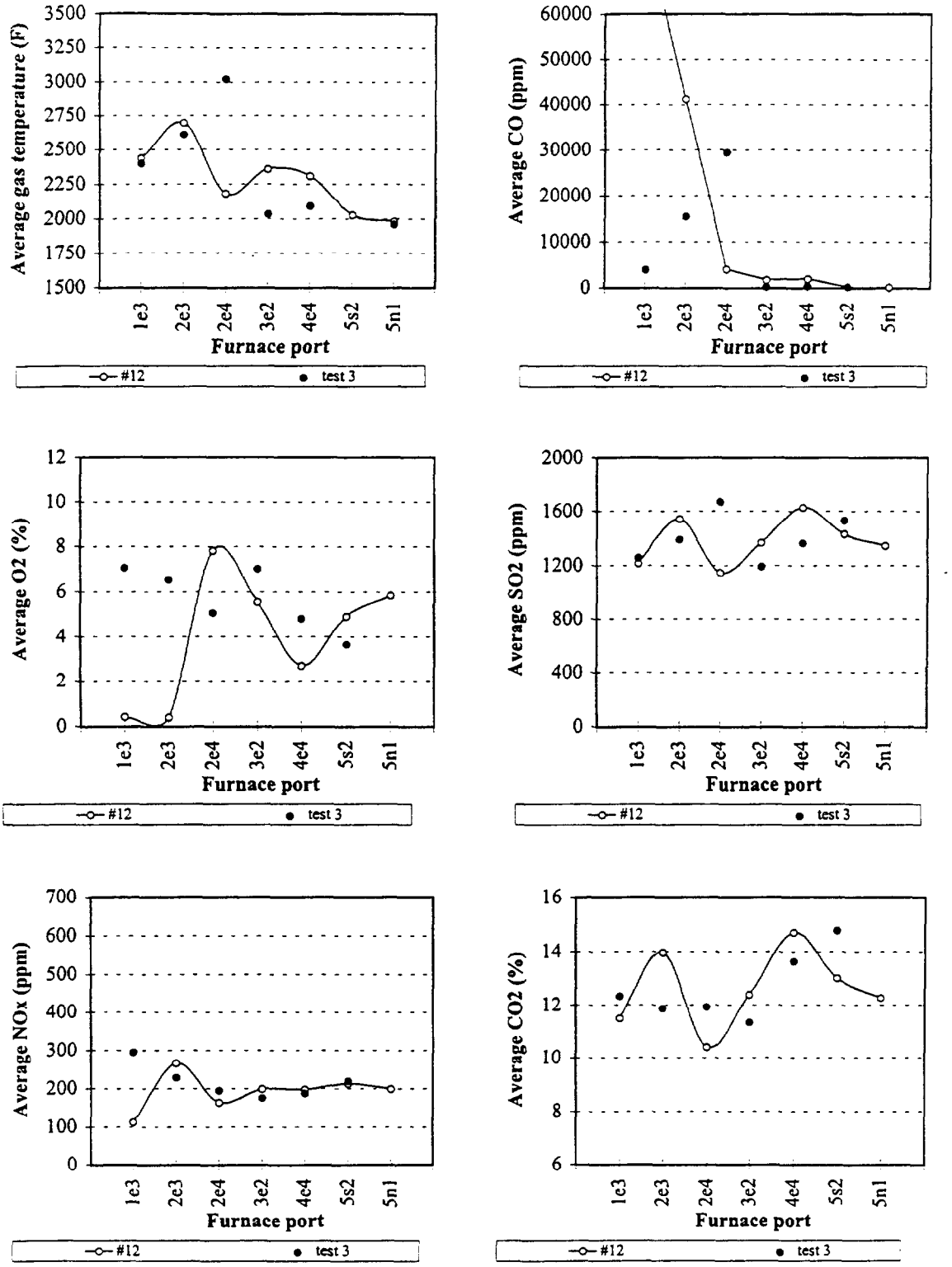

Figure B.1.8 Averaged measured and predicted values for case 12.

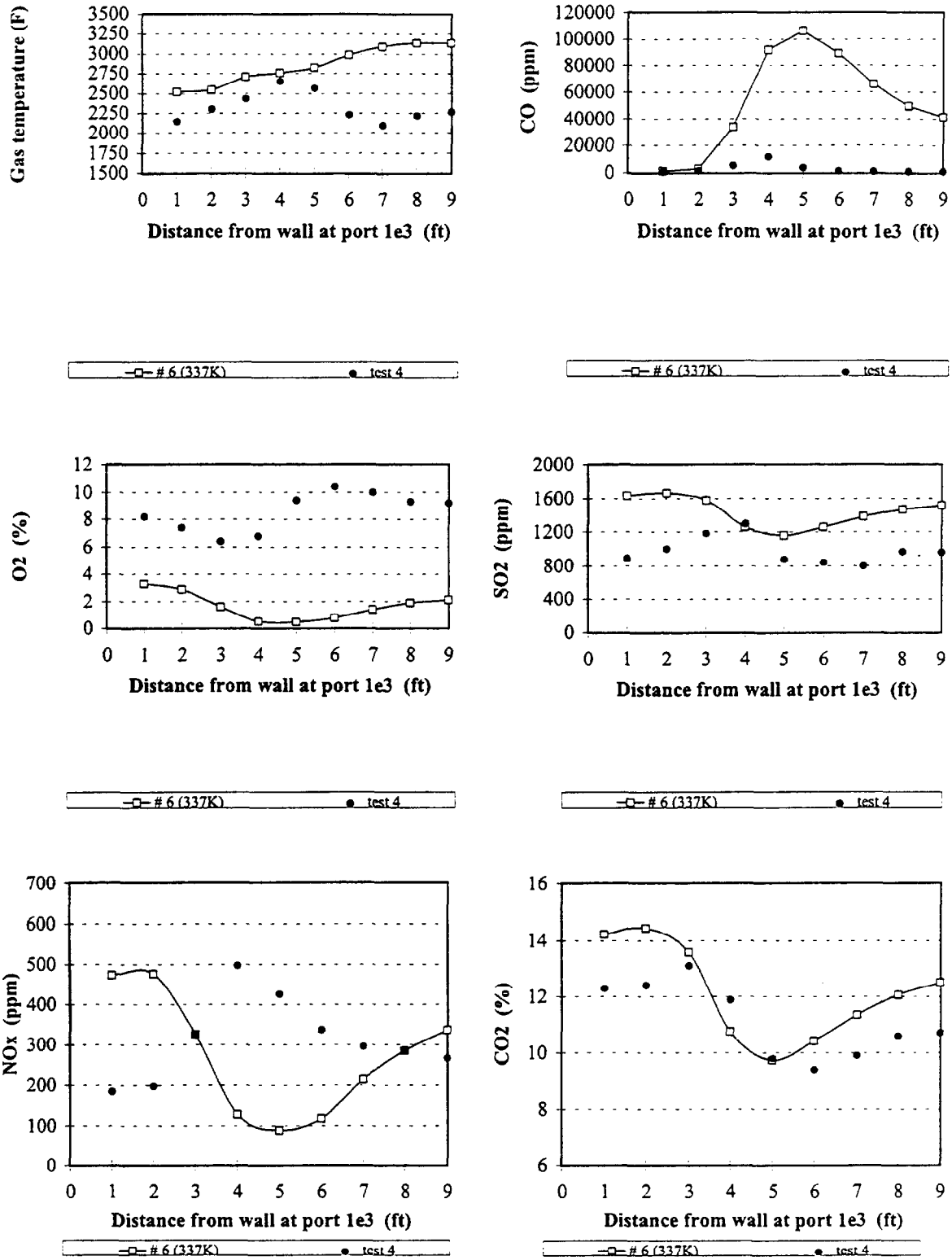

Figure B.2.1 Measured and predicted values for case 6 at port 1e3

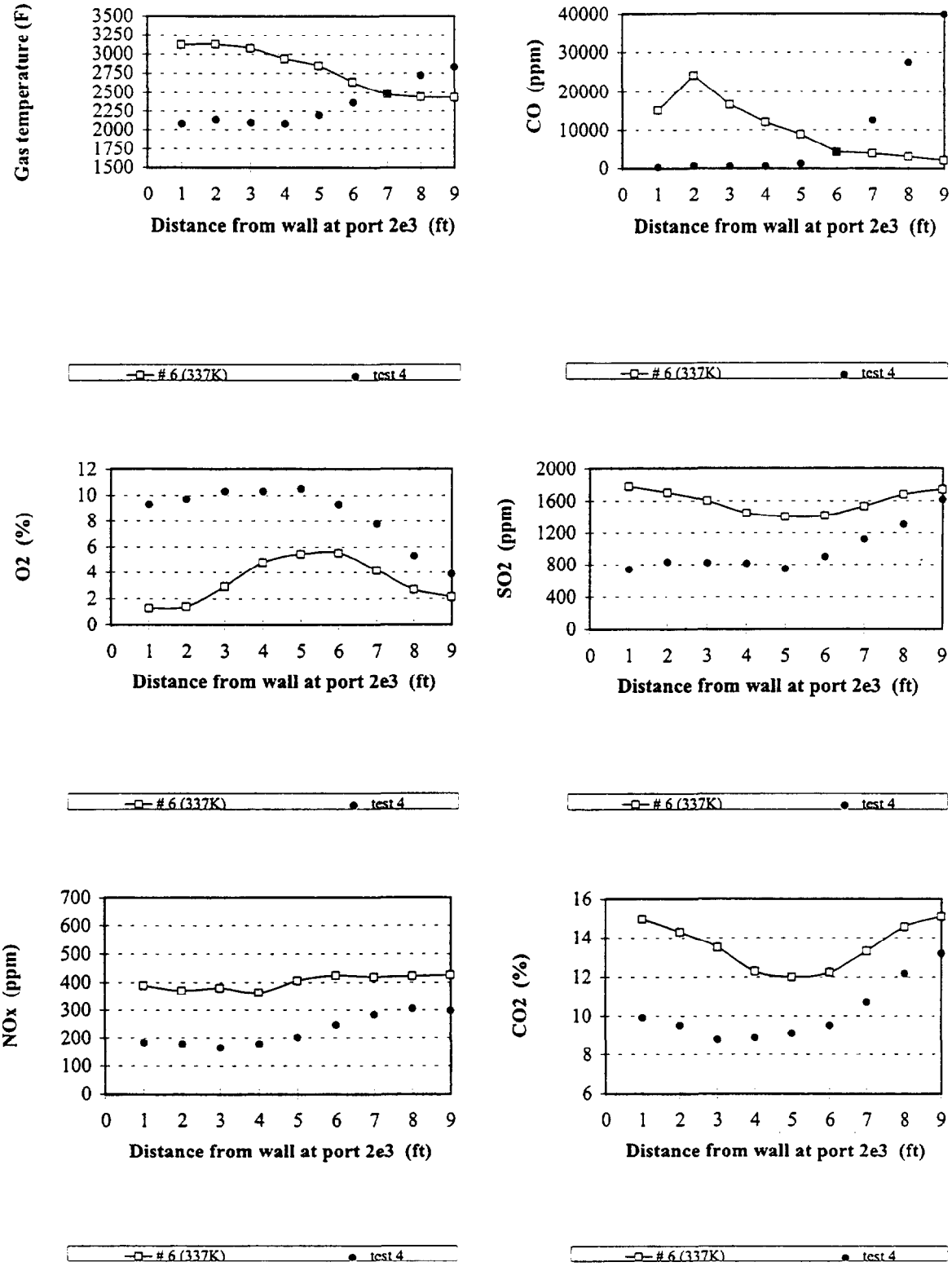

Figure B.2.2 Measured and predicted values for case 6 at port 2e3

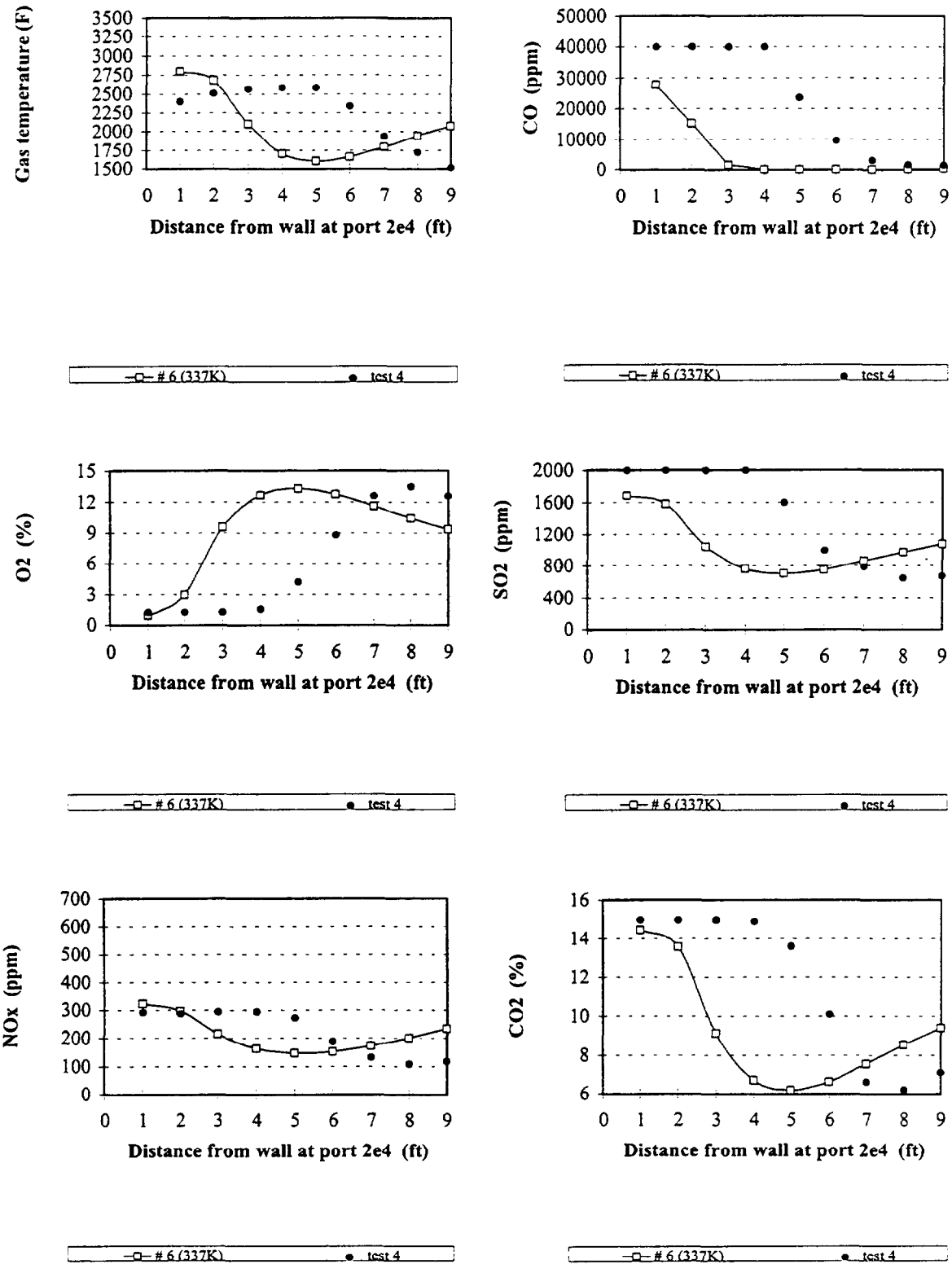

Figure B.2.3 Measured and predicted values for case 6 at port 2e4

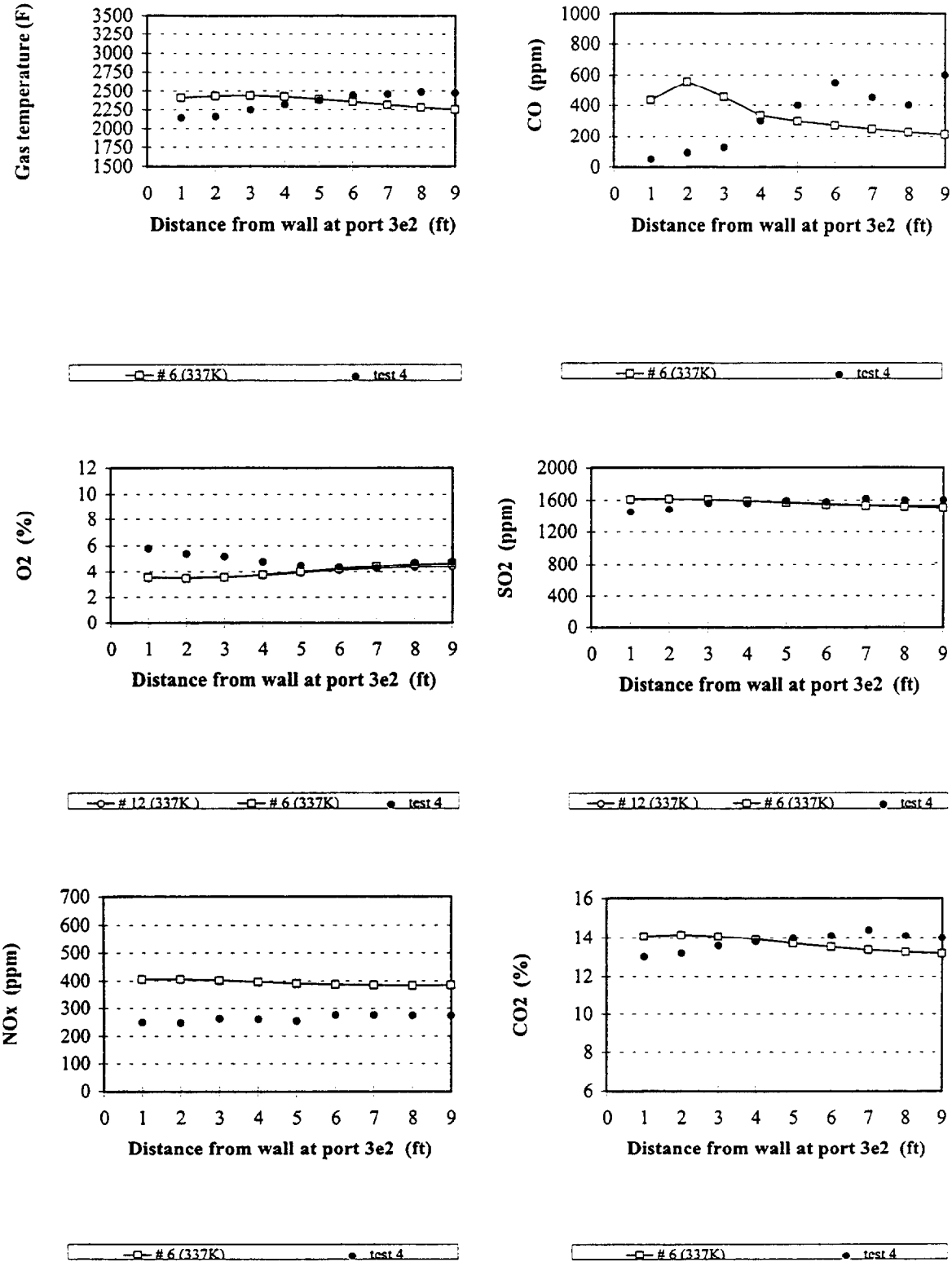

Figure B.2.4 Measured and predicted values for case 6 at port 3e2

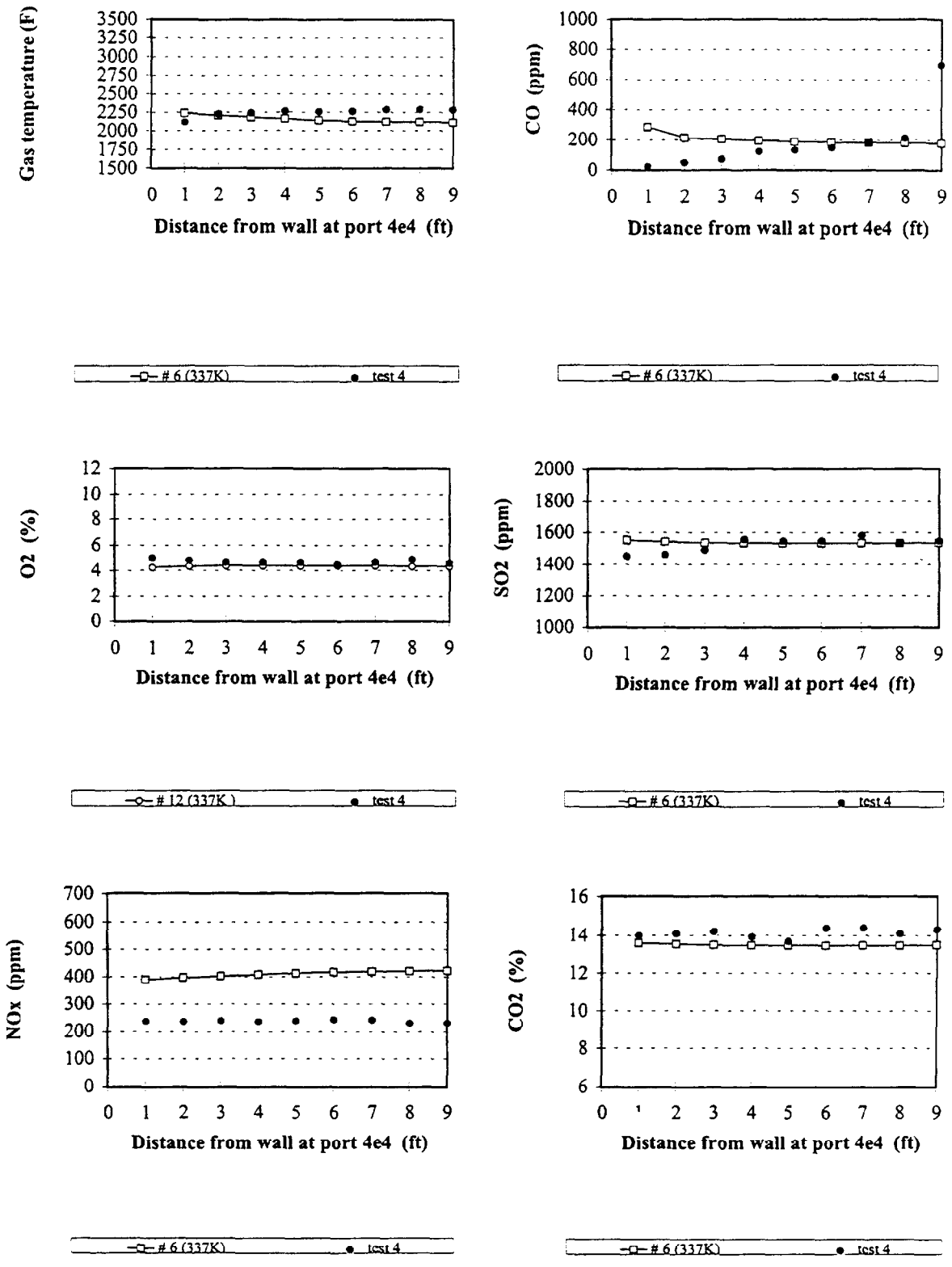

Figure B.2.5 Measured and predicted values for case 6 at port 4e4

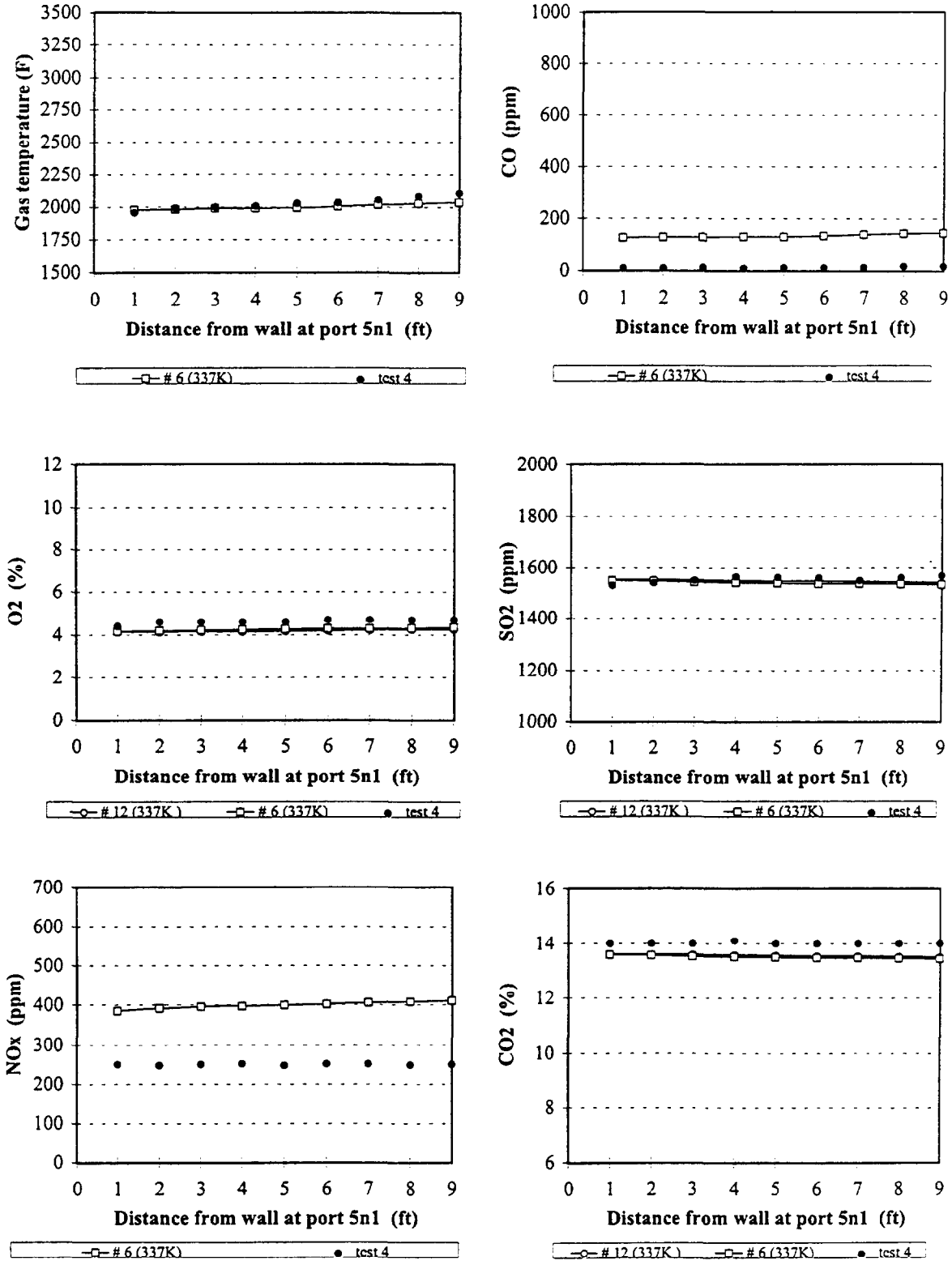

Figure B.2.6 Measured and predicted values for case 6 at level 5

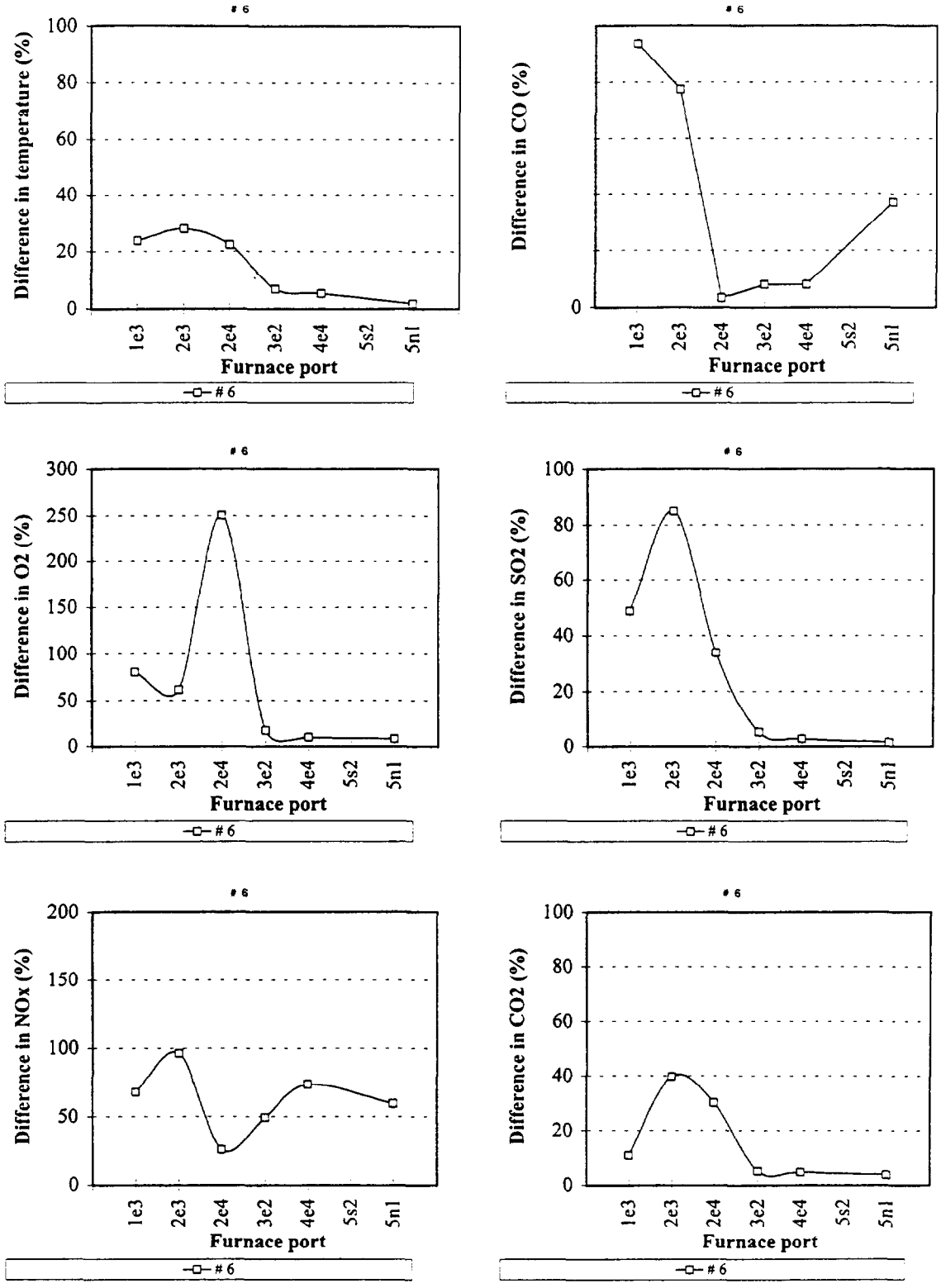

Figure B.2.7 Difference between predictions and measurements for case 6

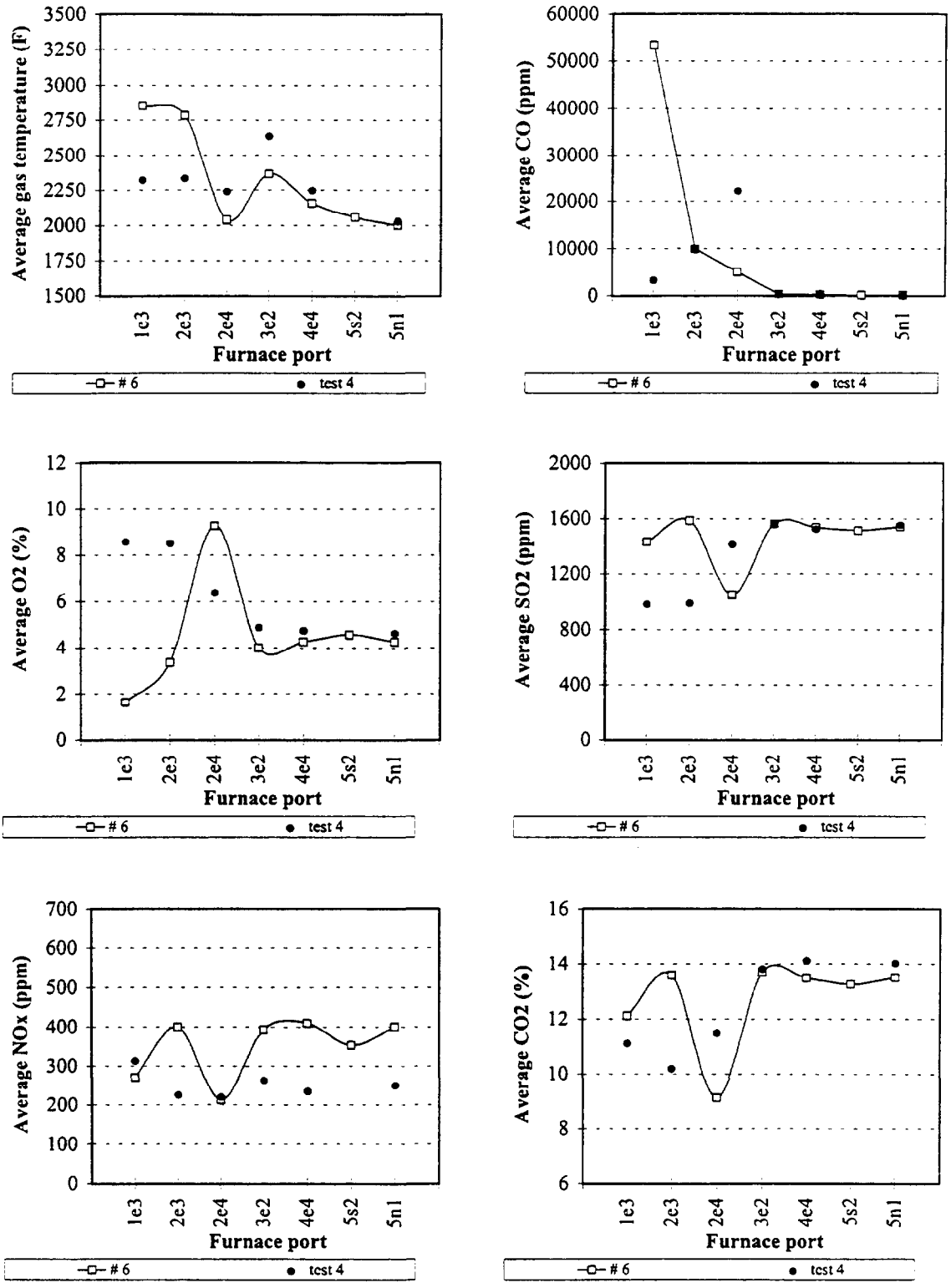

Figure B.2.8 Averaged measured and predicted values for case 6

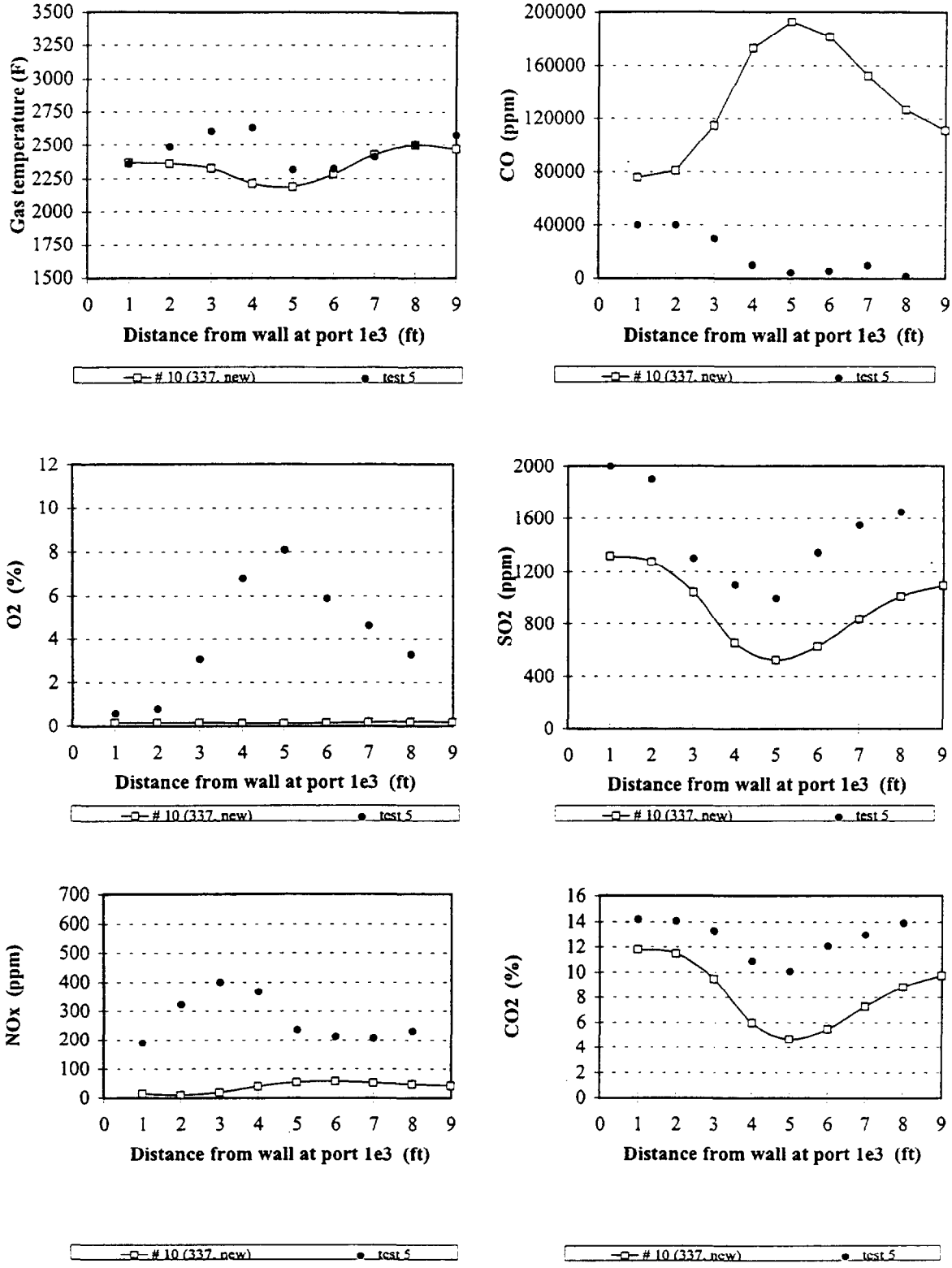

Figure B.3.1 Measured and predicted values for case 10 at port 1e3

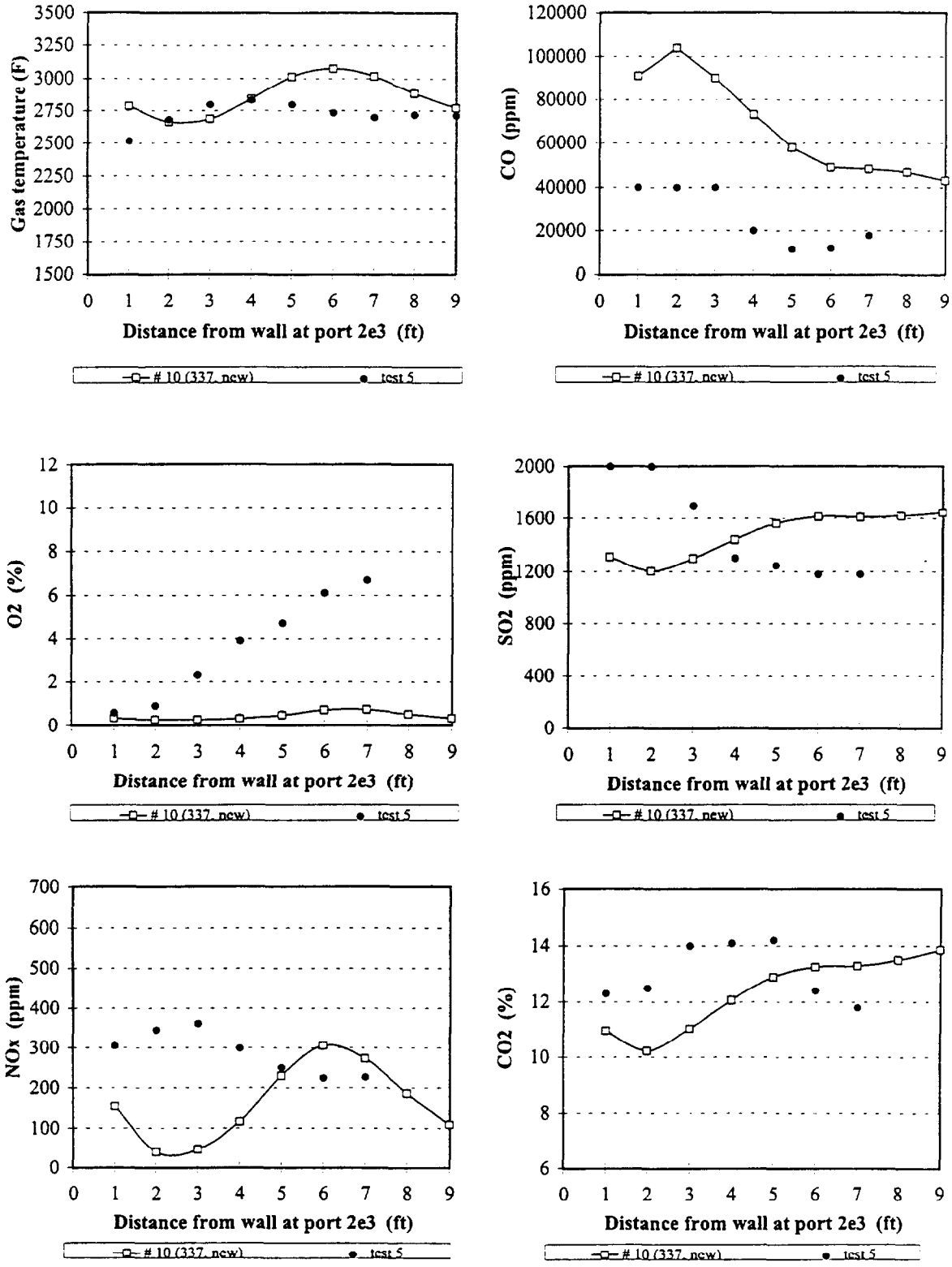

Figure B.3.2 Measured and predicted values for case 10 at port 2e3

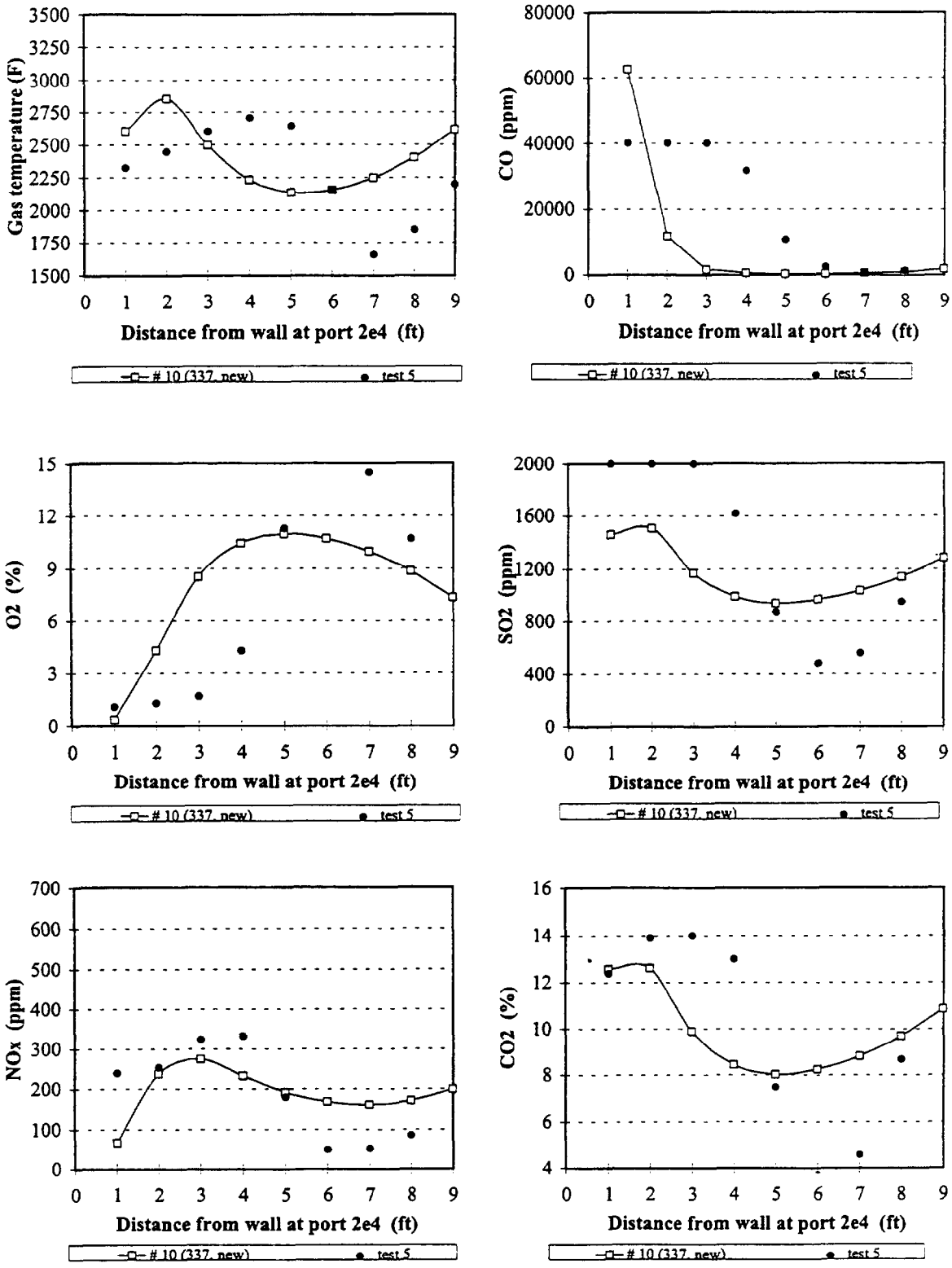

Figure B.3.3 Measured and predicted values for case 10 at port 2e4

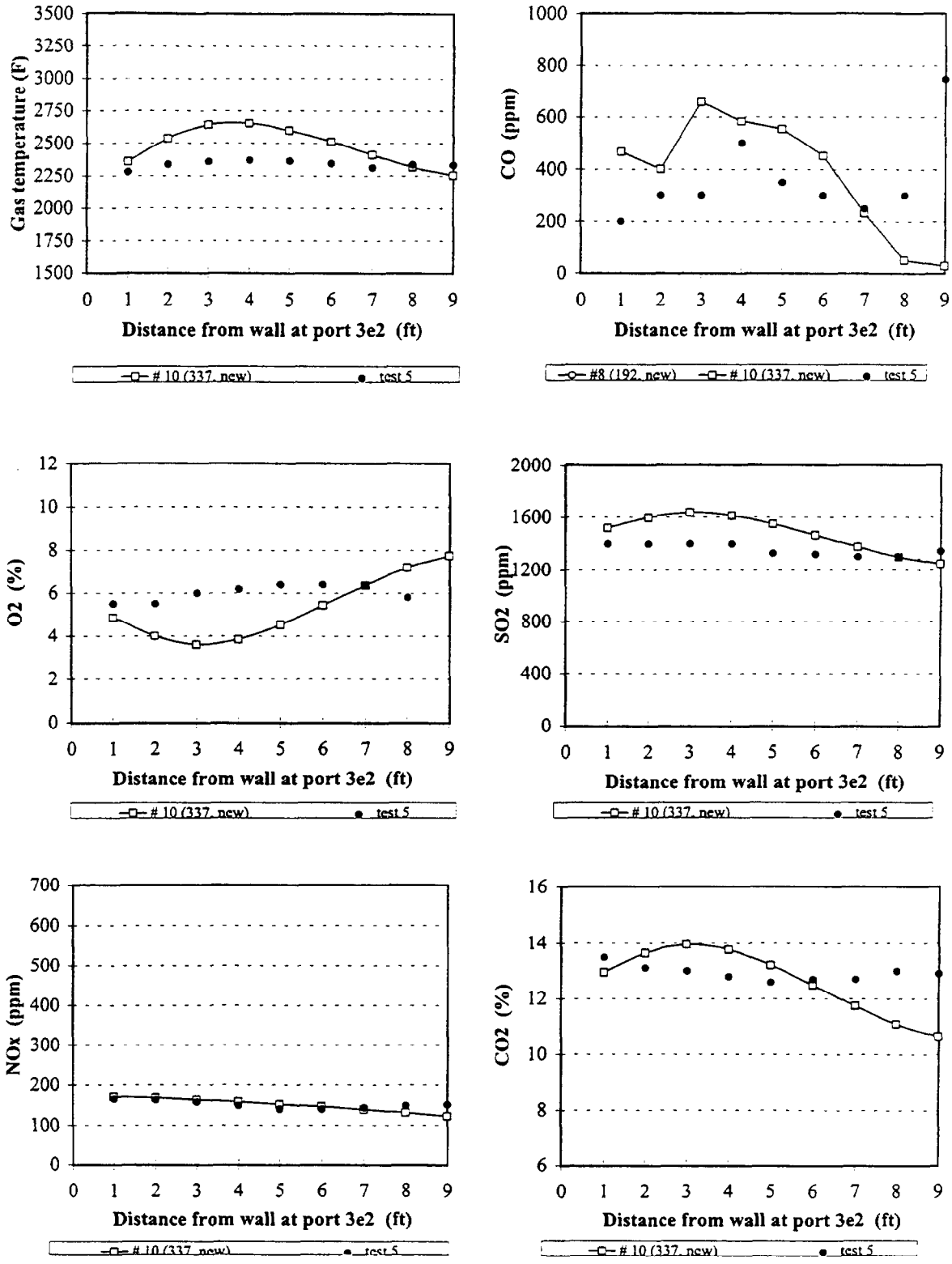

Figure B.3.4 Measured and predicted values for case 10 at port 3e2

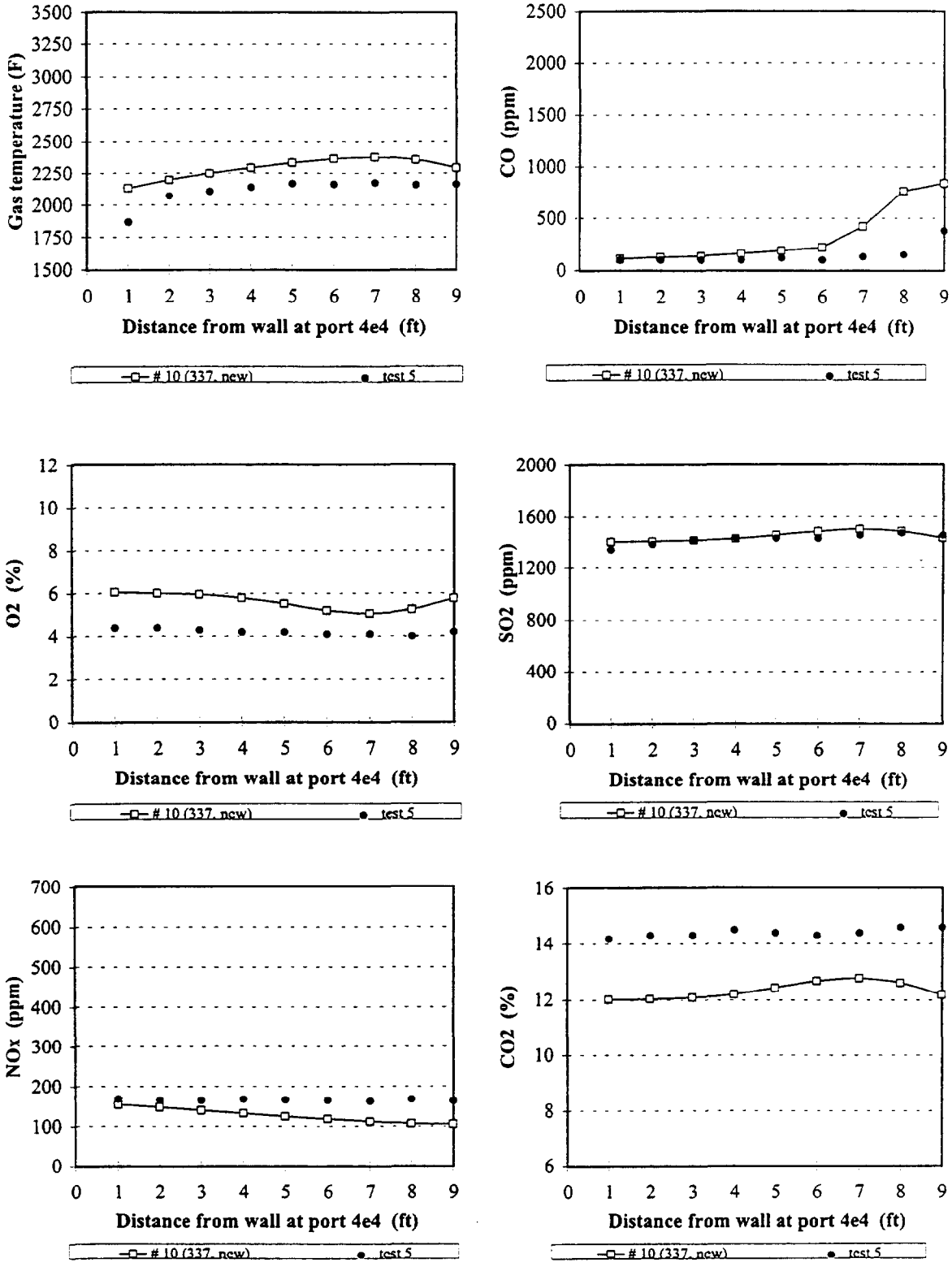

Figure B.3.5 Measured and predicted values for case 10 at port 4e4

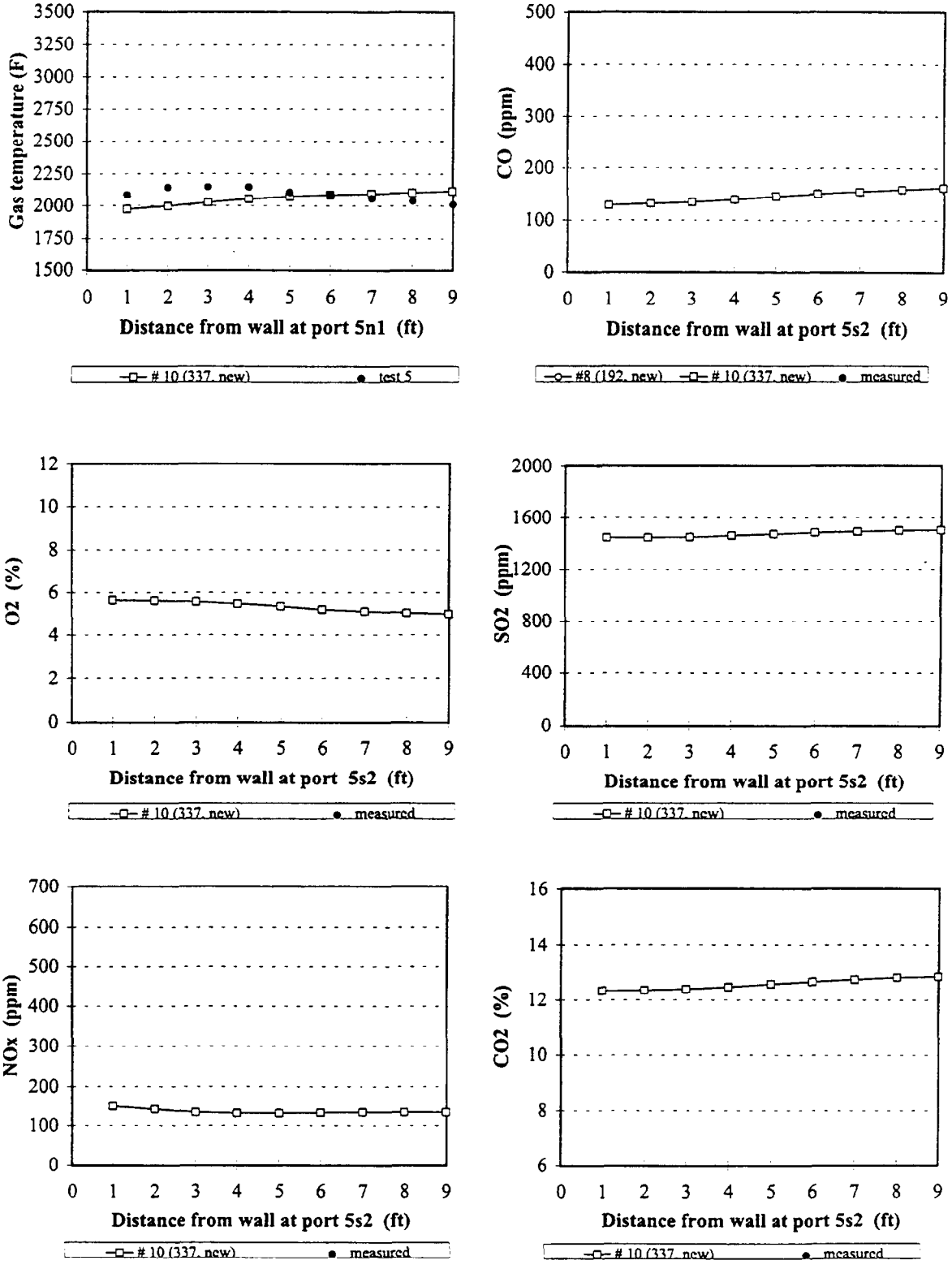

Figure B.3.6 Measured and predicted values for case 10 at port 5n1

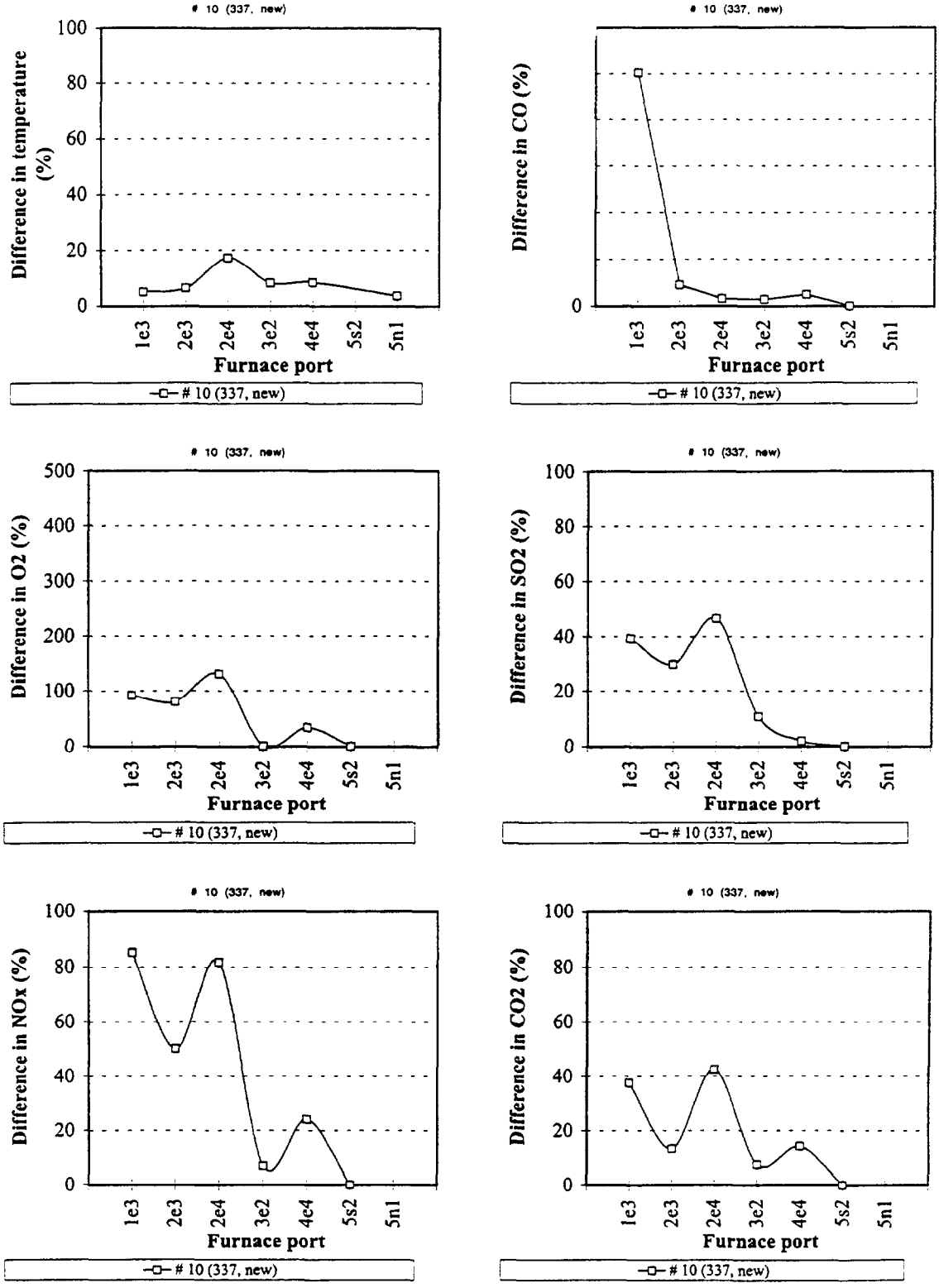

Figure B.3.7 Average Difference between Prediction and Measurement by Port

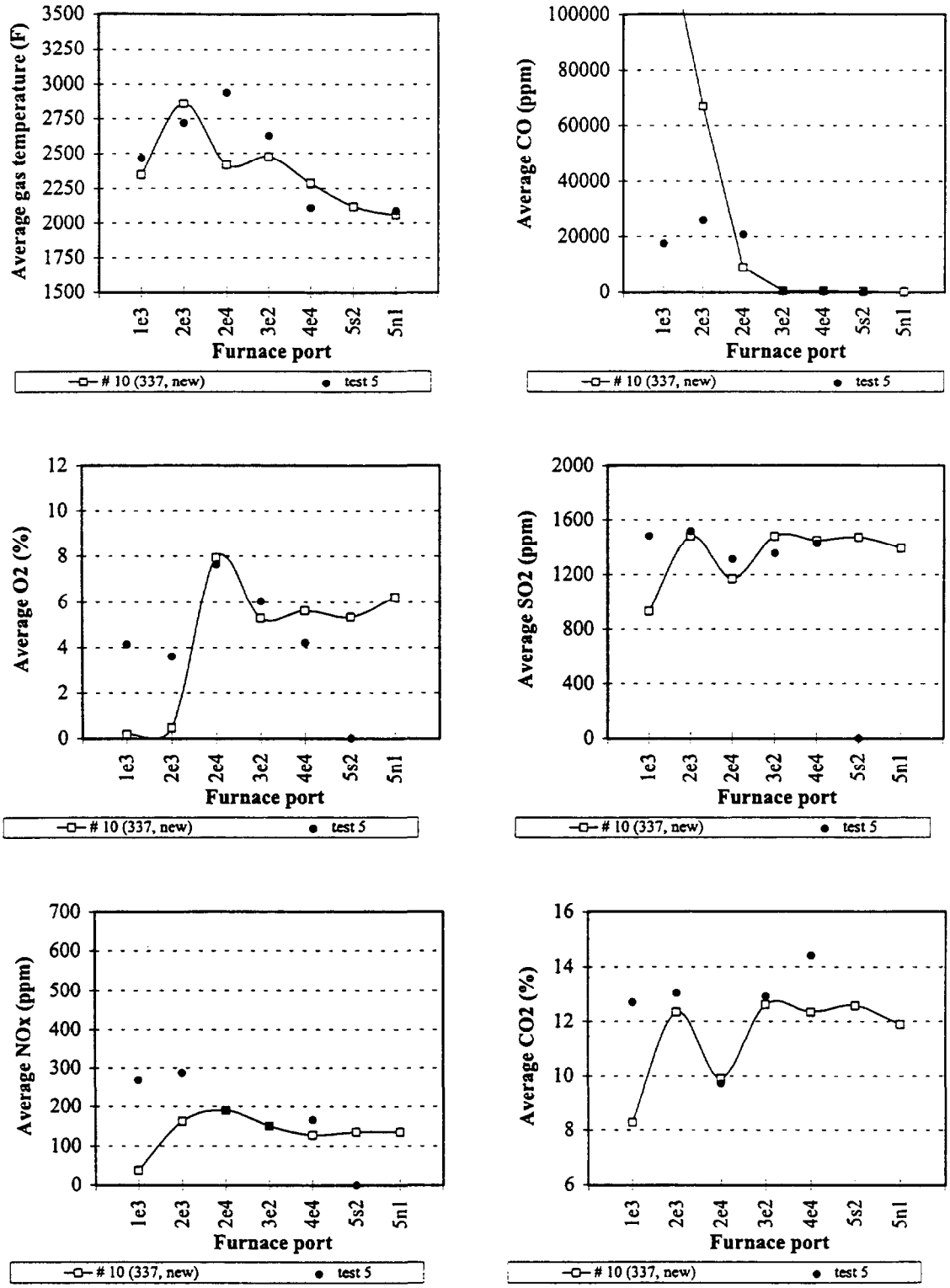

Figure B.3.8 Average measured and predicted values for case 10

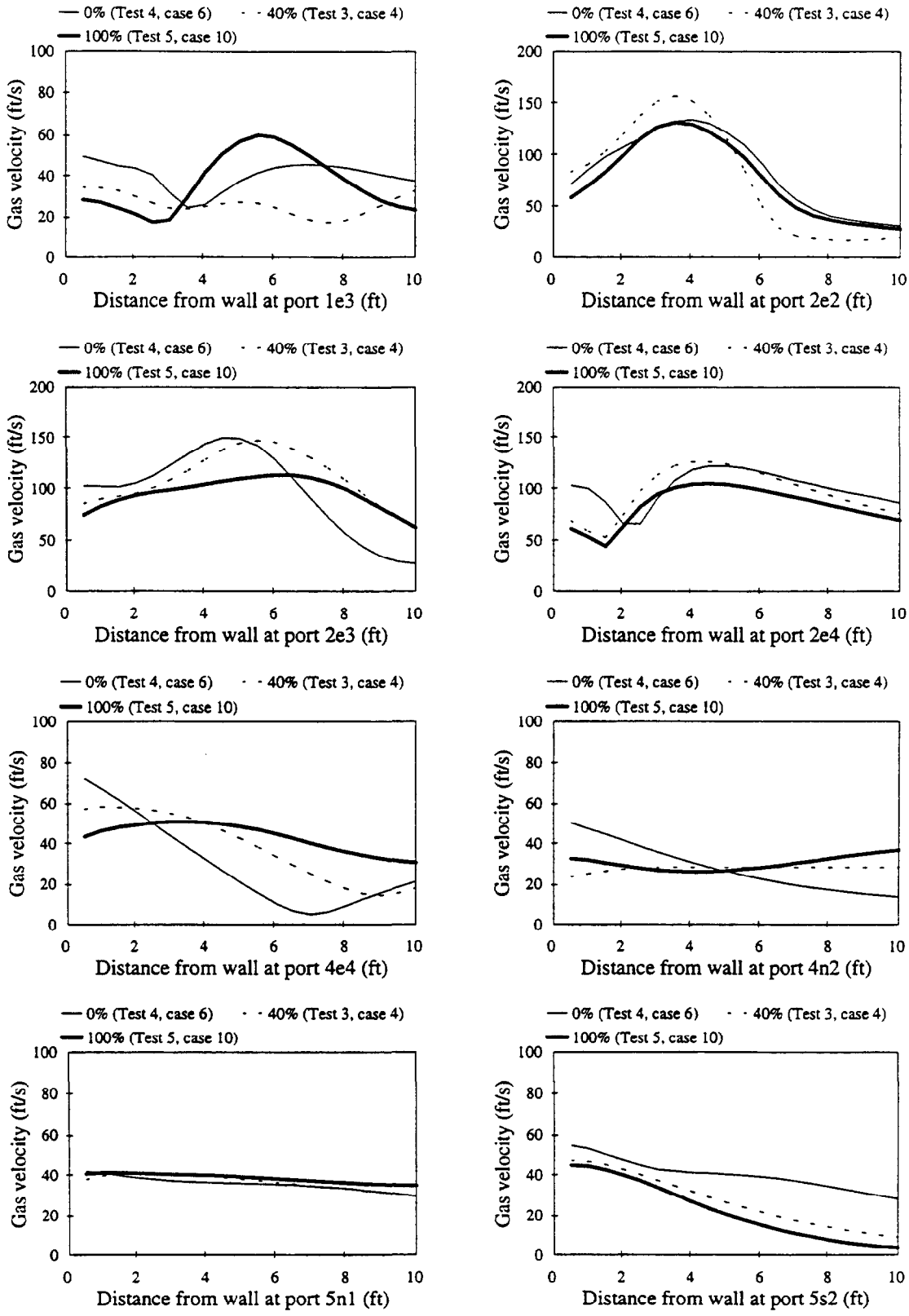

Figure B.4.1 Effect of SOFA on gas velocity predictions (337K grid).

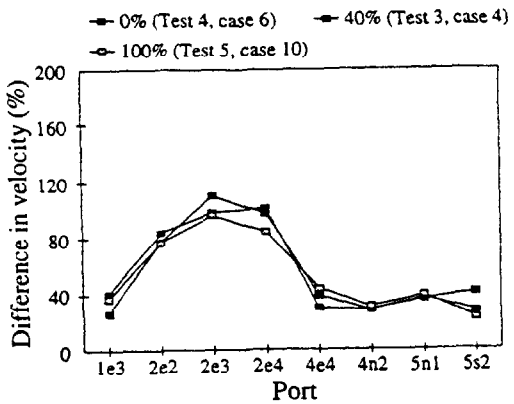

Figure B.4.2 Average difference for337K SOFA settings for each port

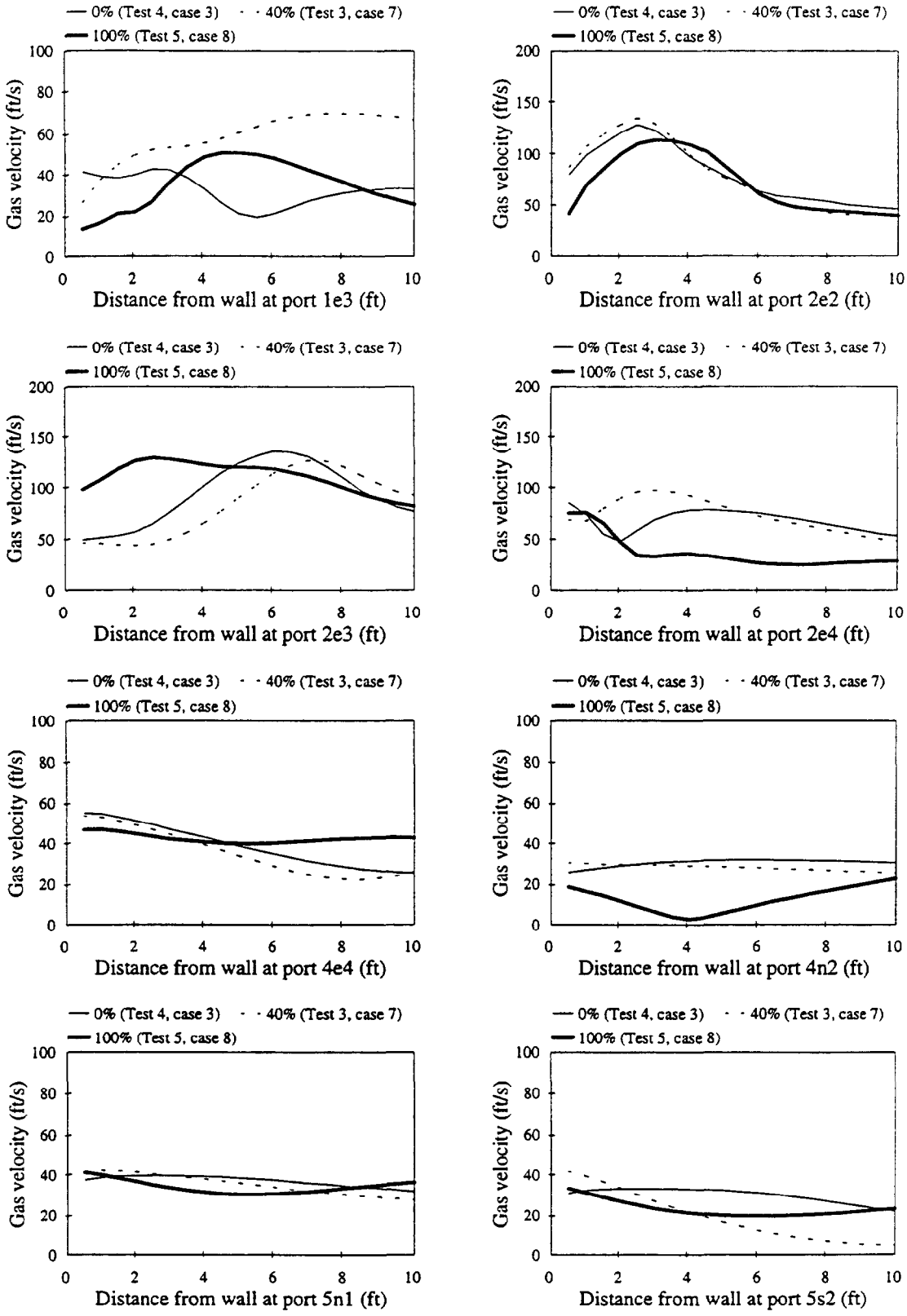

Figure B.4.3 Effect of SOFA on gas velocity predictions (192K grid).

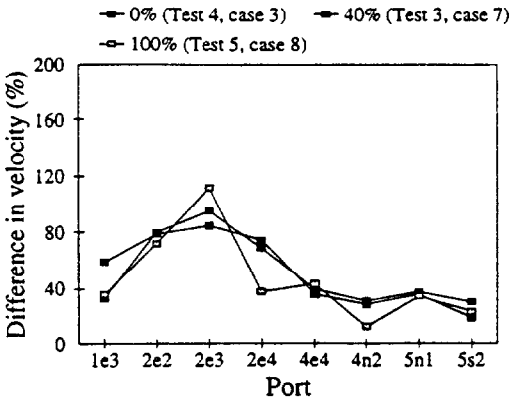

Figure B.4.4 Average Difference for 192K SOFA settings for each port

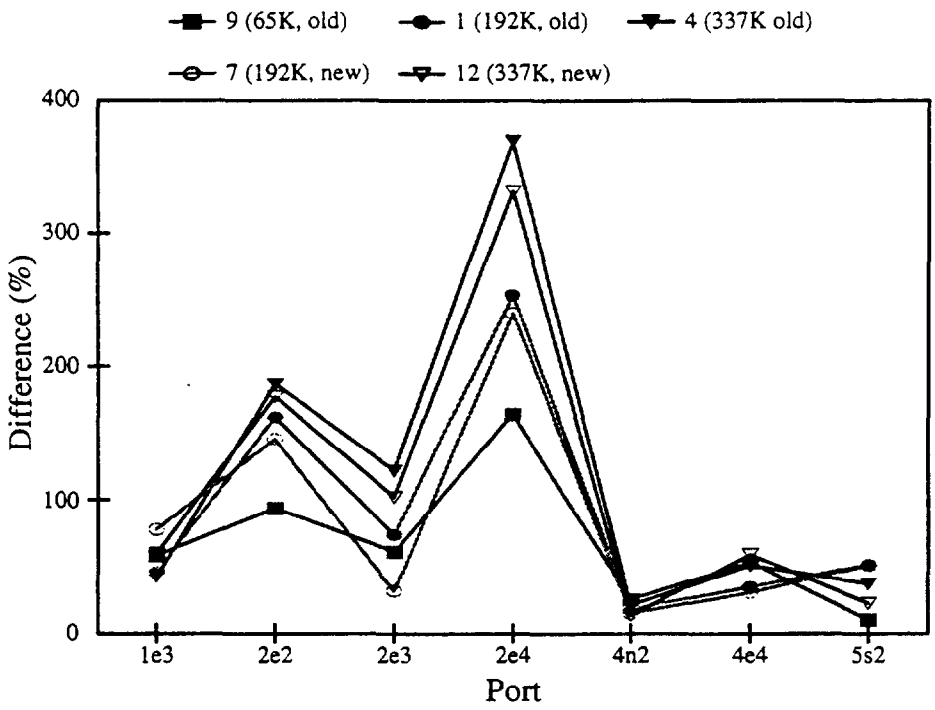

Figure B.4.5. Average percent difference between the predicted and measured gas velocities for test 3.(40% SOFA)

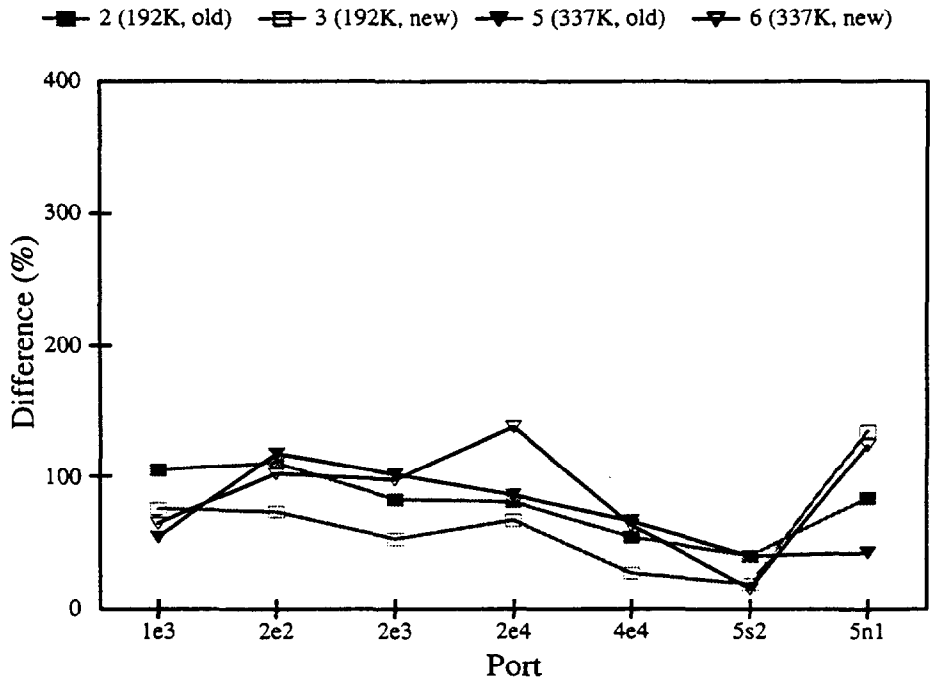

Figure B.4.6. Average percent difference between the predicted and measured gas velocities for test 4. (0% SOFA)

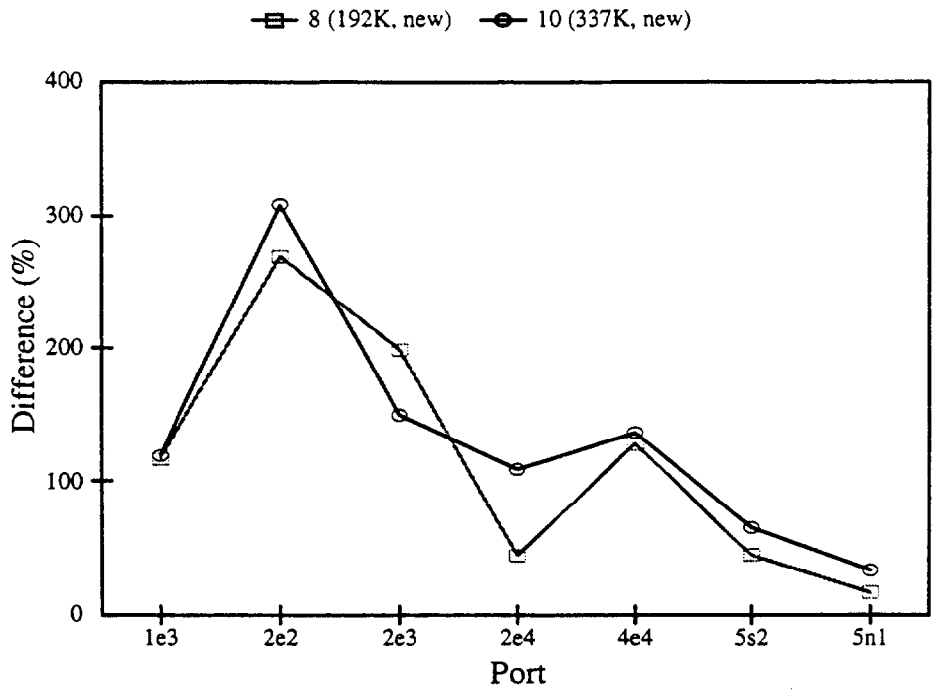

Figure B.4.7. Average percent difference between the predicted and measured gas velocities for test 5.(100% SOFA)

Appendix C

Compares the effect of changing the devolatilization rate constants

Appendix C shows the effect of varying the devolatilization constants (as noted in Table 2) for the 337K grid (C.1) and the 192K grid (C.2) and the velocity measurements (C.3). It is clear that the change in devolatilization constants makes a difference, albeit not as much perhaps as the grid size or SOFA variation, but significant nevertheless, especially in the near-burner field. This would be expected as the devolatilization constants impact where ignition occurs in the prediction program. The "old" devolatilization constants are derived from single particle drop-tube furnace data and are a good beginning point for setting the fundamental constants used in PCGC-3. However, the actual circumstance is not that of a single particle, but that of a cloud, which is significantly different and justifies the use of an alternate constants identified as the "new devolatilization" constants.

While not a clear case, the "new" constants appear to be slightly better than the "old".

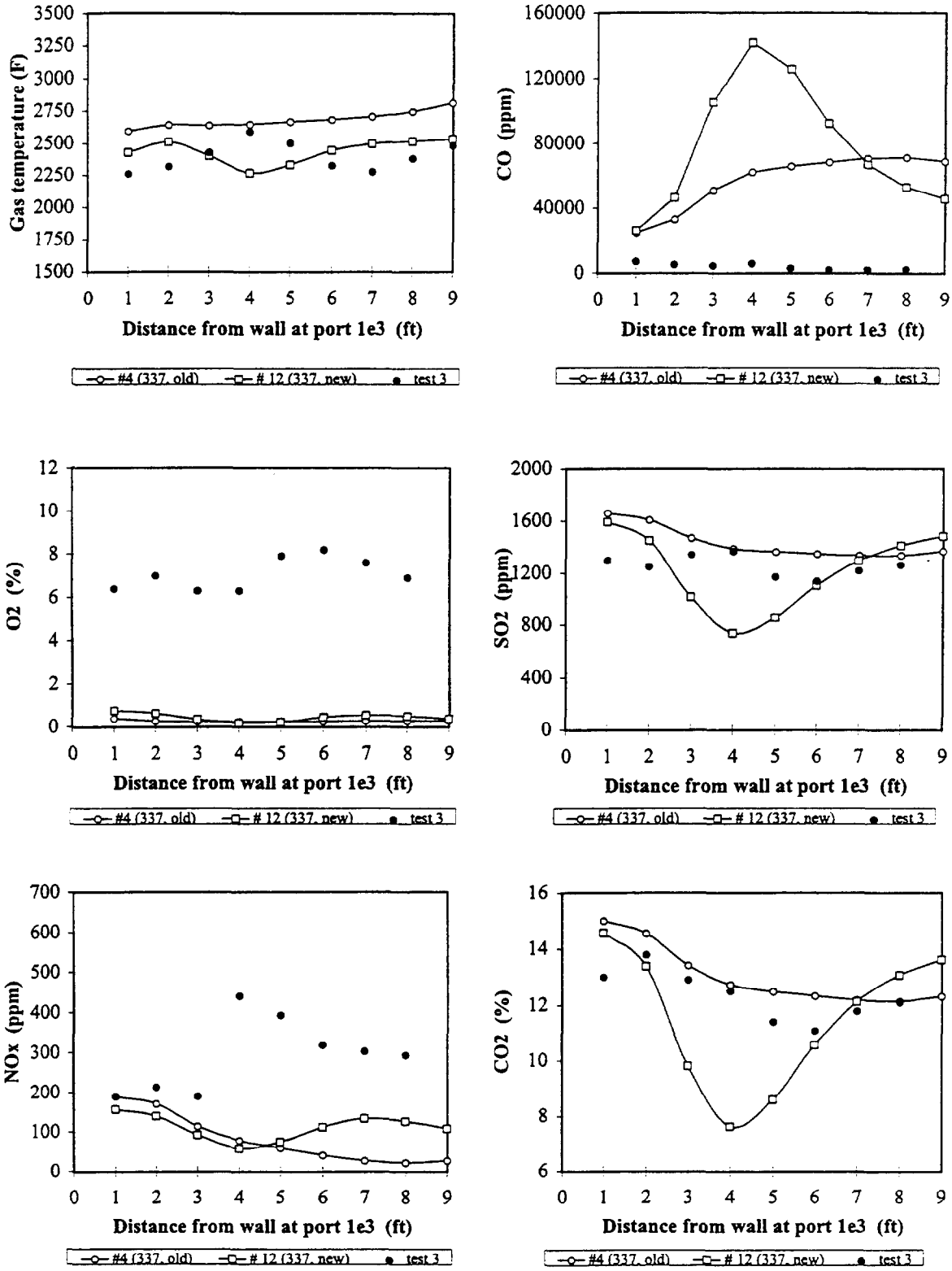

Figure C.1.1 Measured and predicted values for cases 4 and 12 at port 1e3

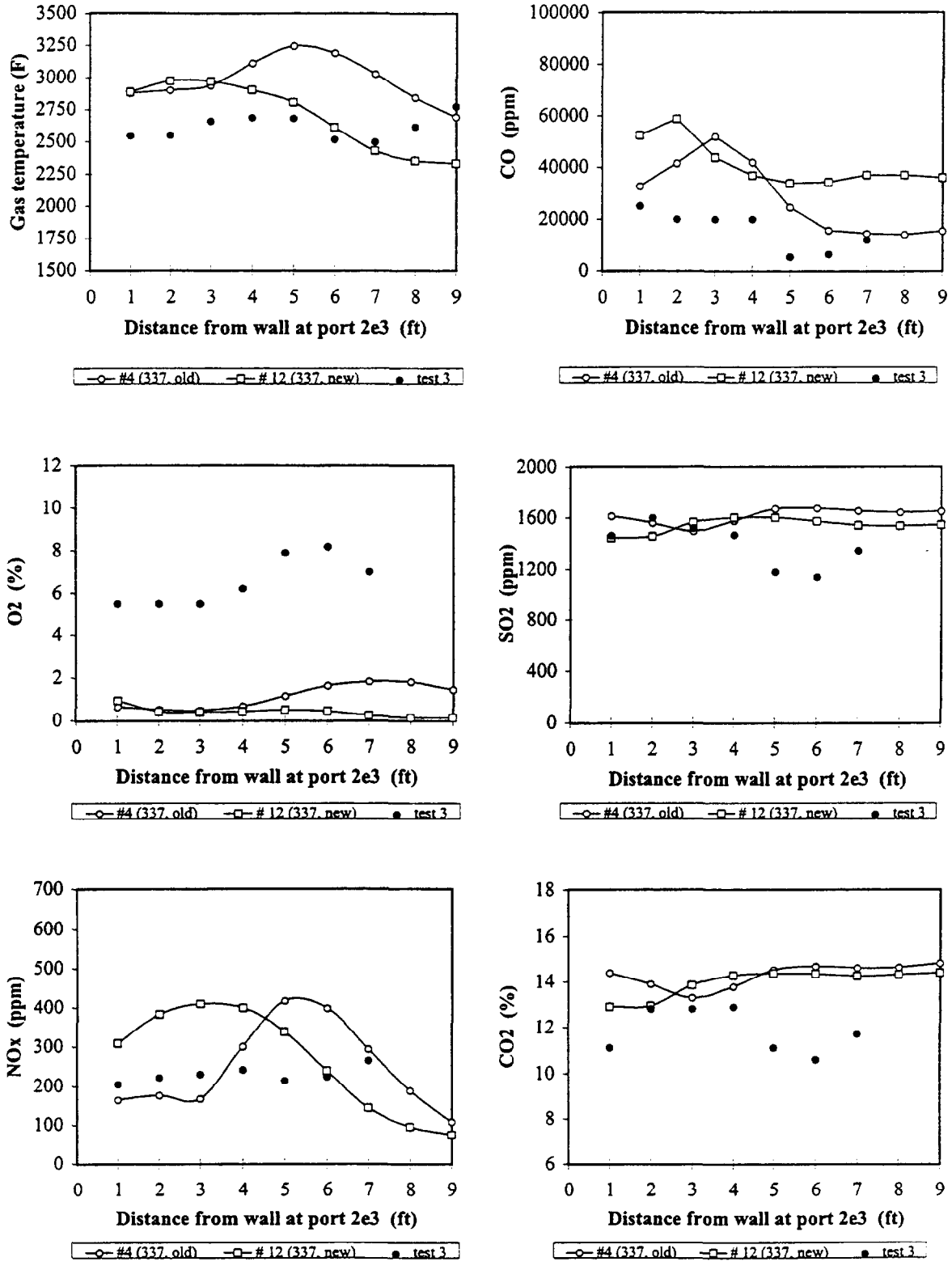

Figure C.1.2 Measured and predicted values for cases 2 and 3 at port 2e3

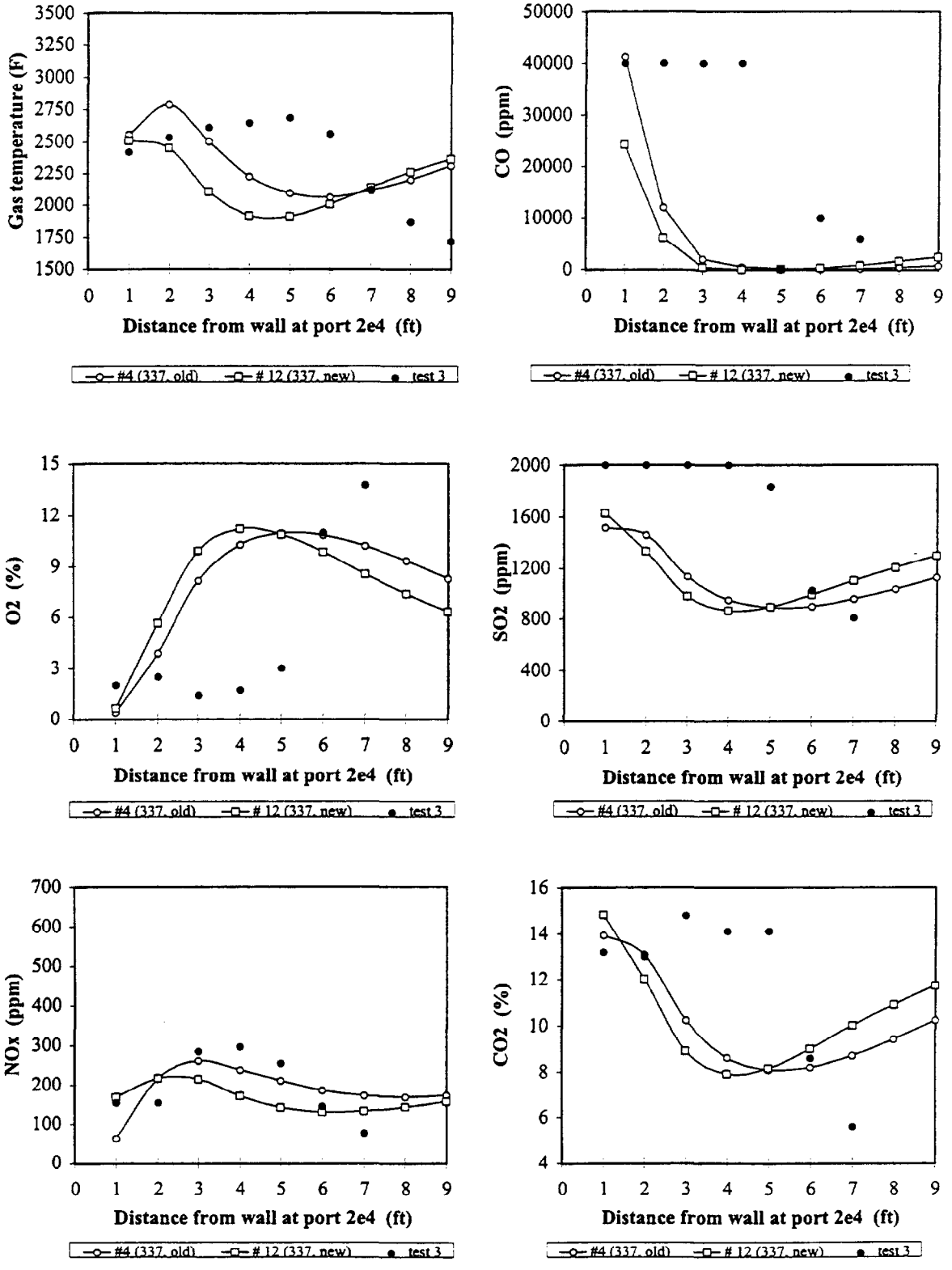

Figure C.1.3 Measured and predicted values for cases 4 and 12 at port 2e4

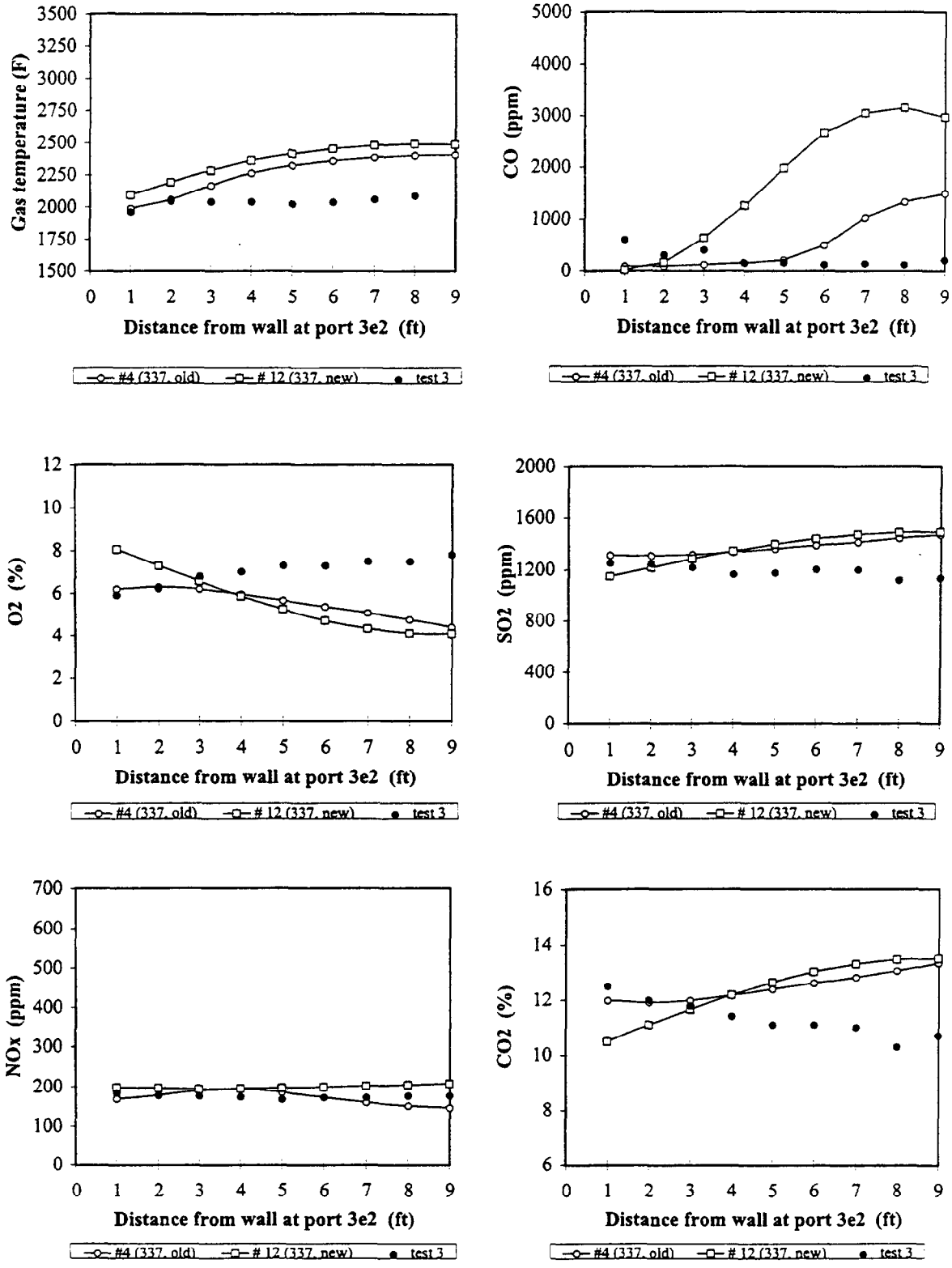

Figure C.1.4 Measured and predicted values for cases 4 and 12 at port 3e2

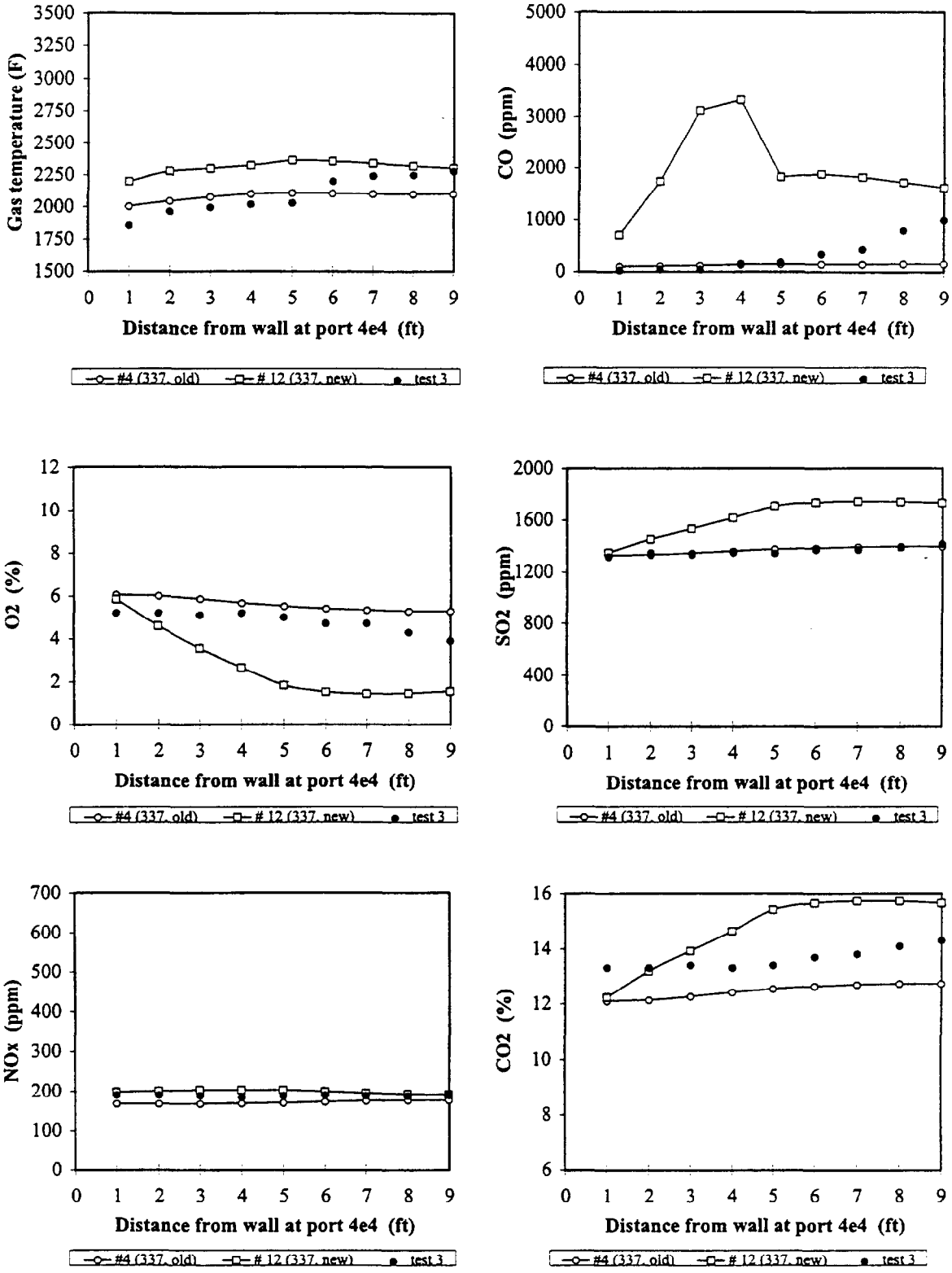

Figure C.1.5 Measured and predicted values for cases 4 and 12 at port 4e4

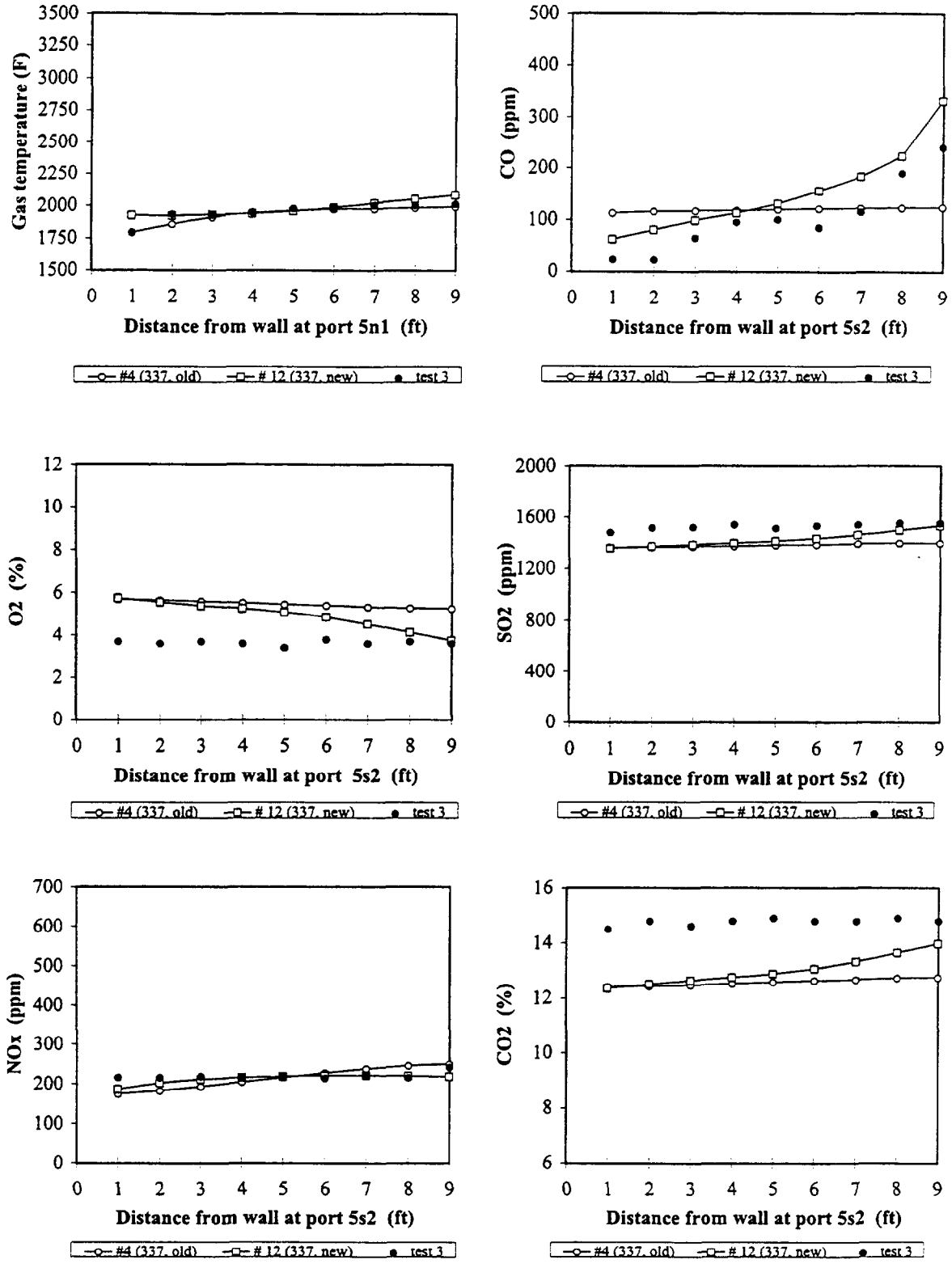

Figure C.1.6 Measured and predicted values for cases 4 and 12 at level 5

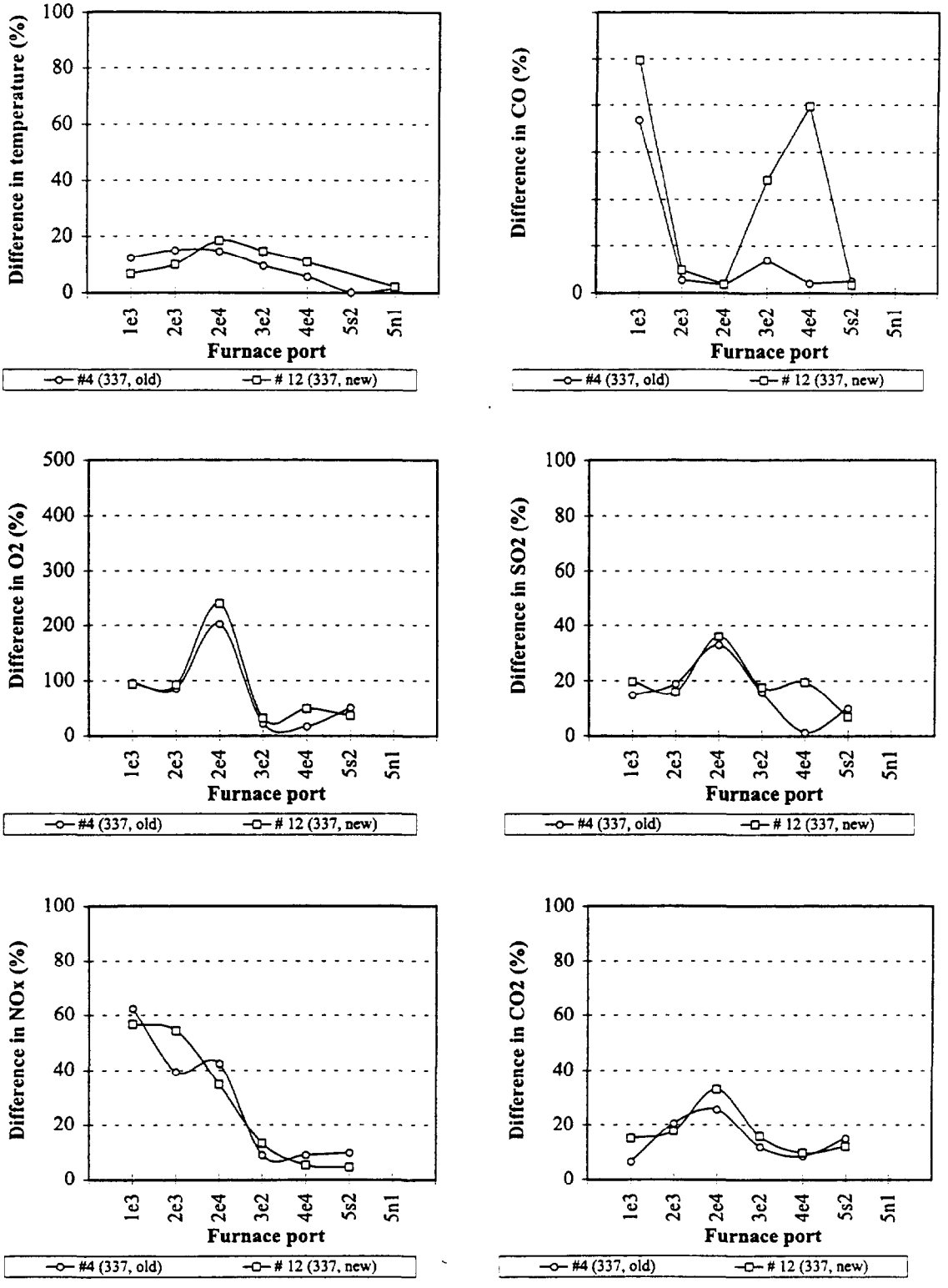

Figure C.1.7 Difference between predictions and measurements for cases 4 and 12

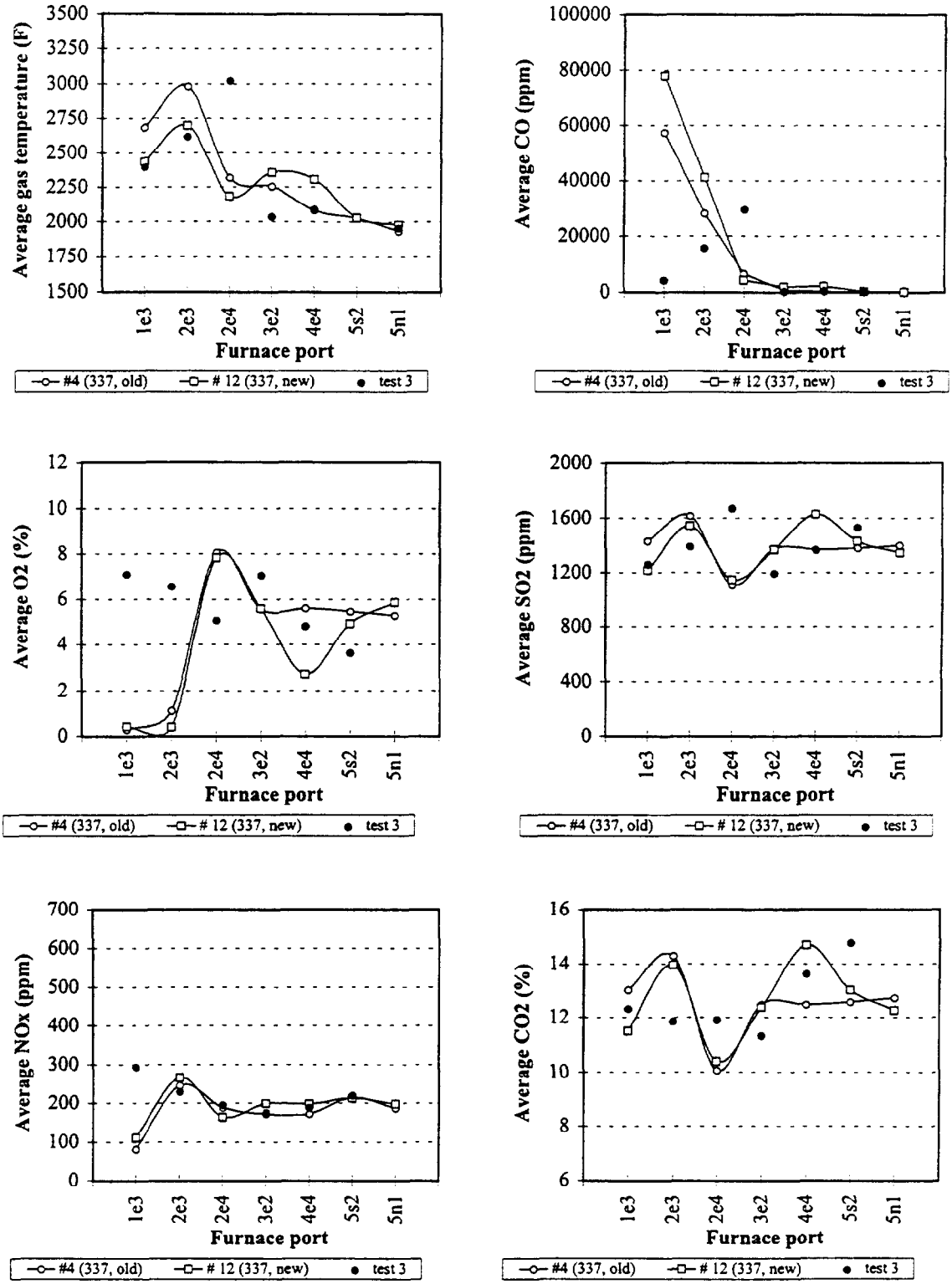

Figure C.1.8 Averaged measured and predicted values for cases 4 and 12

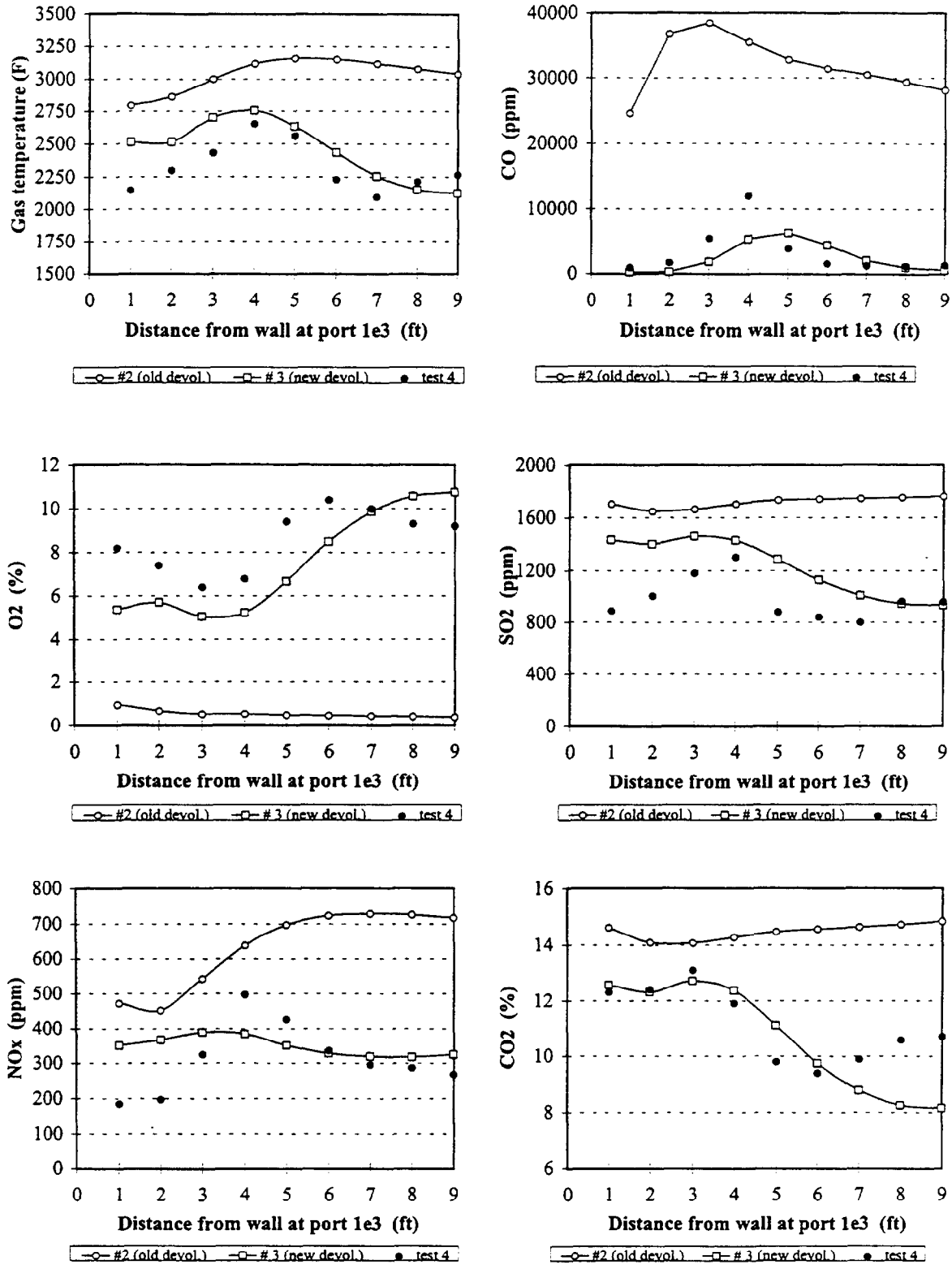

Figure C.2.1 Measured and predicted values for cases 2 and 3 at port 1e3

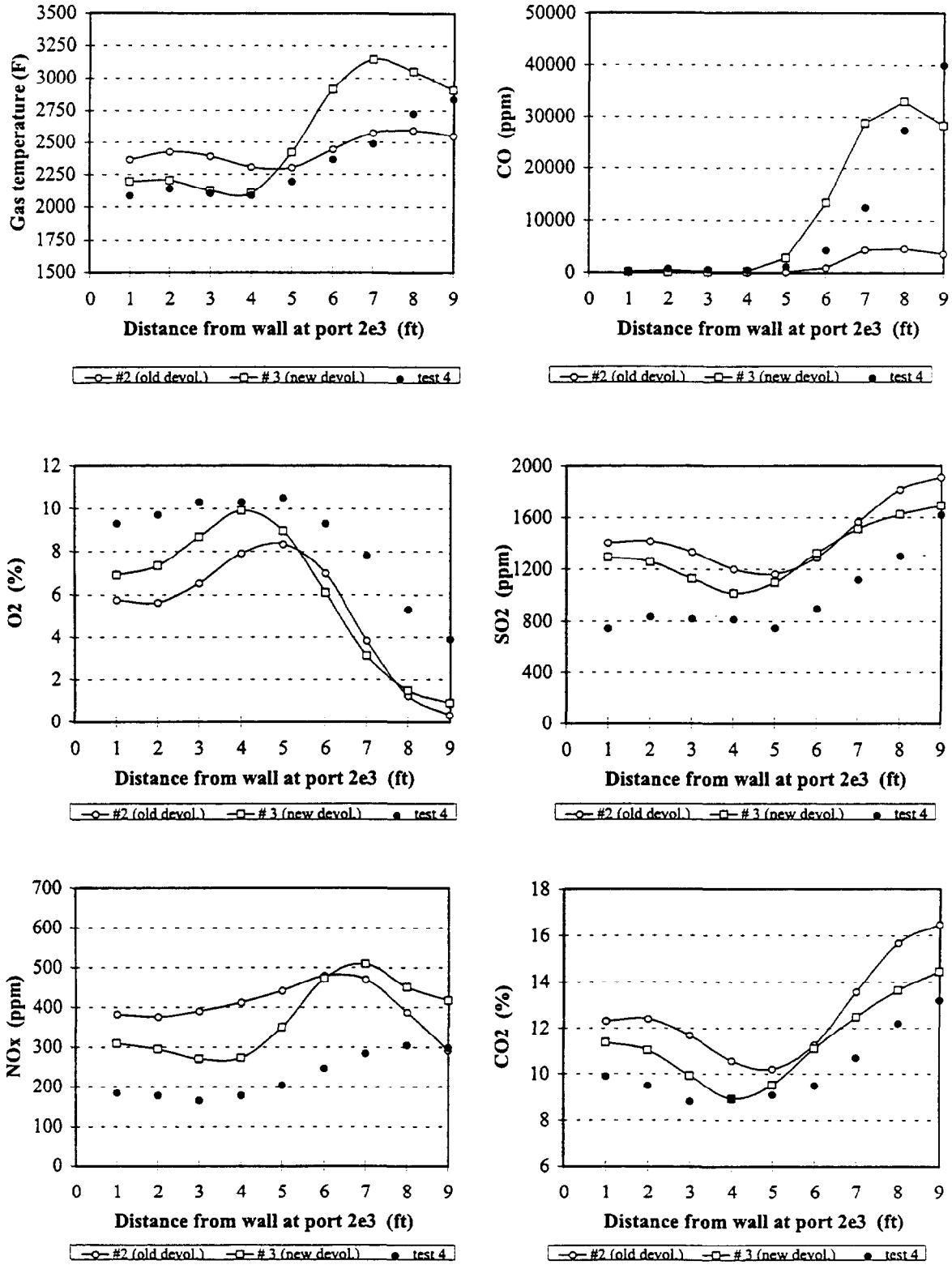

Figure C.2.2 Measured and predicted values for cases 2 and 3 at port 2e3

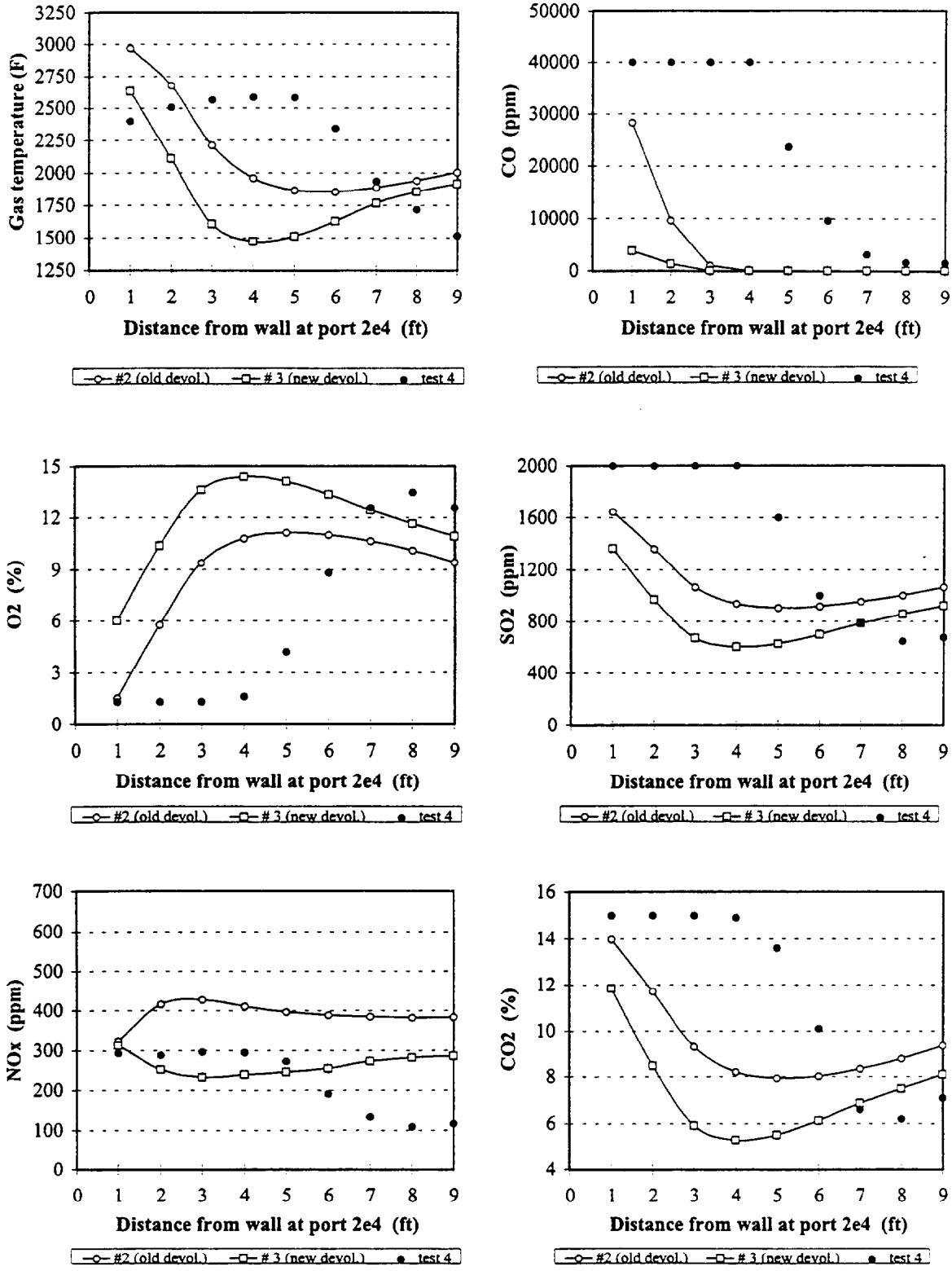

Figure C.2.3 Measured and predicted values for cases 2 and 3 at port 2e4

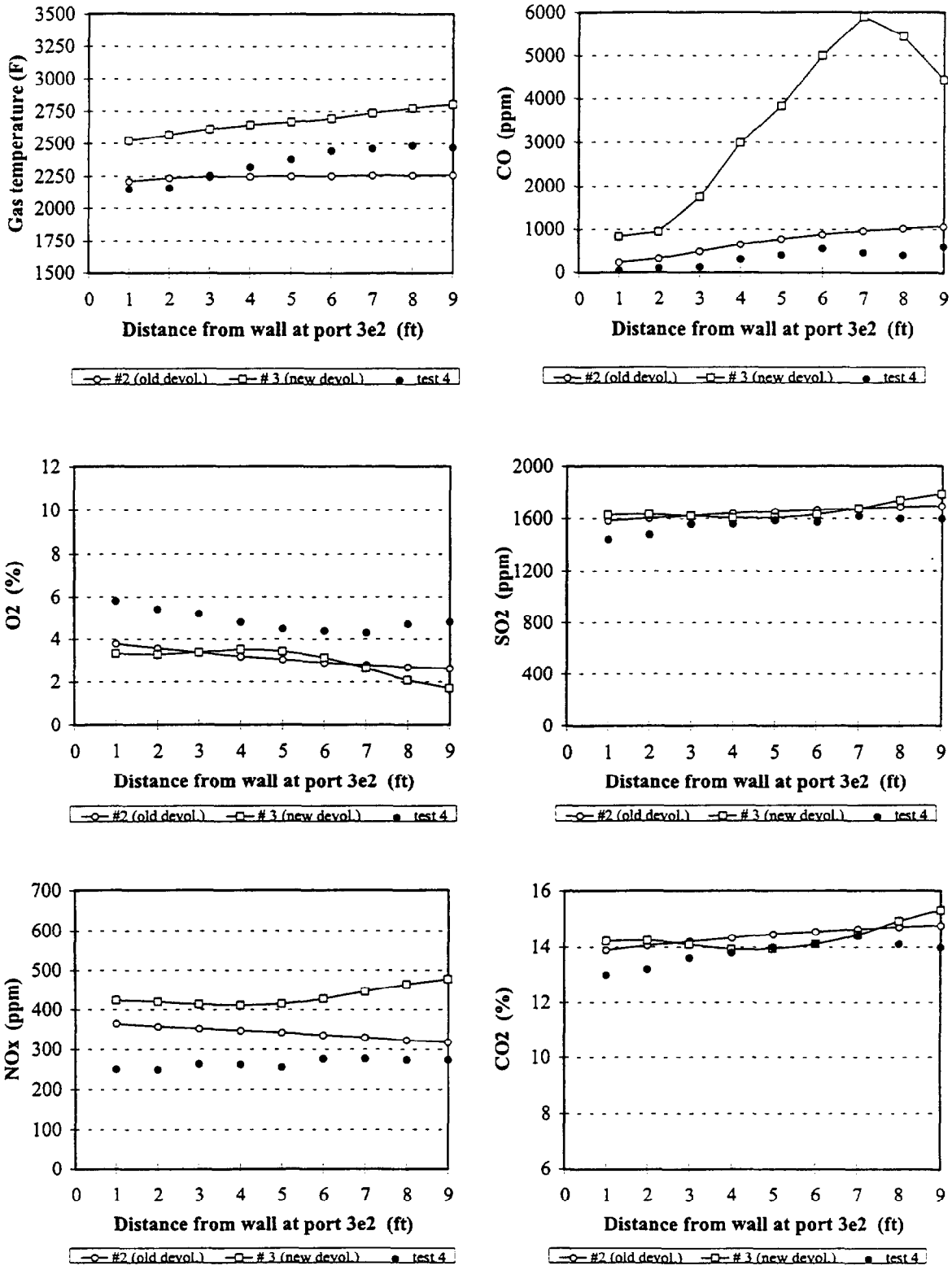

Figure C.2.4 Measured and predicted values for cases 2 and 3 at port 3e2

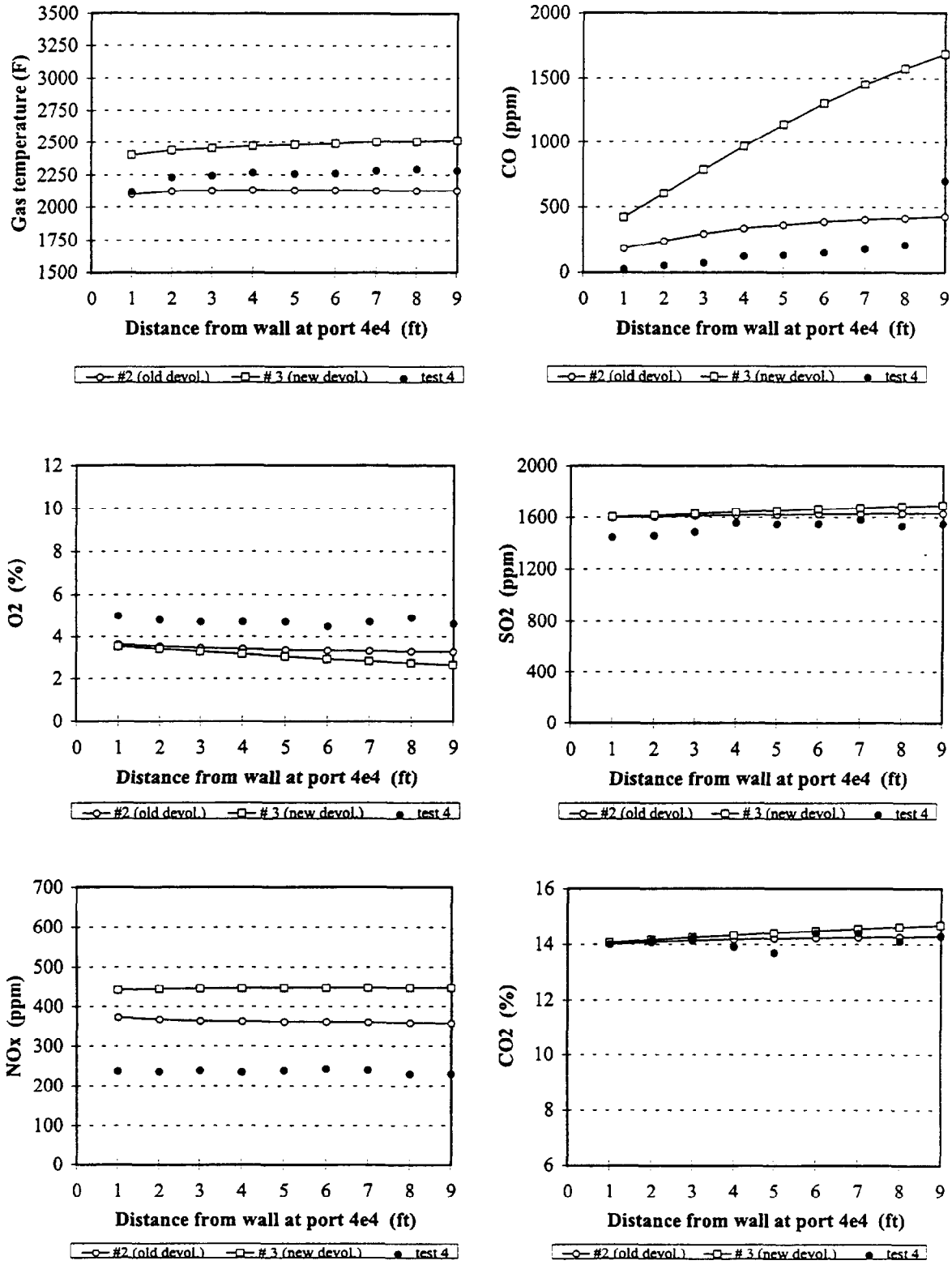

Figure C.2.5 Measured and predicted values for cases 2 and 3 at port 4e4

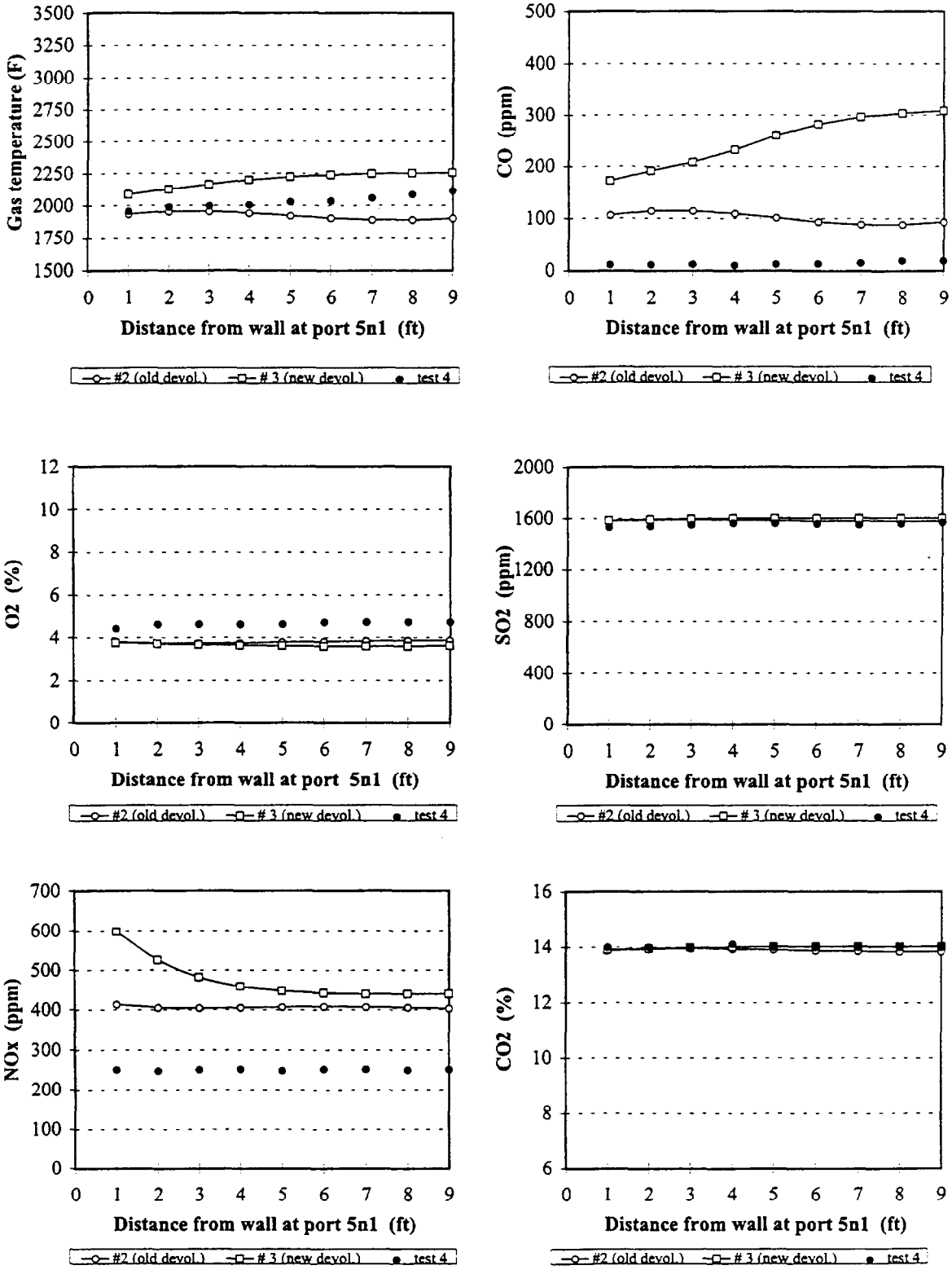

Figure C.2.6 Measured and predicted values for cases 2 and 3 at port 5n1

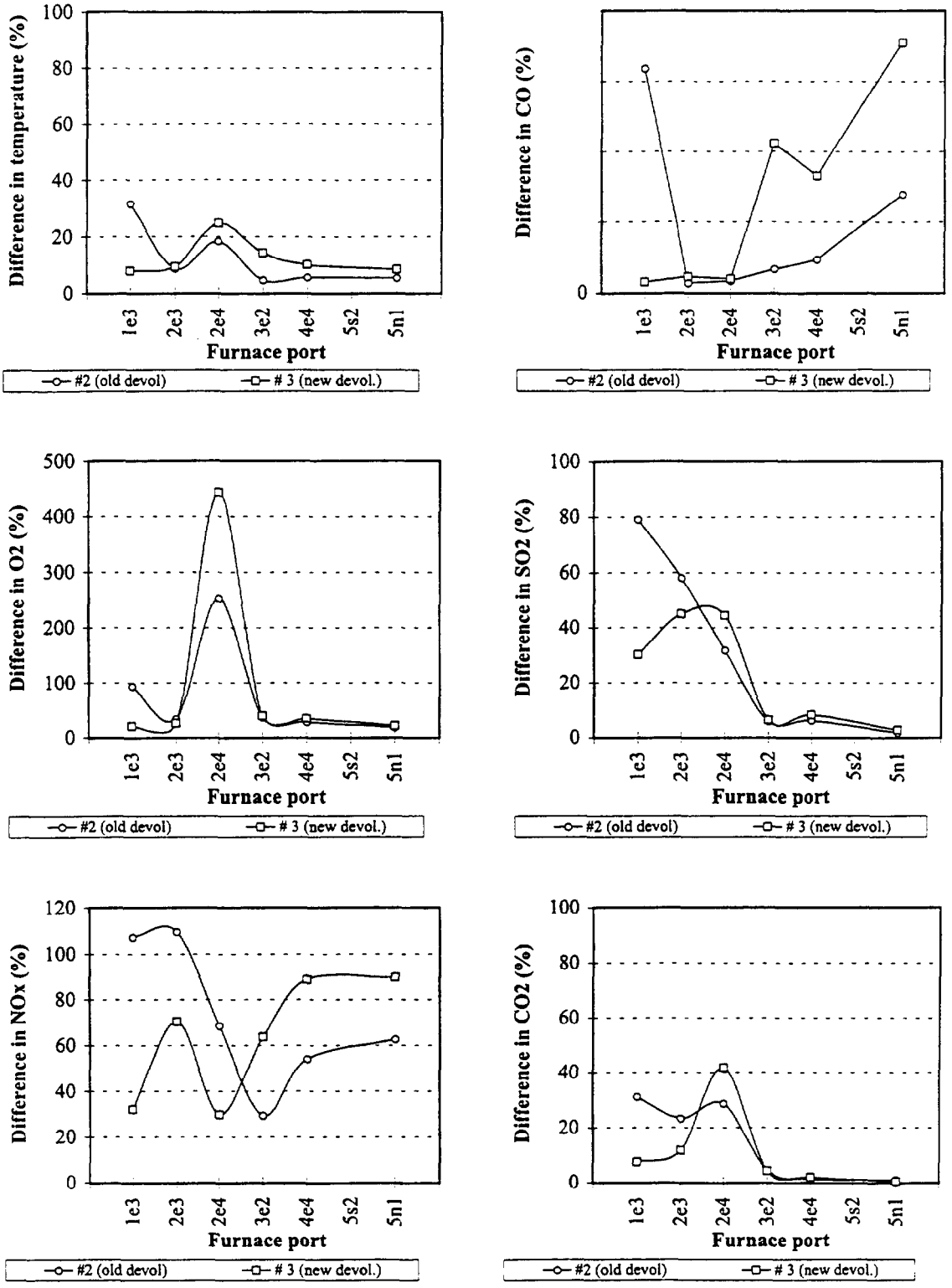

Figure C.2.7 Difference between predictions and measurements for cases 2 and 3

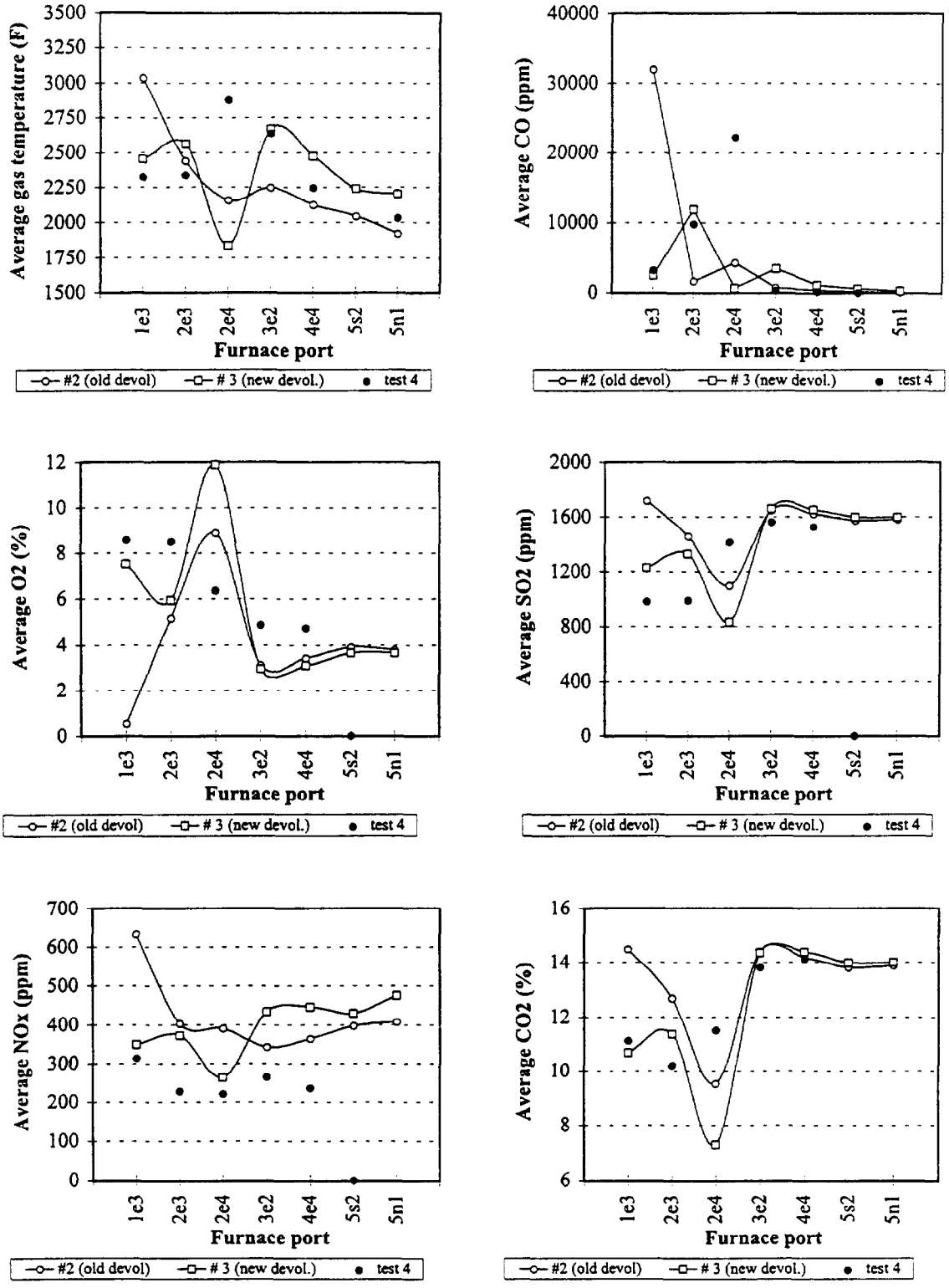

Figure C.2.8 Averaged measured and predicted values for cases 2 and 3

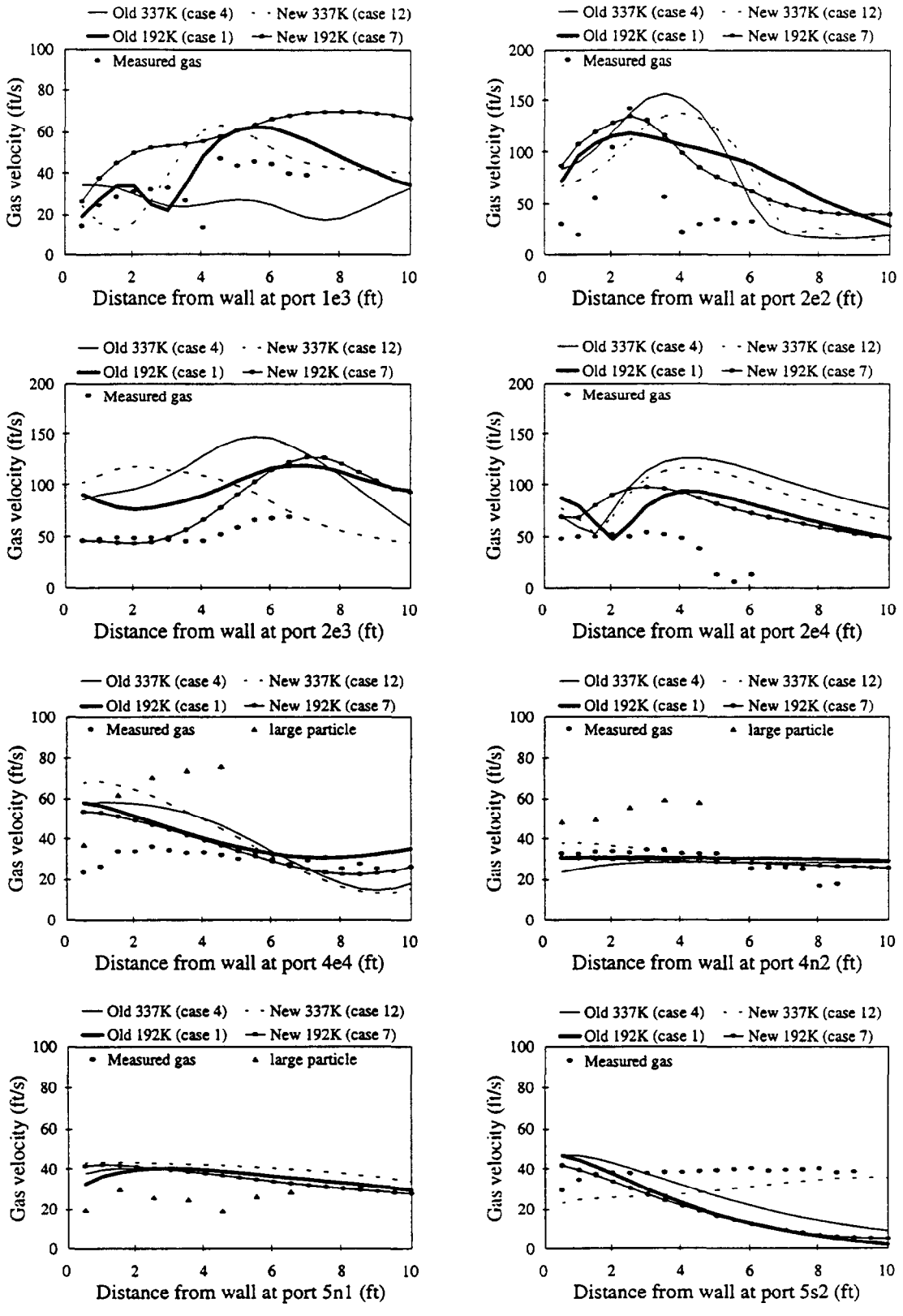

Figure C.3.1 Effect of devolatilization on gas velocity predictions (test 3).

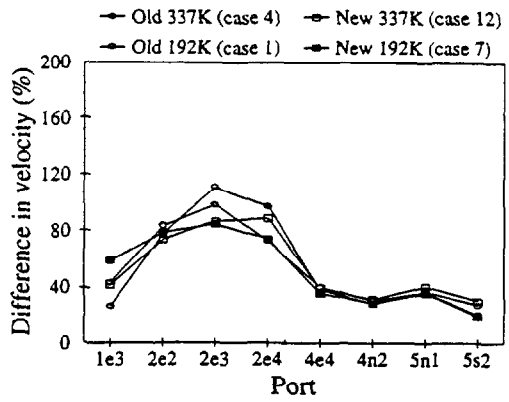

Figure C.3.2 Average velocity difference for test 3 by port

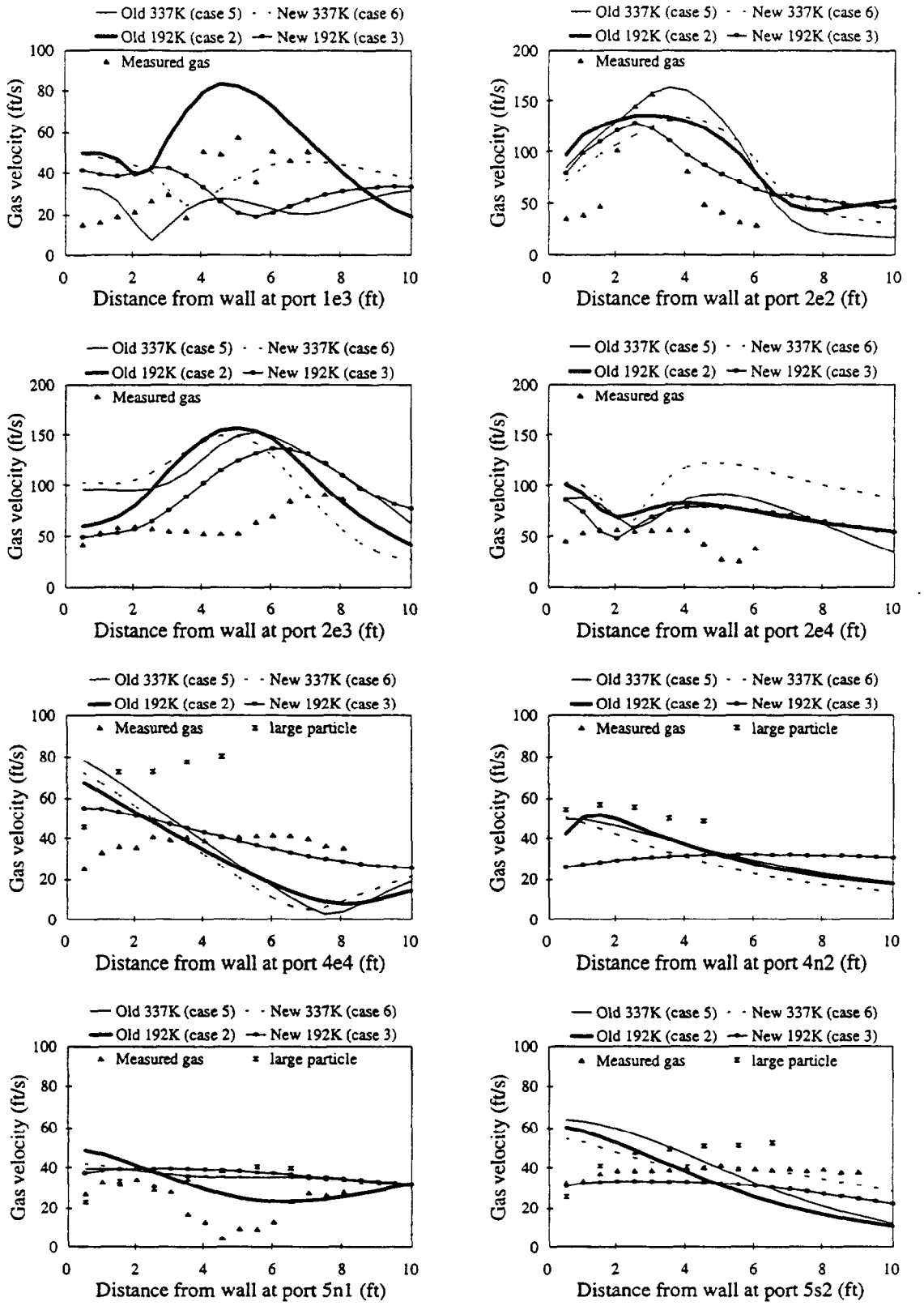

Figure C.3.3 Effect of devolatilization on gas velocity predictions (test 4).

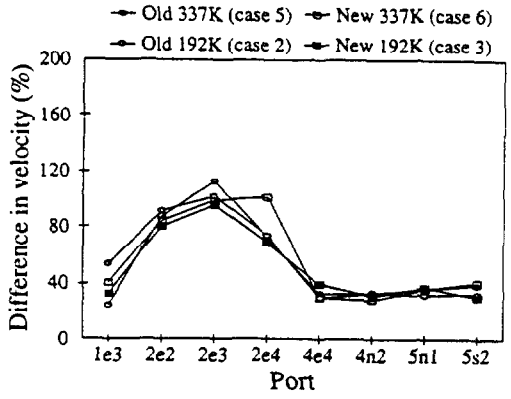

Figure C.3.4 Average velocity difference for test 4 by port

Appendix D

Compares the combined effects of numerical grid size and devolatilization rate constants, plus compares the particle and gas velocities for each of the 12 cases converged

Appendix D.1 shows the combined effects of grid size adjustment and devolatilization constants at the same time .

Section D.2 is a comparison between all twelve cases run on PCGC-3 along with appropriate test data from tests 3, 4, and 5 for velocity. The velocity measurements used are those for the combustion gases using the dusty pitot tube along with the Insitec laser based instrument using the PCSV system (Particle Concentration, Size and Velocity) data reduction. The PCSV unit measures both the large and small particle velocities separately with the large particle data considered to be most accurate. The small particles which would tend to follow the gas velocity give the better comparisons, but not always (see figure D.2.13). Brooks (1997) concluded that the most correct value for the measured velocity was therefore in between the gas measurements and large particle velocity measured values. In any event, the redundant measurements are supportive of each other, suggesting that the near-burner dusty pitot tube measurements (the only ones in that harsh near-field environment) are acceptable even though the PCSV unit could not operate in the near burner-region due to high heat flux and too high a particle flux rate.

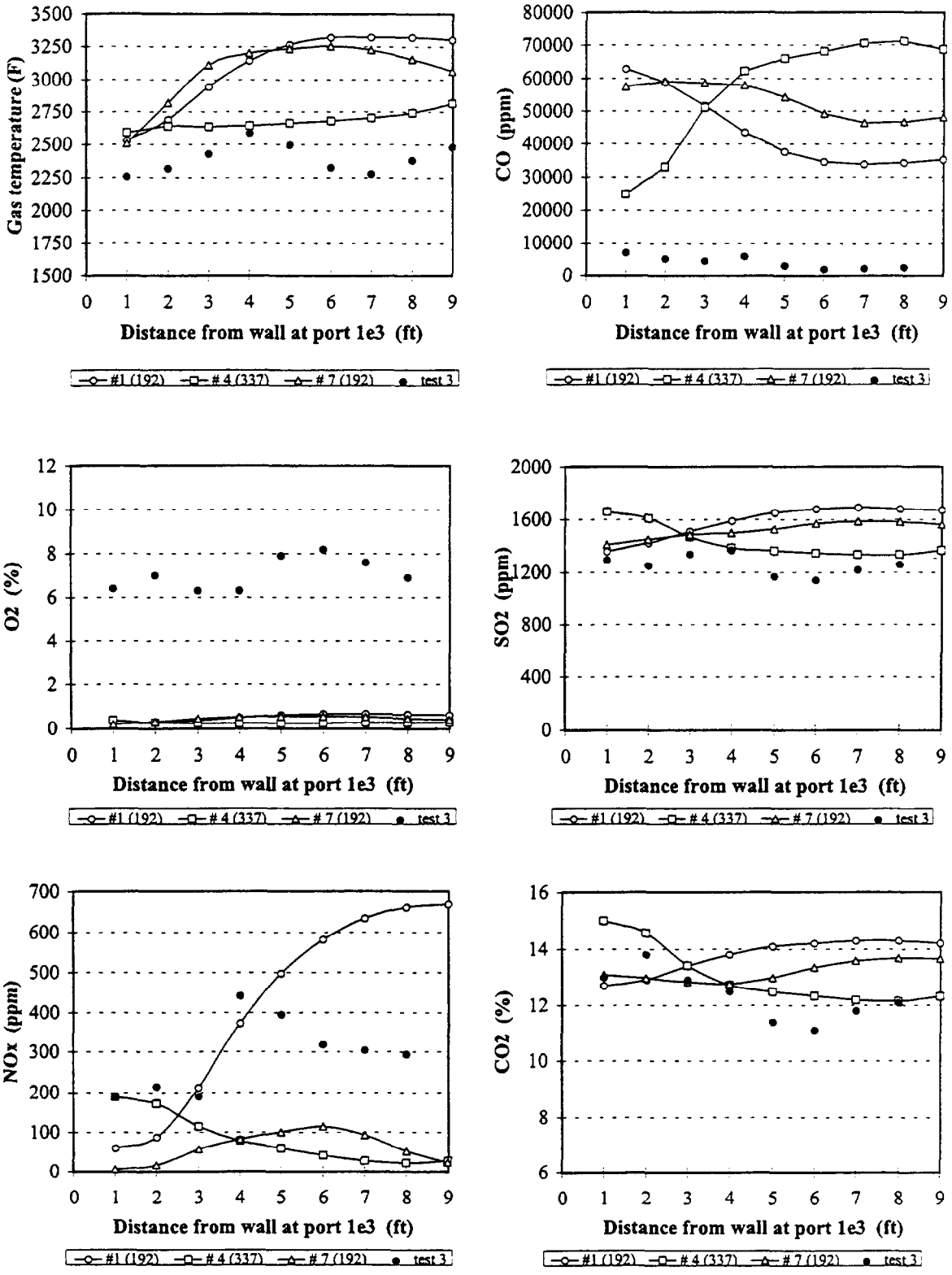

Figure D.1.1 Measured and predicted values for cases 1, 4, and 7 at port 1e3

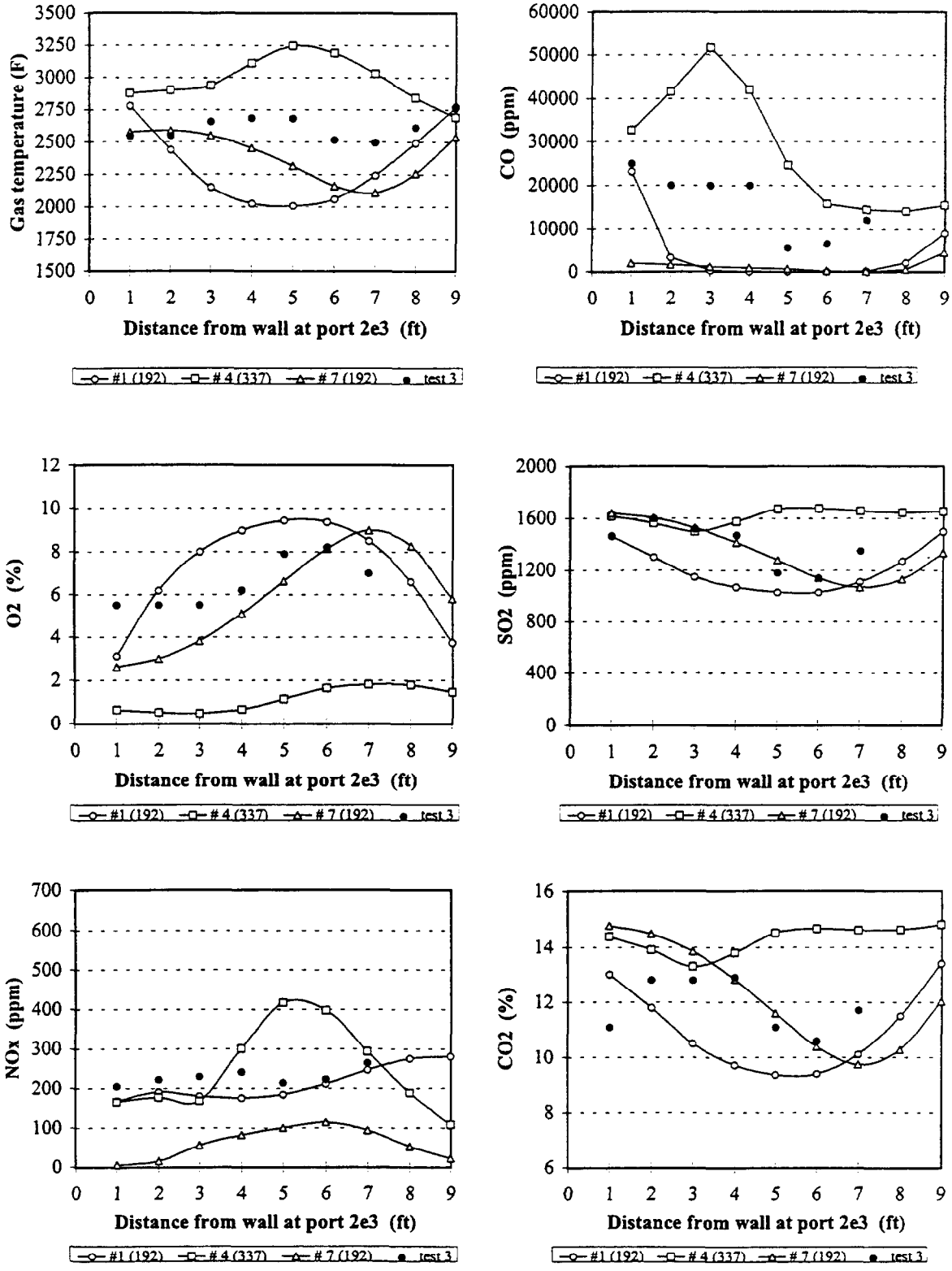

Figure D.1.2 Measured and predicted values for cases 1, 4, and 7 at port 2e3

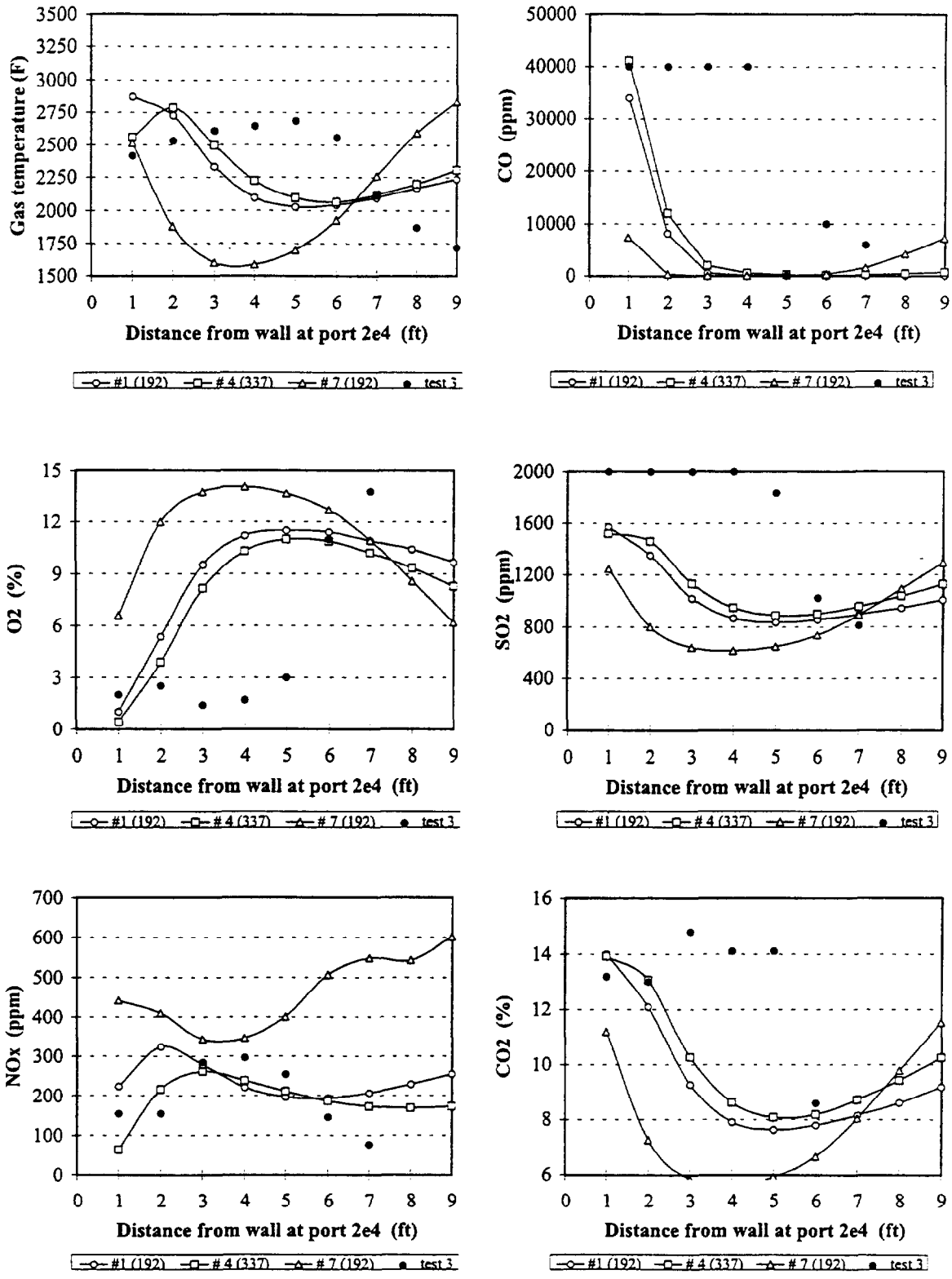

Figure D.1.3 Measured and predicted values for cases 1, 4, and 7 at port 2e4

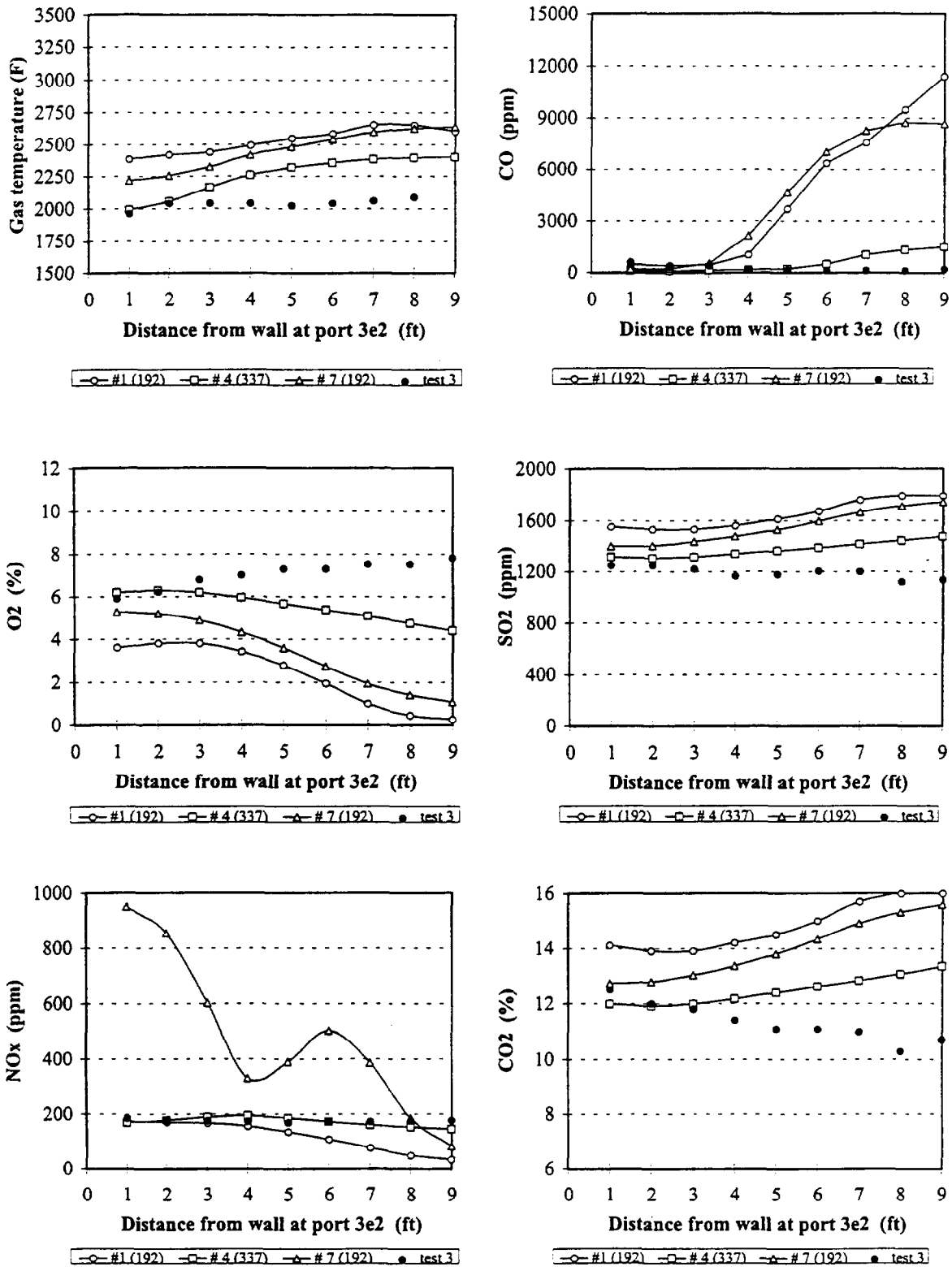

Figure D.1.4 Measured and predicted values for cases 1, 4, and 7 at port 3e2

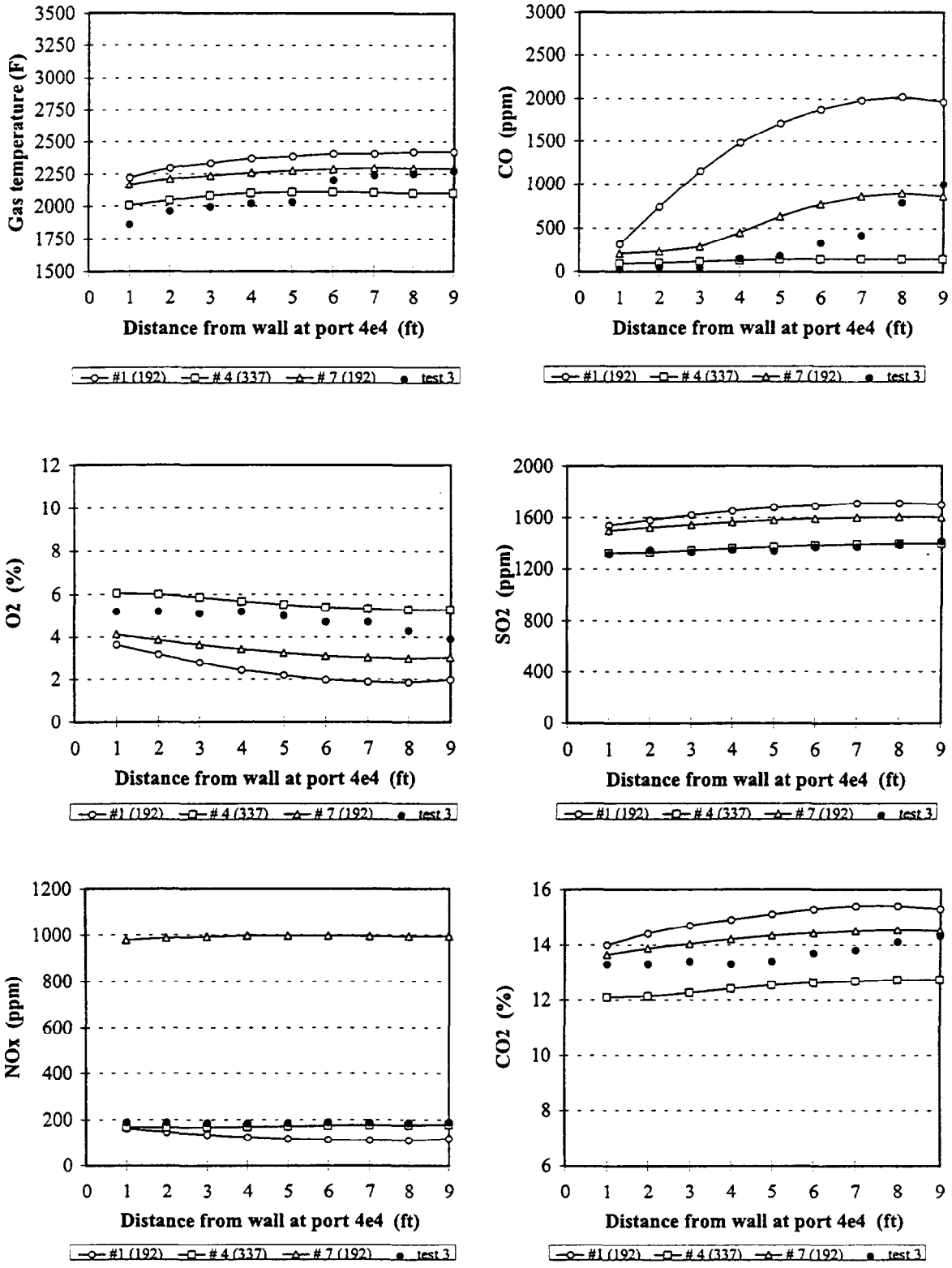

Figure D.1.5 Measured and predicted values for cases 1, 4, and 7 at port 4e4

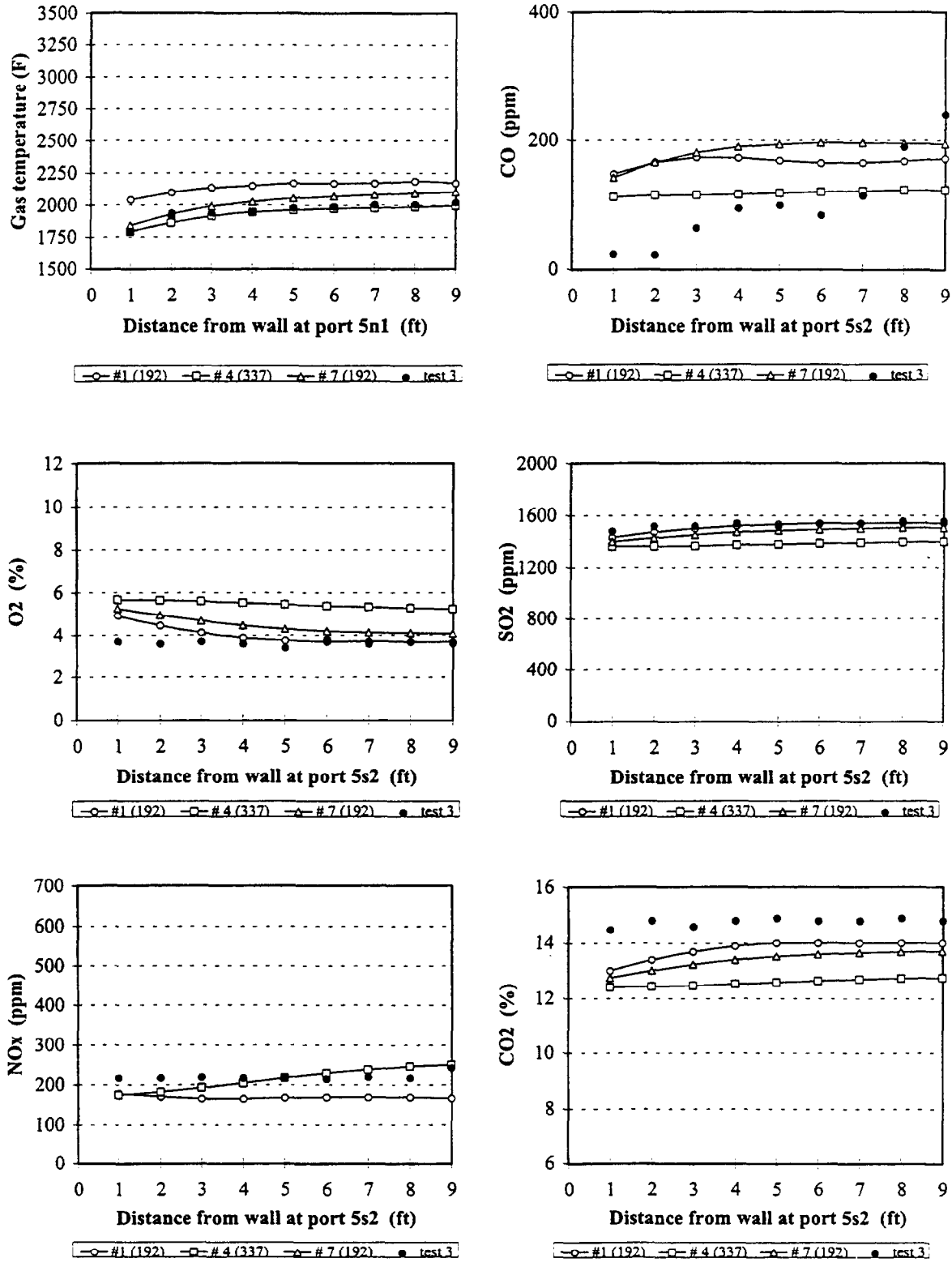

Figure D.1.6 Measured and predicted values for cases 1, 4, and 7 at level 5

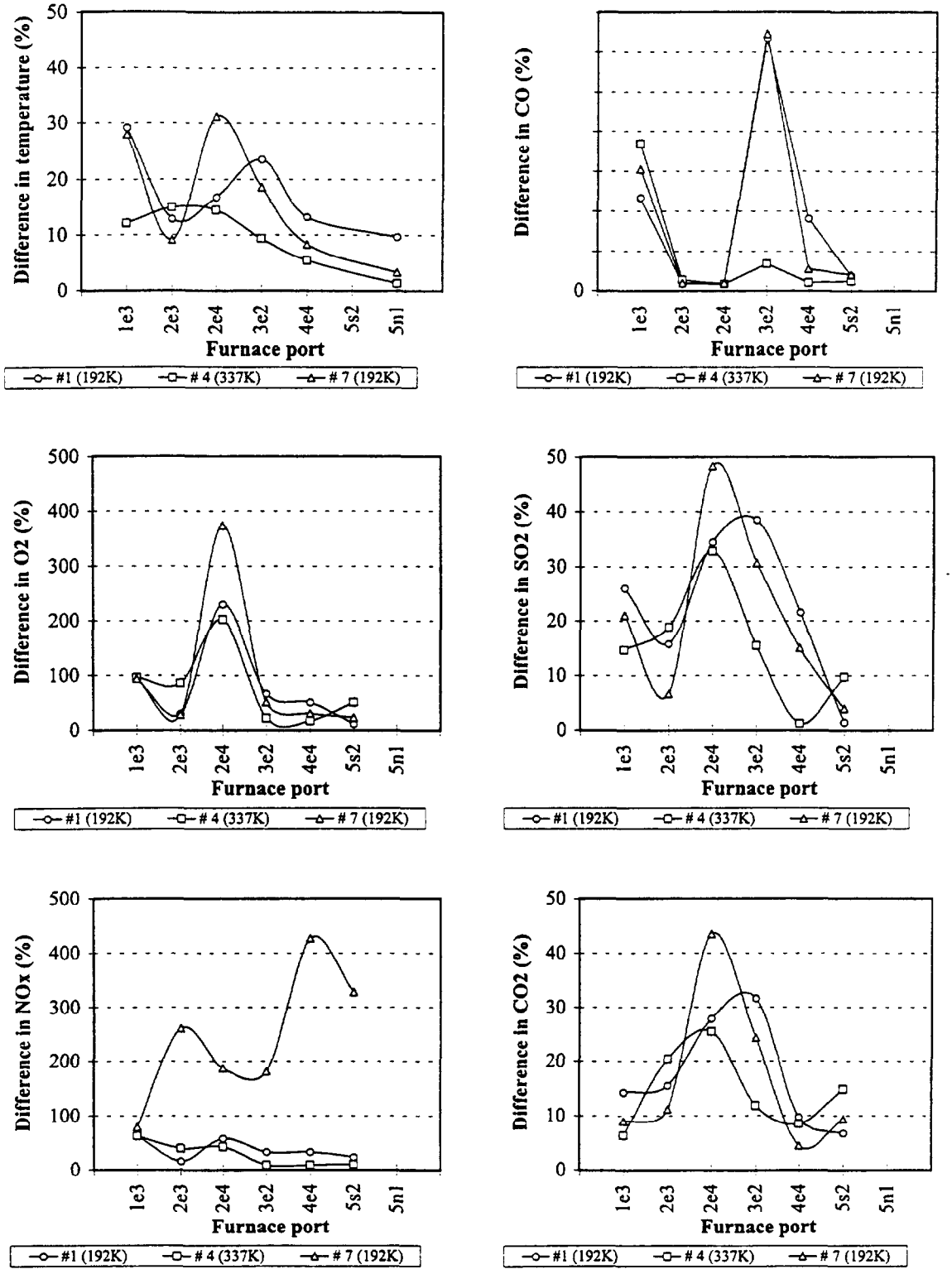

Figure D.1.7 Difference between predictions and measurements for cases 1, 4, and 7.

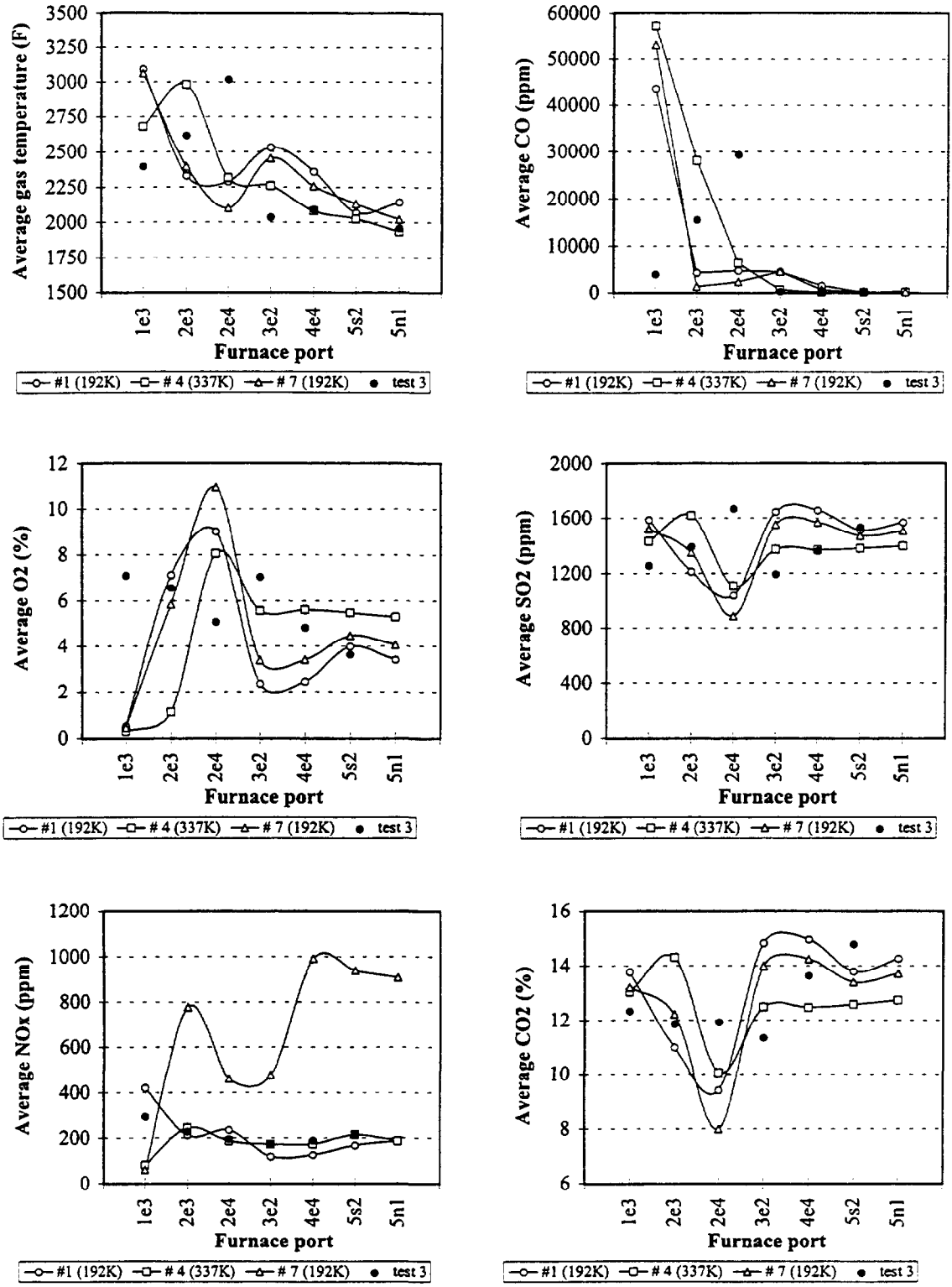

Figure D.1.8 Averaged measured and predicted values for cases 1, 4, and 7.

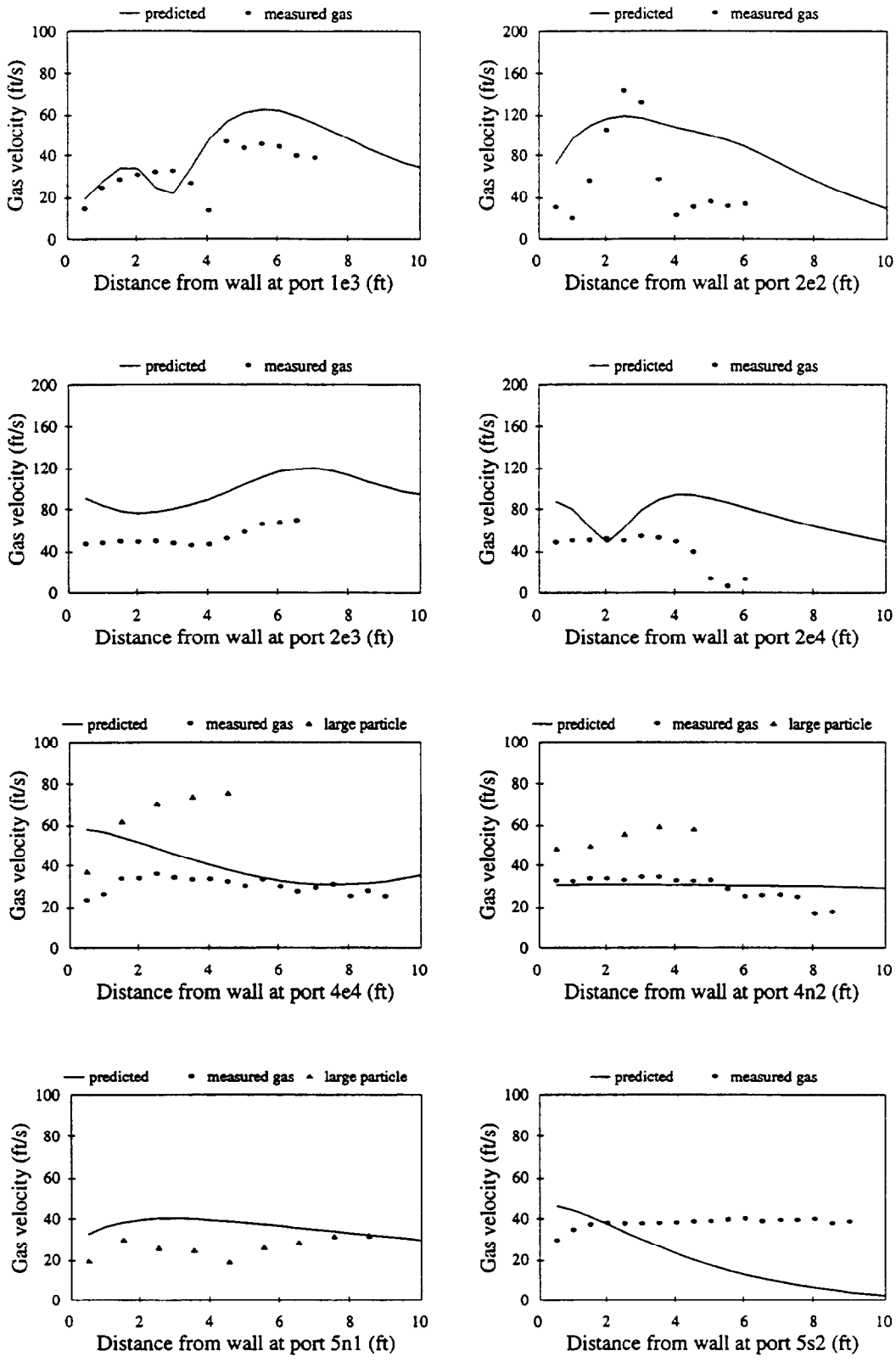

Figure D.2.1. Predicted and measured in-plane velocities for case 1.

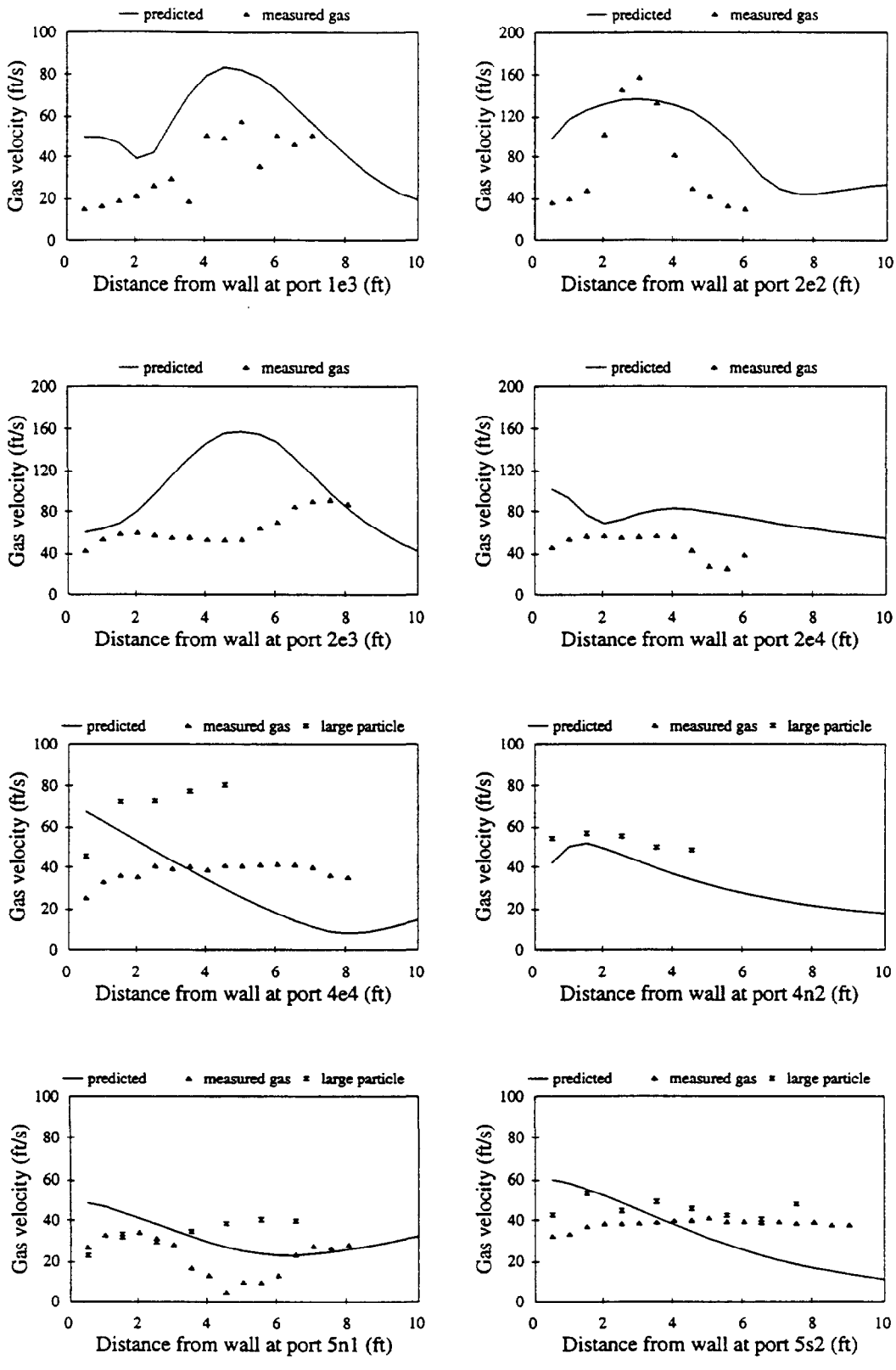

Figure D.2.2. Predicted and measured in-plane velocities for case 2.

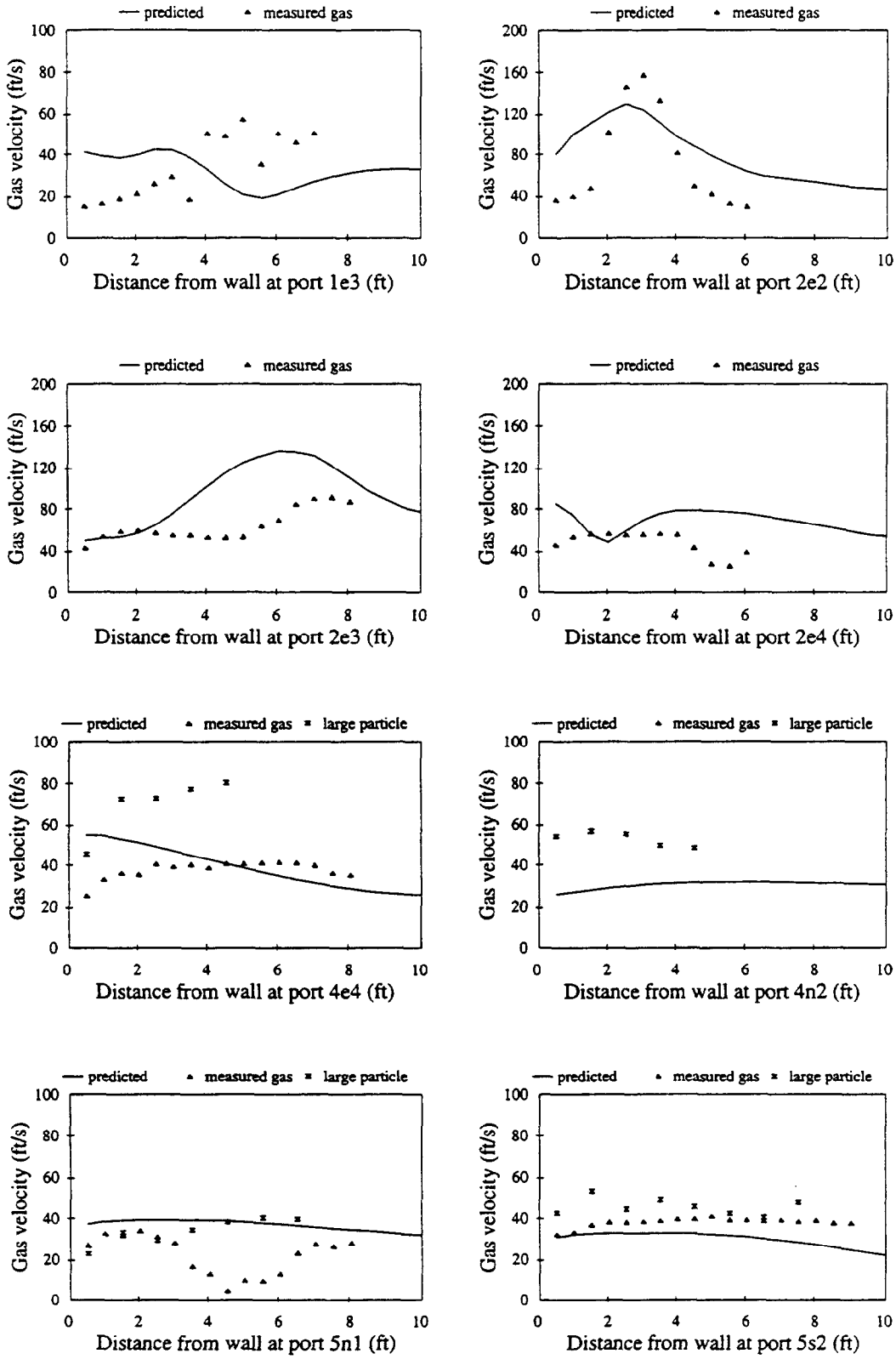

Figure D.2.3. Predicted and measured in-plane velocities for case 3.

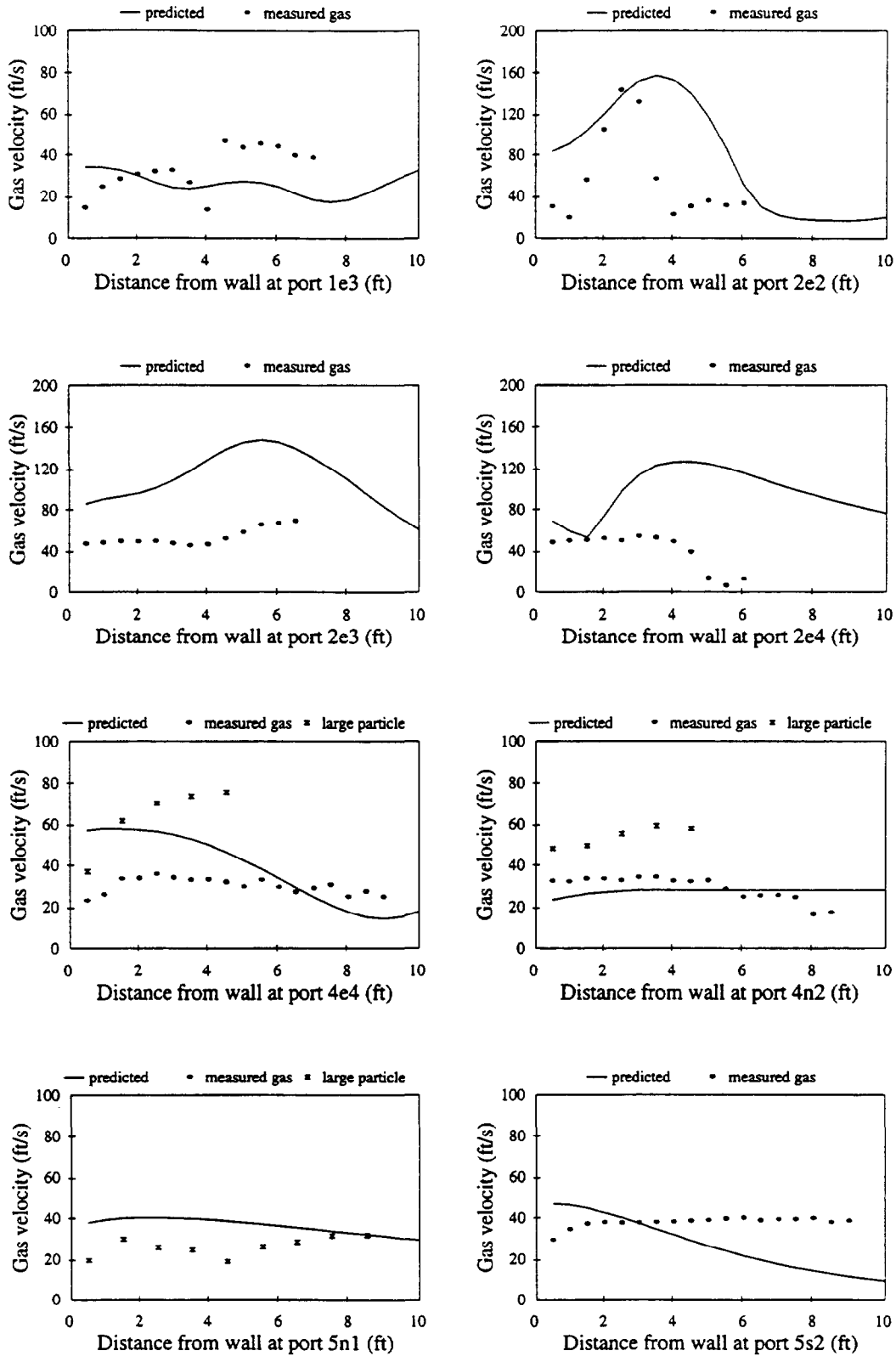

Figure D.2.4. Predicted and measured in-plane velocities for case 4.

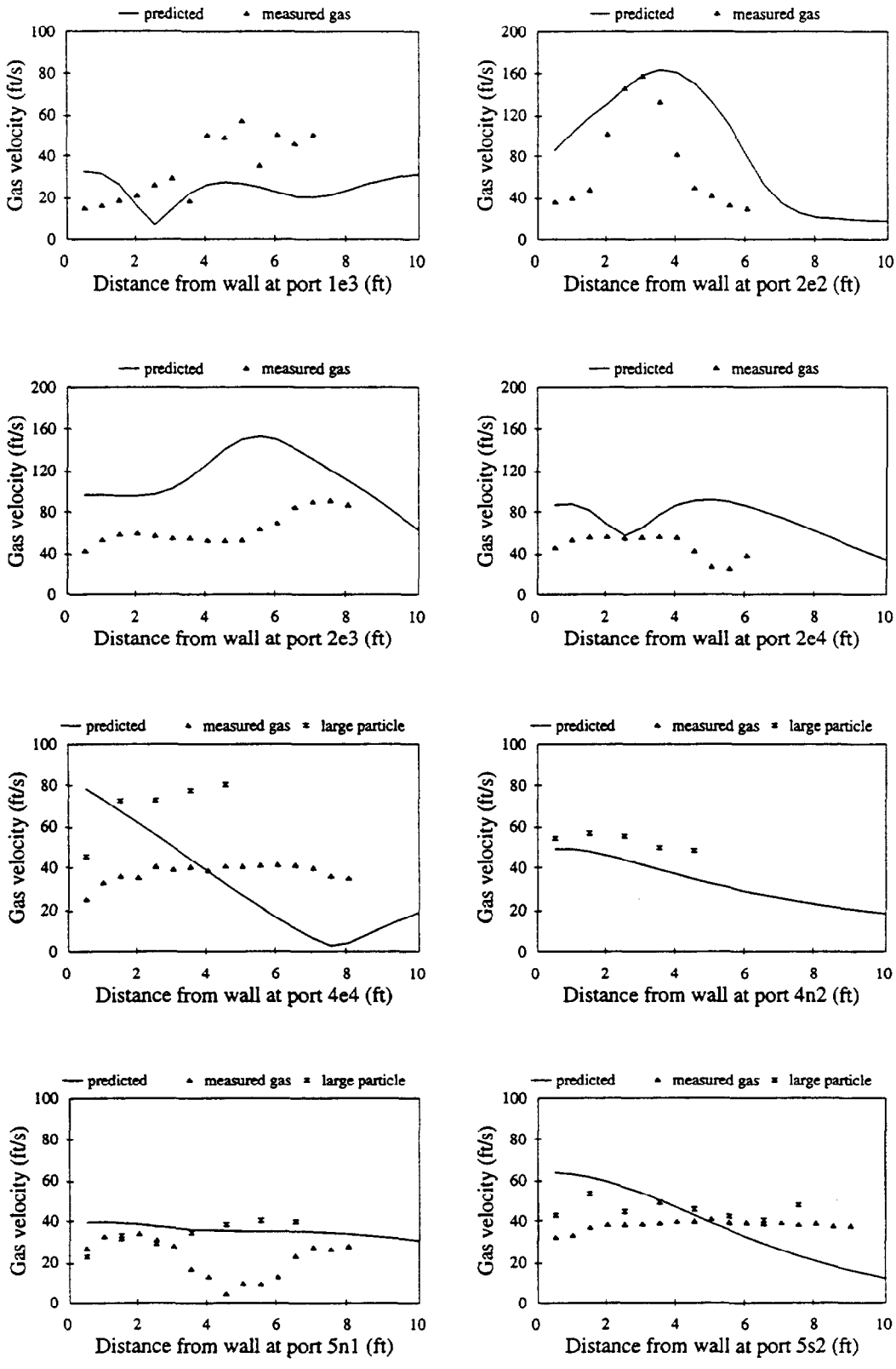

Figure D.2.5. Predicted and measured in-plane velocities for case 5.

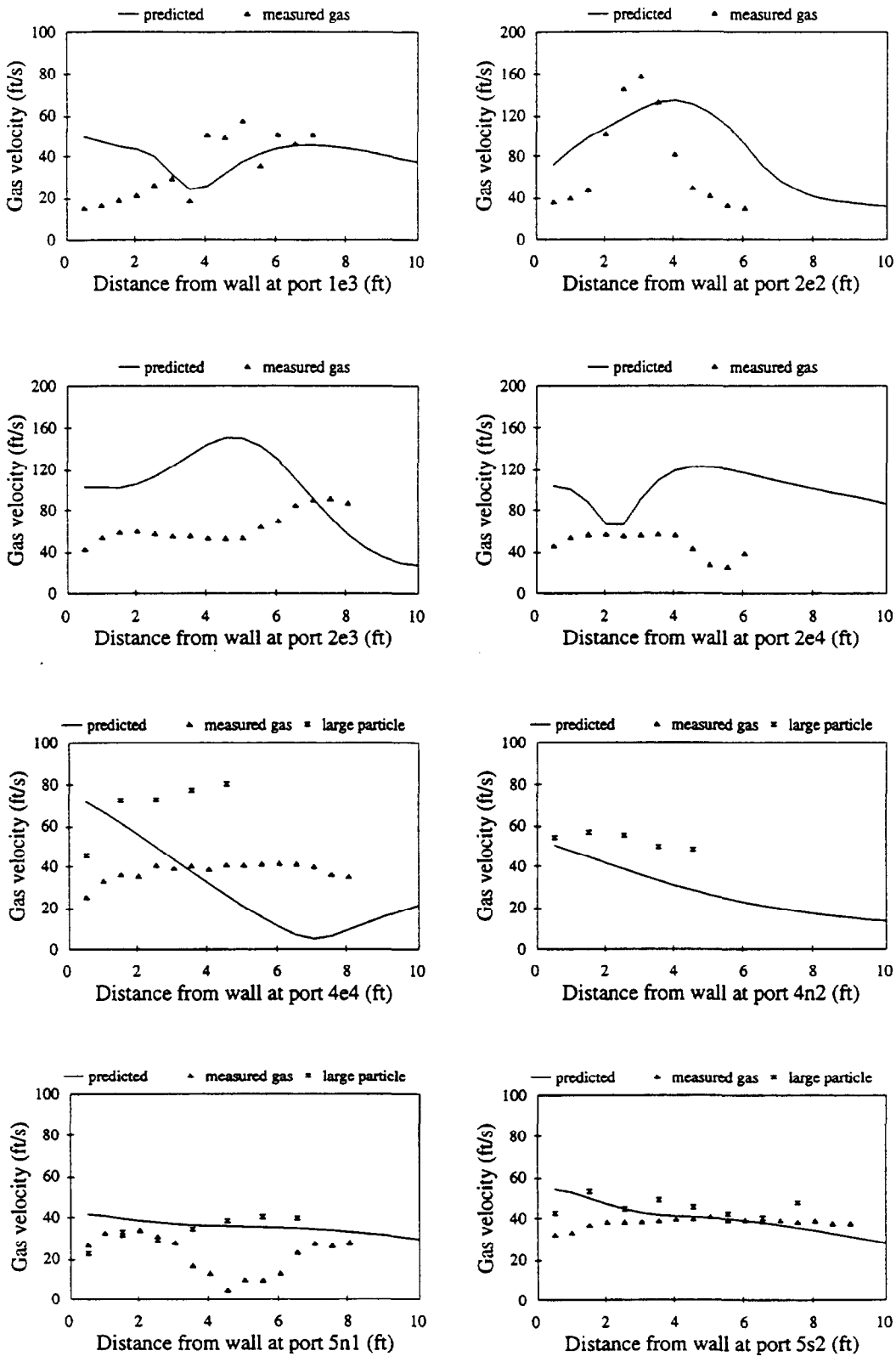

Figure D.2.6. Predicted and measured in-plane velocities for case 6.

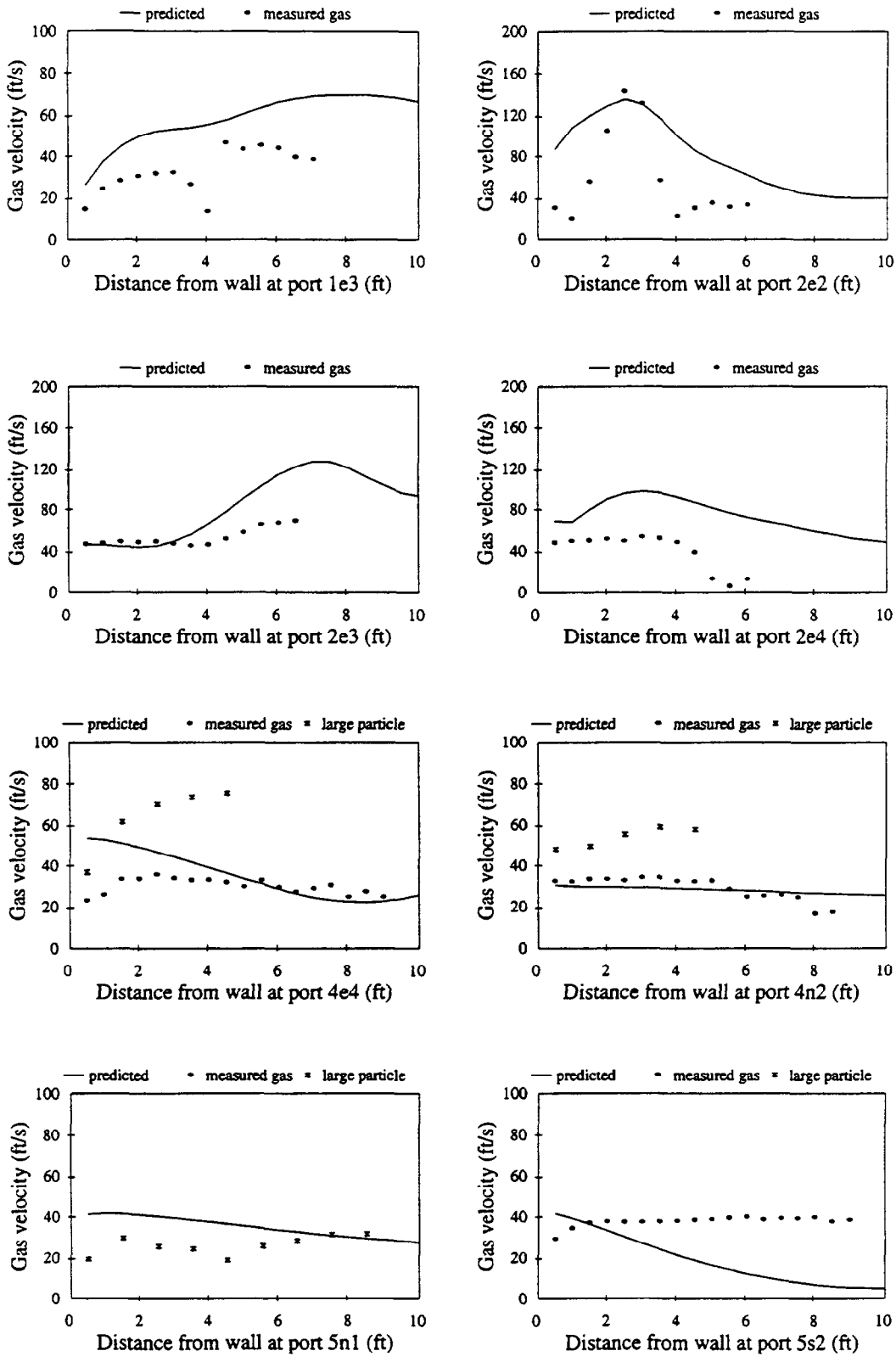

Figure D.2.7. Predicted and measured in-plane velocities for case 7.

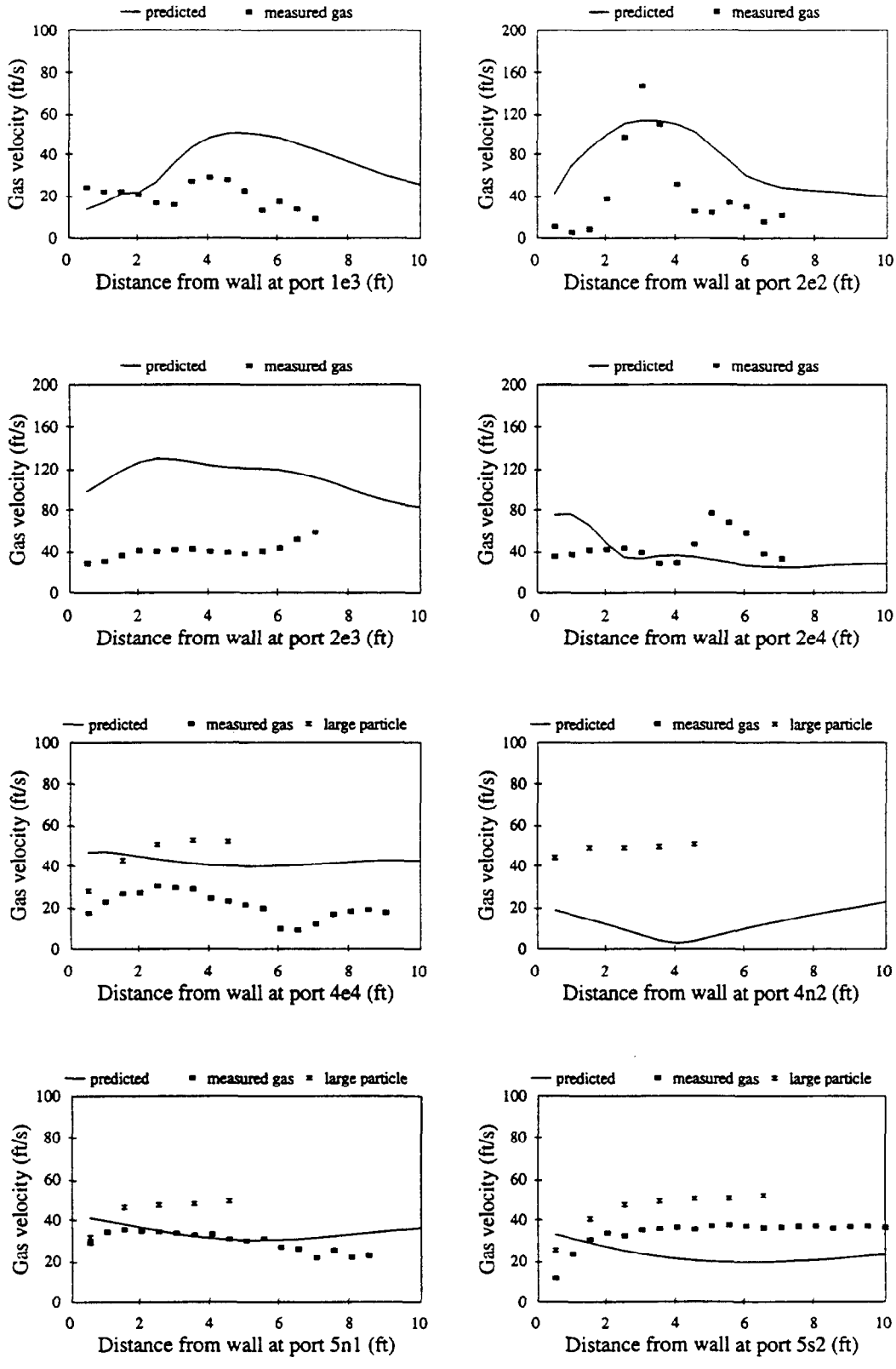

Figure D.2.8. Predicted and measured in-plane velocities for case 8.

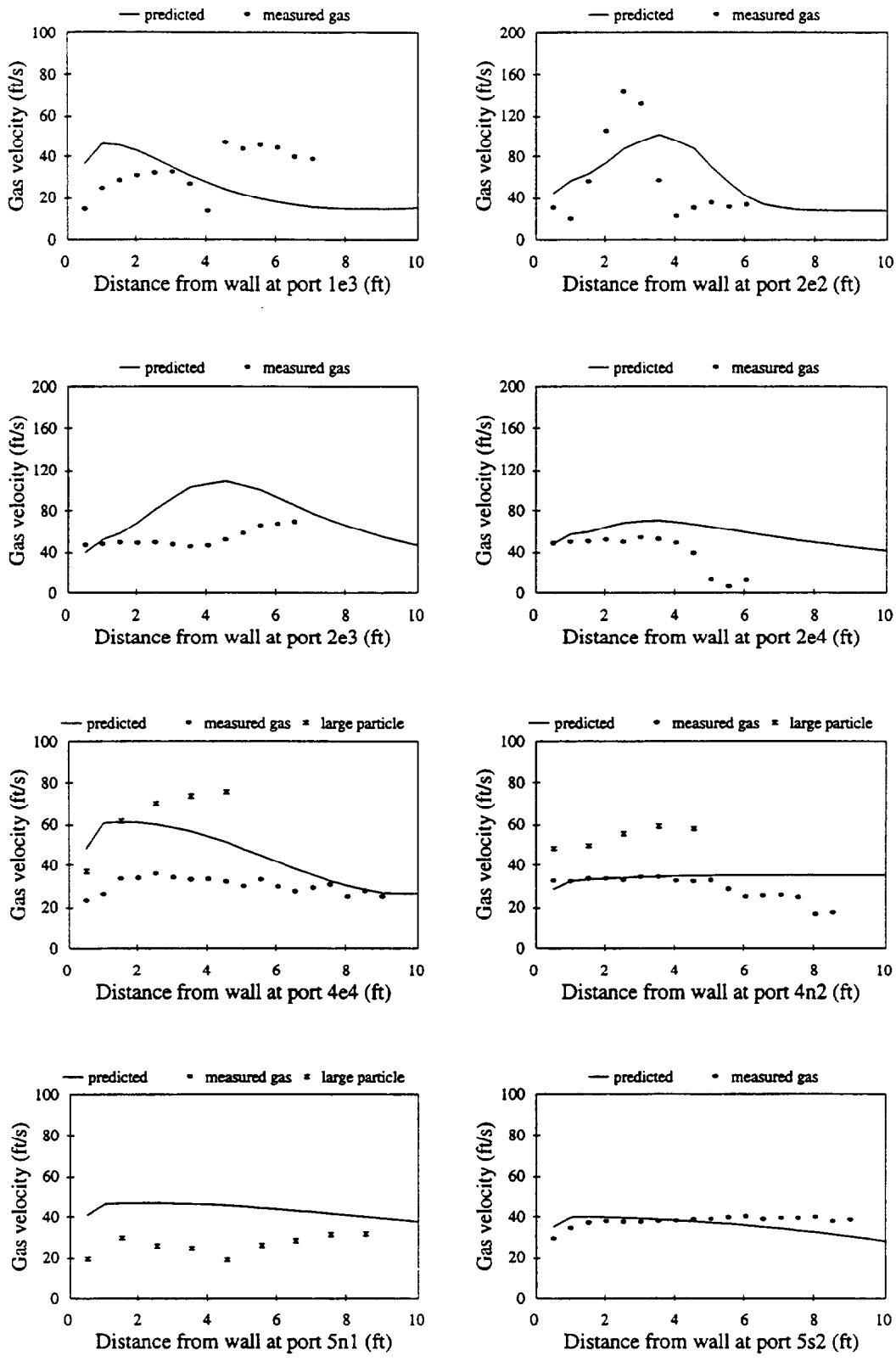

Figure D.2.9. Predicted and measured in-plane velocities for case 9.

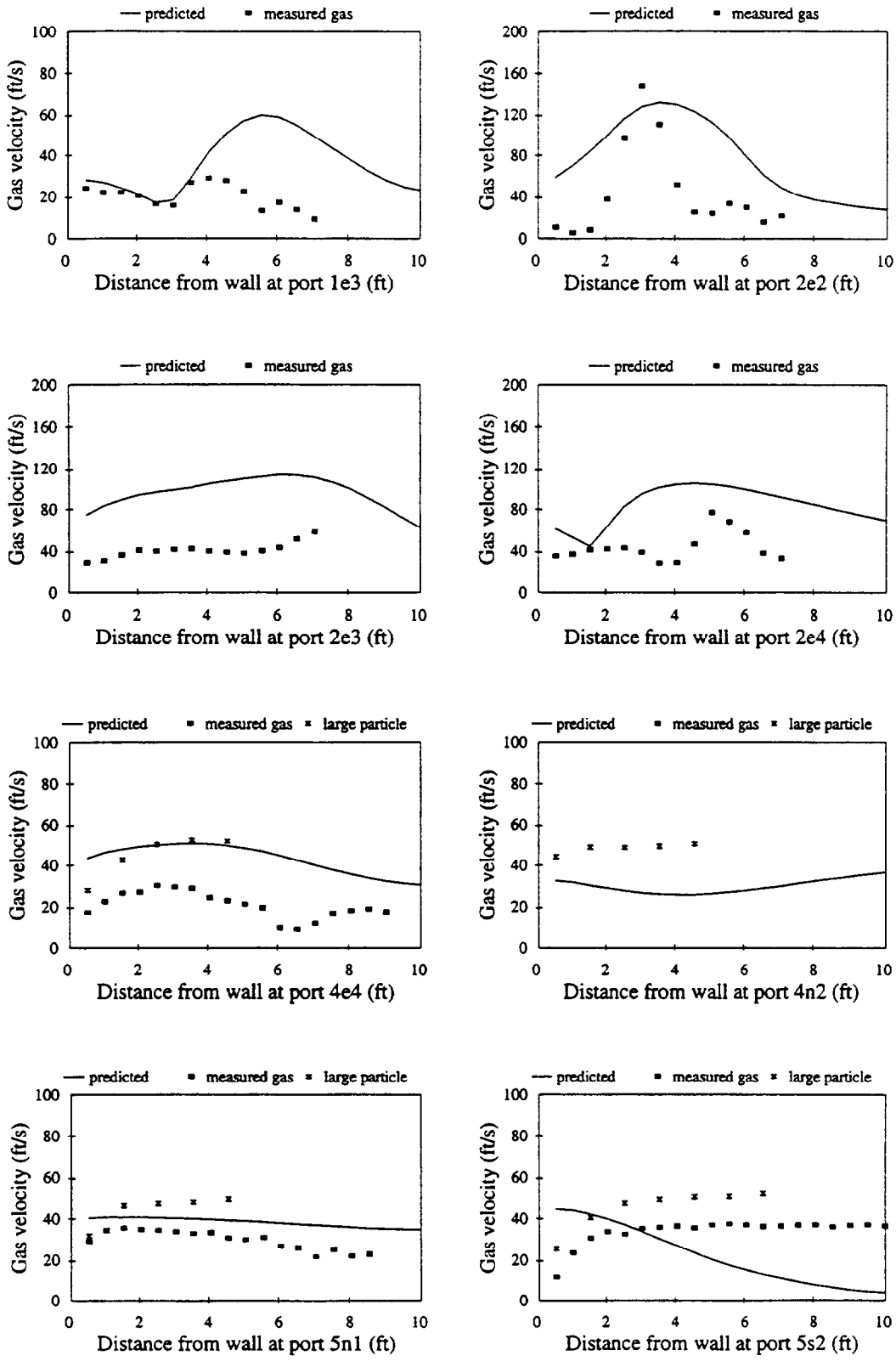

Figure D.2.10. Predicted and measured in-plane velocities for case 10.

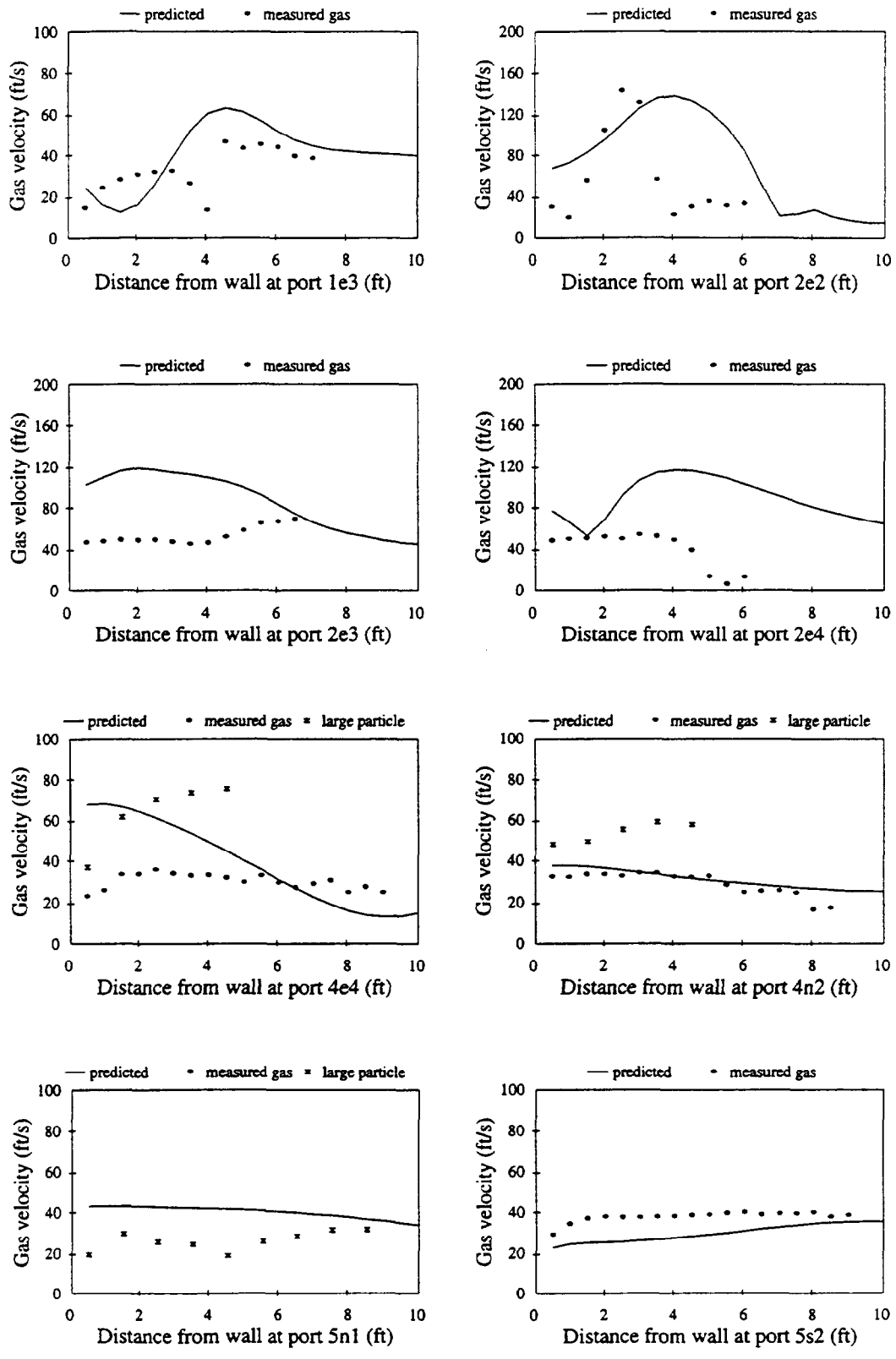

Figure D.2.11. Predicted and measured in-plane velocities for case 12.

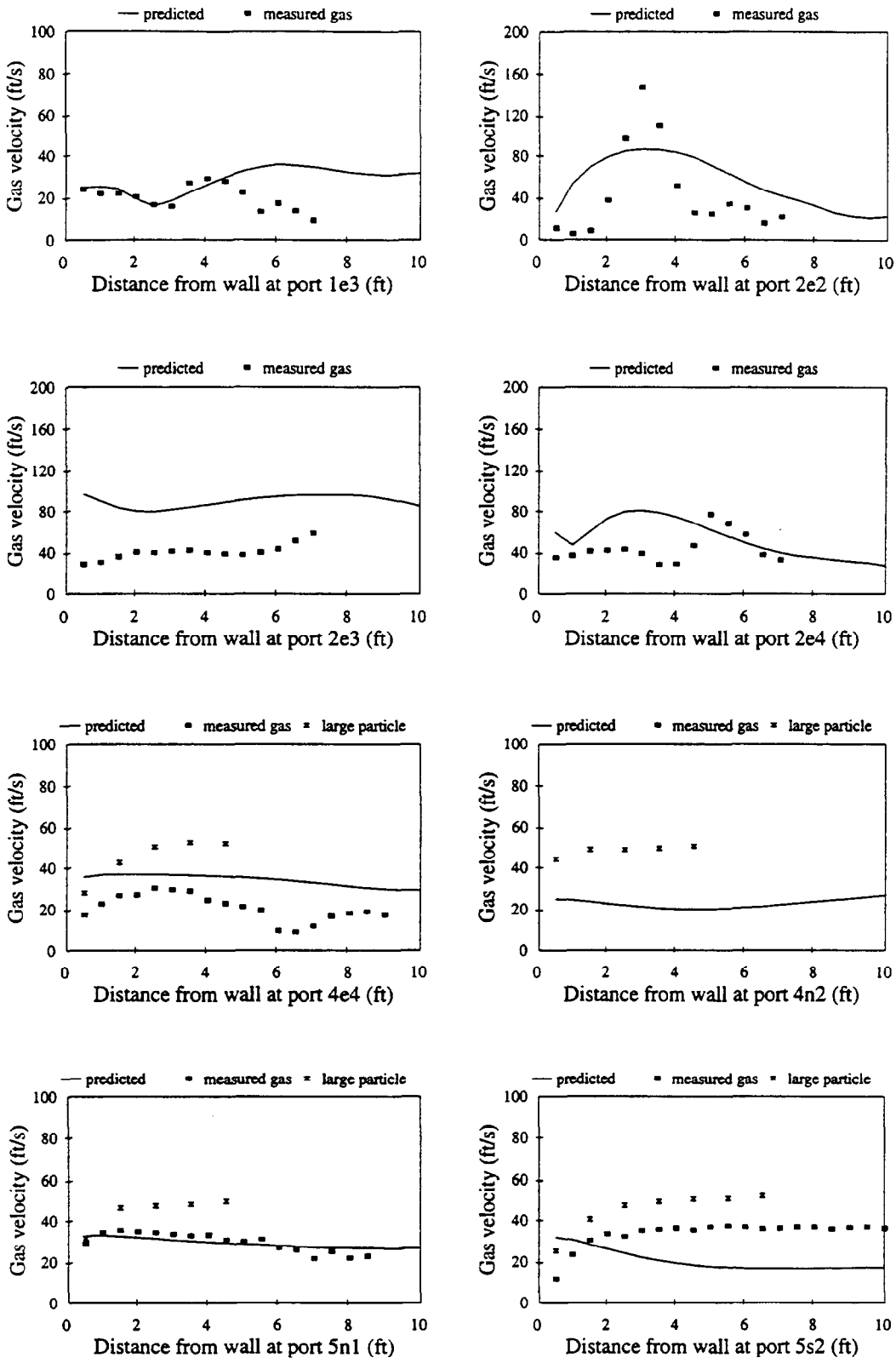

Figure D.2.12. Predicted and measured in-plane velocities for case 13.

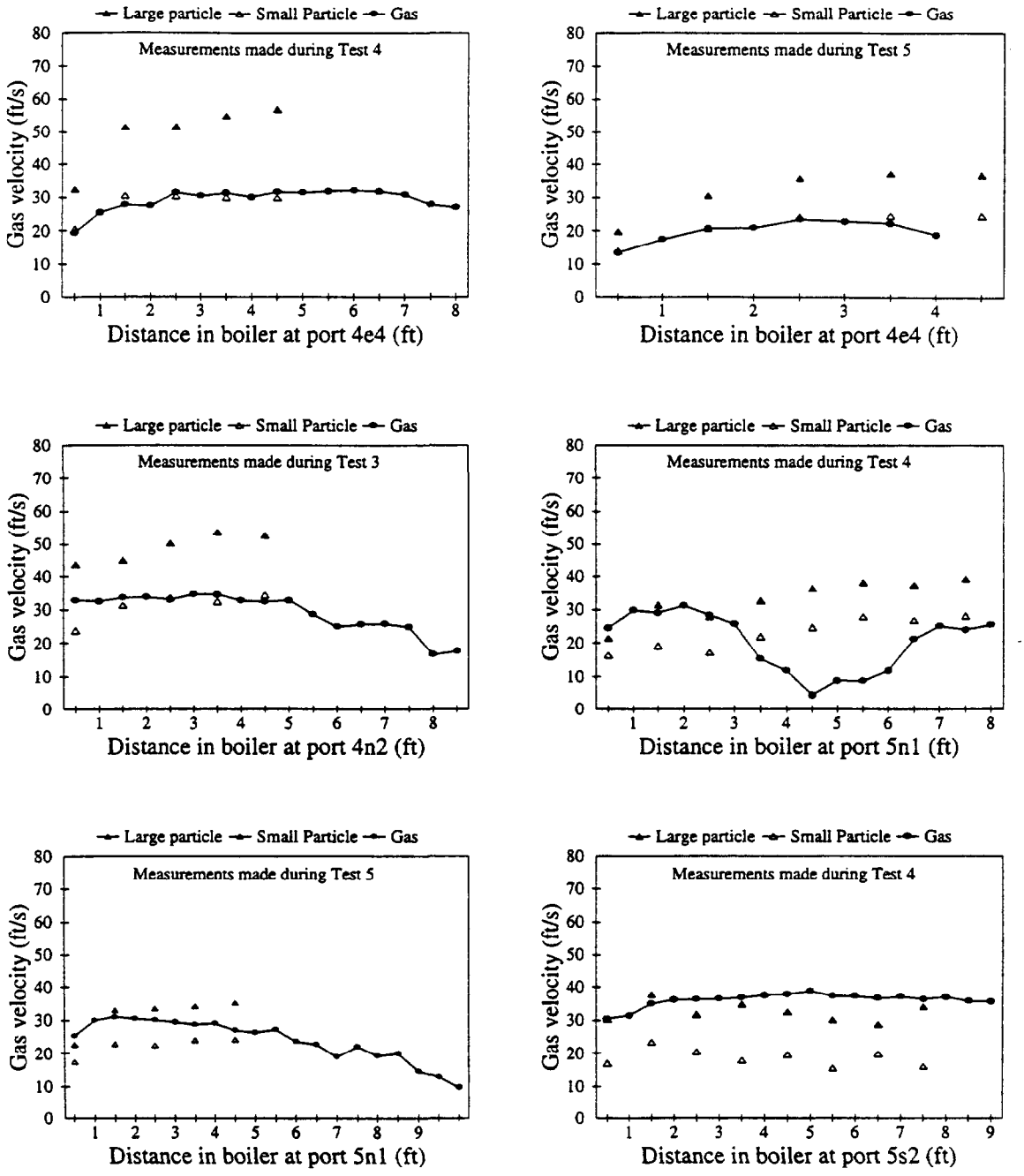

Figure D.2.13. Measured gas and particle velocities taken in the Milliken boiler.

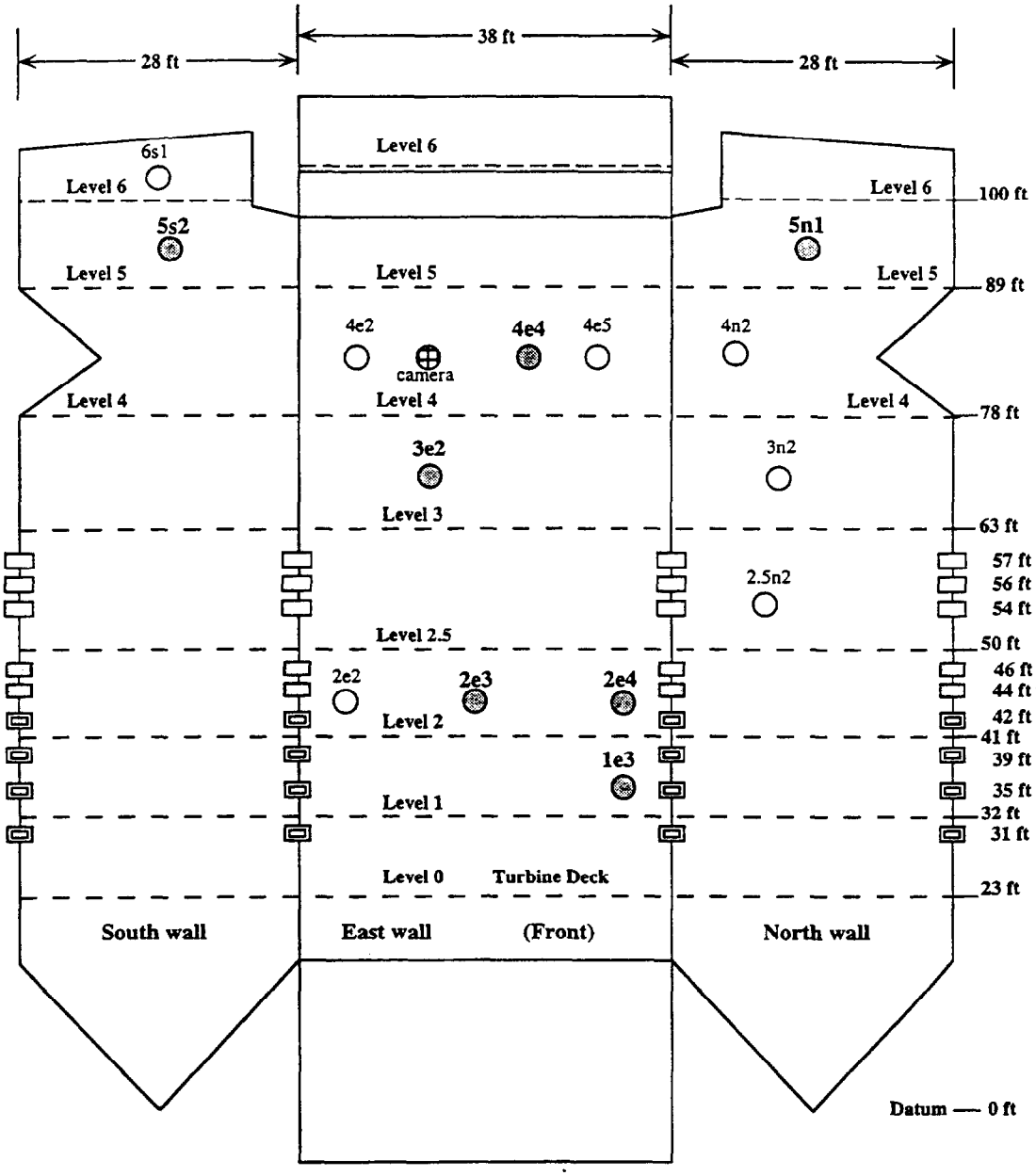

6" diameter ports used for gas and particle composition data collection

other 6" ports

Coal and Primary Air Inlet CCOFA SOFA

Schematic of the Milliken furnace and access ports

Table 2. **Milliken Test Parameters.**

Test	1	2A	2B	2C	3	4	5
Gross Load (MWe)	156	**132**	**155**	158	157	156	157
Net Load (MWe)	147	123	145	148	147	146	146
Coal Feed (t/hr)	55.3	46.1	54.8	54.8	55.6	53.3	54.7
Excess Air (%)	3.9	3.9	4.0	4.1	3.9	3.9	3.7
Tilt (degrees)	- 5	- 5	**- 5**	**+ 5**	- 5	- 5	- 5
SOFA (% open)	40	40	40	40	**40**	**0**	**100**
Coal Type	**B**	C	**C**	C	**A**	A	A

Table · Case comparisons for the PCGC-3 Milliken boiler simluations.

Grid size cases (test 3, old devol.)			
65K grid	192K grid		337K grid
case 9	case 1		case 4
SOFA cases (new devol. except case 4)			
SOFA → / grid ↓	0% open (test 4)	40% open (test 3)	100% open (test 5)
192K grid	case 3	case 7	case 8
337K grid	case 6	case 4	case 10
Devolatilization cases			
SOFA →	0% open (test 4)		40% open (test 3)	
grid ↓ devol. →	old	new	old	new
192K grid	case 2	case 3	case 1	case 7
337K grid	case 5	case 6	case 4	case 12